



# ACTA MINERALOGICA-PETROGRAPHICA

**ABSTRACT SERIES**

**Volume 10**

**2019**

# EC

*European Current Research on  
Fluid Inclusions*



*A meeting dedicated to  
fluid and melt inclusions*

**23-27<sup>th</sup> June 2019, Budapest, Hungary**

# ACTA MINERALOGICA-PETROGRAPHICA

*established in 1923*

## ABSTRACT SERIES

HU ISSN 0324-6523

HU ISSN 1589-4835

### Editor-In-Chief

Elemér Pál-Molnár  
*University of Szeged, Szeged, Hungary*  
*E-mail: palm@geo.u-szeged.hu*

### Guest Editors

Márta Berkesi  
Tibor Guzmics  
Gabriella B. Kiss  
Dóra Cseresznyés

### Contributing Editors

Tamás Spránitz  
Orsolya Gelencsér  
Csilla Király  
Nóra Liptai

### Design

Dóra Cseresznyés and Tamás Spránitz

### Cover Photo

Apatite-hosted fluid inclusions, Kerimasi, Tanzania  
Tibor Guzmics

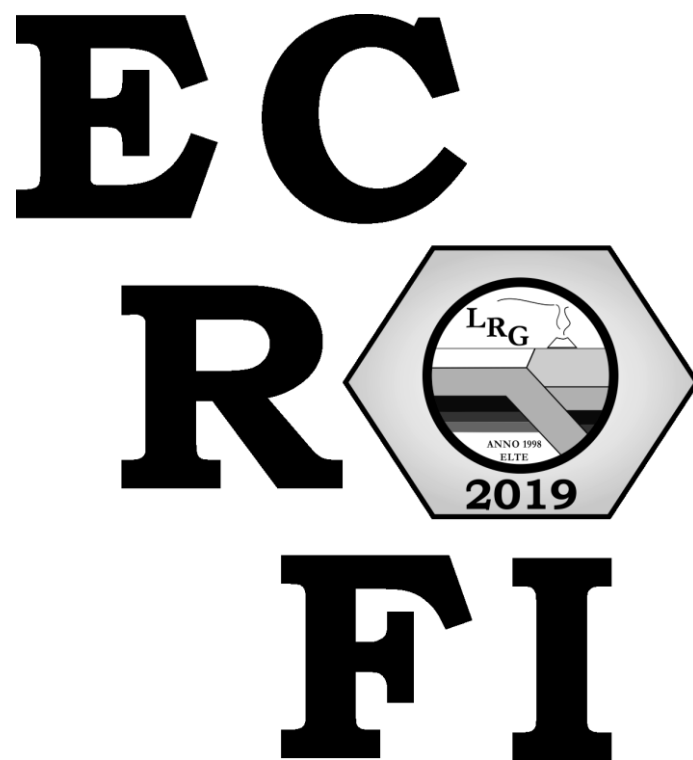
### Sponsors



# **ECROFI XXV**

XXV<sup>th</sup> EUROPEAN CURRENT RESEARCH ON FLUID INCLUSIONS

23-27 June 2019, Budapest, Hungary



## **ABSTRACTS**

Szeged, Hungary  
2019

## Organising committee

Eötvös Loránd University Budapest, Lithosphere Fluid Research Lab  
Márta Berkesi, Tibor Guzmics, Csaba Szabó, Anita Csoma (MOL Nyrt.),  
Dóra Cseresznyés, Orsolya Gelencsér, Tamás Spránitz,  
Ábel Szabó, Anita Erőss, Diamond Congress Ltd.



## Abstracts were reviewed by

Enikő Bali, *University of Iceland, Iceland*  
David Banks, *University of Leeds, United Kingdom*  
Zsolt Benkó, *Institute for Nuclear Physics, ATOMKI, Hungary*  
Márta Berkesi, *Eötvös Loránd University, Hungary*  
Gulcan Bozkaya, *Pamukkale University, Turkey*  
Andrea Ceriani, *University of Science and Technology, United Arab Emirates*  
Anita Csoma, *Unconventional Exploration, MOL Group, Hungary*  
György Czuppon, *RCAES, Hungarian Academy of Sciences, Hungary*  
Larry Diamond, *University of Bern, Switzerland*  
András Fall, *The University of Texas at Austin, USA*  
Simona Ferrando, *University of Torino, Italy*  
Tibor Guzmics, *Eötvös Loránd University, Hungary*  
Jacob Hanley, *Saint Mary's University, Canada*  
Peter Koděra, *Comenius University in Bratislava, Slovakia*  
Dan Marshall, *Simon Fraser University, Canada*  
Jacques Pironon, *Université de Lorraine, France*  
Félix Schubert, *University of Szeged, Hungary*  
Alexander Sobolev, *Université Grenoble Alpes-CNRS, France*  
Alfons Van den Kerckhof, *University of Göttingen, Germany*

---

### Editorial Board

Balázs Koroknai  
Csaba Szabó  
István Dódony  
Magdolna Hetényi  
Mihály Pósfai  
Péter Rózsa  
Szabolcs Harangi  
Tibor Zelenka  
Gábor Papp

György Buda  
István Viczián  
János Földessy  
Péter Árkai  
Péter Sipos  
Sándor Szakáll  
Tamás Fancsik  
Tibor Szederkényi  
Tivadar M. Tóth

### Editorial Office Manager

Szilvia Csató  
*University of Szeged, Szeged, Hungary*  
E-mail: [csato.szilvia@geo.u-szeged.hu](mailto:csato.szilvia@geo.u-szeged.hu)

### Editorial Address

H-6722 Szeged, Hungary  
2 Egyetem Street  
E-mail: [asviroda@geo.u-szeged.hu](mailto:asviroda@geo.u-szeged.hu)

## Preface

It is my great pleasure to welcome all participants of the XXV<sup>th</sup> ECROFI (European Current Research on Fluid Inclusions) conference in 2019, organized by the Lithosphere Fluid Research Lab for the second time in Budapest, Hungary.

Our main goal during the organization of this meeting was to follow the traditions of the ECROFI by putting the main focus on providing the platform for presenting new results and learning about the latest progress in the analytical, experimental and applied aspects of fluid and melt inclusion research. This goal will be fulfilled by the variable topics of the plenary and poster sessions, as well as the first pre-conference workshop on the 23<sup>rd</sup> of June, given by Robert J. Bodnar, which is focusing on the basics of fluid inclusion research and their applications.

Secondly, we aim to provide an opportunity to get acquainted with the research environment at the Research and Instrument Core Facility (RICF) related to fluid inclusion studies at Eötvös University, the institute hosting the conference. Therefore, the second workshop will present the laboratories and facilities of the University involved in melt and fluid inclusion research. Finally, our third goal is to introduce the sub-surface fluids beneath the city of Budapest - the greatest thermal water system in Europe - during the post-conference field trip.

Last but not least, we are happy to have the opportunity to support students' participation by the grant we provide.

For all participants I wholeheartedly wish a professionally successful meeting and a pleasant stay in Budapest!

On behalf of the Organizing Committee,

Márta Berkesi  
Eötvös Loránd University  
Lithosphere Fluid Research Lab

---

# **ABSTRACTS**

---

# Fluid inclusion systematics and mineralogy of the Unique Nictaux Falls Dam Co-Ni-As-Au ( $\pm$ Ag, Bi) occurrence, Meguma Terrane, Nova Scotia, Canada

Adlakha, E.<sup>1\*</sup>, Kennedy, N.<sup>1</sup>, McNeil, N.<sup>1</sup>, Hanley, J.<sup>1</sup>, Kerr, M.<sup>1</sup> & Baldwin, G.<sup>2</sup>

<sup>1</sup>Department of Geology, Saint Mary's University, Canada; <sup>2</sup>Nova Scotia Department of Energy and Mines, Canada; \*erin.adlakha@smu.ca

Polymetallic (Co-Ni-As-Au $\pm$ Ag,Bi) quartz-sulpharsenide veins of the Nictaux Falls Dam Occurrence are currently being investigated to resolve their formation and the potential for 'five-elements' style deposits in Nova Scotia. This showing represents an under-characterised mineralisation style of the Meguma Terrane, Appalachian Orogen, providing an opportunity to study these unique hydrothermal systems.

Two styles of mineralisation occur hosted within fault-bounded quartz veins in late Silurian-aged greenschist Meguma Terrane metasediments: i) laminated, sulpharsenide-quartz veins (Fig. 1A-D) and ii) sulpharsenide mineralised wallrock clasts in quartz breccia (Fig. 1E). Crosscutting relationships with the South Mountain Batholith indicate a maximum age of 370 Ma. The sulpharsenides exhibit unidirectional zoning from Fe-rich (arsenopyrite), to Co-rich (Fe-rich cobaltite), to Ni-rich (Co-rich gersdorffite) rims (Fig. 1B-D). Compositional ( $\mu$ -XRF, EPMA-WDS) mapping indicates inherited arsenopyrite from the wallrock (Fig. 1E). Small (<10  $\mu$ m), Au-Ag alloy grains occur interstitial to Ni-rich rims. Sulpharsenide trace element abundances (LA-ICP-MS) correlate with major element zoning: Fe-rich areas are high in Sb ( $\leq$ 160 ppm) and Bi ( $\leq$ 1600 ppm), and Co-Ni rich areas are high in Au ( $\leq$ 140 ppm), Ag ( $\leq$ 10 ppm) and Se ( $\leq$ 1100 ppm). Based on the solubility of analogous Co-Ni-Fe oxides (Markl et al., 2016) and Se in pyrite (Huston et al., 1995), zoning suggests decreasing pH during mineralisation. Bulk  $\delta^{34}\text{S}_{\text{VPDB}}$  of both types of mineralisation are similar (5.4-6.6 ‰ and 3.9-4.6 ‰, respectively) suggesting a well-mixed, homogenised S source. The values overlap with Meguma Group Slates (Kontak and Smith, 1989) suggesting the wall rock as a S source.

Two fluids are preserved in coeval quartz-hosted fluid inclusions (Fig. 1F) in mineralised and barren veins: i) NaCl-H<sub>2</sub>O $\pm$ CH<sub>4</sub> fluids with salinities of 30 to 35 wt% NaCl equiv. ( $T_h$  via halite dissolution from 160 to 247 °C; n = 18, with some measurements > 250 °C), and ii) CaCl<sub>2</sub>-H<sub>2</sub>O $\pm$ CH<sub>4</sub> fluids with an undetermined but likely high salinity (freezing not observed;  $T_h$  via vapour out between 136 to 240 °C, n = 34 with some measurements >250 °C). Estimates of trapping conditions using microthermometric data (c.f. Lecumberri-Sanchez et al., 2012) show that NaCl-rich fluids were trapped at high confining pressure (>2.65 kbar). Decrepitate salt mound analysis suggests mixing of the two fluids in widely variable proportions as Ca/(Ca+Na) ranges from 0 to 1 (n = 184).

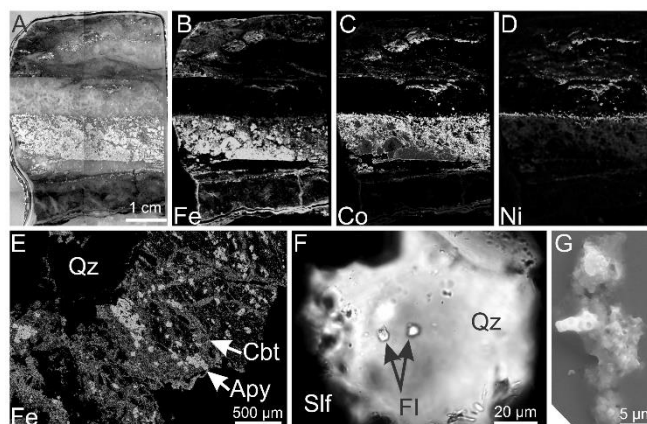


**Fig. 1.** A) Laminated quartz-sulpharsenide vein in thin section. B-D)  $\mu$ -XRF elemental (Fe-Co-Ni) maps of A. E) A WDS map for Fe in a mineralised wallrock clast in quartz (Qz) breccia Arsenopyrite (Apy) cores are disseminated in net-textured cobaltite (Cbt). F) Clustered fluid inclusions (FI) in quartz interstitial to sulpharsenide (Slf). G) SE image of an evaporite mound.

The high fluid salinities combined with a lack of evidence for boiling, low K content and a lack of F in decrepitate mounds preclude a magmatic origin. Based on fluid P-salinity data and the post-Devonian paleotectonic setting of the study area, we suggest the fluids were marine in origin, likely seawater from the unconformably overlying Carboniferous-aged Maritimes Basin. High Ca may reflect Ca-Na exchange with plagioclase-rich amphibolite facies rocks deeper in the metasedimentary succession. Lack of oscillatory zoning and similar  $\delta^{34}\text{S}_{\text{VPDB}}$  in sulpharsenides suggests components were sourced from a single fluid, likely a CaCl<sub>2</sub>-rich basement fluid that scavenged metals, S and As from metasediments.

## Acknowledgement

Min. Resources Develop. Fund. Government of NS

## References

- Markl G. et al. (2016) *Miner. Deposita* 51:703-712.
- Huston D. et al. (1995) *Econ. Geol.* 90:1167-1196.
- Kontak D.J. and Smith P.K. (1989) *Can. J. Earth Sci.* 26:1617-1629.
- Lecumberri-Sanchez P. et al. (2012) *Geochim. Cosmochim. Ac.* 92:14-22.

# Impact and conditions of calcite cementation on reservoir quality evolution of Upper Cretaceous limestones, Onshore Abu Dhabi, United Arab Emirates

**Alsuwaidi, M.<sup>1\*</sup> & Ceriani, A.<sup>1</sup>**

<sup>1</sup>Department of Earth Sciences, Khalifa University of Science and Technology, United Arab Emirates;

\*Mohammad.alsuwaidi@ku.ac.ae

This petrographic, stable isotopic, fluid inclusion and petrophysical study constrains the conditions of calcite cementation and its impact on reservoir quality of limestones of the Upper Cretaceous Simsima Formation across the anticline of an oilfield, onshore Abu Dhabi, UAE. The various crystal morphologies and occurrence habits of calcite cements and paragenetic relationships among them and with other diagenetic minerals suggest various origins and formation timing. Scalenohedral and bladed calcite rims around allochems, which are restricted to packstones and grainstones, have precipitated as early cements from marine pore waters. Syntaxial calcite overgrowths around echinoid fragments engulf dolomite cement. Micro-thermometric measurement of fluid inclusions in one sample containing syntaxial calcite overgrowths revealed  $T_h$  as lower as 64 °C and salinity of nearly 20.5 wt% NaCl equivalent corroborate an origin of fluids from a highly evaporative setting.

The precipitation of coarse equant blocky calcite is common in limestones which display ample evidence of dissolution of peloids, which may have acted as source for this cement. An additional cement source is expected to be by the incipient stylolitisation of the limestones. The presence of this late equant calcite, which post-dates and replaces moldic pore filling dolomite, both in the oil and water zones may pre-date the oil emplacement. However, in the oil zone these moldic pores have, in many cases, escaped cementation by calcite and were instead filled with oil indicating that oil emplacement retarded or even stopped diagenesis.

The higher  $\delta^{18}O_{VPDB}$  values of some of the micrite/microspar rich samples than the values expected for marine calcite precipitated at around 25° C were indicate that the waters were enriched in  $^{18}O$  due to evaporation or that precipitation occurred at low temperatures. Conversely, the coarse equant calcite cements have moderate depletion in  $\delta^{18}O_{VPDB}$  (-6.2 to -3.2‰). Combining these relatively moderately negative oxygen isotopic values with high homogenisation temperatures (76-95 °C) and high fluids salinity (16-19 wt% NaCl) (Fig. 1) suggest precipitation in semi-closed diagenetic systems from geochemically evolved formation waters. The higher homogenisation temperatures than maximum burial temperatures reached suggest that the role of flux of hot basinal brines on diagenesis of the limestones should not be ignored. The formation of secondary pores (e.g.

vugs) might indicate that these brines were charged with organic acids.

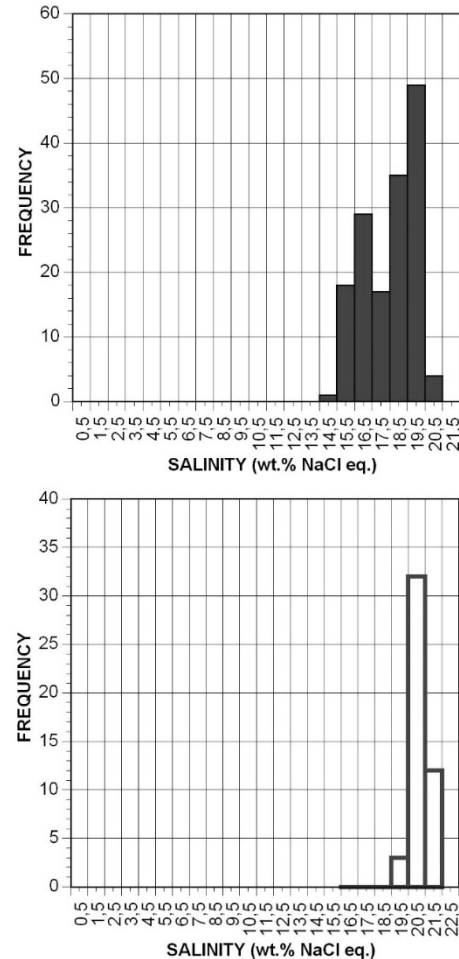


**Fig. 1.** Frequency histograms showing salinity data distribution in blocky calcite cement. Solid bars are for samples in the oil ledge and open bars in the water ledge

## Acknowledgement

This presentation is based upon work supported by the Khalifa University of Science and Technology under Award No. [FSU-2018-15].

# Comendite and Pantellerite melts of the early Mesozoic bimodal associations of Central Mongolia and mechanisms of their formation

**Andreeva, I.<sup>1\*</sup>**

<sup>1</sup>*Institute of Geology of Ore Deposits, Petrography, Mineralogy and Geochemistry, Russia; \*andreeva@igem.ru*

We estimated the composition, evolution and formation conditions of magmas and determined the formation mechanism of melts that produced the comendites and pantellerites of the bimodal volcanic associations of Sant and Dzarta–Khuduk, Central Mongolia, based on electron and ion microprobe analysis of melt inclusions.

Primary melt inclusions were observed in quartz from comendites of the Sant volcanic association, and in quartz from pantellerites of the Dzarta–Khuduk Massif (Andreeva et al., 2018). The inclusions consist of glass + gas phase ± daughter minerals. In addition to glass and gas phases the melt inclusions in quartz from pantellerites contain a fine-grained salt aggregate consisting of Li, Na and Ca fluorides. The phenocrysts of the comendites crystallised at temperatures of 880–960 °C. The phenocrysts of the pantellerites crystallised at higher temperatures of 1000–1060 °C. In addition, heating experiments on quartz-hosted melt inclusions from the pantellerites provided evidence for the formation of immiscible silicate and salt (fluoride) melts at a temperature of 800 °C.

The homogeneous glasses of melt inclusions have both trachydacite and rhyolite compositions. They are characterised by high concentrations of Zr, Nb, Rb, Y, Th and REE. Significant differences were determined in concentrations of Li and volatile component (H<sub>2</sub>O and F) in the glasses: some of the melts are enriched in these components, whereas others are depleted in them.

Using the content of Nb as a differentiation index we correlated variations in different trace element content of melts and rocks (from basalts to rhyolites) relative to Nb in order to estimate the role of crystal fractionation during the formation of the rocks of bimodal associations.

There is a clear positive correlation between the contents of Nb and Zr, Nb and Hf in the whole range of compositions of melts and rocks (including their basic varieties). Similar relations with Nb were observed for Rb, Ta, Th, U, Hf, Y, Be, B and REE. The existence of common trends between melts and rocks of different compositions allowed us to presume a genetic link between basic and acid rocks of the Sant and Dzarta–Khuduk bimodal association.

The glasses of the homogenised melt inclusions from the comendite phenocrysts at Sant are enriched in Li and F. The melts enriched in these elements were found in melt inclusions from pantellerite at Dzarta–Khuduk. The primitive mantle-normalised REE patterns of melt inclusions glasses in phenocrysts of alkalic-salic rocks of both

associations are similar, with the Li maximum being one of the main features.

An extremely important result of studying melt inclusions in phenocrysts from the pantellerites of Dzarta–Khuduk complex was finding Li-enriched fluoride melts along with the silicate melts. This finding suggests the possibility of the generation of a salt melt that extracted significant amounts of Li during the final stages of alkali melt evolution. Such salt melt could subsequently escape from the silicate magma, becoming a source of the rare-metal mineralisation.

The observed general patterns of melt evolution of the Sant and Dzarta–Khuduk Massifs in the Mongolia–Transbaikalia zoned magmatic area, the comparable ages and rock composition suggest a similar formation mechanisms with a dominant role of a crystal fractionation process. The high alkali and volatile component contents (F and H<sub>2</sub>O) of the melts resulted in the significant concentrations of many rare elements. During the final stages of differentiation fluoride melts were separated from the silicate magma, extracting considerable amounts of Li.

## **Acknowledgement**

This study was supported by the Russian Foundation for Basic Research, project no. 17–05–00767.

## **References**

Andreeva I.A. et al. (2018) Dokl. Earth Sci. 481:973-979.

# Magmatic evolution of Wang-Tian'e volcano (NE China): silicate liquid immiscibility or Fenner-type of crystal fractionation?

**Andreeva, O.A.<sup>1\*</sup>, Andreeva, I.A.<sup>1</sup> & Yarmolyuk, V.V.<sup>1</sup>**

<sup>1</sup>*Institute of Geology of Ore Deposits, Petrography, Mineralogy, and Geochemistry, Russian Academy of Sciences (IGEM RAS), Russia; \*oandreeva@igem.ru*

The Changbaishan volcanic area between China and North Korea is the only product of the bimodal magmatism of the Far Eastern part of the Late Cenozoic East Asian Intraplate Volcanic Province. The largest volcanoes of this area in NE China are Changbaishan Tianchi and Wang-Tian'e. In contrast to the Changbaishan Tianchi association of differentiated alkaline rocks lavas of Wang-Tian'e volcano vary from basalt to basaltic andesite and belong mainly to the tholeiitic series and, less frequently, to the alkaline series. Silicic rocks are rare in the area. The goal of this study is to estimate the crystallisation conditions, composition and evolution path of Wang-Tian'e basaltic melts by studying melt inclusions in plagioclase from tholeiitic basalts.

Plagioclase (An<sub>75-80</sub>Ab<sub>19-24</sub>Or<sub>0.8-1.3</sub>) was the first mineral which crystallised in this system. Melt inclusions in plagioclase contain a plagioclase rim and Fe-rich glass, or fine-grained aggregate of clinopyroxene, Ti-magnetite, ilmenite, apatite and sulphides. The composition of the wide rims incrusting the inclusions changes from the outer to inner part of the inclusion from plagioclase (An<sub>46-56</sub>Ab<sub>39-47</sub>Or<sub>4-7</sub>) to anorthoclase (An<sub>13-13.5</sub>Ab<sub>43-50</sub>Or<sub>36-43</sub>). The Fe-rich residual glass and the fine-grained aggregate were analysed by electron microprobe using a 10- $\mu$ m defocused beam. The compositions of Fe-rich glass and the aggregate were identical and show high FeO content – up to 24 wt%, up to 10 wt% CaO, up to 12 wt% MgO, up to 6 wt% TiO<sub>2</sub>, up to 2 wt% Al<sub>2</sub>O<sub>3</sub>, 1 wt% (Na<sub>2</sub>O+K<sub>2</sub>O), 1 wt% P<sub>2</sub>O<sub>5</sub>, 0.3-0.4 wt% SO<sub>3</sub> 98% total at 40-43 wt% SiO<sub>2</sub>. Two types of silicate globules were identified in these inclusions: Fe-rich and Si-rich. Fe-rich globules contain 21-29 wt% FeO, up to 6 wt% MgO, 2-7 wt% Al<sub>2</sub>O<sub>3</sub>, 2 wt% K<sub>2</sub>O, 1 wt% CaO and more than 5 wt% H<sub>2</sub>O at 45-51 wt% SiO<sub>2</sub>. Si-rich globules contain up to 13.5 wt% Al<sub>2</sub>O<sub>3</sub>, 6 wt% K<sub>2</sub>O, 2.2 wt% Na<sub>2</sub>O at 71.5-72 wt% SiO<sub>2</sub>.

The inclusions were homogenised at temperatures of 1180-1190 °C. During thermometric experiments the silicate globules and all the silicate phases dissolved in the melt. Sulphide phases occurring occasionally in the fine-grained aggregate produced sulphide globules with a pure FeS composition. After the heating experiments the inclusions were either completely homogenised or contained glass+gas bubbles±sulphide globules. Their composition in general is identical to the rock composition: 10-12 wt% FeO, 15-16 wt% Al<sub>2</sub>O<sub>3</sub>, 3-3.5 wt% TiO<sub>2</sub>, 4-4.5 wt% MgO, 3-3.5 wt% Na<sub>2</sub>O, 1.3-1.5 wt% K<sub>2</sub>O,

8-9 wt% CaO, 0.6-0.8 wt% P<sub>2</sub>O<sub>5</sub> and 0.3-0.6 wt% SO<sub>3</sub> at 49-51 wt% SiO<sub>2</sub>.

Two possible paths can be suggested for the evolution of the Wang-Tian'e tholeiitic melts. On one hand, in contrast to Bowen's reaction series, the evolution might have followed a Fenner-type fractionation, which proposed that the Ab-An-Di system followed a crystal fractionation path controlled by clinopyroxene fractionation and accumulation of FeO in the melt. As plagioclase was the first mineral to crystallise from the tholeiitic melt of Wang-Tian'e volcano it could form large crystals, especially at relatively high water content, as can be seen in the tholeiitic basalts. Plagioclase crystallisation resulted in melt enrichment in FeO and depletion in SiO<sub>2</sub>, Al<sub>2</sub>O<sub>3</sub> and alkalis, which eventually has led to clinopyroxene crystallisation and Fenner-type fractionation. On the other hand, the presence of Si-rich globules in Fe-rich glasses in the inclusions indicates that low temperature silicate liquid immiscibility could have played a role during tholeiitic melt evolution. This was shown by Roedder (1951) for the quartz-fayalite-leucite system. The formation of hydrous Fe-rich globules in Fe-rich glasses could be attributed to kinetic effects during melt ascent to the surface.

## Acknowledgement

This study was supported by the Grant of the President of Russian Federation, proj. MK-2419.2019.5, and the Russian Foundation for Basic Research, proj. 17-05-00767.

## References

Roedder E. (1951) *Am. Mineral.* 36:282-286.

# Unraveling a hydrous alkaline metasomatic agent beneath the Styrian Basin: an inclusion study from mantle xenolith

Aradi, L.E.<sup>1\*</sup>, Berkesi, M.<sup>1,2</sup> & Szabó, Cs.<sup>1</sup>

<sup>1</sup>Lithosphere Fluid Research Lab, Institute of Geography and Earth Sciences, Eötvös Loránd University, Hungary;

<sup>2</sup>Lendület Pannon Lith<sub>2</sub>Oscope Research Group, Geodesic and Geophysical Institute, Research Centre for Astronomy and Earth Sciences, Hungarian Academy of Sciences, Sopron, Hungary; \*aradi.laszloelod@ttk.elte.hu

The lithospheric mantle was sampled by Plio-Pleistocene alkali basalts across the Styrian Basin (SB), which brought upper mantle xenoliths to the surface. The SB is the westernmost sub-basin of the Pannonian Basin System, located in the transitional zone between the central Pannonian Basin and the Eastern Alps. The lithospheric mantle beneath the SB overlies a region with a fast seismic anomaly, which was interpreted previously (e.g. Qorbani et al., 2015) as a potential remnant of the detached Penninic slab.

In the SB mantle xenolith suite (Aradi et al., 2017) a group of phlogopite-bearing, amphibole-rich xenoliths was found. These xenoliths could be divided into two subgroups, based on the presence or absence of Cl-rich apatite. Relying on the geochemistry of the amphiboles, these rocks were formed during metasomatism, which could have been caused by infiltration of a volatile-rich alkaline mafic melt. This melt reacted with the mantle peridotite mainly via reactive porous melt flow, causing the transformation of Al-rich spinels, orthopyroxenes and clinopyroxenes into Cr-rich spinels, phlogopite and pargasite. Further from the metasomatic agent, the melt might have fractionated along the mantle column, causing even more enrichment in H<sub>2</sub>O, CO<sub>2</sub> and fluid mobile elements (e.g. U, Cl, P), but depletion in basaltic elements (such as Fe and Ti) and potassium. This fractionation led to the formation of the apatite-bearing subgroup.

In the apatite-free xenoliths several primary melt inclusions were found in the newly formed amphiboles (Fig. 1/A), and secondary melt inclusions in the ortho- and clinopyroxenes. The primary inclusions in the amphiboles are partially crystallised, besides silicate glass and CO<sub>2</sub>-rich bubble, clinopyroxene daughter phase was recognised. Secondary inclusions of the pyroxenes are glassy and contain a CO<sub>2</sub>-bearing bubble.

In the apatite-bearing xenoliths primary and pseudosecondary inclusions were found (Aradi et al., 2019; Fig. 1/B). These inclusions, besides the dominating CO<sub>2</sub> (>98 mol. %), contain small amount of H<sub>2</sub>O (<1.2 mol%), N<sub>2</sub> (<0.1 mol%) and SO<sub>4</sub><sup>2-</sup>. The latter one dissolved in the H<sub>2</sub>O-rich fluid. The solid phases of the fluid inclusions in the amphibole consist mostly of different carbonates (magnesite, Na-bearing dawsonite, nahcolite and natrite) and sulphates (anhydrite and Na-bearing thenardite-burkeite). To our best knowledge, such Cl-free, but Na<sup>+</sup> and SO<sub>4</sub><sup>2-</sup>-bearing fluid composition was not described previously in

mantle fluids. Along with the formation of amphiboles, the coexisting fluid phase become enriched in volatiles (C-O-N-S), Na<sup>+</sup>, HCO<sub>3</sub><sup>-</sup> and SO<sub>4</sub><sup>2-</sup>, and then trapped in the amphiboles. Thus, this fluid represents the residual portion of the fractionated volatile-rich alkaline mafic melt (represented by the melt inclusions), which metasomatised the SB subcontinental lithospheric mantle (Aradi et al., 2019).

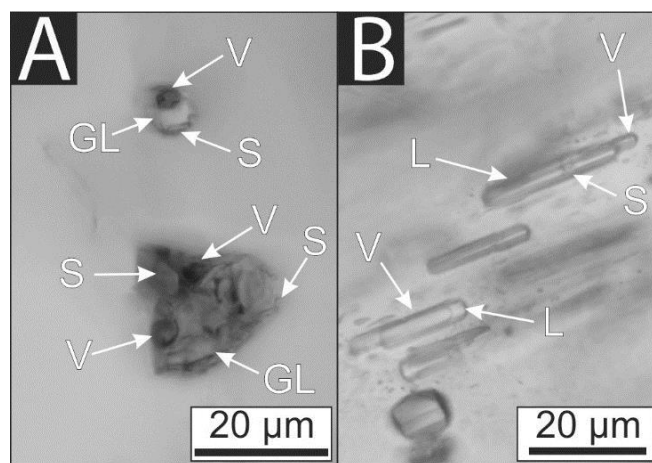


**Fig. 1.** A) Partially crystallised primary melt inclusions in amphibole. B) Pseudosecondary fluid inclusions in amphibole, occurring along the cleavage planes of the host amphibole. L - liquid; V - vapour; S - solid; GL - glass.

## Acknowledgement

This work was completed in the ELTE Institutional Excellence Program (1783-3/2018/FEKUTSRAT) supported by the Hungarian Ministry of Human Capacities. M. Berkesi was supported by the Bolyai Postdoctoral Fellowship Program.

## References

- Aradi L. E. et al. (2017) *Tectonics* 36:2987-3011.
- Aradi L. E. et al. (2019) *Föld. Közl.* 149:35-49.
- Qorbani E. et al. (2015) *Earth Planet. Sc. Lett.* 409:96-108.

## Fluid immiscibility from the suite of hydrothermal deposit

**Avalos, N.<sup>1</sup> & Moncada, D.<sup>1\*</sup>**

<sup>1</sup>Department of Geology, University of Chile, Chile; \*dmoncada@ing.uchile.cl

During the past half-century, numerous fluid inclusion studies of hydrothermal precious metals and base metal deposits have been conducted, and much of our understanding of the physical and chemical environment of metal transport and deposition in the environment has evolved from these studies. The gold and base metal deposits at Alhué mining district, Chile, are a classic example of the hydrothermal type ore deposit. The Alhué mining district of the coastal range of central Chile is located approximately 70 km southwest of Santiago and 24 km east of the illustrious municipality Villa Alhué. The mining activity began in the 16<sup>th</sup> century and continues today in several mines in the district. These deposits form as the result of magma-driven fluid flow in a convecting hydrothermal system, possibly associated with the emplacement of an intermediate composition magma. There still remains considerable debate concerning the source(s) of the fluids (magmatic vs. meteoric), the metals (magma vs. wall rocks) in this important class of ore deposit and the duration of the ore-forming process.

We present a multidisciplinary study that will integrate petrological, geochemical, and structural information with fluid composition to constrain thermodynamic and time conditions and geochemical environment under which the precious and base metals precipitate. There is now a large database of fluid properties in these systems that have shown boiling, mixing of fluids and interaction with wall rock which are all associated with mineralisation in this environment. Once boiling begins at the ascertained depth, the fluid will usually continue boiling up to the surface. Thus, the presence of fluid inclusions indicative of boiling in surface outcrops suggests that the base of the boiling zone, and the highest gold grades, are likely to be encountered at depth.

Another innovative aspect of this project will be the study on the effects of the budget of precious metals and/or base metals in the veins that might have been modified during the different events of boiling and structural controls through time. The low salinities observed in most Au-rich and, to a lesser extent, Ag-rich deposits have been put forth as evidence that Au (and Ag) are transported as sulphur complexes rather than chloride complexes. Another possibility is the interaction between wall rock and fluid, which might contribute to the precipitation of Au in the system. Detailed petrography of samples is necessary to identify individual fluid events, because samples usually contain numerous growth zones and/or planes of inclusions representing fluids of potentially different compositions trapped at different times. *In-situ*

analyses on individual fluid inclusions and mineral textures will be performed using micro-analytical techniques such as infrared (IR) petrography (for opaque minerals), SEM/EDS/EBSD, laser ablation ICP-MS and carbon and nitrogen isotope ratios of fluid inclusion gases, which can be measured online using a crushing device interfaced to an isotopic ratio mass spectrometre (IRMS). These new data will significantly advance our understanding of the Alhué systems and provide basic natural environment data that may be used to estimate thermodynamic properties of complex aqueous fluids at different temperatures, compositions and pressures.

### **Acknowledgement**

I thank the Yamana Gold Inc. exploration team for sample collection and discussion. CONACYT Initiation 1170210

# Superposition of multiple hydrothermal events revealed by coupled SEM-CL and fluid inclusion study in VMS related quartz

**B. Kiss, G.<sup>1\*</sup> & Bendő, Zs.<sup>2,3</sup>**

<sup>1</sup>Department of Mineralogy, Eötvös Loránd University, Hungary; <sup>2</sup> Department of Petrology and Geochemistry, Eötvös Loránd University, Hungary; <sup>3</sup>Flame Spray Hungary Ltd., Hungary; \*gabriella.b.kiss@ttk.elte.hu

Scanning electron microscopy cathodoluminescence (SEM-CL) study of quartz crystals became a prevailing research method aiming to better understand complex hydrothermal ore formation processes. In spite of its obvious benefits, case studies are almost exclusively limited to Cu-porphyry and epithermal systems and only a few examples are known from other deposit types (e.g. orogenic gold, MVT or VMS) (see e.g. Rusk et al., 2004, Frelinger et al., 2015 and the references cited therein). Though several studies point at the possible advantages of SEM CL imaging of quartz in fluid inclusion studies, case studies are scarcely found (e.g. Boiron et al., 1992; Batkhishig et al., 2005), especially in the field of VMS deposits. In the present study we tried to reveal the complex history of quartz formed during submarine hydrothermal process using coupled SEM-CL and fluid inclusion study of quartz.

The studied samples represent VMS stockwork mineralisation related to Jurassic oceanic stage of the Neotethys. Quartz-sulphide veins are hosted in basalt (in Boccassuolo, Reppia and Monte Loreto), gabbro (in Campegli and Bargone) and peridotite (in Vigonzano) (Northern Apennines, Italy).

Fluid inclusion petrography, microthermometry and Raman spectroscopic study was combined with SEM-CL study of quartz. Three quartz generations were already identified by conventional petrography (early, coarse grained euhedral, followed by medium grained subhedral and late stage fine grained anhedral quartz). However, SEM-CL imaging has revealed such details, which were not observable by polarising microscopy. A complex evolution history was observed, with superposition of multiple hydrothermal events, forming the different quartz generations. Crystallisation of CL-bright gray early quartz was interrupted by CL-dark quartz microfracturing, followed by formation of euhedral growth zones. Interstitial quartz precipitated later, followed by micro-brecciation and 2-3 generations of CL-dark/-bright microfractures.

These observations suggest a dynamically changing hydrothermal system. The appearance of growth zones is related to physico-chemical environmental changes during quartz precipitation (Frelinger et al., 2015), while micro-fracturing and micro-brecciation are the results of multiple hydrothermal events (Rusk et al., 2004).

Study of primary fluid inclusions hosted by quartz is in accordance with the above findings. The L+V(+S) inclusions at every locations were trapped from a homogenous parent liquid, showing

homogenisation temperatures of 90-360 °C. Though temperature ranges were slightly different at the different study localities,  $T_h$  trends can be defined. Decreasing  $T_h$  was observed from early (360-240 °C), through transitional (280-150 °C) to late stage quartz (170-90 °C), as well as from core to rim of single crystals (up to 40 °C temperature drop). Not only temperature, but also compositional variability was observed: salinity of  $7.3 \pm 0.75$  to  $3.3 \pm 0.45$  to NaCl equiv. wt% (with a weak correlation with decreasing  $T_h$ ) and average methane content of 0.22 mol/kg (based on Raman spectroscopy analyses) were found. At one location correlation between methane clathrate formation upon cooling and SEM-CL colour was observed: CL-bright core of quartz crystals contained clathrate forming inclusions, while CL-dark outer zones have not shown that feature.

Detailed SEM-CL study of quartz precludes erroneous fluid inclusion microthermometry analyses, as secondary FI in hidden microfractures can be better avoided and small pieces of early quartz within the late fine grained brecciating quartz can be identified. However,  $T_h$  and compositional changes within a crystal or a vein can also be better understood.

Our results show, this approach can be successfully used in understanding VMS deposit forming hydrothermal systems, thus complete our earlier knowledge on this field.

## Acknowledgement

This research was supported by the Hungarian National Science Fund OTKA PD 112580 (to G. B. Kiss) by NKFIH. SEM-CL analyses was available thanks to KMOP 4.2.1/B-10-2011-0002 program.

## References

- Batkhishig B. et al. (2005) *Resour. Geol.* 55:1-8.
- Boiron M. C. et al. (1992) *Geochim. Cosmochim. Ac.* 56:175-185.
- Frelinger S. N. et al. (2015) *Ore Geol. Rev.* 65:840-852.
- Rusk B. et al. (2004) 14<sup>th</sup> International Conference on the Properties of Water and Steam, Kyoto, 296-302.

## Apatite, magnetite, and inclusion compositions from the Buena Vista deposit, Nevada (USA): implications for a new genetic model for Kiruna-type deposits

**Bain, W.M.<sup>1\*</sup>, Steele-MacInnis, M.<sup>1</sup>, Luo, Y.<sup>1</sup>, Pearson, D.G.<sup>1</sup>, Mazdab, F.K.<sup>2</sup>, Marsh, E.E.<sup>3</sup> & Dufresne, A.<sup>1</sup>**

<sup>1</sup>University of Alberta, Canada; <sup>2</sup>University of Alberta, USA; <sup>3</sup>US Geologic Survey, USA; \*wbain@ualberta.ca

Recent studies have proposed hybrid orthomagmatic-hydrothermal models for Kiruna-type iron-oxide apatite (IOA) deposits in which mineralizing fluids comprise both melts and hydrothermal fluids (Tornos et al., 2017; Simon et al., 2018). These models remain controversial but account for the observation of overlapping magmatic and hydrothermal features in many IOA systems.

The Buena Vista IOA deposit (Pershing County, NV) was previously characterised as an endmember hydrothermal IOA systems related to the intrusion of gabbro into carbonate-bearing sedimentary rocks and the subsequent circulation of a magmatic brines around an igneous heat source (Johnson and Barton, 2000). Here we revisit this interpretation and propose a new model for this system based on chemical analysis of apatite, magnetite, and inclusions hosted in Fe-oxide ores and carbonate dikes which cross cut the Fe-oxide ore body.

Characterisation of primary apatite from Fe-oxide ores and carbonate dikes via SEM-CL, EMPA, and LA-ICP-MS showed that both assemblages have similar major and trace element chemistry showing only slight differences in LREE, HREE, and HFSE content. However, both are overprinted by a secondary generation of apatite that shows a distinctive depletion in most trace elements (particularly LREEs), and is intergrown with monazite, REE-bearing allanite, and thorite. Both primary and secondary apatite from Fe-oxide ores and carbonate dikes show positive  $\epsilon\text{Nd}$  values. The compositions of magnetite from Fe-oxide ores was homogenous across individual grains and was relatively rich in Ti and V with variable Al and Si.

Primary and secondary apatite from Fe-oxide ores and carbonate dikes host abundant assemblages of coexisting carbonate melt inclusions and aqueous brines (Fig. 1). The carbonate melt inclusions contain ~10 wt%  $\text{Fe}_2\text{O}_3$ , as well as quartz, anatase and cristobalite. Coexisting brine inclusions are rich in Na-K-Ca and have unusual microthermometric behaviour, with final melting temperatures of +7 to +12 °C. Analysis of decrepitate mounds and crystalline solids in breached brine inclusions showed that in addition to NaCl, carbonate and sulphate are major components of the aqueous fluid and likely explain the positive last-melting temperatures as representing melting of salt hydrates.

Based on the ubiquitous occurrence of carbonate melt inclusions throughout the Buena Vista deposit, as well as the other geochemical data

described here, we interpret that the Buena Vista system is not a purely hydrothermal system as previously suggested. Rather, we propose a hybrid orthomagmatic-hydrothermal model for this system in which Fe transport is accomplished by the circulation of coexisting carbonate melts and aqueous fluids.

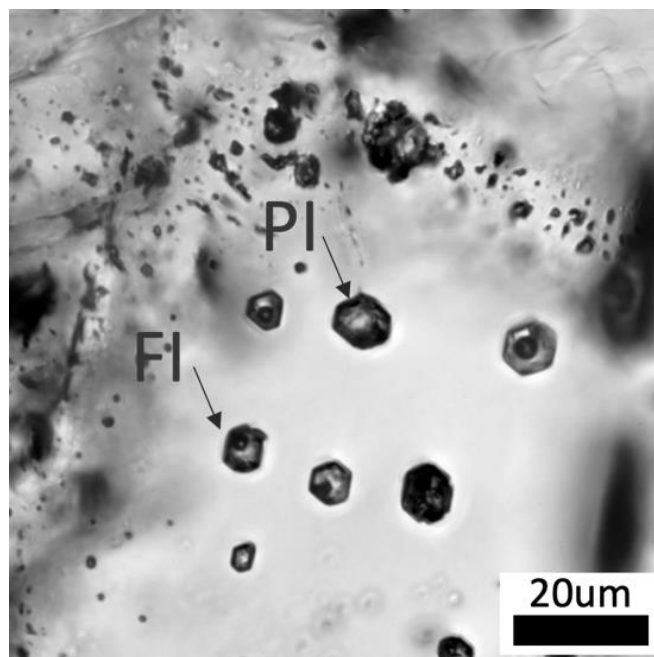


**Fig. 1.** An assemblage of coeval aqueous brine inclusions (FI) and polycrystalline carbonate melt inclusions (PI) hosted in apatite from the Buena Vista deposit.

### References

- Johnson D.A. and Barton M.D. (2000) SEG Guide Book 32:127-144.
- Tornos F. et al. (2017) Econ. Geol. 112:1595-1628.
- Simon A. et al. (2018) SEG Spec. Pubs. 21:89-114.

# Compositions of silicate, salt, and aqueous fluid inclusions hosted in unidirectional solidification textures from the Saginaw Hill Porphyry Stock, Arizona

Bain, W.M.<sup>1\*</sup>, Steele-MacInnis, M.<sup>1</sup> & Marsh, E.E.<sup>2</sup>

<sup>1</sup>University of Alberta, Canada; <sup>2</sup>US Geologic Survey, USA; \*wbain@ualberta.ca

A key process in the formation of porphyry ore deposits is the exsolution of aqueous hydrothermal fluids from silicate melt and the subsequent circulation of these fluid outward from their source. This process is characterised by various types of immiscibility between concentrated and dilute fluids. The most commonly recognised types of immiscibility in magmatic-hydrothermal systems are between saline aqueous liquids and vapours, and between these aqueous fluids and the silicate melts that give rise to them. However, several recent studies of fluid inclusions in veins from shallow and intermediate-depth porphyry systems have shown that hypersaline melt inclusions (salt melts) can also coexist with assemblages of vapour rich inclusions and/or silicate melt inclusions which contain an immiscible saline liquid at high temperature (Kodera et al., 2014; Rottier et al., 2016; Mernagh and Mavrogenes, 2019). This has been interpreted as evidence of exsolution of salt melts directly from a silicate melt, although this process is still not well understood.

Here we present petrographic and microthermometric observations as well as LA-ICP-MS data from fluid and melt inclusions hosted in magmatic and hydrothermal quartz associated with unidirectional solidification textures (USTs) in the Saginaw Hill quartz monzonite-latitude porphyry stock, Arizona (USA). Quartz UST bands are formed as a result of the episodic accumulation and venting of H<sub>2</sub>O-rich fluids produced via immiscibility with silicate melt during crystallisation and degassing (London, 2009). As a result, USTs can trap inclusions of both hydrothermal fluid as well as the silicate melt form which it has exsolved. Thus, the distribution and compositions of UST-hosted fluid and melt inclusions provide insights into the nature of fluids generated at the magmatic-hydrothermal transition in this system.

The cores of UST quartz and quartz phenocrysts in aplite bands from Saginaw Hill contain abundant brine-rich silicate melt inclusions (BSM) that coexist with hypersaline inclusions (>50 wt% NaCl<sub>eq</sub>) and vapour inclusions. At high temperature (>700 °C) BSM inclusions contain silicate melt, a yellow globular liquid (hydrous salt melt), and vapour in consistent phase proportions. LA-ICP-MS analysis of BSM and hypersaline inclusions showed high concentrations of Cu, Fe, and Zn indicating that these fluids are involved in metal partitioning and transport in this system. In contrast, the rims of UST quartz and quartz phenocrysts in aplite bands contain assemblages of primarily brine and vapour inclusions with variable base melt concentrations (Fig. 1). Data

from this project provides a better understanding of how hydrothermal fluid compositions evolve during the episodic P-T fluctuations which accompany UST formation.

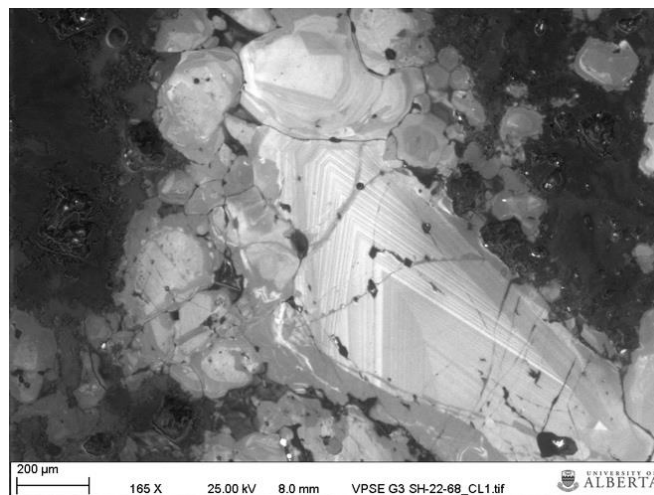


**Fig. 1.** CL image of UST quartz showing hydrothermal (CL-gray) and magmatic quartz (CL-bright, growthzoned)

## References

- Kodera P. et al. (2014) *Geology* 42:495-498.
- London D. (2009) *Can. Min.* 47:697-724.
- Mernagh T.P. and Mavrogenes J. (2019) *Chem. Geol.* 508:210-224.
- Rottier B. et al. (2016) *Chem. Geol.* 447:93-116.

## Fluid inclusions in fluorites from North Hameimet, Tebessa, Algeria

**Bakelli, A.<sup>1,3\*</sup>, Sami, L.<sup>2,3</sup>, Kolli, O.<sup>1,3</sup>, Boutaleb, A.<sup>1,3</sup> & Meddane, S.<sup>1,3</sup>**

<sup>1</sup>University of Sciences and Technology Houari Boumediene (FSTGAT/Geology, Algeria); <sup>2</sup>University of Mouloud Mammeri Tizi Ouzou (Natural Sciences/Geology, Algeria); Laboratoire de Métallogénie et Magmatisme de l'Algérie (FSTGAT/ Geology, Algeria); \*[aboulykdane@gmail.com](mailto:aboulykdane@gmail.com)

The Mineralisation of North Hameimet Massif is 1700 m long and 600 m wide and, oriented in NW-SE. It is located 17 km away from Tebessa city. The sedimentary outcrop of the massif has Triassic and Cretaceous ages and, is characterised by fluorite, barite and galena mineralisation. The Triassic part is consisting of a breccia with dolomite-rich elements, silicified small fragments of eruptive rocks which are carried near to the surface during the ascent of the diapir. Here, two types of mineralisation event can be distinguished:

1) breccia enriched in barite, fluorite and sometimes in galena, its formation is related to the Triassic-cover contact;

2) vein mineralisation outcrops in the eastern part of the massif related to the contact between the Albo-Aptian and the Vraconian.

We have studied primary hydrous fluid inclusions (FI) hosted in fluorite. FIs are two-phase (aqueous liquid + vapour) at room temperature in the non-brownish fluorite. In the brownish fluorite we have additionally recognised primary two-phase (hydrocarbon liquid + vapour, Fig. 1) and three-phase (hydrocarbon liquid + aqueous liquid + vapour) fluid inclusions at room temperature.

Our microthermometry suggested the system H<sub>2</sub>O-NaCl-CaCl<sub>2</sub> for the hydrous FIs. In the same FIs the homogenisation temperatures ranged between 104 and 152 °C, the final ice melting temperatures (T<sub>m</sub>) varied between -26 and -23 °C. The aqueous liquid in the three-phase hydrocarbon inclusions could be characterised by the system H<sub>2</sub>O-NaCl binary. Here the T<sub>m</sub> was determined to be between -21 and -17 °C, which can be corresponded to the salinity from 20 to 25 wt% eq. NaCl (Bodnar, 1993).

We analysed O, C and S stable isotopes in calcite and galena. The collected data show  $\delta^{13}\text{C} = -1 \text{ ‰}$ ;  $\delta^{18}\text{O} = 17 \text{ ‰}$  and  $\delta^{34}\text{S} = \text{from } 2.2 \text{ to } 10 \text{ ‰}$ . These are in good accordance with the results on sulphides and sulphurs (Mesloulou district, Laouar et al., 2016) originated from Triassic sulphates via thermochemical reduction. The residual sulphate was enriched in <sup>34</sup>S, which is reflected in the composition of barite in the residual deposition. The  $\delta^{13}\text{C}$  values of the calcite minerals, indicate an inorganic carbon origin.

Our observations suggest that there was a highly saline and hot (~150 °C) fluid when the crystallisation of fluoride happened. The fluid might undergone a dilution during evolution. The origin of the mineralisation that replaced the limestone and filled the open spaces was hydrothermal. The hydrothermal event might be related to Diapir

movement resulted from different tectonic events, such as in Ouenza, Mesloulou, Essouabaa and Sakièt-Koucha in Tunisia (Sami et al., 2011).

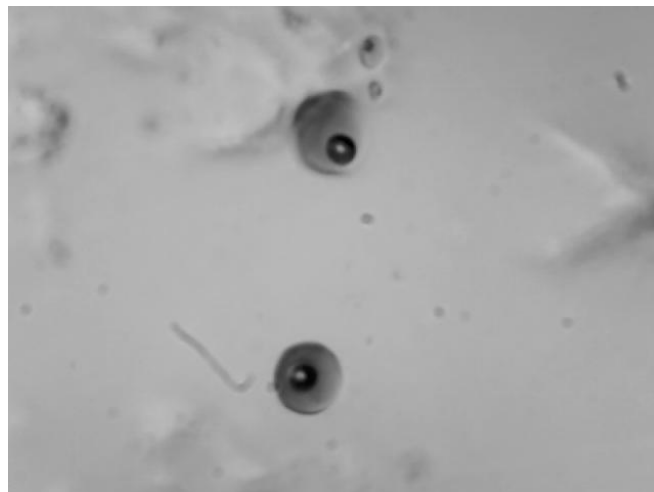


**Fig. 1.** Brownish fluorite-hosted two-phase hydrocarbon inclusions at room-T. North Hameimat, Algeria. Photomicrograph. The fluid inclusions are 60  $\mu\text{m}$  large.

### References

- Bodnar R. J. (1993) *Geochim. Cosmochim. Ac.* 57:683-684.  
Laouar R. et al. (2016) *J. Afr. Earth Sc.* 121:119–135.  
Sami L. (2011) *Thèse Doct. D'Etat, USTHB (FSTGAT), Alger. Algérie.*

# Fluids in granulitic garnetites: high density CH<sub>4</sub> fluids versus H<sub>2</sub>O-CO<sub>2</sub> bearing cordierites, Khabarny Massif (Ural, Russia)

**Bakker, R.J.<sup>1\*</sup> & Puskarev, E.<sup>2</sup>**

<sup>1</sup>Resource Mineralogy, Department of Applied Geosciences and Geophysics, Montanuniversität Leoben, Austria;

<sup>2</sup>Institute of Geology and Geochemistry, Ural Branch, Russian Academy of Sciences, Russia;

\*bakker@unileoben.ac.at

The Khabarny complex is one of the largest ophiolite allochtones along the western part of the Sakmara Zone (Ural, Russia), and consists of mafic-ultramafic rock, such as mantle peridotites (harzburgite, dunite), gabbroic rock (olivine gabbro, gabbro), dolerite dike swarm, plagiogranites, in addition to sedimentary-volcanic sequences. The rocks investigated in the present study are garnetites that form a lens and block-like small bodies among two-pyroxene crystalline schists in the north-eastern part of the Khabarny Massif. These rocks are metamorphosed volcano-sedimentary rock at granulitic facies conditions, and consist mainly of almandine-pyrope-rich garnets, Mg-cordierite, quartz and rutile.

Fluid components are characterised in fluid inclusions in quartz, garnet and in large channel sites of the six-membered ring structure of cordierite. The cordierite structure can attain maximally 1 mole fluid species per formula unit. In terms of mass percentage one mole of H<sub>2</sub>O equals to 2.99 mass%, one mole of CO<sub>2</sub> equals 6.99 mass%, and one mole of N<sub>2</sub> equals 4.57 mass% in a Mg-rich cordierite. The presence of H<sub>2</sub>O, CO<sub>2</sub>, and N<sub>2</sub> at channel sites can be visualised and quantified with Raman spectroscopy.

Garnet, quartz and cordierite in the garnetites contain abundant solid and fluid inclusions. Quartz occurs in larger irregular elongated nodules, with a maximum length of a few mm. Quartz also occurs in clusters of about 10 to 20 isolated euhedral crystals (each with 5 to 20 µm in diameter) in the centre of each garnet grain. Locally, these quartz inclusions reveal re-equilibration textures with numerous irregular channels and cracks (max. 10 µm length) extending from the quartz surface into the garnet. Moreover, some of these quartz inclusions are identified by Raman as cristobalite.

Complex fluid inclusions with small entrapped pyrophyllite and siderite crystals, in addition to a fluid mixture of CH<sub>4</sub> (79 ± 4 mol%) and N<sub>2</sub> (21 ± 4 mol%) are rarely observed within the garnet. These inclusions are smaller than 3 µm in diameter. In quartz, fluid inclusions are monophase at room temperature. Raman spectroscopy reveals the presence of CH<sub>4</sub> (>96 mol%), and locally minor amounts of C<sub>2</sub>H<sub>6</sub>, N<sub>2</sub> and H<sub>2</sub>S. The inclusions occur mainly in trails that are restricted within single quartz grains. Locally, inclusions with similar properties occur in clusters. The fluid inclusions have a regular and equant shape with diameters varying between 1 and 10 µm. A large part of the fluid inclusions contain graphite in

addition to CH<sub>4</sub>. This graphite is deposited on the fluid inclusion walls, causing a dark appearance of the entire inclusion. The inclusions are locally attached to aragonite crystals that also precipitated within the trails. The calculated densities (from microthermometric data) of the inclusions vary between are 0.349 to 0.367 g/cm<sup>3</sup>.

Two types of H<sub>2</sub>O vibration modes are visualised in cordierite: a Raman band at 3598.1 cm<sup>-1</sup> and a relative low shoulder at 3580.5 cm<sup>-1</sup>. CO<sub>2</sub> within the cordierite channels reveals a main Raman band at 1382.2 cm<sup>-1</sup> and a minor band at 1269.9 cm<sup>-1</sup>, corresponding to the Fermi double. The Raman bands of N<sub>2</sub> in cordierite channels can be distinguished from atmospheric N<sub>2</sub>, with centre positions at 2325.5 cm<sup>-1</sup> and 2330.1 cm<sup>-1</sup>, respectively.

The contrast in fluid composition between fluid inclusions and cordierite encourages a discussion about the ability of both environments to preserve its fluid content during the exhumation path of granulites under varying temperature-pressure-redox conditions.

Is the entrapped CH<sub>4</sub>-rich fluid representative of peak metamorphic conditions of the garnetites? Isochore reconstruction of CH<sub>4</sub>-rich fluid inclusions in quartz results in a pressure calculation of 541 to 612 MPa at 800 °C. Garnet-cordierite geothermometric calculations reveal slightly higher pressures of 600 to 700 MPa in the temperature range 750-800 °C. The peak metamorphic redox conditions of the garnetites are assumed to be highly reduced due to the presences of a CH<sub>4</sub>-rich fluid with minor amounts of C<sub>2</sub>H<sub>6</sub>, H<sub>2</sub>S and N<sub>2</sub>. In contrast, the CO<sub>2</sub>-H<sub>2</sub>O-N<sub>2</sub> rich fluid in cordierite represents a relative oxidised environment, with fluid components that are expected to occur in granulite facies rock.

To be continued...

## Proper iso- $T_h$ curves in the H<sub>2</sub>O-NaCl system

**Bakker, R.J.**<sup>1\*</sup>

<sup>1</sup>*Resource Mineralogy, Department of Applied Geosciences and Geophysics, Montanuniversität Leoben, Austria;*  
<sup>\*</sup>*bakker@unileoben.ac.at*

The software *AqSo\_NaCl* (Bakker, 2018) can be used to characterise the properties of phases that may exist in the binary H<sub>2</sub>O-NaCl system up to 1000 °C and 500 MPa. The model replaces all available correlation equations and other equations of state that are restricted to narrow temperature, pressure and composition intervals. Liquid-vapour, liquid-solid, and vapour-solid immiscibility fields emerge with increasing salinity at relative high temperatures, and already occur at mass fractions of a few µg per gram, at salinities that cannot be detected by microthermometry. Properties such as density, molar volume, composition, and volume fraction of liquid, vapour, and solid phases in fluid inclusions can be calculated in heating and freezing experiments. Isochores can be calculated within the homogeneous fluid field (all-liquid or all-vapour), within immiscibility fields (coexisting two-phase fields *LV*, *SL*, and *SV*), and along the *SLV* (solid-liquid-vapour) curve. Iso- $T_h$  lines are obtained by modifying the total volume of the fluid inclusions by taking account of the volumetric properties of quartz. In addition, the software *AqSo\_NaCl* may calculate bulk properties of fluid inclusions directly from microthermometric data.

The isochores within the two-phase fields and along the three-phase curve (further indicated with "sub-isochore") are not isochores in the sense of one homogeneous fluid, but the combination of two or three phases with specific properties and volume fractions that sum up to a constant bulk density and composition. These restrictions can be directly applied to closed-system fluid inclusions at variable temperatures. The isochores and sub-isochores calculated with *AqSo\_NaCl* describe the properties of each individual phase (composition, density, and volume fraction) within fluid inclusions during a heating and freezing experiment.

The interpretation of microthermometric analyses from fluid inclusions that are suspected to contain mainly H<sub>2</sub>O and NaCl was based on the use of highly simplified fluid models also known as "correlation" equations, due to lack of comprehensive algorithms that describe the  $p$ - $T$ - $V$ - $x$  properties of liquids, vapours and solids of the H<sub>2</sub>O-NaCl system over the complete range of conditions of interest. Experimental studies of synthetic fluid inclusions were used to develop simplified models that relate experimental trapping conditions to homogenisation temperatures (e.g. Zhang and Frantz 1987; Bodnar, 1995). These models were used to design the so-called "iso- $T_h$ " lines, i.e. temperature-pressure conditions in the homogeneous fluid field (liquid) that result in the same homogenisation conditions ( $LV \rightarrow L$ ), without

any knowledge about density. These iso- $T_h$  lines are per definition linear, and they are derived from a best-fit to at least two  $p$ - $T$  data points (i.e. homogenisation and experimental conditions). However, these iso- $T_h$  lines may be highly inaccurate at conditions between the two points or at extrapolated conditions. Moreover, the uncertainty of these lines has not been quantified.

The equation of state that describes the variability of the molar volume of quartz (e.g. Hosieni et al., 1985) can be used to calculate the modification of the fluid density in fluid inclusions in quartz with the software *AqSo\_NaCl*. These modified isochores correspond to true iso- $T_h$  lines in fluid inclusion studies, and appear to have highly variable slopes in  $p$ - $T$  diagrams.

True iso- $T_h$  curves are significantly curved in the liquid-solid field (i.e. brine and halite) and in the homogeneous liquid field. Iso- $T_h$  curves are not steeper in the liquid-solid field than in the homogeneous liquid field. The slope of iso- $T_h$  curves in the homogeneous liquid field change significantly at the  $\alpha$ - $\beta$  transition of quartz and may be negative in a small temperature interval close to this transition.

The software *AqSo\_NaCl* can be downloaded from the website of Ronald J. Bakker at the University of Leoben (<http://fluids.unileoben.ac.at>) and from the supplementary data related to the publication in *Computer and Geosciences* (Bakker, 2018).

### References

- Bakker R.J. (2018) *Comp. Geosci.* 115:122-133.
- Bodnar R.J. (1995) *Pure Appl. Chem.* 67:873-880.
- Hosieni et al. (1985) *Am. Mineral.* 70:782-793.
- Zhang and Frantz (1987) *Chem. Geol.* 64:335-350.

## Fluid inclusion study in quartz vein of the Kekura gold deposit, Western Chukchi Peninsula, Russia

**Baksheev, I.A.<sup>1</sup>, Nagornaya, E.V.<sup>2,1\*</sup>, Komarova, M.M.<sup>3</sup>, Khabibullina, Y.N.<sup>1</sup> & Kalko, I.A.<sup>1</sup>**

<sup>1</sup>Faculty of Geology, Lomonosov Moscow State University, Russia; <sup>2</sup>Vernadsky Institute of Geochemistry and Analytical Chemistry of Russian Academy of Sciences, Russia; <sup>3</sup>Institute of Geology of Ore Deposits, Petrography, Mineralogy and Geochemistry RAS (IGEM RAS), Russia; \*chp312@gmail.com

Kekura is the largest gold deposit in the Studukhino gold district located 50 km south away from Bilibino, Western Chukchi Peninsula, Russia. It is spatially related to the shallowly eroded Late Cretaceous granodiorite pluton that intrudes Lower Triassic deformed terrigenous sequence enriched in organic matter. Gold-bearing quartz veins and lenses occur within the pluton and near-contact country rocks. Three types of alteration were recognised at the deposit: propylitic, dolomite-quartz-sericite and argillic. Greenish fine-grained propylite is composed of quartz, oligoclase, actinolite, clinocllore, and carbonate. The most abundant whitish dolomite-quartz-sericite rock is altered and contains relict biotite, K-Na feldspar, oligoclase, newly formed muscovite, dolomite and quartz. This alteration is occasionally cut by veinlets with tourmaline, which in turn are cut by carbonate veinlets. Carbonate pods are found in the altered rock. Relict REE phosphates, apatite, and rutile are accessory minerals. The presence of argillic alteration is marked by illite that replaces muscovite in dolomite-quartz-sericite rock.

Fluid inclusions (FI) were identified in quartz (1) isolated or clustered inclusions in the crystal core; in some samples these inclusions are distributed in the growth zones; and (2) misoriented isolated inclusions or inclusion groups healing fractures crossing several grains. According to the criteria of Roedder (1984), the type 1 and 2 FI were attributed to the primary and secondary, respectively.

Primary fluid inclusions are negative crystal shaped and ranging from 2 to 10  $\mu\text{m}$  and their clusters. Secondary inclusions of 2 to 20  $\mu\text{m}$  in size are more frequent than primary inclusions. Secondary fluid inclusions are divided into two subtypes: (1) contain liquid  $\text{CO}_2$  and (2) liquid  $\text{CO}_2$ -free.

Microthermometric study has been carried out on both primary and secondary fluid inclusions. The studied FI homogenised into liquid at 120–300  $^\circ\text{C}$ ; final ice melting temperature ranges from -7.0 to -1.8  $^\circ\text{C}$ ; fluid salinity varies from 3.1 to 10.5 wt% NaCl equiv. On the basis of eutectic temperature ranging from -35 to -21  $^\circ\text{C}$ , fluid is dominated by Na- and Mg-chlorides. Based on homogenisation temperatures, primary FI could be divided into three groups: 120–180, 220–270, and 300–310  $^\circ\text{C}$ . Homogenisation temperatures of primary FIs observed in a single quartz crystal decrease from 220–230  $^\circ\text{C}$  to 120–140  $^\circ\text{C}$  from the core to the rim.

Vein quartz from the Kekura deposit is frequently cut by later quartz veinlets. The homogenisation

temperatures measured in the later quartz veinlets range in 130–140  $^\circ\text{C}$  and fall into the first group of temperature range.

These observations show that the first temperature range is related to the crystal rims or later thin veinlets. The second range is related to the crystal cores, and the third range is possibly related to the earliest quartz generation.

We have determined homogenisation temperatures of primary FI in quartz vein along an 800 m long bore hole. The homogenisation temperatures range in 125–240  $^\circ\text{C}$  at the surface and in 122–230  $^\circ\text{C}$  at the bottom. These values testify to the absence of vertical temperature zoning at the deposit.

Both the subtype (1) and (2) secondary FIs homogenised into the liquid phase at 140–180  $^\circ\text{C}$  and 220–310  $^\circ\text{C}$ , respectively. Secondary and primary FIs showed similar homogenisation temperatures but different compositions, which indicates a presence of a pulse hydrothermal system for a long time at the Kekura deposit.

### Acknowledgement

This study has been supported by the Russian Foundation for Basic Research (project no. 18-35-20034).

### References

Roedder E. (1984) in: Rev. Mineral. 12:644 p.

## Fluid composition in the deepest part of the IDDP-2 deep borehole in Iceland, based on fluid inclusions

**Bali, E.<sup>1\*</sup>, Aradi, L.E.<sup>2</sup>, Szabó, Á.<sup>2</sup>, Szabó, Cs.<sup>2</sup>, Friðleifsson, G.Ó.<sup>3</sup> & Zierenberg, R.<sup>4</sup>**

<sup>1</sup>Institute of Earth Sciences, University of Iceland, Iceland; <sup>2</sup>Lithosphere Fluid Research Lab, Eötvös Loránd University, Hungary; <sup>3</sup>HS Orka, Iceland; <sup>4</sup>University of California, Davis, USA; \*eniko@hi.is

The main purpose of the Iceland Deep Drilling Project (IDDP) is to explore the possibilities to utilise supercritical fluid in geothermal industry. The second IDDP borehole in Iceland (IDDP-2) was drilled at the Reykjanes geothermal field in 2016-2017. The borehole reached 4659 m depth where the fluid pressure and temperature were measured during drilling to be 34 MPa and 426 °C, respectively (Friðleifsson et al., 2017). Drill cores were recovered at various depths, including the deepest part of the borehole. The core samples at the deepest part show amphibolite facies metamorphism where hornblende is accompanied by ortho- and clinopyroxene as secondary minerals. Felsic veins, composed of quartz, plagioclase and biotite, are also present in the cores at the bottom of the borehole (Friðleifsson et al., *in press*).

Fluid inclusions were studied from the felsic veins of the IDDP-2 drill core samples taken in the depth range of 4634.20 to 4638.00 m. We focused on secondary fluid inclusion assemblages as these are more representative of the current geothermal fluid than the primary ones. We characterised the physical state, temperature and the chemical composition of the geothermal fluid. Vapour-rich and solid-rich brine fluid inclusions as well as silicate melt inclusions were distinguished. The bubble to brine ratio is variable in the fluid inclusions, which indicates the fluid is not a single supercritical fluid but is separated into two phases.

Based on low to high temperature Raman microspectrometric measurements, vapour-rich inclusions are dominated by H<sub>2</sub>O (~97.5 mol%), but also contain CO<sub>2</sub> (~1.5 mol%), H<sub>2</sub>S (0.7 mol%) and traces of H<sub>2</sub> (calculated by the method of Dubessy et al., 1989). These inclusions homogenise into the vapour phase at temperatures between 580 and 600 °C.

Based on optical microscopy, microthermometry, Focused Ion Beam-Scanning Electron Microscopy slice & view combined with Energy Dispersive Spectrometry (FIB-SEM-EDS) and Raman microspectrometry, brine inclusions are composed of four major solid phases, a vapour bubble +/- minor liquid phase. Solid1 and Solid2 are two different Fe-K chloride hydroxides, based on FIB-SEM-EDS. Solid3 is a sylvite-halite solid solution, whereas Solid4 is a Fe-Cu sulphide with molybdenite-like structure (based on their Raman spectra). Additionally, we observed CaCl<sub>2</sub>, Ba-rich chloride and Fe-rich chloride-hydroxide as minor phases in the brine by FIB-SEM-EDS. Upon heating, phase transformations in the brine

inclusions happen within very narrow temperature ranges, typically phase disappearances occur within 20 °C. The last solid phase, the Fe-Cu sulphide, disappears at 600±20 °C, but none of the brine inclusions were completely homogenised below 780 °C due to the accidental entrapment of excess vapour in each analysed inclusion. Based on the composition and the volume proportion of the solid phases within the brine inclusions, we estimate that a brine with up to 29 wt% Fe, 20 wt% K, 6000 ppm Ba and 8000 ppm Cu coexists with a low salinity vapour at ~4600 m depth in the geothermal system of Reykjanes Peninsula.

The disappearance of the Fe-Cu sulphide in the brine inclusions and the disappearance of the liquid film in the vapour-rich inclusions during microthermometric measurements happens at 600±/-20 °C, which is assumed to be representative of the real geothermal fluid temperature. This temperature is higher than the measured T close to the bottom of the bore hole during drilling, after only 6 days heating. However, it is similar to the lower T estimates based on alteration minerals in the drill cores (590-710 °C, Zierenberg et al., *in prep*). As melt inclusions are commonly found in the secondary inclusion assemblage, it is clear that a melt was also percolating in the system after the formation of the felsic veins.

### References

- Dubessy J. et al. (1989) Eur. J. Mineral. 1:517-534.
- Friðleifsson G.Ó. et al. (2017) Sci. Dril. 23:1-12.
- Friðleifsson G.Ó. et al. (in press) J. Volcanol. Geoth. Res.
- Zierenberg R. et al. (in prep)

# Non-equilibrium fluid composition in quartz-hosted fluid inclusions from carbonatites, Murun Mount (Russia)

**Bazarkina, E.F.<sup>1,2\*</sup>, Akinfiev, N.N.<sup>1</sup>, Dubessy, J.<sup>3</sup>, Szabó, Cs.<sup>4</sup>, Aradi, L.E.<sup>4</sup>, Kovalenker, V.A.<sup>1</sup> & Prokofiev, V.Y.<sup>1</sup>**

<sup>1</sup>Institute of Geology of Ore Deposits, Petrography, Mineralogy, and Geochemistry, RAS, Moscow, Russian Federation; <sup>2</sup>Néel Institute CNRS-UGA, France; <sup>3</sup>GeoRessources Laboratory CNRS-UL-CREGU, France; <sup>4</sup>Lithosphere Fluid Research Lab, Eötvös Loránd University, Hungary; \*elena.f.bazarkina@gmail.com

The goal of this study is to estimate the redox properties of igneous paleo-fluids circulating during formation of Murunsky igneous massif (Russia). The fluid inclusions in the magmatic quartz of Sr-Ba carbonatites were analysed by FIB-SEM and confocal Raman spectroscopy methods in Lithosphere Fluid Research Lab (Budapest, Hungary) and GeoRessources (Nancy, France) Laboratories, correspondingly.

Two types of primary fluid inclusions were found: 1) single-phase gas inclusions; and 2) multiphase inclusions represented by multiple anisotropic solid phases, vapour bubble and interstitial aqueous liquid.

The composition of the single-phase inclusions (in mol%) is N<sub>2</sub> 98–92, CH<sub>4</sub> 1–7 and CO<sub>2</sub> 0.5. These inclusions homogenize into the liquid phase between the temperatures of -164.5 and -149.5 °C, which corresponds to density of pure N<sub>2</sub> 0.48–0.64 g/cm<sup>3</sup>. At 610–650 °C the nitrogen pressure inside these inclusions is estimated to be between 2.4 and 5.5 kbar (Prokofiev and Vorobiov, 1991).

Homogenisation temperature of multiphase inclusions was determined in the T-range of 610–650 °C. The gas bubble is dominantly CH<sub>4</sub> with trace amounts of CO<sub>2</sub>. Among solid phases, we identified nahcolite, barite (with some Sr content), siderite, anhydrite, pyrite, sphalerite and calcite. Moreover, two rare phases containing Fe-S and K-Al(S) were detected. One of them was identified as ferrottychite, Na<sub>6</sub>Fe<sup>(II)</sup><sub>2</sub>(SO<sub>4</sub>)(CO<sub>3</sub>)<sub>4</sub>. The other K-Al(S) phase could not be identified. In the aqueous liquid phase, we detected SO<sub>4</sub><sup>2-</sup>, H<sub>2</sub>S/HS<sup>-</sup>, CH<sub>4</sub>, and NH<sub>3</sub> species. The estimated composition with  $mSO_4^{2-} > mH_2S(aq) \sim mCH_{4(aq)} > mCO_{2(aq)}$  was used to estimate the redox properties of the fluid.

Results of our thermodynamic modeling in the system C-S-O-H-Na over the temperature range of 25–500 °C revealed that methane and sulphate cannot coexist under equilibrium (Fig. 1). Our observations may indicate a non-equilibrium interaction between a magmatic fluid, originated from a carbonatite magma, and an organic matter derived from the sedimentary rock, which the carbonatite intruded to. Likely, the observed fluid has been quickly quenched after entrapment, thus retained non-equilibrium compositions up to the present.

We suggest that the observed non-equilibrium nature of the fluid can be responsible for the

formation of unusual minerals in the Murunsky Massif, including the unique charoite.

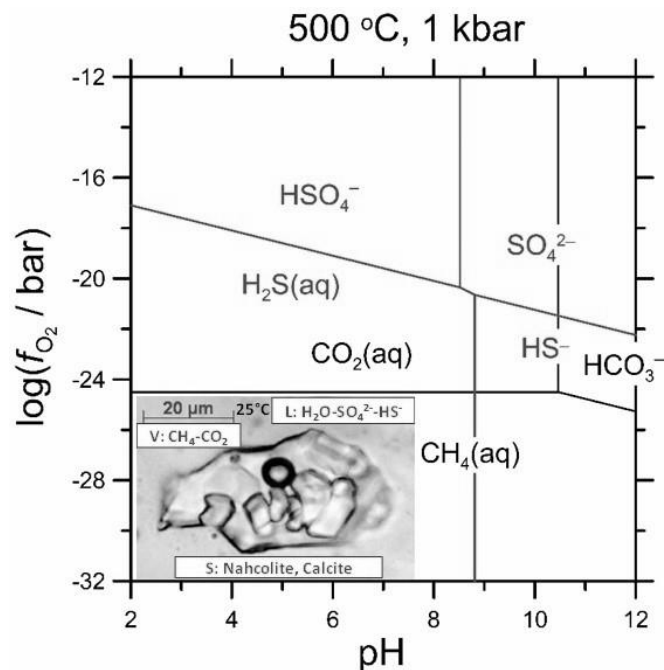


**Fig. 1.**  $\log f_{O_2}$  – pH diagram showing the stability fields of species in the system C-O-H-S at 500 °C and 1 kbar. Fields of SO<sub>4</sub><sup>2-</sup> and CH<sub>4(aq)</sub> do not overlap; however, these species coexist in the fluid inclusions, which indicates a possible non-equilibrium state of the fluid entrapped.

## Acknowledgement

This study was supported by Project ANR 16-CE31-0017 and the Russian Academy of Sciences basic research project 0136-2018-0021.

## References

Prokofiev V. and Vorobiov E. (1991) *Geochem. Int.* 10:1444-1452.

# Extremely alkaline carbonatite melts at Oldoinyo Lengai: a melt inclusion study

**Berkesi, M.<sup>1\*</sup>, Bali, E.<sup>2</sup>, Szabó, Cs.<sup>1</sup> & Guzmics, T.<sup>1</sup>**

<sup>1</sup>Lithosphere Fluid Research Lab, Institute of Geography and Earth Sciences, Eötvös Loránd University, Hungary;

<sup>2</sup>Faculty and Institute of Earth Sciences, University of Iceland, Iceland; \*martaberkesi@caesar.elte.hu

Nephelinite rock from the only active carbonatite volcano, Oldoinyo Lengai (OL), was selected for a detailed melt inclusion study in order to better understand how natrocarbonatites associated to nephelinites form. The fresh natrocarbonatite rocks at OL are dominantly composed of nyerereite and natrite<sub>ss</sub> (natrite solid solution).

The studied rock contains euhedral clinopyroxene (aegirine-augite) and nepheline phenocrysts. In the growth zones of nepheline numerous primary melt inclusions have been found, besides clinopyroxene, titanite and schorlomite crystal inclusions. At room temperature the Raman spectroscopy discovered characteristics of natrite<sub>ss</sub>, based on the main band at 1078 cm<sup>-1</sup>, when focusing the laser in the carbonate melt phase. Microthermometry-combined Raman spectroscopy showed a melting of carbonate at 600-610 °C by the appearance of its meniscus and also by the significant broadening of the main Raman band of natrite<sub>ss</sub>. Further heating results in the appearance of an immiscible nephelinite melt and a carbonate melt (Fig. 1) at around 800 °C. These melts coexisted and trapped heterogeneously during the nepheline crystallisation.

Besides microthermometry, quenching experiments (from 810 °C) of handpicked nepheline grains revealed bubbles in their melt inclusions. These are interpreted to be shrinkage bubbles. Only a few of them contain very low density vapour CO<sub>2</sub>, suggesting almost complete outgassing before melt entrapment.

Raman spectroscopy, SEM-EDS and EPMA analyses on the quenched and subsequently exposed melt inclusions revealed a strongly peralkaline silicate melt composition (peralkalinity index between 3.5 and 7.2) with extremely low H<sub>2</sub>O-content (less than 0.1 wt%). At the same time the carbonate melt shows dominantly a natrite- and rarely a nyerereite-normative compositions with high fluorine-content (9-14 wt%). F plays an important role in maintaining the natrite-normative carbonate melts with 17-29 wt% CaO in the coexistence with the nephelinite melt. The natrite-normative carbonate compositions are proved to be originated from an alkali carbonate fluid, whereas CaO-rich nyerereite-normative compositions are melt-originated (Guzmics et al., 2019).

CaCO<sub>3</sub>/(CaCO<sub>3</sub>+Na<sub>2</sub>CO<sub>3</sub>+K<sub>2</sub>CO<sub>3</sub>) values of the quenched carbonate melts are highly variable and continuous between 0 and 42 and, thus, widely overlapped on the natrite<sub>ss</sub>-nyerereite eutectic (~26). This indicates a mixing of a fluid-, and a melt-

originated carbonate melts, which might be enabled by the outgassing of a CO<sub>2</sub>+H<sub>2</sub>O-dominated vapour. During outgassing, the remaining and immiscible silicate-carbonate melts could be enriched in Na<sub>2</sub>O+K<sub>2</sub>O, contributing to the formation of the strong peralkalinity in the silicate melt.

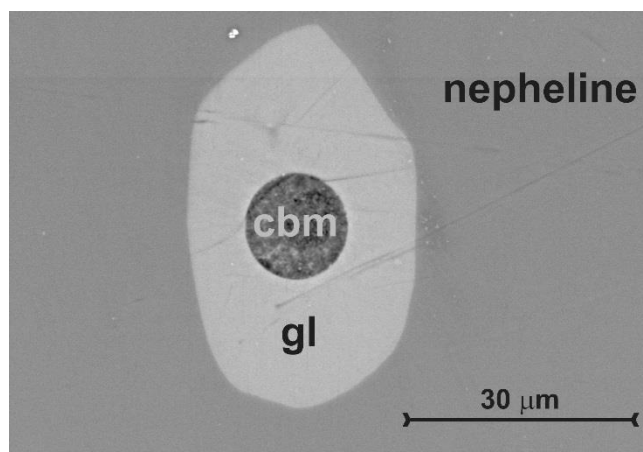


**Fig. 1.** Backscattered electron image of a quenched and exposed, nepheline-hosted primary melt inclusion from Oldoinyo Lengai nephelinite. gl- quenched silicate glass, cbm- quenched carbonate melt

Previous models suggested a peritectic reaction between aegirine-augite and a moderately alkaline carbonatite, which may be responsible for the formation of extremely peralkaline nephelinites at OL (Weidendorfer et al., 2019). In contrast, our samples show the role of outgassed and fluid-derived (natrite-normative) carbonate melts in the formation of natrocarbonatites and strongly peralkaline nephelinites at OL.

## Acknowledgement

This study was supported by the project NKFI K-119535

## References

- Guzmics T. et al. (2019) *Geology* 47:527-530.  
Weidendorfer D. et al. (2019) *Earth. Planet. Sc. Lett.* 510:219-230.

# Fluid inclusion characterisation of Alpine-type quartz tension gashes of Thassos Island (Rhodope massif, Greece)

Bitte, M.<sup>1\*</sup>, Tarantola, A.<sup>1</sup>, Scheffer, C.<sup>1,2</sup>, Voudouris, P.<sup>3</sup> & Valero, M.<sup>1</sup>

<sup>1</sup>GeoRessources lab., Université de Lorraine, France; <sup>2</sup>Département de Géologie et de Génie Géologique, Université Laval, Canada; <sup>3</sup>Department of Geology and Geoenvironment, National and Kapodistrian University of Athens, Greece; \*marie.bitte8@etu.univ-lorraine.fr

Thassos Island is part of the “Southern Rhodope Core Complex” (SRCC), NE Greece. The island is made of three geological units: (i) the lower metamorphic unit is mainly composed of marbles, mica schists and paragneisses; (ii) the intermediate metamorphic unit is made of orthogneisses (metamorphism of Hercynian plutons), paragneisses and mica schists with interbedded marbles; (iii) the upper unit is composed of crystalline rocks (granites and migmatites) and tertiary clastics rocks. The intermediate and lower units are separated by a major detachment fault (Wawrzenitz and Krohe 1998), close to which Alpine-type tension gashes are described (Voudouris et al., 2004).

Regional metamorphism of paragneisses of the intermediate unit is recorded by a kyanite-garnet-biotite-plagioclase-hematite±staurolite±sillimanite paragenesis that indicates *PT* conditions of 7.8-10.4 kbars and 630-710 °C in the amphibolite facies. Structural features indicate ENE-WSW extension regime during the exhumation of the high-*P* units from ductile to brittle conditions. The exhumation, starting during middle Oligocene, is marked by intense mylonitisation of the different metamorphic rocks, boudinage, shallow-dipping and high-angle normal faults, and NNW-trending Alpine-type tension gashes. Post-metamorphic metasomatic reactions lead to the formation of secondary skarn-like mineral assemblages, including gems, suggesting decarbonation reactions during exhumation (Tarantola et al., *subm.*).

The present work shows the properties (*VX*, sources, *PT* conditions of entrapment) of fluid inclusions (FIs) trapped in Tessin-habitus quartz crystals (Maneta and Voudouris, 2010) from Alpine-type fissures obtained by microthermometry, Raman spectroscopy and stable isotope analyses.

Two types of FIs are observed in the euhedral quartz crystals. Type 1 is composed of three-phase CO<sub>2</sub>-H<sub>2</sub>O-N<sub>2</sub>-NaCl isolated primary FIs and pseudosecondary FIs within planes that do not cross-cut the edges of the quartz crystals. Type 2 is represented by secondary two-phase H<sub>2</sub>O-NaCl-N<sub>2</sub> FIs.

FIs of Type 1 are found in assemblages (FIA) homogenising at temperatures close to the critical point of pure CO<sub>2</sub>, but either to LCO<sub>2</sub> or to VCO<sub>2</sub> for a given FIA, indicating pressure fluctuation during fluid entrapment. In both cases, the salinity is always lower than 2.3 wt% NaCl. Bulk

homogenisation to the carbonic phase occurs at comparable temperatures for both types of FIA at 290-340 °C.  $\delta^{13}\text{C}$  of these inclusions is highly positive (up to +8 ‰), underlining the origin of CO<sub>2</sub> by decarbonation reactions. Type 2 inclusions have salinity up to 5.9 wt% NaCl and homogenise at temperatures comprised between 270 and 230 °C.

These data associated with the temperatures derived from the chemical composition of associated chlorite crystals (rose-shaped and late vermicular) reveal a continuous event with vein opening by crack-and-seal mechanism at ductile-brittle to brittle conditions from 360 to 170 °C and at pressures lower than 2 MPa. Carbonic-rich fluids associated with metasomatic reactions are replaced by surficial fluids, certainly issued from evaporated sea-water, in the last period of exhumation.

## References

- Maneta V. and Voudouris P. (2010) Bull. Geol. Soc. Greece 43:685-696.  
Tarantola A. et al. (*subm.*) Minerals  
Voudouris P. et al. (2004) Documenta Naturae 151:23-45.  
Wawrzenitz N. and Krohe A. (1998) Tectonophys. 285:301-33.

## Colloidal gold in epithermal mineralising fluids

**Bozkaya, G.<sup>1\*</sup>, Banks, D.A.<sup>2</sup> & Bozkaya, O.<sup>1</sup>**

<sup>1</sup>Department of Geological Engineering, Pamukkale University; <sup>2</sup>School of Earth and Environment, University of Leeds; \*gbozkaya@pau.edu.tr

The Arapucandere deposit can be considered as an intermediate-sulphidation epithermal deposit hosted by Palaeozoic metamorphic rocks and Permo-Triassic clastic rocks related to collisional and post-collisional tectonic regimes in the Biga Peninsula (NW Turkey). Mineralisation at Arapucandere, a base metal deposit, resulted from episodic lithostatic-hydrostatic pressure variations within fault and fracture systems creating space for mineralisation and providing a mechanism that induced massive ore deposition. Quartz is present as largely pre-ore coarse crystals and syn- to post-ore finer grained crystals. Different episodes of deposition for each type of quartz are evident indicating repeated influx of fluids. Large euhedral quartz crystals grew after the deposition of sulphides. Overgrowths have a fibrous texture that grew perpendicular to the existing crystal faces and facilitated trapping of large, elongate fluid inclusions between the quartz fibers. Episodic periods of trapping of fluid inclusions occurred throughout the growth of quartz. Sulphides (sphalerite, galena and chalcopyrite) cut the coarser grained quartz and also show evidence of multiple periods of deposition. Pyrite is an early phase, occurring within the quartz that is cut by the other sulphides.

Primary fluid inclusions, predominantly L-V, are located in zones where they were trapped in significant numbers in linear arrays originating from pre-existing crystal faces, and are typically between 20 and 100  $\mu\text{m}$  in size. V-rich inclusions are much less common, but may occur with L-V inclusions in these linear trails. V-rich inclusions frequently occur in fractures that appear to be pseudosecondary in origin; inclusion trails originate from the outer surface of quartz crystals, however they may also be of secondary origin. There are also examples of clearly secondary fluid inclusions, as seen in CL images, where trails of inclusions cut the outer face of euhedral crystals and through numerous growth bands.  $T_h$  values are between 270 and 340  $^{\circ}\text{C}$  and the majority of the salinities are low (< 2 wt% NaCl equiv.) but a small number of areas, where the inclusions appear to be secondary, have higher salinities (up to 8 wt% NaCl equiv.)

Although V-rich inclusions can be large (> 30  $\mu\text{m}$ ), the small amount of liquid made determination of bulk salinity impossible. They do exist in inclusion clusters together with what appear to be V-only inclusions and inclusions with variable L/V ratios. Overall, the measured  $T_h$  values of V-rich inclusions (homogenise to vapour) are consistent with the  $T_h$  values of L-V inclusions

(homogenise to liquid). Therefore, in some of the zones homogenisation to both liquid and vapour occurs at similar temperatures, indicating boiling.

Trapped within primary fluid inclusions are numerous particles of gold, the largest observed is approximately 1  $\mu\text{m}$  in size, but most are smaller. Scanning electron microscopy (SEM) element mapping shows these gold particles to contain Au, Ag, Cu + Hg. LA-ICP-MS analysis of fluid inclusions confirms Au and Ag are not present in solution, rather they exist in numerous particles. The concentration of gold in fluid inclusions are orders of magnitude greater than has been previously measured, or thought likely, in crustal fluids. The average Ag and Au concentrations are approximately 32 and 41 ppm, respectively, but maximum concentrations may reach several 100s to 1000s ppm. Au-Ag particles could not have precipitated in the fluid inclusions; therefore, they have precipitated elsewhere and were transported by the hydrothermal fluid.

The suggestion that gold can be transported as colloids has been proposed for some time (Herrington and Wilkinson, 1993; Saunders, 1990) as a means of transporting gold at elevated concentrations greater than is possible in solution. Our observation, for the first time, of sub-micron gold particles being carried in a mineralising fluid, and trapped in fluid inclusions, is consistent with this process. The high concentrations of Au measured indicate that this method of Au transport is potentially more important than dissolved Au.

### References

- Herrington R.J. and Wilkinson J.J. (1993) *Geology* 21:539-542.  
Saunders J.A. (1990) *Geology* 18:757-760.

# Coupled Sr-Nd-Pb isotope and trace element ratios in olivine-hosted melt inclusions from subduction-related magmatism in central Italy

**Bracco Gartner, A.J.J.<sup>1\*</sup>, Nikogosian, I.K.<sup>1</sup>, Luciani, N.<sup>1</sup>, Davies, G.R.<sup>1</sup> & Koornneef, J.M.<sup>1</sup>**

<sup>1</sup>Faculty of Science, Vrije Universiteit Amsterdam, The Netherlands; \*a.j.j.braccogartner@vu.nl

The complex intercontinental collision zone of peninsular Italy is characterised by diverse potassium-rich magmatic products that reflect large temporal and spatial variations in subducted material in the mantle source. Understanding the chemical geodynamics of Italy –a post-collisional subduction setting marked by large sediment input– is key to deciphering both the extent and mechanisms of subduction recycling worldwide. However, primary melt systematics and thereby source characteristics are obscured in bulk lavas by magma mixing/mingling and crustal assimilation at shallow levels. Hence the need for isotope, major and trace element data on melt inclusions (MIs) trapped in high-forsterite olivine, which represent partial melts that have by-passed such secondary modifications, and thus more fully record the geochemical heterogeneity of the mantle source.

Previously the analysis of coupled Sr-Nd-Pb isotope systems in small ( $\varnothing < 300 \mu\text{m}$ ) MIs was hindered by analytical limitations. Recent advances in TIMS technology, i.e. the use of  $10^{13} \Omega$  resistors in the feedback loop of Faraday cup amplifiers (Koornneef et al., 2015), now allow isotope analysis of exceedingly low abundances of Sr (2 ng), Nd (30 pg) and Pb (100 pg).

In contrast to *in situ* techniques, chemical separation of the elements of interest prior to TIMS analysis eliminates matrix effects and interfering isotopes, and thus leads to more accurate and precise data. Although this approach requires dissolution of the MI and host olivine, the latter contains insignificant amounts of Sr, Nd and Pb (De Hoog et al., 2010), meaning its contribution is negligible. Nonetheless, wet chemistry procedures require miniaturised, ultra-low blank techniques to minimise blank contributions (Koornneef et al., 2015). Total procedural blanks for these techniques are typically  $<20 \text{ pg Sr}$ ,  $<1 \text{ pg Nd}$  and  $<10 \text{ pg Pb}$ , but can be corrected for using the elemental abundances of Sr, Nd and Pb determined through isotope dilution by means of single (Sr and Nd) and double spike techniques (Pb; Klaver et al., 2016).

In addition, the residual matrix, collected as eluate during column chemistry, is analysed for trace element ratios by ICP-MS (e.g. Koornneef et al., 2017). Repeat analyses of small, representative aliquots of international rock standards AGV-1 (4–8 ng Sr; 200–400 pg Nd; 250–500 pg Pb;  $n = 6$ ) and JB-2 (17 ng Sr; 600 pg Nd; 500 pg Pb;  $n = 3$ ), corrected for column yields for each element, yield trace element ratios (e.g. La/Sm, Cs/Ba, Sm/Gd) typically reproducible to

within 5–15% 2RSD. Sr-Nd-Pb isotope data for AGV-1 ( $^{87}\text{Sr}/^{86}\text{Sr} = 0.70400 \pm 2$ ;  $^{143}\text{Nd}/^{144}\text{Nd} = 0.51278 \pm 8$ ;  $^{206}\text{Pb}/^{204}\text{Pb} = 18.93 \pm 2$ ;  $^{207}\text{Pb}/^{204}\text{Pb} = 15.65 \pm 2$ ;  $^{208}\text{Pb}/^{204}\text{Pb} = 38.55 \pm 6$ ; 2SD;  $n = 8$ ) and JB-2 ( $^{87}\text{Sr}/^{86}\text{Sr} = 0.703685 \pm 8$ ;  $^{143}\text{Nd}/^{144}\text{Nd} = 0.51307 \pm 8$ ;  $^{206}\text{Pb}/^{204}\text{Pb} = 18.340 \pm 5$ ;  $^{207}\text{Pb}/^{204}\text{Pb} = 15.56 \pm 1$ ;  $^{208}\text{Pb}/^{204}\text{Pb} = 38.27 \pm 4$ ; 2SD;  $n = 3$ ) are in excellent agreement with the GeoReM preferred values (Jochum et al., 2016).

The new combined methods are applied to ~20 homogenised high-potassium (HKS) to melilitite MIs hosted by primitive ( $\text{Fo}_{92-90}$ ) olivines from three key Quaternary volcanic centres (Vulsini, Sabatini and Alban Hills) in the Roman Magmatic Province, central Italy. Most MIs were previously analysed for major and trace elements by EPMA and LA-ICP-MS. Systematic covariations are recorded between proxies for sediment metasomatism such as  $\text{K}_2\text{O}$ , U/Th, U/Nb, Cs/Rb, Be and  $^{87}\text{Sr}/^{86}\text{Sr}$  within the MIs. Whereas  $^{143}\text{Nd}/^{144}\text{Nd}$  show little variation, marked unradiogenic Pb isotope compositions far exceed those reported for regional volcanic rocks.

The primitive melt compositions indicate the involvement of isotopically distinct and trace element-enriched mantle domains below central Italy. We infer that the covariations reflect melt extraction from a small-scale heterogeneous mantle source that was modified by sediment melts derived from the subducted Adriatic slab. These findings will ultimately be used to improve our understanding of subduction recycling and deep mantle element fluxes.

## Acknowledgement

This research is funded by the European Research Council (ERC) under the European Union's Horizon 2020 research and innovation programme under grant agreement No. 759563 (ERC-StG ReVolutions).

## References

- De Hoog J.C.M. et al. (2010) Chem. Geol. 270:196-215.
- Jochum K.P. et al. (2016) Geostand. Geoanal. Res. 40:333-350.
- Klaver M. et al. (2016) J. Anal. At. Spectrom. 31:171-178.
- Koornneef J.M. et al. (2015) Chem. Geol. 397:14-23.
- Koornneef J.M. et al. (2017) Nat. Commun. 8:648.

# Numerical simulation of base metal sulphides in a geothermal system

**Calisto, D.<sup>1</sup>, Moncada, D.<sup>1\*</sup>, Sonnenthal, E.<sup>2</sup> & Chinchilla, D.<sup>3,4</sup>**

<sup>1</sup>Department of Geology, Faculty of Physical and Mathematical Sciences, University of Chile, Chile; <sup>2</sup>Energy Geosciences Division, Lawrence Berkeley National Lab, USA; <sup>3</sup>Department of Crystallography and Mineralogy, Faculty of Geology, Complutense University of Madrid, Spain; <sup>4</sup>Geosciences Institute (IGEO), Spain; \*dmoncada@ing.uchile.cl

We use fluid inclusion data, chemical compositions of base metal sulphides and flow rates to constrain a numerical model to predict thermodynamic and geochemical conditions of a fossil geothermal system, the Patricia Zn-Pb-Ag deposit located in northern Chile. This deposit consists of quartz and base metal sulphides veins of hydrothermal origin with structural control hosted in a volcanic succession (Fig. 1).

Fluid inclusion analysis indicates that the hydrothermal fluids had circulation temperatures that range from 215 to 140 °C, and salinities between 22 to 1 wt% NaCl, with no evidence of boiling in the system (Chinchilla et al., 2016).

Models of fluid-rock interaction were made using the reactive-transport code TOUGHREACT (Xu et al., 2011) to identify relevant geochemical and transport parameters controlling the formation of the fossil geothermal system. The paragenesis of the deposit is mimicked by a model of successive stages consistent with the observed mineral assemblage distribution and fluid inclusion data.

Our model couples fluid flow and mineral precipitation and dissolution under kinetic and mass balance constraints; our results suggest that the precipitation of base metal sulphides is controlled by:

(1) The chemical composition of the ore fluid, acid fluids with low contents of reduced sulphur (<10 ppm) are required to transport ore forming concentrations (~10-25 ppm) of base metals under the temperature ranges of the ore stage.

(2) The presence of reduced sulphur in the epithermal system during the circulation of the ore forming solution, this sulphur is sourced by either a different fluid or previously precipitated sulphides, pyrite, being an important precursor for sphalerite and galena precipitation.

(3) Fluid upflow rate and in minor degree the ore fluid metal content, constrain the time necessary to precipitate all the metal budget of the deposit.

We use conservative values for the system hydrological properties from active geothermal systems, and theoretical models. With a permeability of  $5 \cdot 10^{-13} \text{ m}^2$ , fluid flow rates ~100 kg/sec, and 10,000 years of constant fluid circulation. Although simple our model, achieve a similar alteration and ore mineralogy after this period. The ore stage period deposits the estimated metal budget of the deposit in ~3000 years.

Lastly this mineralisation is controlled by the permeability distribution of the ore system,

sulphides accumulates on the fractured portion of the porous media.

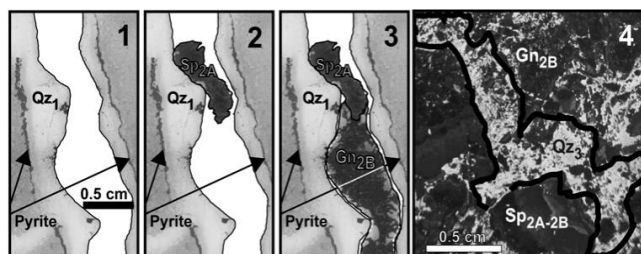


**Fig. 1.** Mineral assemblage of the Patricia base metal ore stage, (1) Pre-ore stage, pyrite+quartz; (2) and (3) Ore stage sphalerite+galena; (3) Post-ore Stage numerical modeling with TOUGHREACT replicates the depositional sequence observed in this vein. Modified from Chinchilla et al. (2016).

## References

Chinchilla D. et al. (2016) Ore Geol. Rev. 73:104-126.  
Xu T. et al. (2011) Comput. Decis. 37:763-774.

## Deep carbon in CAMP and the T-J mass extinction: new perspectives on LIPs through melt inclusions

**Capriolo, M.<sup>1\*</sup>, Marzoli, A.<sup>1</sup>, Aradi, L.E.<sup>2</sup>, Callegaro, S.<sup>3</sup>, Dal Corso, J.<sup>4</sup>, Bartoli, O.<sup>1</sup>, Newton, R.J.<sup>4</sup>, Wignall, P.B.<sup>4</sup>, Mills, B.J.W.<sup>4</sup>, Baker, D.R.<sup>5</sup>, Youbi, N.<sup>6,7</sup>, Spiess, R.<sup>1</sup> & Szabó, Cs.<sup>2</sup>**

<sup>1</sup>Department of Geosciences, University of Padova, Italy; <sup>2</sup>LRG, Institute of Geography and Earth Sciences, Eötvös Loránd University, Hungary; <sup>3</sup>CEED, University of Oslo, Norway; <sup>4</sup>SEE, University of Leeds, UK; <sup>5</sup>Department of Earth and Planetary Sciences, McGill University, Canada; <sup>6</sup>Department of Geology, Faculty of Sciences-Semlalia, Cadi Ayyad University, Morocco; <sup>7</sup>IDL, University of Lisbon, Portugal; \*manfredo.capriolo@phd.unipd.it

A multidisciplinary and innovative study on melt inclusions (MIs) has been carried out on basaltic rocks from the Central Atlantic Magmatic Province (CAMP; Marzoli et al., 1999), in order to investigate the volatile C species degassed during the emplacement of this Large Igneous Province (LIP). LIPs are closely related to mass extinction events, as their magmatic activity can trigger climatic changes implying catastrophic consequences. The CAMP (ca. 201 Ma) is one of Earth's largest LIPs and is synchronous with the end-Triassic mass extinction, which is one of the most severe biotic crises during the Phanerozoic (Davies et al., 2017). The Triassic-Jurassic boundary corresponds to a hyperthermal event due to a fourfold increase of atmospheric CO<sub>2</sub> (McElwain et al., 1999), and the CAMP magmatic activity is identified as the potential trigger mechanism (Wignall, 2001). Moreover, the sedimentary record displays multiple negative C isotope excursions (Hesselbo et al., 2002), testifying to an important disruption of the global C cycle at the end-Triassic.

We combined optical microscopy, confocal Raman microspectroscopy, SEM-EDS and EMP to study the C compounds (mainly CO<sub>2</sub>, rarely replaced by elemental C) in gas exsolution bubbles within MIs. These represent a direct proxy of volatiles degassed into the ocean-atmosphere system during the magmatic activity. The MIs containing the studied CO<sub>2</sub>-bearing bubbles are hosted in clinopyroxene (augitic composition) crystal clots.

This work shows that CAMP basaltic melts rose from the mantle towards the Earth surface through a mush reservoir, in which crystals, melt and exsolved fluids interacted. The CO<sub>2</sub> exsolved into bubbles within the melt during its ascent from lower to intermediate crust depths. The bubble-bearing melt was occasionally entrapped in interstices between growing crystals, forming MIs. The confining host mineral phase prevented significant post-entrapment phenomena from influencing the MIs during magma ascent and cooling. However, post-entrapment crystallisation (PEC) processes often occurred, and the entrapped melt partially crystallised the host crystal (on MI rims) and other mineral phases, leading to a differentiation of the residual melt (generally andesitic composition) within the MIs. The fO<sub>2</sub> decrease, likely due to the

crystallisation of oxides in some MIs, rarely caused the reduction of CO<sub>2</sub> into elemental C within bubbles. Moreover, in bubble-free MIs the differential shrinkage between the melt and the host mineral phase may have caused the nucleation of empty bubbles.

The C involved in this process, mainly in the form of CO<sub>2</sub>, was mostly degassed during the emplacement of CAMP. Nevertheless, the fraction entrapped in MIs allows us to understand the processes that brought C from the lithosphere into the hydrosphere-atmosphere system. Considering the inferred pressures of MIs formation, the entrapped C may be derived from the mantle and/or be inherited from C-rich crustal material. This demonstrates that at least part of the total amount of the degassed C has a mantle and/or metasedimentary origin, at lower or intermediate crustal depth. Hence, the C degassed as volcanic CO<sub>2</sub> was not totally derived from assimilation of organic-rich sediments at shallow depth.

### References

- Davies J.H.F.L. et al. (2017) Nat. Commun. 8:15596.  
Hesselbo S.P. et al. (2002) Geology 30:251-254.  
Marzoli A. et al. (1999) Science 284:616-618.  
McElwain J.C. et al. (1999) Science 285:1386-1390.  
Wignall P.B. (2001) Earth-Sci. Rev. 53:1-33.

# Melt inclusion constraints on the plumbing architecture of the Bárðarbunga-Veiðivötn volcanic system, Iceland

Caracciolo, A.<sup>1,2\*</sup>, Bali, E.<sup>1,2</sup>, Guðfinnsson, G.H.<sup>1</sup>, Kahl, M.<sup>1</sup> & Halldórsson, S.A.<sup>1</sup>

<sup>1</sup>NordVulk, Institute of Earth Sciences, Iceland; <sup>2</sup>Institute of Earth Sciences, University of Iceland, Iceland; \*alc10@hi.is

Magmas in Iceland commonly carry disaggregated crystal mush fragments that can be used to study the architecture of their volcanic plumbing systems. Here, we have studied four well-characterised, mush fragment-bearing units from the Bárðarbunga-Veiðivötn magmatic system in order to resolve the temporal evolution of magma storage reservoirs within this most extensive volcanic system of Iceland. Studied units are: Ljósufjöll (pillow lava, subglacial), Brandur, Fontur and Saxi (tephra cones, early-Holocene), Þjórsárdalshraun and Drekahraun (middle-Holocene lava flows) and Veiðivötn eruption (fresh scoria, ~1477 AD). This sample set allowed us to investigate the plumbing system evolution from a glacial stage to the present time.

Glassy melt inclusions (MIs) (Fig. 1) from all units, corrected for post entrapment processes, cluster at Mg#58-68 (MgO up to 10.05 wt%) without any significant temporal variation. Macrocryts found in the old units preserve a tight and primitive compositional range that is skewed towards more evolved compositions as the samples become younger.

Several thermobarometres have been applied to clinopyroxene, groundmass glasses and melt inclusions to constrain magma storage conditions and their variation with time. Cpx-melt barometry (Neave and Putirka, 2017) and OPAM barometry (Yang et al. 1996) on groundmass glasses record similar pressures of  $2.2 \pm 0.7$  kbar ( $7.8 \pm 2.5$  km) and  $1.9 \pm 0.8$  kbar ( $6.8 \pm 2.8$  km), respectively.

OPAM barometry reveals that olivine and plagioclase-hosted MIs from all studied units outline a reservoir located in the mid-crust crust between 7-11 km. This coincides/overlaps with the last equilibration of the crystal cargo with the carrier melts in all units. In addition, old units contain a primitive crystal cargo (Fo/An >86.5) that originates from the lower crust ( $4.7 \pm 1$  kbar), revealing the occurrence of an additional magma storage zone located at around  $16.8 \pm 3.6$  km depth. Our results suggest that, in the older units, magma(s) from deep reservoir(s) have erupted without complete mixing and re-equilibration in the shallow reservoir (7-11 km depth). On the other hand, we can rule out the involvement of a deep reservoir(s) as a direct source for lavas during the time covered by the recent units.

At the end of the Weichselian glaciation, magma eruption rates were up to 20-30 times higher than the present-day production (Sigvaldason et al., 1992). This effect has been connected to the glacial unloading having increased the melting rate

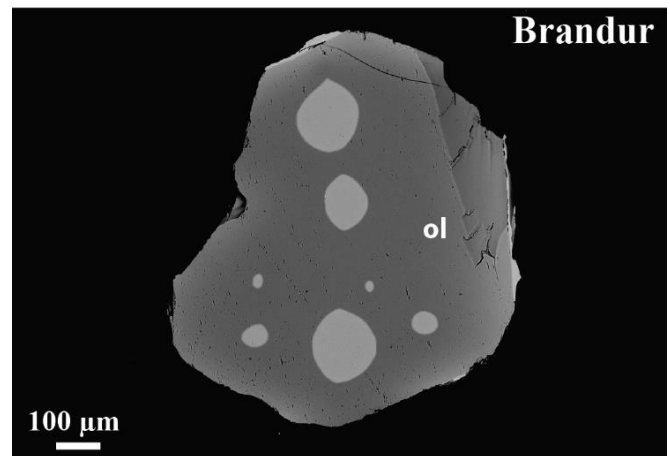


**Fig. 1.** Typical melt inclusions as seen in BSE image. Glassy MIs hosted in an olivine crystal from the Brandur tephra cone.

in the upper mantle (Jull and McKenzie, 1996). Most likely, this process, coupled with the bending of the crust above the reservoirs (Gudmundsson, 1986), allowed magma from deep regions to erupt.

In contrast, the absence of a petrological signature of the deep reservoir(s) in the recent units could be linked to steady-state magma production rates, with the shallower reservoir(s) dominating the plumbing architecture, so that magmas from deep regions are well mixed at relatively shallow depths before eruptions, as is the case at the present.

## References

- Gudmundsson A. (1986) *J. Geophys. Res.* 91:12711-12721.
- Jull M. and McKenzie D. (1996) *J. Geophys. Res.* 101:21815-21828.
- Neave D.A. and Putirka K.D. (2017) *Am. Mineral.* 102:777-794.
- Sigvaldason G.E. et al. (1992) *B. Volcanol.* 54:385-392.
- Yang H.J. et al. (1996) *Contrib. Mineral. Petr.* 124:1-18.

# Effect of petroleum charge on diagenesis of reservoir: evidence from synthesised fluid inclusions

Chen, Y.<sup>1\*</sup>, Ge, Y.J.<sup>2</sup>, Zhou, Y.Q.<sup>1</sup> & Zhou, Z.Z.<sup>3</sup>

<sup>1</sup>School of Geosciences, China University of Petroleum, China; <sup>2</sup>Research Institute of Yanchang Petroleum (GROUP) Co. Ltd., China ; <sup>3</sup>College of Geological Science and Engineering, Shandong University of Science and Technology, China; \*yongchenzy@upc.edu.cn

Formation of fluid inclusions (FI) is a common process during diagenesis and migration of hydrocarbons in sedimentary basins. They can be used to track the migration pathways of oil and gas, determine the temperature and pressure of diagenesis, assess the time and stages of oil accumulation. Moreover, investigation of FIs contributes to the setout of ancient interface between water and oil by GOI (Grains containing Oil Inclusions), identification the origin of petroleum using biomarkers and evaluation exploration potential. But, there are still some arguments about the records of fluid inclusions in hydrocarbon-bearing reservoirs.

In order to understand the effect of oil accumulation on the formation of fluid inclusions together with the diagenesis in reservoir rocks, we synthesised hydrocarbon-bearing and aqueous FIs in calcite under natural reservoir conditions using different oil-water volume ratios. Fluid inclusions were synthesised according to the method of Sterner and Bodnar (1984) with some modifications. In our study we followed experimental procedures described by Chen et al. (2016).

In our synthetic calcite crystals, fluid inclusions were selected under UV microscopy for further microthermometry. The results show that fluid inclusions can be formed at 150 °C and 40 MPa with the oil-water ratio from 30% to 100%. The number of hydrocarbon-bearing inclusions increases with volume ratio of oil to water, but decreases after the oil volume content beyond 70% (Fig. 1). However, the oil-water ratio had a little effect on the homogenisation temperature of hydrocarbon and aqueous inclusions. Based on

the observations under optical microscope, it indicates that the growth of calcite was affected by charge of oil because the healing of fractures became imperfect with increasing of oil-water ratio. The synthesised hydrocarbon inclusions in crude oil system (contain 0.4 % water), implies that diagenesis (or growth of calcite) was not completely stopped even when the reservoir is saturated with oil.

As the hydrocarbon-bearing inclusions were formed at any ratio of oil to water in calcite, it means that the whole history of oil accumulation can be recorded by fluid inclusions. The experimental evidence confirmed that diagenesis of reservoir would be weakened during the charge of petroleum.

## Acknowledgement

The research was co-funded by the National Natural Science Foundation of China (Grant No. U1762108 and 41873070).

## References

Sterner S.M. and Bodnar R.J. (1984) *Geochim. Cosmochim. Ac.* 48:2659-2668.  
Chen Y. et al. (2016) *Mar. Petrol. Geol.* 76:88-97.

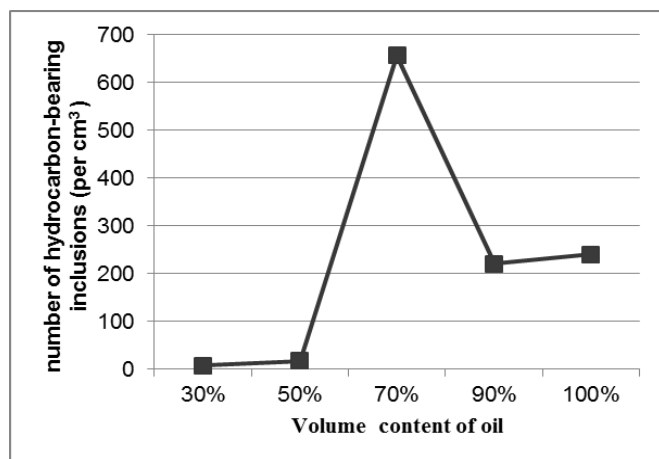


Fig. 1. Number of hydrocarbon inclusions formed in one cm<sup>3</sup> synthetic calcite versus oil-water vol%.

# Acquisition of equations of state of aqueous solutions by using hydrothermal diamond-anvil cell, fused silica capillary optical cell and Raman spectroscopy

**Chou, I-M.<sup>1\*</sup>**

<sup>1</sup>CAS Key Laboratory for Experimental Study under Deep-sea Extreme Conditions, Institute of Deep-sea Science and Engineering, Chinese Academy of Sciences, China; \*imchou@idsse.ac.cn

Even though aqueous solutions are essential agents involved in many geological processes, our knowledge of their volumetric properties is inadequate when applied to natural or experimental systems. For improvement, an experimental protocol has been established for the acquisition of the equations of state (EOS's) of aqueous solutions containing salt(s) at elevated pressure (P)-temperature (T) conditions. This protocol is similar to that used previously by Shen et al. (1993) during the early development stage of the hydrothermal diamond-anvil cell (HDAC), but with significant improvements. In their experiments, a doubly polished quartz chip and H<sub>2</sub>O were loaded in the sample chamber of HDAC and the  $\alpha$ - $\beta$  quartz phase transition temperatures ( $T_{tr}$ 's) were measured at 0.1 MPa and along five isochores of H<sub>2</sub>O during the phase transitions, which were detected by using the interferometric method. For each measured  $T_{tr}$ , the  $\alpha$ - $\beta$  quartz phase transition P ( $P_{tr}$ ) was then calculated based on the P-T equation reported by Mirwald and Massonne (1980). The sample was then cooled to nucleate vapour bubble(s) and the liquid-vapour homogenisation temperature ( $T_h$ ) was determined, which defined the bulk density of H<sub>2</sub>O and homogenisation P ( $P_h$ ), based on the EOS of H<sub>2</sub>O. The line connecting ( $P_h$ ,  $T_h$ ) and ( $P_{tr}$ ,  $T_{tr}$ ) two points defined the isochore of H<sub>2</sub>O for that particular density. They concluded that the EOS of H<sub>2</sub>O reported by Haar et al. (1984) is the most accurate one.

The newly established protocol has three improvements: (1) the newly modified HDAC (HDAC-VT; Li et al., 2016) provides a perfect seal of the sample solution under minimal compression of the diamond anvil faces against the metal gasket, and therefore closely maintains the isochoric property of the sample during cooling cycle of the experiment; (2) the use of a new Raman spectroscopic criterion for the detection of  $T_{tr}$ . When compared with the commonly used  $\alpha$ -quartz Raman band near 465 cm<sup>-1</sup> (defined at 24 °C and 0.1 MPa), the one near 128 cm<sup>-1</sup> is much more sensitive for  $T_{tr}$  detection; and (3) the use of fused silica capillary optical cell (Chou et al., 2005; Applegarth et al., 2015) for accurate vapour pressure measurements of aqueous solutions, which define  $P_h$  at each measured  $T_h$ .

The  $T_{tr}$ 's during heating cycle at 0.1 MPa and also along 18 H<sub>2</sub>O isochores (densities between 0.622 and 0.907 g/cm<sup>3</sup>) in HDAC were determined based on the improved Raman spectroscopic criterion (Chou and Li, 2017). The  $P_{tr}$  at each measured  $T_{tr}$

was calculated based on three different models of EOS of H<sub>2</sub>O: Haar et al. (1984), Wagner and Pruß (2002), and Zhang and Duan (2005). The three thus obtained  $\alpha$ - $\beta$  quartz phase boundaries, each of which was defined by 19 evaluated  $P_{tr}$ - $T_{tr}$  data points, were then evaluated by comparing them with available experimental data. The best one, formulated by Wagner and Pruß (2002), was chosen to define this quartz pressure calibrant, which will be used in future HDAC experiments to determine  $P_{tr}$  at each measured  $T_{tr}$ . To obtain isochores of geologically important aqueous fluids containing salt(s),  $P_h$  value at each measured  $T_h$  is needed, and these data are currently being collected by using fused silica capillary optical cell (Chou et al., 2005; Applegarth et al., 2015). The composition of the sample solution will be verified by the melting point of ice measured after the determination of isochore(s) at elevated P-T conditions. This experimental protocol is now well established for the acquisition of EOS's of geologically important aqueous solutions at elevated P-T conditions.

## Acknowledgement

I thank W.A. Bassett, J.K. Li and S.H. Li for their inputs and discussions, and the Key Frontier Science Program (QYZDY-SSW-DQC008) of CAS for financial support.

## References

- Applegarth L.M. et al. (2015) Appl. Spectrosc. 69:972-983.
- Chou I-M. et al. (2005) in: Advances in High-Pressure Technology for Geophysical Applications. 475-485.
- Chou I-M. and Li S.H. (2017) JpGU-AGU Joint Meeting, at Makuhari Messe, Chiba, Japan.
- Haar L. et al. (1984) NBS/NRC Steam Tables.
- Li J.K. et al. (2016) Rev. Sci. Instrum. 87:053108-1-9.
- Mirwald P.W. and Massonne H.J. (1980) J. Geophys. Res-Sol. Ea. 85:6983-6990.
- Shen A.H. et al. (1993) Am. Mineral. 78:694-698.
- Wagner W. and Pruß A. (2002) J. Phys. Chem. Ref. Data 31:387-535.
- Zhang Z.G. and Duan Z.H. (2005) Phys. Earth Planet. In. 149:335-354.

# Climate variations during the Messinian: evidence from fluid inclusion studies of Selenite deposits from Calabria, Southern Italy

Cipriani, M.<sup>1\*</sup>, Costanzo, A.<sup>2</sup>, Feely, M.<sup>2</sup> & Dominici, R.<sup>1</sup>

<sup>1</sup>Department of Biology, Ecology and Earth Science, University of Calabria, Italy; <sup>2</sup>Earth and Ocean Science, School of Natural Sciences, National University of Ireland Galway, Ireland; \*mara.cipriani@unical.it

Petrographic and fluid inclusion (FI) studies are used to investigate the formation of Miocene twinned selenite crystals (Primary Upper Gypsum) (Cianflone et al., 2012) from the Catanzaro Trough (Calabria, Southern Italy). These crystals were formed during the Messinian salinity crisis (MSC) (about 6 Ma) during a period of approx. 600.000 years. This is the only primary selenite deposit in Calabria. Petrographic studies of the selenite crystals reveal the presence of alternating growth intervals, *i.e.* *cloudy* (FIs rich) and *clear* intervals (FIs poor). The presence of these intervals, at both macro- and micro-scale, is significant because these stratigraphic occurrences have not been observed to date in similar Italian MSC evaporitic deposits. Primary FIs observed are Type 1 monophasic (L) aqueous, Type 2 aqueous two-phase liquid-rich (L>V) and Type 3 multiphase solid (L±V+S). Microthermometric analyses revealed temperature of last melting ( $T_{LM}$ ) between -7.7 °C and -0.1 °C corresponding to a salinity range between 0.18 and 11.34 eq. wt% NaCl (Costanzo et al., 2019). These results are similar to salinities reported for other Messinian basins and indicate that the selenite precipitated from brines with a significant proportion of non-marine waters (Natalicchio et al., 2014).

A well-preserved outcrop (1.70 m in high) with eight cycles of selenite bedding, was selected in order to investigate intra- and inter- salinity variations in crystals from each deposition cycle (Fig. 1). Microthermometric results reveal variations in the salinity range throughout the cycles, *i.e.* salinity increases from the first to the third cycle (from ~0.7 to ~3.9 eq. wt% NaCl), decreases in the fourth cycle (~2.1 eq. wt% NaCl), increases again in the fifth (~3.5 eq. wt% NaCl), decreases in the sixth (from ~2.5 eq. wt% NaCl) and finally increases in the seventh and eighth cycle (from ~2.6 to ~2.9 eq. wt% NaCl) (Fig. 1).

The observed variations in salinity between cloudy and clear intervals in the crystals within each of the eight cycles may reflect the alternation between arid and humid conditions (daily or seasonal) that may have been controlled by precessional orbital forcing (Reghizzi et al., 2018).

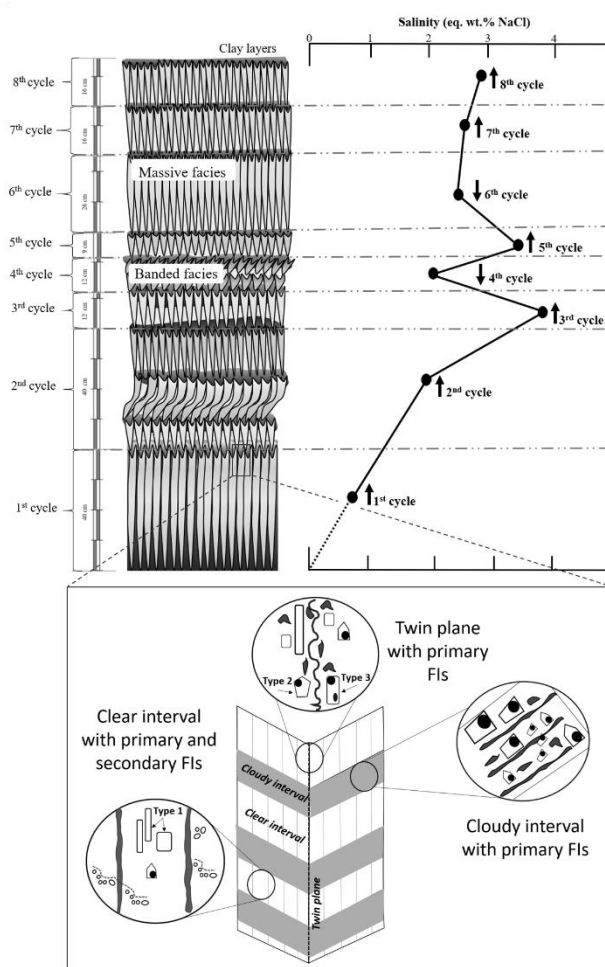


**Fig. 1.** Stratigraphic column of the massive selenite deposit with a single crystal (red square) showing FIs distribution in cloudy and clear intervals. Banded facies (BF) are observed in the 4<sup>th</sup> and 5<sup>th</sup> cycles. Average salinity values reflecting the fluctuations in salinity from the 1<sup>st</sup> cycle through to the 8<sup>th</sup> cycle are shown on the right-hand side of the column.

## References

- Cianflone et al. (2012) Rendiconti Online Soc. Geol. It. 21:71-73.
- Costanzo et al. (2019) Carbonate. Evaporite. (in press).
- Natalicchio et al. (2014) Geology 42:179-182.
- Reghizzi et al. (2018) Paleoclimatology Palaeocl. 33:716-731.

## The 8.2 k.y. event recorded in speleothem from Central Europe: unusual stable isotope composition of fluid inclusions

**Czuppon, Gy.<sup>1\*</sup>, Demény, A.<sup>1</sup>, Leél-Őssy, Sz.<sup>2</sup>, Óvári, M.<sup>3</sup>, Lin, K.<sup>4</sup>, Molnár, M.<sup>5</sup>, Siklósy, Z.<sup>1</sup>, Baykara, O.<sup>4</sup> & Shen, C-C.<sup>4</sup>**

<sup>1</sup>Institute for Geological and Geochemical Research, HAS, RCAES, Hungary; <sup>2</sup>Department of Physical and Applied Geology, Eötvös Loránd University, Hungary; <sup>3</sup>Institute for Danube Research, HAS, Hungary; <sup>4</sup>High-Precision Mass Spectrometry and Environment Change Laboratory (HISPEC), Department of Geosciences, National NTU, Taiwan, <sup>5</sup>Institute for Nuclear Research, HAS, Hungary; \*czuppon.gyorgy@csfk.mta.hu

During the Holocene several short term climate anomalies occurred, among which the 8.2 k.y. event was the most pronounced. Several proxy records spreading from the North Atlantic to monsoonal regions indicate this event suggesting its semi-global impact, at least (mostly cooling). Large amount of freshwater release into the North Atlantic has been invoked as a main cause of the slowdown of the oceanic thermohaline circulation, resulted in temperature drop in West and North Europe (von Grafenstein et al., 1998; Barber et al., 1999).

Here we present new isotopic data of calcite and inclusion hosted water of stalagmite from Central Europe (Béke Cave, NE Hungary), covering the time interval from 10500 to 4500 yr. BP. The carbon and oxygen isotopic composition of the stalagmite calcite recorded the 8.2 k.y. event by elevated  $\delta^{18}\text{O}$  and  $\delta^{13}\text{C}$  values between 8000 and 8400 yr. BP.

Beside the C and O isotope compositions of the speleothem calcite, we determined the hydrogen and oxygen isotopic composition of the inclusion water using vacuum crushing and cavity ring-down spectroscopy. The relatively high water content allowed us to achieve ~5 mm sampling (and ~50 yr. timing) resolution. Both hydrogen and oxygen isotopic composition of inclusion water shows positive excursions around 8.2 kyr where the host calcite yielded elevated oxygen isotope compositions.

The observed positive anomalies in O isotopic composition in both the host calcite and its fluid inclusion water is in contrast to other western European speleothems, which recorded this cooling event by marked decreasing of  $\delta^{18}\text{O}$  values of the calcite. The different response to this event in the Carpathian Basin might be caused by 1) decrease of the amount of winter precipitation and summer temperatures, resulting in relatively higher infiltration of summer precipitation, leading to enhanced annual isotopic composition; or 2) increased influence of air masses originated from above the Mediterranean delivering precipitation with enhanced  $\delta^{18}\text{O}$  values (i.e. relative lower proportion of Atlantic air characterised by lower  $\delta^{18}\text{O}$ ).

Relatively drier and cooler conditions have been inferred from other paleoclimate archives in Europe for the 8.2 k.y. event. The dataset presented in this paper would be in agreement with these

observations, if the relative amount of winter precipitation decreased along with temperature drop resulting in lower evaporation rate during the warm seasons. This would increase the relative contribution of warm season precipitation – and elevated  $\delta\text{D}$  and  $\delta^{18}\text{O}$  values – in the dripwater from which the stalagmite was formed. The trace element composition supports this later explanation rather than moisture source changes.

### Acknowledgement

We express our thanks for the financial support of the National Research, Development and Innovation Office (project No. OTKA NK 101664, PD 121387). György Czuppon also thanks the János Bolyai Research Scholarship of the Hungarian Academy of Sciences for their support. This research was also supported by the European Union and the State of Hungary, co-financed by the European Regional Development Fund in project GINOP-2.3.2.-15-2016-00009 'ICER'.

### References

von Grafenstein et al. (1998) *Clim. Dynam.* 14:73-81.  
Barber et al. (1999) *Nature* 400:344-348.

## Fluid inclusion study of the Eastern Sayan orogenic gold deposits

**Damdinov, B.B.<sup>1\*</sup> & Damdinova, L.B.<sup>1</sup>**

<sup>1</sup>Geological Institute SB RAS, Buryat State University, Russia; \*damdinov@mail.ru

Eastern Sayan orogenic gold deposits are presented by gold-quartz and gold-sulphide-quartz types, which localised in the shear-zones, melanges and fracture zones. The largest gold-sulphide-quartz deposits are spatially associated with ophiolitic belts in the margin of the Archean foundation of Tuva-Mongolian microcontinent, whereas gold-quartz type deposits are hosted directly by Archean gneisses. Ore bodies of these deposits are presented by quartz veins and quartz-sulphide mineralised zones. The main ore minerals of both types of deposits are analogous: pyrite, galena, sphalerite, chalcopyrite, sphalerite, native gold. Accordingly, in the chemical composition of ores Fe, Pb, Zn, Cu, Au, Ag are predominated. Gold-quartz deposits are distinguished only by lower concentrations of these elements. Spatially associated with orogenic gold deposits, pyrrhotite ores represent metamorphosed analogs of the ancient “black-smoker” sulphide ores (VMS type deposit). These ores are classified as gold-pyrrhotite type.

The sulphur isotopic compositions of the gold-sulphide-quartz, gold-quartz and gold-pyrrhotite type ores are similar. Values vary from 0 to +6‰ corresponding to the isotope composition of the modern “black smokers” (Seal, 2006). The calculated oxygen isotopic composition of the equilibrium fluid correspond to a metamorphic fluid.

Fluid inclusions (FI) study of the ore-bearing quartz allowed us to estimate the P–T conditions of the orogenic gold formation. The highest homogenisation temperature (450 – 550° C) has been shown by the gold-pyrrhotite ores. FI trapped the two-phase fluid heterogeneously, which is indicated by the coexistence of gas and gas-liquid FIs. At 300-400 °C, gold-polysulphide deposits were formed. The formation of gold – quartz deposit occurred at the temperatures of 200-350 °C. The average pressure values for the mineral formation in all studied deposits were 360–430 bar. The compositions of the solutions in all studied types of deposit are the same and correspond to the systems FeCl<sub>2</sub>-FeCl<sub>3</sub>-MgCl<sub>2</sub>-NaCl-H<sub>2</sub>O (Fig. 1).

FIs entrapped at high temperature from pyrrhotite ores contain highly concentrated brines with a salinity up to 33 wt% eq. NaCl, whereas the salinity in the FIs from the gold-sulphide-quartz and gold-quartz types is varying in the range of 5–15 wt% eq. NaCl.

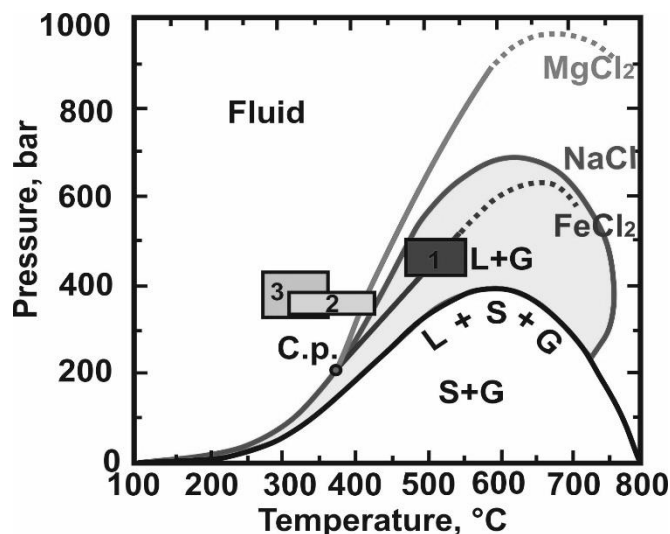


**Fig. 1.** P-T projections from the systems NaCl-H<sub>2</sub>O, MgCl<sub>2</sub>-H<sub>2</sub>O and FeCl<sub>2</sub>-H<sub>2</sub>O (Steele-MacInnis et al., 2015) indicating the trapping conditions of FIs from various deposit types studied. 1 – gold-pyrrhotite, 2 – gold-sulphide-quartz, 3 – gold-quartz. C.p. – H<sub>2</sub>O critical point, L – liquid, S – solid, G – gas.

The results of complex geological, structural, mineralogical, geochemical and fluid inclusion studies of the Eastern Sayan orogenic gold deposits allow to conclude that the formation of gold-sulphide-quartz ores occurs due to ore-forming components migration into the water fluids from primary “black smoker” sulphide ores (submarine metalliferous deposits) during its metamorphic transformations. Further migration of these fluids leads to the gold-quartz deposit appearance.

### Acknowledgement

Study is supported by RFBR, project №18-05-00489a

### References

- Seal R. R. (2006) Rev. Mineral. Geochem. 61:633-677.
- Steele-MacInnis M. et al. (2015) Geochim. Cosmochim. Ac. 148:50-61.

# Formation conditions and metal content of fluid inclusions from Pervomaiskoe molybdenum ore deposit (Dzhida ore field, South-Western Transbaikalia)

**Damdinova, L.<sup>1\*</sup>, Damdinov, B.<sup>1</sup> & Bryansky, N.<sup>2</sup>**

<sup>1</sup>Geological Institute SB RAS, Russian Federation; <sup>1</sup>Buryat State University; <sup>2</sup>Institute of Geochemistry. A.P. Vinogradov SB RAS, Russian Federation; \*ludamdinova@mail.ru

Our knowledge on the formation of the W-Mo (Be) stockwork deposits is currently incomplete. This is especially true for data on the fluid regime, gas-salt composition, P-T-X parameters, as well as the evolution and metal content of solutions forming the vein-stockwork mineralisation. In Dzhida ore field (South-Western Transbaikalia) there are one of the largest resources of W and Mo in Russia where the above problems potentially can be solved.

The purpose of this study is to determine the composition of ore-forming solutions and physico-chemical conditions of molybdenum mineralisation in the Pervomaiskoe stockwork deposit. The stockwork is formed by a network of variously oriented quartz-molybdenite veinlets (Stelmachonok, 1994). Mineralogical, petrographic and geochemical studies allowed us to identify the mineral and chemical composition of the quartz-molybdenum veins and near-veinlet zones. Microthermometry, Raman spectroscopy and LA-ICP-MS analyses were applied to examine fluid inclusions hosted in quartz from both bonanza and poor quartz-molybdenite veinlets. Gas composition and metal concentrations in the solutions, formed the quartz-molybdenite veinlets, were determined.

The study of fluid inclusion showed that the quartz-molybdenite veins were formed in the temperature range of  $\geq 186\text{--}314$  °C from a homogeneous fluid (Fig. 1). Total salinity varies from ~6.3 to 11.7 wt% eq. NaCl. The gas phase contains CO<sub>2</sub>, CH<sub>4</sub> and N<sub>2</sub>. Using LA-ICP-MS method, the concentrations Li, Be, B, F, Na, Mg, Al, Cl, K, Ca, Mn, Fe, Cu, Zn, Nb, Mo, Ag, Sn, La, Ce, Ta, W, Au, Pb, Th, U were determined. For quantification of the element concentration in ore-forming solutions, the method described by Borovikov et al. (2016) was applied. NIST-610 was used as an external standard. Molybdenum concentration in the fluid inclusions from bonanza quartz-molybdenite veinlets was measured to be up to 559 ppm (182 ppm in average), whereas it does not exceed 85 ppm (13 ppm in average) in the poor quartz-molybdenite veinlets. Bonanza veinlets were formed by near-neutral solutions with a high content of Mo, S and F, while the poor veinlets were precipitated from a highly alkaline solution. Therefore we suggest considering the pH value of solutions as an important parameter of ore deposition.

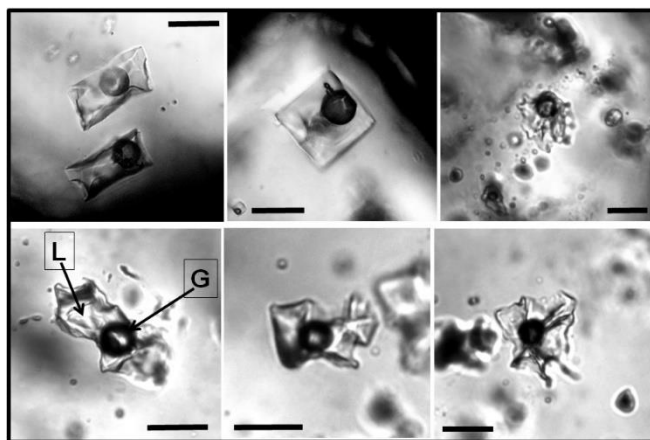


**Fig. 1.** Primary fluid inclusions in quartz from quartz-molybdenite veinlets. Scale bar is 10  $\mu\text{m}$ .

## Acknowledgement

This work was supported by the RFBR grant N 18-45-030002r\_a.

## References

- Borovikov A.A. et al. (2016) Russ. Geol. Geophys+ 57:647-662.
- Stelmachonok K.Z. (1994) Dokl. Ras. 337:382-385 (in Russian).

# Fluid flow evolution in the Albanide fold-and-thrust belt: insights from $\delta^2\text{H}$ and $\delta^{18}\text{O}$ isotope ratios of vein-hosted fluid inclusions

De Graaf, S.<sup>1\*</sup>, Nooitgedacht, C.W.<sup>2</sup>, Vonhof, H.B.<sup>1</sup> & Reijmer, J.J.G.<sup>3</sup>

<sup>1</sup>Max Planck Institute for Chemistry, Climate Geochemistry Department, Germany; <sup>2</sup>VU University Amsterdam, Department of Earth Sciences, The Netherlands; <sup>3</sup>King Fahd University of Petroleum and Minerals, College of Petroleum Engineering & Geosciences, Saudi Arabia; \*stefan.graaf@mpic.de

Tectonic forces generated during thrust emplacement along active margins may drive complex fluid flow patterns in fold-and-thrust belts and foreland basins. In this study, isotope data ( $\delta^2\text{H}$  and  $\delta^{18}\text{O}$ ) of fluid inclusions hosted in calcite vein cements were used to reconstruct regional fluid migration pathways in the Albanide fold-and-thrust system. The fluid inclusion isotope data were acquired using the continuous-flow set-up of Vonhof et al. (2006). This technique involves crushing of mineral samples at a relatively low temperature (110 °C) and allows for on-line analysis of both  $\delta^{18}\text{O}$  and  $\delta^2\text{H}$  ratios of bulk fluid inclusion water. To date, such continuous-flow techniques have mainly been used to study fluid inclusion isotope compositions of speleothems, and have not yet found a widespread application on vein systems for hydrogeological reconstructions.

The studied calcite veins developed in a sequence of naturally fractured Cretaceous to Eocene carbonate rocks as a result of episodic throughput of fluids from the early stages of burial onward. The acquired fluid inclusion isotope data demonstrate that fluids circulating in the carbonates were derived from an underlying reservoir that consisted of a mixture of meteoric water and evolved marine fluids, probably derived from deep-seated evaporites (Fig. 1). The meteoric fluids infiltrated in the hinterland before being driven outward into the foreland basin and ascended as soon as fracturing induced a sufficient increase in permeability. Structural and petrographic observations provide time constraints for various phases of fracture infilling and reveal an increasing dominance of meteoric water in the system through time as migration pathways shortened and marine formation fluids were progressively flushed out. Similar fluid flow evolutions have previously been recorded in various fold-and-thrust belt settings elsewhere in the world (e.g. Fitz-Diaz et al., 2011).

Despite the Cretaceous to Tertiary age of the studied vein system, oxygen isotope signatures of the fluid inclusions appear to still be original. Oxygen isotope exchange processes between the fluid inclusion water and host mineral could have been inhibited, because veins have not been exposed to elevated temperatures (i.e. <80 °C). Diagenetic stability of fluid inclusion water has been recognised in similar low-temperature vein systems (e.g. De Graaf et al., 2017). In contrast, fluid inclusions hosted in veins from high-

temperature hydrothermal settings are more prone to diagenetic alteration (De Graaf et al., 2019). Although more research into the diagenetic stability of fluid inclusion isotope ratios is required, the fluid inclusion isotope record has potential as a powerful tool for fluid provenancing in subsurface fluid flow systems.

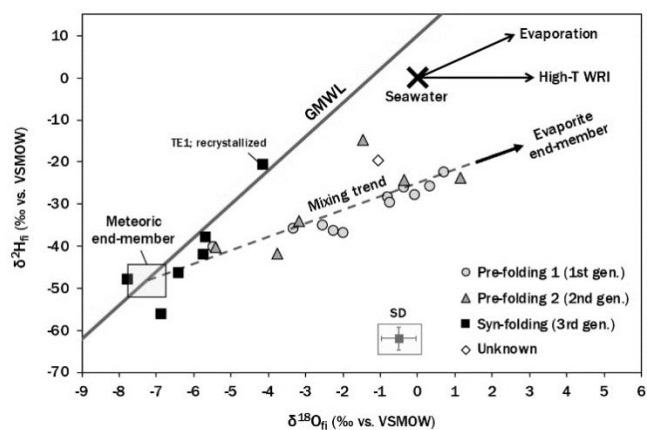


**Fig. 1.** Fluid inclusion isotope data of calcite veins from the Albanide fold-and-thrust belt exhibit a distinct correlation in the  $\delta^{18}\text{O}$ - $\delta^2\text{H}$  space, reflecting the isotope evolution of fluids circulating in the foreland fold-and-thrust system. Early pre-folding veins precipitated from a mixture of meteoric water and evolved marine formation fluids, whereas later stage syn-folding veins precipitated from a fluid dominated by the meteoric end-member.

## References

- De Graaf S. et al. (2017) *Mar. Petrol. Geol.* 80:382-393.
- De Graaf S. et al. (2019) *Miner. Deposita* (in press).
- Fitz-Diaz E. et al. (2011) *J. Struct. Geol.* 33:1237-1253.
- Vonhof H.B. et al. (2006) *Rapid. Commun. Mass Sp.* 20:2553-2558.

# Identifying deep hydrothermal fluids that leach metals from the oceanic crust and generate seafloor VMS deposits

Diamond, L.W.<sup>1\*</sup> & Richter, L.<sup>1</sup>

<sup>1</sup>Institute of Geological Sciences, University of Bern, Switzerland; \*diamond@geo.unibe.ch

Volcanogenic massive sulphide (VMS) deposits in basaltic lavas are widely viewed as products of metal-leaching from the oceanic crust by hot circulating seawater. Greenschist-facies alteration of the basalts produces spilites (rocks consisting of chlorite + albite + quartz ± actinolite ± epidote) at low water/rock ratios, and epidosites (rocks consisting of epidote + quartz + titanite + Fe-oxides) at high water/rock ratios. Which of these alteration types liberates the metals for VMS deposits is debated. Richardson et al. (1987) proposed epidosites as source rocks, whereas Jowitt et al. (2012) showed that spilites may be just as metal-depleted as epidosites. Other contentious points are the phase-state and salinity of the epidosite-forming fluids. Juteau et al. (2000) advocated hypersaline brines formed by boiling whereas Schiffman & Smith (1998) argued for single-phase water of seawater-salinity. To clarify these issues we have investigated fluid inclusions in altered lavas, sheeted dikes and plagiogranites in the Semail ophiolite, Oman.

Samples from plagiogranites show clear timing relations: (1) magmatic–hydrothermal quartz overgrown by (2) hydrothermal quartz belonging to spilite alteration, in turn overgrown by (3) quartz belonging to epidosite alteration. The magmatic–hydrothermal quartz is the only stage that contains liquid + vapour + halite (LVH) inclusions with coexisting vapour-rich inclusions (Richter and Diamond, 2019). In contrast, spilite-stage inclusions in the plagiogranites and in quartz amygdales in lavas all consist exclusively of LV with uniform phase proportions, implying entrapment from single-phase water with salinity of 2.4–4.0 wt% NaCl<sub>eq</sub> (cf. seawater salinity = 3.1–3.7 wt% NaCl<sub>eq</sub>). Homogenisation (LV→L) temperatures vary from 130–140 and 160–180 °C in lavas to 380–390 °C in spilited plagiogranites.

The epidosite-fluid occurs as primary LV inclusions in epidote + quartz in epidotised plagiogranites as well as in massive, pervasively epidotised dikes and lavas, and associated veins. Uniform phase proportions show the inclusions were trapped from single-phase water with salinity of 2.4–4.0 wt% NaCl<sub>eq</sub>, similar to the spilite-fluid. Homogenisation (LV→L) temperatures show narrow ranges (<12 °C) in individual fluid inclusion assemblages, with overall values of 220–315 °C in epidotised sheeted dikes and lavas, and 365–370 °C in epidotised plagiogranites.

Element concentrations in the fluids were determined by LA-ICP-MS analysis of individual fluid inclusions in petrographically well-defined inclusion assemblages in spilite-stage and

epidosite-stage quartz. Figure 1 demonstrates that recharging seawater decreases its Mg content by >2 orders of magnitude and increases its Ca content by ~1 order of magnitude as it converts its basaltic wall rocks to spilites. Also Mn, Fe, Cu and Zn become enriched as seawater evolves to spilite-fluid. The epidosite-fluid has an even lower Mg content and a higher Ca/Mg ratio, consistent with its epidote + quartz mineralogy.

In the epidosite-fluid, the contents of the VMS-metals Fe, Cu, Zn and Mn are all >1 order of magnitude lower than in the spilite-fluid (Fig. 1). This is because epidosites replace spilites that are already metal-depleted. We therefore view the spilite fluid, rather than the epidosite fluid, as the essential carrier of metals to VMS deposits at seafloor vents. The vent fluids themselves (Fig. 1) contain little Fe, Cu and Zn because they are sampled after their metals have been removed as sulphide precipitates at and below the seafloor.

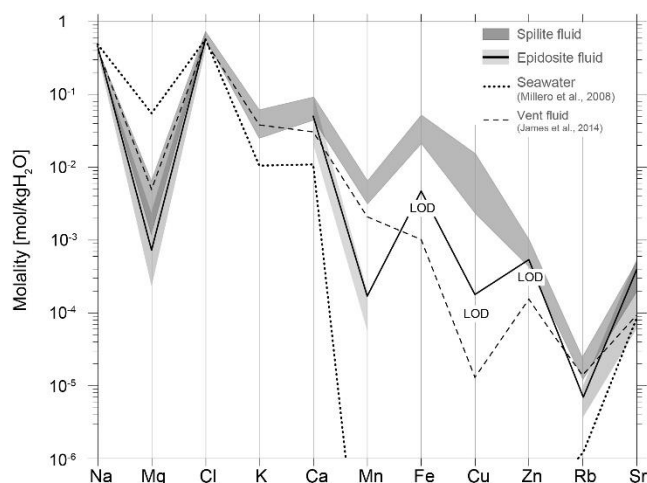


Fig. 1. Multi-element plot of spilite- epidosite-fluids (this study) compared to seawater and seafloor-vent fluid.

## References

- Jowitt S. et al. (2012) *J. Geochem. Explor.* 118:47-59.
- Juteau T. et al. (2000) *Mar. Geophys. Res.* 21:351-385.
- Richardson J.R. et al. (1987) *Earth Planet. Sc. Lett.* 84:243-253.
- Richter L. and Diamond L.W. (2019) in: *ECROFI 2019* (this volume).
- Schiffman P. and Smith B.M. (1988) *J. Geophys. Res.* 93:4612-4624.

# Spatial pattern of stable isotope composition of Holocene precipitation across Eurasia: a fluid inclusion study of speleothems

Dublyansky, Y.<sup>1\*</sup>, Scholz, D.<sup>2</sup> & Spötl, C.<sup>1</sup>

<sup>1</sup>Institute of Geology, University of Innsbruck, Austria; <sup>2</sup>Institute of Geosciences, Johannes Gutenberg University Mainz, Germany; \*yuri.dublyansky@uibk.ac.at

In a spatial sense, the isotopic composition of meteoric precipitation changes systematically over continents, in response to the evolution of humidity in the air masses as they travel from the moisture source regions (oceans) inland. In a temporal sense, the isotopic composition of precipitation changes with changing climate in response to a plethora of factors, such as changes in composition of oceans, changes in air temperature, readjustments of air circulation systems to new climate conditions, etc.

Fluid inclusions in speleothems (flowstones and stalagmites) trap dripwater from which speleothems grow. Drip waters represent a close proxy of local meteoric precipitation, temporally averaged during the transit through the soil and epikarst. Fluid inclusion-bearing speleothem layers can be precisely and accurately dated by the U-Th method. The analysis of water from speleothem fluid inclusions allows reconstructing the stable isotope composition of past precipitation in a given area.

This approach was applied in a study of the Holocene speleothems along a 8,500 km-long longitudinal transect extending from the Atlantic coast of the Europe to eastern Siberia (Lake Baikal), following the direction of the moisture transport from the Atlantic Ocean deep into the largest continental mass on Earth. Another 900 km-long transect was studied in NS direction along the Ural Mountains at the Europe-Asia divide.

88 stalagmites were collected from 33 caves. After precisely dating them using the U-Th method, 9 Holocene samples were selected for fluid inclusion work.

Analyses of the stable isotope composition of fluid inclusion water were performed on a dedicated line at Innsbruck University (Dublyansky and Spötl, 2009). The data were used to reconstruct isotopic characteristics of precipitation over Northern Eurasia during the last 11,700 yrs.

Fluid inclusions were found to faithfully record the isotopic compositions of ancient precipitation. Similarly to modern-day precipitation, the Holocene precipitation becomes isotopically "lighter" as moisture travels from the Atlantic coast eastward reaching minimum values in the vicinity of Lake Baikal (Fig. 1). It also varies in north-south direction showing more depleted values in stalagmites from Central Ural caves compared to their counterparts in Southern Ural (no Holocene stalagmites were found in Northern Ural).

Applying this method to Pleistocene stalagmites will allow to reconstruct the isotopic composition and patterns of rainfall in the more distant past, during climates that were substantially different from today's.

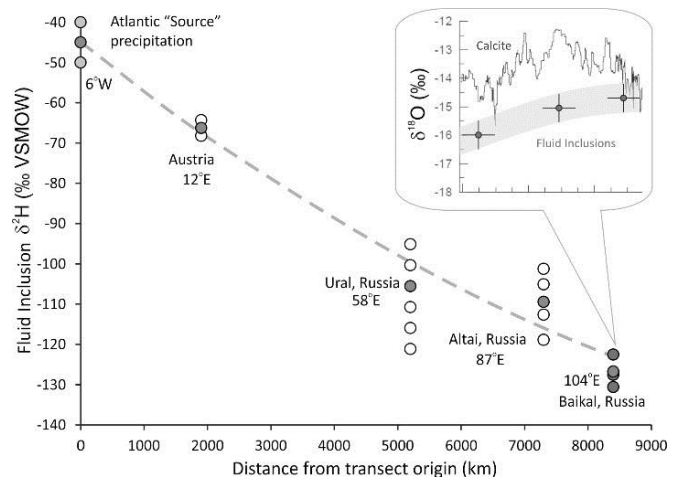


**Fig. 1.** Isotope composition of fluid inclusions water in the Holocene speleothems along the trans-Eurasian transect. Insert shows fluid inclusion water isotope values (circles with error bars and grey band) compared to the time-series of the stable isotopes in the host speleothem calcite (thin line).

## Acknowledgement

The work was funded by FWF grant P25716-N19 to YD.

## References

Dublyansky Y. and Spötl C. (2009) Rapid Comm. Mass Spectrom. 23:2605-2613.

# Fluid circulations and diagenesis of carbonate reservoirs in a foreland basin: evidences of thermal disequilibrium between fluid and host rocks

Elias-Bahnan, A.<sup>1\*</sup>, Carpentier, C.<sup>1</sup>, Pironon, J.<sup>1</sup> & Gaucher, E.C.<sup>2</sup>

<sup>1</sup>GeoRessources lab, CNRS, CREGU, Université de Lorraine, France; <sup>2</sup>TOTAL, CSTJF, France;

\*alexey.elias-bahnan@univ-lorraine.fr

Fluids circulating in foreland basins can have strong impacts on petroleum systems and reservoir properties. This applies to the Upper Cretaceous Lacq reservoir of the Aquitaine Basin in southwestern France. In this area, dolomitic reservoirs were considered as products of a surficial dolomitisation process (Biteau et al., 2006). However, a recent revisiting of the geodynamic model of the Pyrenean and South Aquitaine domain involving Early Cretaceous hyperextension with mantle exhumation led to suppose the impact of deeply sourced hydrothermal fluids on the diagenesis of reservoirs (Salardon et al., 2017; Renard et al., 2019). This new understanding of the geodynamics of the region requires a reappraisal of the diagenetic models of petroleum reservoirs.

Despite its importance, little is known about the nature, origin and timing of fluid circulation in the basin. Therefore, this work aims to (1) revisit and reconstruct the diagenetic history of the Lacq field, (2) investigate the types of sources of fluids involved and (3) link the obtained data to the geodynamic context of the basin. For these purposes, in addition to classical petrography and geochemistry techniques utilised on core samples, Aqueous Inclusion Thermodynamics (AIT) and Petroleum Inclusion Thermodynamics (PIT) tools, which rely on Confocal Scanning Laser Microscopy (CSLM), were used to determine P-T conditions of fluid circulations.

Microthermometry data were obtained from fluid inclusions (FIs) in matrix dolomites, saddle dolomites and calcite phases. FIs in both calcite and dolomite phases have the same  $T_h$  mode values of 80 °C with identical salinities being equal to or less than that of seawater. Oil inclusions in blocky calcites have  $T_h$  mode values of 67 °C. AIT and PIT modelling on aqueous and oil inclusions in the blocky calcites indicate a trapping temperature range of 82 to 92 °C and pressures of 136 to 210 bars.

To have a time constraint on these P-T conditions, Petromod 1D is used to model the basin subsidence and the evolution of hydrostatic and lithostatic pressures with time. Under normal burial conditions, the hottest temperatures recorded by the Upper Cretaceous reservoirs of Lacq would not exceed 50 °C, while the trapping temperatures of the aqueous and oil inclusions are too hot to be in thermal equilibrium with the reservoir (Fig. 1).

This gap between modelled burial temperatures and fluid inclusion  $T_h$  is indicative of a pulse of hot hydrothermal fluids that influenced the diagenesis

of the petroleum reservoir. By extrapolating the fluid pressures to the domain of hydrostatic and lithostatic gradients, we estimate a timing between 56 and 47 Ma, with an overpressure of nearly 80 bars (difference from hydrostatic gradient). This coincides with the maximum compression of the Pyrenean orogeny, and was similarly concluded by Renard et al. (2019) in the Rouse field.

Therefore, using a multitude of modelling techniques, we document the impact of hot deeply sourced fluids, circulating during the Pyrenean orogenic compression, whose circulations were not in thermal equilibrium with the host rocks.

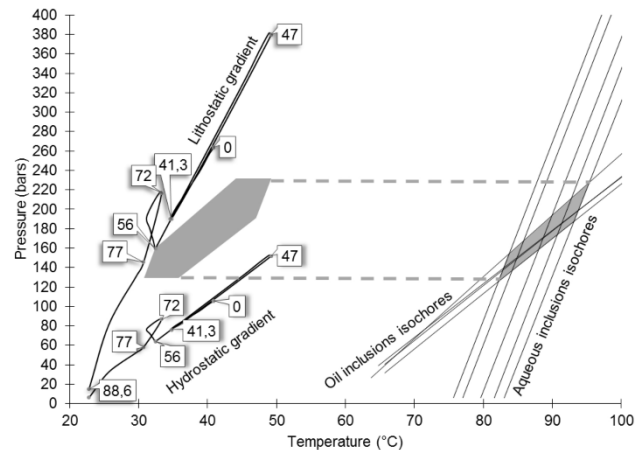


**Fig. 1.** Evolution of hydrostatic and lithostatic gradients experienced by the Upper Cretaceous reservoirs of Lacq. The isochores of aqueous and oil inclusions are also plotted. Their intersection indicate the trapping P-T conditions (grey shaded area). Number tags are ages in Ma. Loops in the gradients represent unconformities.

## References

- Biteau J-J. et al. (2006) *Petrol. Geosci.* 12:247-273.
- Renard S. et al. (2019) *Chem. Geol.* 508:30-46.
- Salardon R. et al. (2017) *Mar. Petrol. Geol.* 80:563-586.

# Paleotemperature constraints of calcite fracture cementation in shale: a comparison of fluid inclusion and carbonate clumped isotope thermometry

Fall, A.<sup>1\*</sup>, Dennis, P.F.<sup>2</sup>, Gale, J.F.W.<sup>1</sup> & Ukar, E.<sup>1</sup>

<sup>1</sup>Bureau of Economic Geology, Jackson School of Geosciences, The University of Texas at Austin, USA; <sup>2</sup>School of Environmental Sciences, University of East Anglia, UK; \*andras.fall@beg.utexas.edu

Natural fractures in sedimentary basins provide pathways for fluid flow and associated heat and mass transfer, especially in rocks with low intrinsic permeability, such as shales. Fractures form as a result of various combinations of tectonic, burial and thermal loading (stress), pore fluid pressure, and evolving rock strength. Timing of fracturing and cementation is a key element in building predictive fracture models, but obtaining the timing of fracturing is difficult. In naturally cemented fractures fluid inclusion temperatures, when correlated with burial and thermal history models, can be used to unlock the history of fracturing (e.g. Fall et al., 2015).

However, not all fracture cements contain fluid inclusions suitable for microthermometry, and consequently timing of fracture formation. In such cases an alternative method for obtaining temperatures of fracture cementation is necessary. In cases where carbonate cement fills the natural fractures, carbonate clumped isotope paleothermometry is a potential alternative to fluid inclusion microthermometry.

Carbonate clumped isotope thermometry ( $T-\Delta_{47}$ ), a technique relying on the thermodynamic tendency of heavy isotopes of carbon ( $^{13}\text{C}$ ) and oxygen ( $^{18}\text{O}$ ) to bond, or “clump” together in carbonate minerals (Ghosh et al., 2006) has recently been applied to a range of geologic problems (Huntington and Lechler, 2015), including dolomite cementation in shallow crustal settings (Came et al., 2017) and genesis of hydrothermal skarn and carbonate-hosted ore deposits (Mering et al., 2018, Dennis et al., 2019). A few recent studies (e.g. Came et al., 2017; MacDonald et al., 2018), have previously compared fluid inclusion and clumped isotope temperatures, though they all used the homogenisation temperatures ( $T_h$ ) of the inclusions for the comparison, disregarding potential pressure correction effects on the actual inclusion trapping ( $T_t$ ) and carbonate formation temperatures. Moreover, Honlet et al. (2017) used the  $T-\Delta_{47}$  to determine the magnitude of pressure correction of fluid inclusions, without independently establishing the accuracy of the temperatures derived from the  $T-\Delta_{47}$  method.

Here we present a study where we directly compare fluid inclusion and clumped isotope temperatures based on calcite-filled bed-parallel veins (BPV or beef) in the calcareous shales of the Vaca Muerta Formation, Argentina. Calcite in BPVs is fibrous and growth zoning and host rock inclusions trapped in the calcite indicate antitaxial

calcite cements growth concurrent with fracture opening (synkinematic). The calcite-filled BPVs are cut by narrow bed-parallel microfractures, and four sets of bed-normal, opening-mode fractures, all containing carbonate cement.

All fracture cements contain fluid inclusion assemblages (FIA) consisting of coexisting primary aqueous inclusions (salinity ~15 wt% NaCl equivalent) and methane-dominated hydrocarbon gas inclusions ( $T_h$  ~-75 °C to -65 °C). The coexistence of the two types of inclusions within the same FIA indicates that  $T_h$  of the inclusions will represent the actual  $T_t$ , or the temperature at which calcite precipitated. These temperatures are then directly comparable to the clumped isotope temperatures.

Preliminary results of the comparison, however, show a discrepancy in the compared temperatures.  $T_h$  of the primary aqueous fluid inclusions in various beef zones show a range from 175 °C to 208 °C, with no systematic trends between the zones. Late BPV-parallel fracture cements show  $T_h$  ranging from 165 °C to 183 °C, while three sets of vertical fractures show  $T_h$  ranging from 142 °C to 161 °C. In contrast  $T-\Delta_{47}$  of the fibrous calcites ranges from ~123 °C in the earlier Zone 1 and 2 cements, to ~116 °C in the later Zone 3 cements. Although care was taken to avoid younger fractures cutting BPVs possible causes of temperature differences are mixing of various generations of calcite cements, reequilibration of the fluid inclusions, and/or resetting of  $\Delta_{47}$  values of calcite due to possible post-cementation thermal and mechanical effects.

## References

- Came R.E. et al. (2017) *Geochim. Cosmochim. Ac.* 199:31-47.
- Dennis P.F. et al. (2019) *J. Geol. Soc. Lond.* (in press).
- Fall A. et al. (2015) *G.S.A. Bull.* 127:61-75.
- Ghosh P. et al. (2006) *Geochim. Cosmochim. Ac.* 70:1439-1456.
- Huntington K.W. and Lechler A.R. (2015) *Tectonophys.* 647-648:1-20.
- MacDonald J.M. et al. (2018) *Geol. Soc. Spec. Pub.* 468:189-202.
- Mering J.A. et al. (2018) *Econ. Geol.* 113:1671-1678.

# Hydrocarbon migration and accumulation characterisation in Yinan-2 gas reservoir, Kuqa depression (Tarim Basin, China)

Fan, J.J.<sup>1\*</sup>, Liu, S.B.<sup>1</sup>, Lu, X.S.<sup>1</sup>, Meng, Q.Y.<sup>1</sup> & Zhuo, Q.G.<sup>1</sup>

<sup>1</sup>Research Institute of Petroleum Exploration and Development, State Key Laboratory of Enhanced Oil Recovery, China; \*fanjunjia@petrochina.com.cn

Yinan-2 gas reservoir is a typical tight gas reservoir in Kuqa depression (Tarim Basin). In the relevant studies there seems to be a consensus about the filling characteristics of early oil and late gas in Kuqa. However, there are controversies on the distribution and migration path of oil and gas in Yinan-2. In order to reveal hydrocarbon migration pathway and charging history, from the Yinan-2 well, 26 sand samples were studied by using quantitative fluorescence techniques (Fig. 1), microscopic observation and homogenisation temperature measurement of fluid inclusions. Based on the fluid inclusions observation, well log curves and comprehensive geological data analysis, it is indicated that the Yinan-2 gas reservoir experienced oil charge of early stage, oil leakage and gas charging in late stage. The following conclusions can be drawn:

1) the early oil of Yinan-2 gas reservoir could be originated mainly from deep Triassic mudstone strata by vertical migration pathways. The ancient oil reservoir likely suffer structural damage and leakage, and no large-scale paleo-oil reservoir expected to be formed,

2) the migration paths of the late natural gases pushed vertically, and a large-scale gas-bearing area might be formed below 4750 m of the reservoir,

3) Yinan-2 gas reservoir is featured by mixed source characteristics, the natural gas originated from Jurassic coal formation and Triassic lacustrine mudstones,

4) a deep layer in Yinan-2 is a favorable area for the development of continuous tight gas reservoirs.

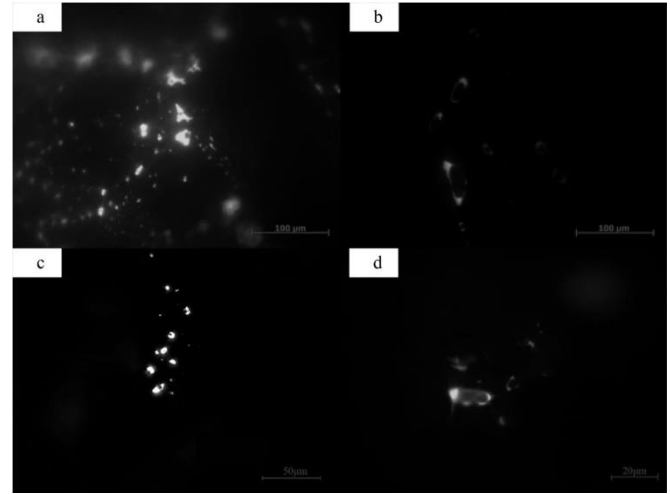


**Fig. 1.** Photomicrographs taken under fluorescent microscope, showing the hydrocarbon inclusions of sandstone samples in Yinan-2. The oil inclusions show different fluorescent colours.

# Tectonic hydrothermal dolomitisation in Ordos Basin: evidence from fluid inclusions

Feng, Y.W.<sup>1\*</sup>, Chen, Y.<sup>1</sup> & Zhao, Z.Y.<sup>2</sup>

<sup>1</sup>School of Geosciences, China University of Petroleum, China; <sup>2</sup>Research Institute of Petroleum Exploration and Development, PetroChina, China; \*fengyw1994@outlook.com

Fluid inclusions occurring along structural fractures of minerals may record the composition, the temperature and pressure of the fluids related to gas migration or water-rock interaction. A large number of fluid inclusions are found in a carbonate vein from the Majiagou Formation, Ordos Basin. The vein-filling minerals were identified by laser Raman spectroscopy. Results show the presence of calcite, dolomite (1099 cm<sup>-1</sup>) and magnesite (1095 cm<sup>-1</sup>) (Fig. 1). Some dolostone chips (residues of wall rock) with different sizes were cemented with dolomite. The dolomite cement crystals near the residues are small, while those far away from the residues are bigger. This indicates that the dolomite and magnesite formed along the structural fractures due to the migration of Mg-rich fluid and its interaction with the wall rock.

Our microthermometric experiments on the fluid inclusions in dolomite and magnesite show homogenisation temperatures ( $T_h$ ) in the ranges 236.9-262.3 °C and 313.2-342.1 °C, respectively. These  $T_h$ s exceed the maximum temperatures corresponding to the burial history of studied formation in this region, indicating that the Mg<sup>2+</sup> rich fluids should be hydrothermal fluids from deep basin. The formation of dolomite and magnesite veins may be the result of tectonic hydrothermal dolomitisation. The above geological setting favors recrystallisation of dolomite and change the reservoir properties, including improvement of rocks porosity and permeability. This resulted in the formation of high quality reservoirs for oil and gas.

## Acknowledgement

This work was supported by the National Natural Science Foundation of China (No. U1762108 and 41873070).

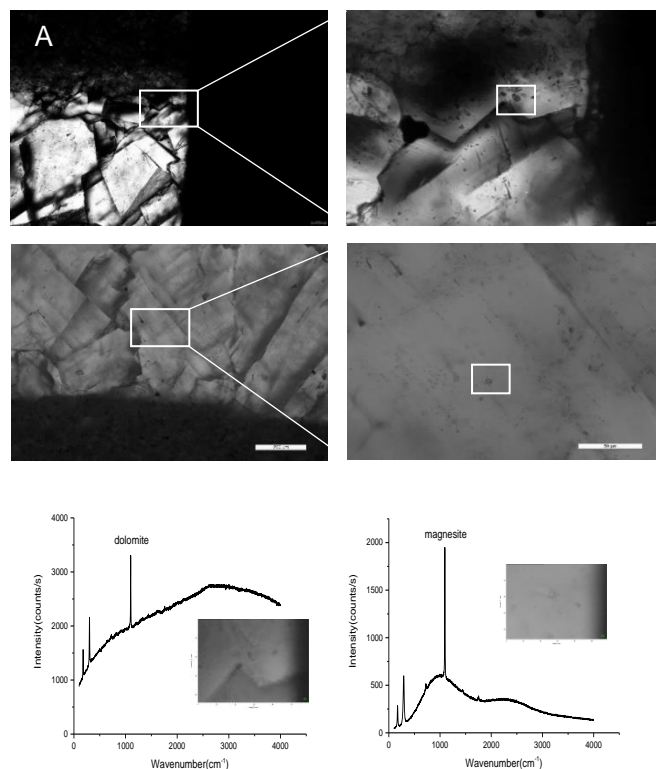


**Fig. 1.** Fluid inclusions in dolomite (A) and magnesite (B) veins. Raman spectra show the characteristic peaks of dolomite and magnesite.

## UHP fluid inclusions: indicators of the petrological and geochemical role of the fluids released at sub-arc depths

**Ferrando, S.<sup>1\*</sup>**

<sup>1</sup>Department of Earth Sciences, University of Torino, Italy; \*simona.ferrando@unito.it

Fluids released by dehydration reactions within the slab during its subduction at sub-arc depths have strong petrological and geochemical effects on the metamorphic evolution of the subducting rocks and on the metasomatism of the overlying mantle wedge.

An increasing number of fluid inclusion studies in ultra-high pressure (UHP) lithologies from both the slab and the overlying mantle wedge reveals: i) the widespread occurrence of subduction-related UHP fluids (or melts); ii) the presence of three distinct populations of UHP fluid inclusions (i.s.), i.e. chlorite-bearing aqueous  $\pm$  non-polar gaseous inclusions, multiphase-solid inclusions and melt inclusions; iii) the preservation, in some inclusions, of the chemical composition of the trapped UHP fluid.

The data obtained from UHP fluid inclusions indicates that: a) along cold geothermal gradients, a deep subducted slab can release water-dominated solutions containing moderate concentrations of chlorides, Si, Al, and alkalis,  $\pm$  non-polar gases; b) along intermediate geothermal gradients, the slab can release alkali-aluminosilicate-rich aqueous fluids at *P-T* conditions near or just above the second critical end-point of H<sub>2</sub>O–silicate systems, and their amounts of solutes [Si, Al, Ca, Fe, alkalis, (SO<sub>4</sub>)<sup>2-</sup>, (CO<sub>3</sub>)<sup>2-</sup> and incompatible trace elements] can gradually increase at rising temperature; c) along hot geothermal gradients, UHP dehydration melting of the subducting slab releases hydrous-silicate melts enriched in incompatible trace elements; d) the overlying mantle wedge is metasomatised by subduction-related solute-rich COH fluids or subduction-related melts, both enriched in incompatible trace elements.

These studies reveal that, although the chemical composition of natural subduction-related UHP fluids is more complex than that considered by experiments, the data on alkali-aluminosilicate-rich aqueous fluids are in agreement with experiments on mineral dissolution and element fractionation at UHP conditions. In fact, the major- and trace-element content in alkali-aluminosilicate-rich aqueous fluids results to be related to a progressive-to-complete dissolution of UHP minerals such as phengite, carbonate and epidote *s.l.* The remarkable occurrence of trace elements in alkali-aluminosilicate-rich aqueous fluids is also in agreement with experiments in which these fluids result to incorporate similar or even higher amounts of trace elements than a hydrous-silicate melt generated at the same P-T conditions. Fluid

inclusion studies on natural samples also support experiments and thermodynamics on physical properties of subduction-related UHP fluids. In fact, the large element solubility and mobilisation exhibited by the aqueous solutions released at sub-arc depths are in agreement with the idea that they are polymerised fluids, with a metasomatic efficiency much more similar to that of hydrous-silicate melts than that of typical crustal fluids dominated by halite ligands.

The relevant data so far obtained suggest that, although hampered by some analytical difficulties, the research on UHP fluid inclusions from slab and mantle-wedge lithologies will provide exciting new results in the coming years and it will supply an added value to experimental and thermodynamic data on subduction-related fluids and to petrology and geochemistry of orogenic magmatism.

# Speleogenesis of hypogene caves in Veľká Fatra (Slovakia): fluid inclusion and stable isotope evidence

**Filipčíková, P.<sup>1\*</sup>, Dublyansky, Y.<sup>2</sup>, Spötl, C.<sup>2</sup> & Koltai, G.<sup>2</sup>**

<sup>1</sup>Department of Environmental Geochemistry, Comenius University in Bratislava, Slovakia; <sup>2</sup> Institute of Geology, University of Innsbruck, Austria; \*filipcikova2@uniba.sk

Hydrothermal speleogenesis is a specific category of hypogene karst, commonly but not always hosting euhedral calcite crystals lining cave walls and/or isotopic alteration halos in the adjacent wall rock (Dublyansky, 2013; Dublyansky and Spötl, 2009).

Samples of euhedral calcite crystals and bedrock were obtained from three caves in the area of Veľká Fatra (Slovakia). Prior to this study, hydrothermal speleogenesis has not been identified in the area. The presence of euhedral calcite crystals, however, suggest a deep-seated hydrothermal origin of some of these caves. We applied a suite of methods including stable isotope analyses on wall rock and calcite crystals, fluid-inclusion petrography, microthermometry and isotope analysis of fluid inclusion water to identify speleogenetic phases and constrain the nature of the fluids involved.

The initial dissolution phase is represented by isotope alteration halos in the cave wallrock where carbon isotope values significantly decrease towards the cave wall (from 1.5 ‰ to -10.3 ‰) showing a partially sigmoidal shape. The  $\delta^{18}\text{O}$  data show a weak trend towards higher values (about -2.9 ‰ VPDB) compared to the unaltered Triassic host rock (-4.5 ‰ VPDB). A different (and presumably late-stage) alteration signal was obtained for two locations, where  $\delta^{18}\text{O}$  values range from -8.1 to -7.1 ‰, and  $\delta^{13}\text{C}$  between -4.1 and -1.6 ‰.

Homogenisation temperatures of two-phase fluid inclusions range between 41 and 74 °C in three caves. The temperature variation within a single crystal is 10 to 20 °C and the measured FIA indicate either stable conditions or a cooling trend. Salinity decreases in the same manner from 3.6 to 0.7 mass% NaCl equiv. from the base to the top of the crystals. The stable isotopic composition of the inclusion water was analysed in five samples. All samples show moderate (1.5-2.0 ‰) positive  $\delta^{18}\text{O}$  displacement relative to the Global Meteoric Water Line, suggesting some degree of water-rock interaction.

The early phase of calcite formation involved fluids of likely sea water origin while the later phase of calcite growth suggests a meteoric water influx. Changes in crystallisation conditions are also reflected in the changing crystal habit.

The study of scalenohedral calcite and associated bedrock yielded evidence of temperature decrease in a range 74 to 41 °C and the fluid composition evolution from the marine

towards low-salinity meteoric that likely occurred during the uplift and exhumation of the area.

We conclude the cave Tajná Túžba (TT) and Lubená II (LUB-II) formed under the same conditions represented by the early (sea-water) dissolution, however the bedrock signal in TT was likely overprinted by late, meteoric fluid. The overprint signal was detected (along with the marine signal) in samples of loose boulders topped by calcite lying on the cave floor, and corrosive environment is suggested also by the presence of highly corroded crystals lining the cave walls. The precipitation phase was characterised by progressively diluted fluid where the calcite in TT yielded higher temperatures (74 to 52 °C) suggesting earlier precipitation than in LUB-II (66 to 47 °C).

The formation of Lubenna I cave took place subsequent to the marine phase, represented by meteoric signal in the wall rock and in calcite spar, crystallising at temperatures 63 to 41 °C.

Timing of the speleogenetic process, related to tectonic uplift and stage involving marine water is tentatively placed in the Paleogene–Lower Miocene.

## References

- Dublyansky Y.V. (2013) in: Treatise on Geomorphology 57-71.  
Dublyansky Y.V. and Spötl C. (2009) in: Hypogene Speleogenesis and Karst Hydrogeology of Artesian Basins. 45-50.

# Fluid inclusion study in the Portas gold deposit (Lugo, NW of Spain): preliminary results

**Fuertes-Fuente, M.<sup>1\*</sup>, Cepedal, A.<sup>1</sup>, Martin-Izard, A.<sup>1</sup>, Arias, D.<sup>1</sup> & Aragón, D.<sup>2</sup>**

<sup>1</sup>Department of Geology, University of Oviedo, Spain; <sup>2</sup>Sondeos y Perforaciones Industriales del Bierzo S.A., Spain; \*mercedf@uniovi.es

## Introduction

Gold occurrences are abundant in the NW Iberian Peninsula, and mining companies currently explore several gold prospects. This research focuses on one of them, the Portas deposit (Cepedal et al., 2018). This work presents a preliminary fluid inclusion study to determine the composition of the fluids involved in the mineralising process.

## Geological Setting

The Portas deposit is located in the Variscan belt of the NW of Iberian Peninsula. The succession that hosts the deposit is a sequence of alternating slates, metasandstones and quartzites, culminating in the Armorican Quartzite. Slates of Llanvirn age overlie the quartzite. Iron-rich metasediments occur in the transitional stratigraphic levels to the Armorican Quartzite. This Ordovician sequence is affected by three coaxial Variscan deformation phases, and by metamorphism at greenschist facies.

## The Portas deposit

The deposit is associated with a quartz-vein system that crosscuts Ordovician metasediments. The veins show different degrees of deformation, and the less deformed and undeformed quartz-veins are associated with the ore mineralisation. They are mainly composed of quartz and chlorite, and lesser amounts of, ankerite, apatite and rutile. In the veins, the ore minerals are arsenopyrite, and pyrite that overgrows or heals fractures in the arsenopyrite. This pyrite is associated with galena, chalcopyrite, sphalerite, and gold.

## Fluid inclusion study

Quartz samples from the ore-bearing veins were collected for fluid inclusion petrography and microthermometry. Two fluid inclusion types were recognised in all the sampled veins:

Type 1: Carbonic fluid inclusions. They are abundant in all the studied samples. At room temperature, they are monophasic and have a dark appearance (Fig. 1). They form three-dimensional arrays in the quartz crystals. Microthermometry data show a  $T_m(\text{CO}_2)$  range of between -64 and -61.8 °C. The volumetric fraction of the carbonic liquid phase varies between 0.25 and 0.5. The  $T_h(\text{CO}_2)$  is to the vapour state with two temperature intervals from -26 to -21.5 °C, and from -10.5 to -7.2 °C. The homogenisation temperatures are consistent within the fluid inclusion assemblages.

Type 2: Aqueous fluid inclusions. At room temperature, they are biphasic inclusions with  $\phi_{\text{liq}} = 0.7-0.8$ . They occur as intragranular and transgranular fluid inclusion planes.  $T_e$  is

around -20.8 °C and  $T_m(\text{ice})$  is from -5.3 °C to -2.8 °C.  $T_h(\text{total})$  is between 230 °C and 316 °C to the liquid state.

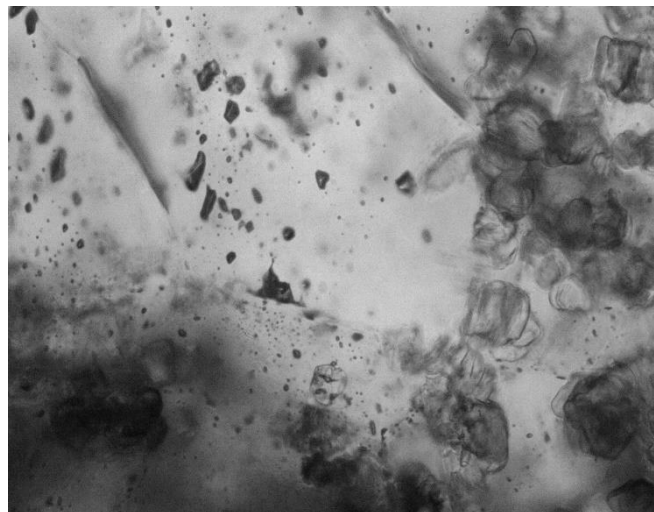


**Fig. 1.** Type 1 fluid inclusions containing a single fluid phase in a quartz crystal. The crystal also shows abundant inclusions of vermicular chlorite (on the right).

## Conclusions

From this preliminary study, a mixture of volatiles,  $\text{CO}_2\text{-CH}_4\text{-N}_2$ , (Van den Kerkhof and Thiéry, 2001) seems to have had a role in the ore mineral deposition. Further studies are necessary to establish the actual composition of this fluid, and its implication for the genesis of this gold deposit.

## Acknowledgement

This work has been financed by the CGL2016-76532-R project of the Spanish National Plan I+D+i.

## References

- Cepedal A. et al. (2018) in: 15<sup>th</sup> IAGOD Symposium Proceedings Anales 56-SEGEMAR:148-149.
- Van den Kerkhof A. and Thiéry R. (2001) Lithos 55:49-68.

# Fluid inclusion study and burial depth of deep-seated Evate carbonatite deposit

**Gajdošová, M.<sup>1\*</sup>, Huraiová, M.<sup>1</sup> & Hurai, V.<sup>2</sup>**

<sup>1</sup>Department of mineralogy and petrology, Comenius University, Slovakia; <sup>2</sup>Earth Science Institute, Slovak Academy of Science, Slovakia; \*misa.gajdos@gmail.com

The Evate carbonatite deposit is located in the Monapo structure in Mozambique. As calcite and dolomite are the major mineral phases, the rock can be classified as calciocarbonatite and ferric calciocarbonatite. Apatite, olivine, amphibole, phlogopite, magnetite, ilmenite, anhydrite and spinel are other abundant minerals of the carbonatite and associated nelsonite (Hurai et al., 2017; Barbosa et al., 2016). No comprehensive research has been carried out from the Evate deposit yet and the recent views on its genesis remain contentious. The Evate deposit may represent an example of deep-seated post-orogenic carbonatites occurring rarely in the Earth.

We studied fluid inclusions in the metasomatic fenite, subjacent to the Evate deposit, consisting of quartz, albite, K-feldspar, amphibole, magnetite, pyrrhotite and pyrite. Accessory minerals are titanite, monazite and rutile with small apatite and calcite inclusions. The observed mineral assemblage allowed us to combine data from various thermometers with the isochores determined from the fluid inclusions.

The presence of rutile needles in quartz (Fig. 1) indicates the system saturated in Ti. Therefore, the crystallisation temperature of quartz could be calculated by using Ti-in-quartz thermometer (Thomas et al., 2010). The Ti-content determined by EPMA (13-38 ppm) returned crystallisation temperature of  $421 \pm 18$  °C (at 1 bar). Temperature calculated by using the Zr content in rutile determined by EPMA (40-78 ppm) corresponded to  $493 \pm 11$  °C (at 1 bar), according to the calibration of Tomkins et al. (2007).

Numerous monophasic fluid inclusions in quartz had rounded or elongated shapes and diameters ranging from 1 to 16  $\mu\text{m}$ . Raman spectroscopy revealed low-density secondary gaseous inclusions of  $\text{N}_2\text{-CO}_2$  composition and higher density primary fluid inclusions of  $\text{CO}_2$ -rich fluid with minor admixture of  $\text{CH}_4$  and  $\text{N}_2$ . In the primary inclusions, the homogenisation of V (vapour phase) and L (liquid phase) took place into the L between  $-31.5$  and  $21.8$  °C with a top frequency at  $-3.2$  °C. Temperatures of melting ranged from  $-57.7$  to  $-56.6$  °C. A super-dense inclusion was also observed, showing a metastable total homogenisation of V into the L at  $-57.6$  °C, stable partial homogenisation of V into the L at  $-57.4$  °C and total homogenisation by the dissolution of solid in the L at  $-56.9$  °C.

Nahcolite was a ubiquitous daughter phase identified by Raman spectroscopy within  $\text{CO}_2$ -rich primary inclusions (Fig. 1). Dawsonite frequently occurred only within  $\text{CO}_2$ -rich inclusions adhered to

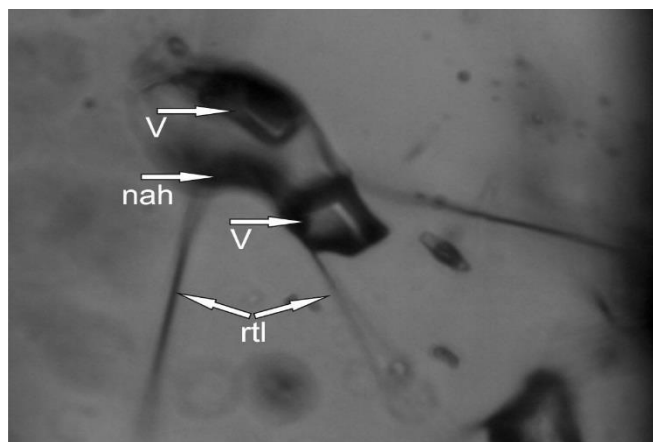


**Fig. 1.** Quartz-hosted fluid inclusion containing nahcolite-nah,  $\text{CO}_2$  phase-V and rutile-rtl (size  $11 \times 5 \mu\text{m}$ ).

albite. Thenardite was also rarely present. Solitary monophasic nahcolite inclusions were also observed in quartz.

Isochores of  $\text{CO}_2$  inclusions combined with the Ti-in-quartz and Zr-in-rutile thermometers returned temperatures and pressures of  $420\text{-}530$  °C and  $3\text{-}7.2$  kbar, respectively. Burial depths are estimated to be  $26\text{-}29$  km, assuming the changing lithostatic and hydrostatic fluid regimes, thus corroborating our assumption about the deep-seated carbonatite formed during the post-collisional break-up of Gondwana. This interpretation is supported by the EPMA U-Pb-Th monazite age of  $573 \pm 13$  Ma in the studied rock, corresponding to the thrust-faulting exhumation phase of east-African orogen (Grantham et al., 2013).

## Acknowledgement

This work was supported by the Comenius University grant for young scientists (UK/205/2019).

## References

- Barbosa R.O. et al. (2016) 35<sup>th</sup> IGC, Cape Town, Abstracts volume.
- Grantham G.H. et al. (2013) *Precambrian Res.* 234:85-135.
- Hurai V. et al. (2017) *Ore Geol. Rev.* 80:1072-1091.
- Thomas J.B. et al. (2010) *Contrib. Mineral. Petr.* 160:743-759.
- Tomkins H.S. et al. (2007) *J. Metamorph. Geol.* 25:703-713.

## FTIR and fluid inclusion study of hydrothermal quartz crystals in the Certej epithermal gold deposit, Apuseni Mts., Romania

**Gál, Á.<sup>1\*</sup>, Kovács, I.J.<sup>2</sup>, Szabó, Cs.<sup>3</sup>, Berkesi, M.<sup>3</sup>, Szakács, A.<sup>4</sup> & Ionescu, C.<sup>1,5</sup>**

<sup>1</sup>Department of Geology, Babeş-Bolyai University Cluj-Napoca, Romania; <sup>2</sup>Kövesligethy Radó Seismological Observatory, Geodetic and Geophysical Institute, Research Centre for Astronomy and Earth Sciences, Hungarian Academy of Sciences, Hungary; <sup>3</sup>Lithosphere Fluid Research Lab, Institute of Geography and Earth Sciences, Eötvös Loránd University Budapest, Hungary; <sup>4</sup>Institute of Geodynamics, Romanian Academy, Romania; <sup>5</sup>Archeotechnologies and Archeological Material Sciences Laboratory, Institute of International Relations, History and Oriental Studies, Kazan (Volga Region) Federal University, Russia; \*agi.gal@ubbcluj.ro

The Certej low sulphidation epithermal Au deposit, one of the most important ones in Romania, occurs at the south-eastern part of the Apuseni Mts. within the well-known “Gold quadrangle”, related to Miocene (14.7-7.4 Ma) calc-alkaline volcanics and intrusives. The disseminated Au mineralisation is hosted by andesites and Cretaceous and Neogene breccias. Our research focuses on fluid inclusions in hydrothermal quartz crystals aiming to obtain information on the ore-forming hydrothermal fluids, which will provide a better understanding of the paleoenvironment and the chemical and thermodynamic conditions in which the Au deposit was formed. The fluid inclusion studies were performed using a heating/cooling stage. The investigation methodology was completed by Raman spectroscopy applied to the fluid inclusions and by Fourier Transform Infrared Spectroscopy on selected quartz crystals.

The quartz crystals show heterogeneity in their infrared spectra. Both structural hydroxyl and molecular water contents vary not only among different specimens but also within a single crystal. The most important substitutions of structural hydroxyl are related to the linked substitutions:  $\text{Li}^+ + \text{OH}^-$  in interstitial positions (band at  $3480 \text{ cm}^{-1}$ ) or  $\text{Al}^{3+} + \text{OH}^-$  into a vacant  $\text{Si}^{4+}$  site (triplet of bands at  $3420$ ,  $3380$  and  $3320 \text{ cm}^{-1}$ ). There are also indications for the trace presence of  $\text{B}^{3+} + \text{OH}^-$  substitution into vacant  $\text{Si}^{4+}$  sites (band at  $3600 \text{ cm}^{-1}$ ). The broad band of molecular water in the  $3400 - 3300 \text{ cm}^{-1}$  range is usually present with extremely variable intensities. The structural hydroxyl content is usually below 5 ppm wt. (expressed in molecular water equivalent) but varies considerably within and among crystals. The molecular water content in sub-microscopic inclusions is low ( $\sim 10-15$  ppm). The structural hydroxyl and molecular water content is at the lower end of the array defined by quartz grains from various igneous and metamorphic assemblages. The various substitution mechanisms of structural hydroxyl and the strong heterogeneity in water concentrations may be in line with the complex nature of shallow hydrothermal systems as manifested in their strongly time-dependant chemical and physical properties. Such complexity at Certej might be the result of boiling in the deeper part of the hydrothermal system, input of meteoric water to the

fluids of prevalently magmatic origin and resulting variations in fluid temperatures and concentrations, and interaction with the host rocks of various composition (e.g. organic-rich shales).

The determined eutectic temperatures of the fluid inclusion brines range between  $-19.3$  and  $-24.4 \text{ }^\circ\text{C}$  (corresponding to a KCl-bearing  $\text{H}_2\text{O}-\text{NaCl}$  system), whereas the freezing point depressions range from  $-4.1$  to  $-0.1 \text{ }^\circ\text{C}$ . The final melting temperature occurred between  $-0.1$  and  $-3.3 \text{ }^\circ\text{C}$ . The fluid inclusion salinity is between 0.18 and 5.41 wt% NaCl. These data allowed for pressure calculations and determination of the corresponding depths of the paleo-watertable (100-300 m) at the time of the mineralisation processes. Vapour-rich fluid inclusions consist of  $\text{H}_2\text{O}=67.0-99.9 \text{ vol}\%$ ,  $\text{N}_2=0.0-7.2 \text{ vol}\%$ , and  $\text{CO}_2=0.0-29.7 \text{ vol}\%$ , as the main components.

# Insight into Miocene seawater composition from fluid inclusions in halite, Praid, Transylvanian Basin Romania

Gelencsér, O.<sup>1,2\*</sup>, Berkesi, M.<sup>1</sup>, Palcsu, L.<sup>2</sup>, Futó, I.<sup>2</sup>, Aradi, L.E.<sup>1</sup> & Szabó, Cs.<sup>1</sup>

<sup>1</sup>Lithosphere Fluid Research Lab, Institute of Geography and Earth Sciences, Eötvös Loránd University, Hungary;

<sup>2</sup>Laboratory of Climatology and Environmental Physics, Institute for Nuclear Research, Hungarian Academy of Sciences, Hungary; \*gecso@caesar.elte.hu

The middle Miocene Badenian Salinity Crisis (BSC) event during the closing of the Paratethys ca. 13.8 Ma ago (Peryt, 2006), resulted in the deposition of massive amounts of marine salt rocks in the eastern margin of the Transylvanian Basin (Romania). Fluid inclusions in halite, collected from the locality of Praid, offer insights into the properties and history of marine fluids and paleoenvironment in this region.

The halite trapped both primary (p) and secondary (s) fluid inclusions (FI). The negative crystal shaped pFI (50-100 µm in diameter) are distributed along growth zones of halite and represent droplets of the paleo seawater from which halite precipitated. These FI appear only as single-phase liquid inclusions at room temperature, and are possibly in a metastable state. Therefore, the bubble nucleation was induced by cooling the inclusions to -20 °C to overcome the metastable barrier. The pFI show homogenisation temperatures ( $T_h$ ) to liquid ranging from 10 °C to 24 °C, values typical for a marine formation environment. The measured eutectic temperatures ( $T_e$ ) during low-temperature microthermometry range from -55 °C to -42 °C, indicating the potential presence of Ca and Mg besides Na in the fluids.

Cryogenic Raman spectroscopy was performed on the pFI to better determine their chemical composition. Raman spectra were collected following the secondary freezing method of Ni et al. (2006) to avoid the formation of disequilibrium solid assemblages, and to observe the series of all bands of various salt hydrates. Initial freezing to -190 °C indicates only the peak for water ice (Fig. 1). A heating of the inclusions to -70 – -50 °C followed by re-freezing causes recrystallisation in the FI, and the appearance of characteristic bands of salt-hydrates on the Raman spectra of these inclusions. Several salt phases such as Na-, Ca- and Mg-hydrates can be distinguished on the spectra (Fig. 1), in agreement with the observed low  $T_e$  values. The collected spectra show fairly consistent peak positions with sharp/narrow bands. Typical wavenumbers are at 3404, 3422, 3436, 3538 cm<sup>-1</sup>, only the presence of Mg-hydrate (~3513 cm<sup>-1</sup>) is varying in the measured samples. The pFI also contain SO<sub>4</sub><sup>2-</sup> besides H<sub>2</sub>O, as confirmed by the Raman band at 983 cm<sup>-1</sup>.

The sFI appear along healed microfractures and halite grain boundaries, containing gas-rich fluids. Based on Raman spectroscopy at room temperature the gas phase contains low density N<sub>2</sub>

and CH<sub>4</sub>. These later fluids may be originated from organic matter trapped during later burial.

The examined fluid inclusions in halite at Praid suggest a complex fluid evolution beginning at the precipitation of the halite and through to deformation during burial. The pFI are proxy to paleo-seawater and show its complex salinity during salt deposition, while the sFI are witnesses of a possible fluid migration event potentially related to the halokinetic deformation of halite.

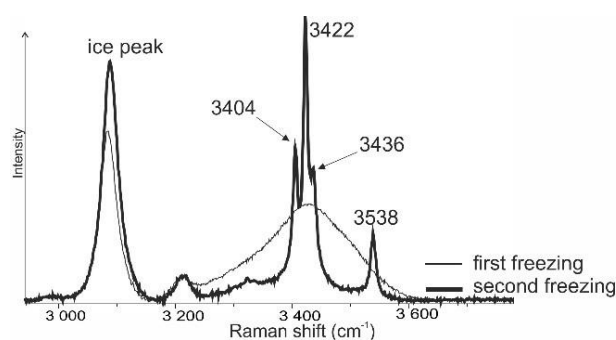


**Fig. 1.** Characteristic Raman spectra of P-type fluid inclusions on -190 °C after first (hairline) and second (thick black) freezing in the stretching regions of structural H<sub>2</sub>O.

## Acknowledgement

This work was supported by the ELTE Excellence Program (1783-3/2018/FEKUTSTRAT) supported by the Hungarian Ministry of Human Capacities and by the European Union and the State of Hungary, co-financed by the European Regional Development Fund in the project of GINOP-2.3.2-15-2016-00009 'ICER'.

## References

- Ni P. et al. (2006) Chin. Sci. Bull. 51:108-114.
- Peryt T.M. (2006) Sediment. Geol. 188-189:379-396.

## Fluid inclusion in apatite of the Sorkhe-Dizaj magnetite deposit (Tarom, NW Iran)

**Ghahramani, S.<sup>1\*</sup>, Tarantola, A.<sup>2</sup>, Whitechurch, H.<sup>1</sup> & Jannessary, M.R.<sup>3</sup>**

<sup>1</sup>Université de Strasbourg CNRS, IPGS-EOST, France; <sup>2</sup>Université de Lorraine, CNRS, GeoRessources, F-54506 Vandœuvre-lès-Nancy, France; <sup>3</sup>Geological Survey of Iran; \*sghahramani@unistra.fr

The Sorkhe-Dizaj magnetite-apatite deposit is located in the Alborz-Azarbaijan magmatic belt in the Tarom volcano-plutonic zone (NW Iran). Field, petrography and geochemistry investigations demonstrate that the quartz-monzodiorite to monzogranite pluton of Early Oligocene age (41 Ma) (Nabatian et al., 2014), intrudes Eocene volcanic rocks including high-K calc-alkaline pyroclastic and lava flows (Amand Member of Karaj Formation). The mineralisation of magnetite and apatite is associated with large lenticular bodies, stockwork, veins and dykes that crosscut intrusive plutonic rocks. The mines are currently, exploited for iron. However, geochemical studies indicate high concentrations of REE in the apatite and the associated accessory minerals (monazite and thorite). The aim of the present study is to (1) characterise the REE ore deposit, associated with the Kiruna-type Fe-deposit, (2) determine the temperature and depth of formation of the REE-bearing phases, (3) understand the fluid characteristics (*T*, composition, redox state) in equilibrium with the REE phases.

Through petrographic studies, fluid inclusions (FIs) of sub to euhedral apatite crystals (within magnetite) classified to the primary which most trapped during crystals growth, secondary FIs as transgranular and rare pseudosecondary. 7 types of primary FIs are recognised: Monophase Type A1 and A2, containing only liquid (L) and only vapour (V); two-phase Type B, subdivided into Type B1 (L+V), the most common liquid-rich, with 10 to 30 vol% vapour; type B2 (L+V) vapour-rich between 50 to 60 vol% and Type B3 (L+S), containing liquid and opaque daughter minerals; multiphase Type C (L+V+S) liquid-vapour with halite and opaque daughter minerals subdivided into Type C1 (Fig. 1) the second most frequent type with 10 to 40 vol% vapour, and Type C2 multiphase solid vapour-rich with 50 to 60 vol% vapour; Multisolid Type C3, containing saturated aqueous salt, more than 50 vol% salt crystals and opaque daughter minerals. 5 types of secondary FIs are classified into monophase A1, A2, two-phase B1, B3 and multiphase C1.

First primary FIs are trapped as heterogeneous saturated solution with suspended solids type C3, Microthermometry results show Type C3 have two ranges  $Th_{LV-L}$  (340-401 °C) and (179-240 °C) contain the highest salt content (23-43 wt% NaCl eq.); concurrence homogeneous saturation Type B2 and C2, high  $Th_{LV-L}$  (304-406 °C); then, homogeneous shrinkage type B1 and C1, having low  $Th_{LV-L}$  (150-274 °C), type B1 have lower salinity (0-13 wt%); at the end secondary FIs of types C1

and B1 show low  $Th_{LV-L}$ , (137-234 °C) and (115-228 °C) salinity of 3-23 wt% were trapped in secondary healed fractures. Boiling solution results in type A1, A2 and B3. The low eutectic temperatures (-50 to -20 °C) suggest that NaCl and CaCl<sub>2</sub> are present in the aqueous solution of the FIs. Phase ratios, compositions and Raman spectrometry indicate a series of FIs that have been trapped in different proportions of vapour and liquid-like density together with salt crystals. The daughter mineral phase was identified as magnetite. The vapour phase does not show any presence of CO<sub>2</sub>, CH<sub>4</sub> or N<sub>2</sub>.



**Fig. 1.** Primary fluid inclusion (Type C1) containing vapour, liquid, a halite crystal and 2 opaque daughter minerals; doubly polished section visualised by PPL at room temperature. (Sorkhe-dizej-Tarom)

The geochemical results (REE patterns) suggest that the apatite crystallised from magmatic fluids. The results of the present study of fluid inclusions in the apatite show that they have an elevated homogenisation temperature and high salinity. These results suggest a magmatic origin high temperature and high salinity (type C3, B2 and C2) followed quickly by lower temperature and salinity hydrothermal fluids (type B1 and C1) during the crystallisation of the REE-bearing phases. These results corroborate those of Nabatian and Ghaderi (2013), but attribute a preponderant role to the magmatic-hydrothermal fluids of high temperature for the crystallisation of the first generation of REE-bearing phase.

### References

- Nabatian G. et al. (2014) *Lithos* 184-187:324-325.  
Nabatian G. and Ghaderi M. (2013) *Int. Geol. Rev.* 55:397-410.

# Idiomorphic quartz replacements in Late Jurassic reef limestones of the East Cameros Basin (N Spain)

González-Acebrón, L.<sup>1\*</sup>, Pérez-Garrido, C.<sup>1</sup>, Arribas, J.<sup>1,2</sup>, & Mas, J.R.<sup>1,2</sup>

<sup>1</sup>Faculty of Geology, Complutense University of Madrid, Spain; <sup>2</sup>Geosciences Institute (IGEO-CSIC), Spain;

\*lgcebron@geo.ucm.es

Euhedral quartz crystals appear as a replacement in the Late Jurassic reef limestones in the south area of the East Cameros Basin (N Spain), close to San Felices town (Soria province). This reef unit is 31 m thick and is built up by crystalline inequigranular limestones, which show dull orange luminescence and non-ferroan calcite composition. This calcite contains Mg-rich muscovite solid inclusions and isolated 35-40  $\mu\text{m}$ -size fluid inclusions with variable liquid: vapour ratio and  $T_m(\text{Ice})$  around 0 °C. In these limestones, pebble size quartzite discharges appear as a lateral facies change, which can be interpreted as delta fans.

The quartz hexagons are sticks of 3-8 cm long and up to 0.5 cm thick, with a dirty centre (Fig. 1A). Under the microscope, they show a cloudy nucleus very rich in solid inclusions of non-ferroan calcite, Mg-rich muscovite and two types of fluid inclusions (Fig. 1A). Type 1 are primary, 40-70  $\mu\text{m}$ -size and present variable L:V ratios (50:50 to almost all-gas, Fig. 1B). No response under freezing runs (until liquid nitrogen temperature) has been observed in this type of fluid inclusions. Type 2 are pseudosecondary, 6-18  $\mu\text{m}$ -size and present a liquid:vapour:solid ratio of 90:5:5, in which the solid is halite daughter mineral (Fig. 1C). These fluid inclusions freeze around -100 °C. No other nucleation temperature has been observed during freezing runs (until liquid nitrogen temperature). Upon heating, these fluid inclusions show a final melting of a solid at -56.6 °C and eutectic temperatures around -52 °C, pointing to a  $\text{NaCl}+\text{CaCl}_2+\text{H}_2\text{O}+\text{CO}_2$  system. Next observed measurement is the homogenisation of the gas bubble to the liquid, which is between 260 and 282 °C, followed by the melting of the halite -  $T_m$  (Halite)-at temperatures of 277-288 °C.

Some quartz crystals of small size (<1 mm) are detected in the conglomeratic unit located stratigraphically below the reef limestones, as well as some replazative nodules of Mg-rich muscovite, quartz and Fe-rich chlorite. They present oval shape and are around 0.3-2.2 cm-long. Inside the nodules, some quartz grains present quartz overgrowths, showing a rim of Mg-rich muscovite solid inclusions around the boundary of the grain.

The origin of both the nodules and the idiomorphic crystals is related to the hydrothermal process which occurred after basin infilling during the mid-Cretaceous. The  $T_m(\text{Halite})$  of primary fluid inclusions in the idiomorphic crystals are in agreement with previous studies in the area:  $T_h(\text{total})$  of 195-350 °C were measured in primary

fluid inclusions in quartz veins cutting Tithonian sandstones and limestones (González-Acebrón et al., 2011). The fluid which formed the idiomorphic crystals was of higher salinities than for the quartz veins, as manifested by the presence of halite daughter minerals.

Finally, the fluid inclusions in the crystalline limestone with variable L:V ratios and  $T_m(\text{Ice})$  around 0°C indicate the limestone has suffered recrystallisation in a vadose environment during telodiagenesis.

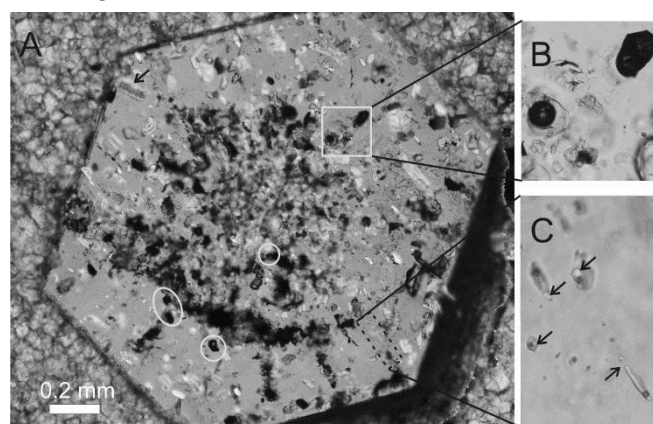


**Fig. 1.** A) Quartz hexagon crystal showing calcite nucleus, solid inclusions of muscovite (arrow) and two types of fluid inclusions: Type 1 (solid lines), B) and type 2 (dotted line), C) arrows point to halite daughter minerals.

## Acknowledgement

Spanish DIGICYT Project CGL2014-52670, research group "Sedimentary Geology, Paleoclimate and Environmental Change (CLIMSED) Ref: 910198" of the Complutense University of Madrid.

## References

González-Acebrón L. et al. (2011) Int. J. Earth Sci. 100:1811-1826.

# Rinneite daughter minerals in highly saline inclusions of the Nepa potash deposit (Siberia)

Grishina, S.<sup>1\*</sup>, Polozov, A.G.<sup>2</sup> & Maximovich, Y.<sup>3</sup>

<sup>1</sup>Sobolev Institute of Geology and Mineralogy Siberian Branch of the Russian Academy of Sciences, Russia;

<sup>2</sup>Institute of Geology of Ore Deposits, Petrography, Mineralogy and Geochemistry, Russia; <sup>3</sup>Novosibirsk State University, Russia; \*grishina@igm.nsc.ru

Little information is provided in the literature concerning the characterisation of potash deposits (Kemp et al., 2013). The origin of barren zones is one of the unsolved problems. The Nepa potash deposit, situated on the Siberian Platform is one of the largest potash deposits in the world. Magnetite mineralisation and oil are common within the Nepa deposit. A characteristic feature of the Nepa potash deposit is the presence of barren zones, represented by halite-calcite and halite-calcite-anhydrite rocks, replacing the potassium salts horizons. Along dolomite and calcite, the mineral assemblages contains silicates, sulphides and oxides that are unusual for worldwide barren zones of other potassium deposits. According to the most common model the formation of such specific zones was linked to the presence of dolerite sills, dikes and explosion pipes within the deposit.

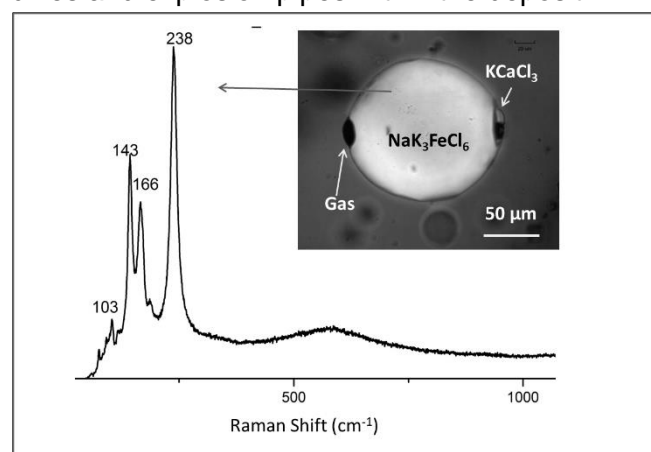


**Fig. 1.** Raman spectra of a rinneite daughter mineral in polyphase inclusion in halite from the Nepa potash deposit.

“Black salts” are another specific feature of the Nepa deposit. The impregnation of ore minerals (pyrrhotite, pyrite and magnetite) is a characteristic feature of black salts. In this study we compare fluid and mineral inclusion associations from the barren zones, where magmatic activity was not detected, and from black salts in the vicinity of dolerite sills. Borehole 194 was drilled at the centre of the potash deposit and intersects the salt interval at 700-960 m, and dolerite sills at 842.5-885 m. Black salts were picked up at 1.5 and 6 m from the upper contact, and at 10 m below the sill.

Rinneite ( $\text{NaK}_3\text{FeCl}_6$ ) was identified based on SEM-EDS and Raman analysis, both as individual inclusions and as daughter minerals, in association with chlorocalcite ( $\text{KCaCl}_3$ ) and hydrates ( $\text{CaCl}_2 \cdot n\text{H}_2\text{O}$ ) in the highly saline inclusions.

Raman spectra of rinneite presented here for the first time from natural samples (Fig. 1). It is very close to the reported spectra of saltonseite ( $\text{K}_3\text{NaMnCl}_6$ ) (Kurosawa et al., 2016), which is isostructural with rinneite (Kampf et al., 2012). Rinneite was documented in halite-calcite rocks from barren zones and in black salts near dolerite sills.

Highly saline Fe-bearing brine inclusions were found at the upper and lower contact zones of the sill in well 194 from the Nepa potash deposit, in contrast to reported characteristic anhydrous  $\text{CaCl}_2$ -bearing inclusions, documented on the contact of bedded salts with dolerite intrusions (Grishina et al., 1992). Formation of Fe-bearing fluids could be related to a hydrothermal system that provided leaching of Fe from dolerite, process that agrees well with experimental data.

The observed Fe-bearing highly saline fluid inclusions support a post-sedimentation model for the formation of barren zones.

## Acknowledgement

This work is partly supported by Russian Foundation for Basic Research (grant 18-05-00682).

## References

- Grishina S. et al. (1992) *Eur. J. Mineral.* 4:1187-1202.
- Kampf A.R. et al. (2012) *Mineral. Mag.* 76:807-817.
- Kemp S.J. et al. (2016) *Econ. Geol.* 11:719-742.
- Kurosawa M. et al. (2016) *Geochim. Cosmochim. Ac.* 182:216-239.

# Sulphate-rich melt inclusions as evidence of interaction between chloride xenoliths and kimberlites in Udachnaya-East pipe

Grishina, S.<sup>1\*</sup>, Maximovich, Y.<sup>2</sup>, Tomilenko, A.A.<sup>1</sup> & Smirnov, S.Z.<sup>1,2</sup>

<sup>1</sup>V.S. Sobolev Institute of Geology and Mineralogy, Siberian Branch of the Russian Academy of Sciences, Russia;

<sup>2</sup>Novosibirsk State University, Russia; \*grishina@igm.nsc.ru

Association of alkali sulphates and chlorides have been found in inclusions of different settings ranging from magmatic (Abersteiner et al., 2018 and references therein) to sedimentary (Lowenstein et al., 2016). In this study we document similar assemblage of daughter minerals in polyphase sulphate-rich inclusions found in chloride xenoliths from kimberlites of Udachnaya-East pipe.

Two halite generations: carbonate free (halite-1) and carbonate-bearing (halite-2) were distinguished in xenoliths according to mineral and fluid inclusion study by SEM-EDS and Raman analyses. Inclusion assemblage of halite-1 is similar to those in metamorphosed halite from bedded salts (Grishina et al., 1992). Sulphate-rich inclusions were found in halite-2 along with mineral assemblage identical to the host kimberlite: calcite, olivine, monticellite, perovskite, titanomagnetite, ilmenite, alkali sulphates, alkali sulphide (rasvumite).

Globular sulphate-rich inclusions occur along distinct planes cutting across the halite crystals. The globules vary in size from 10 µm to 300 µm in diameter. Sulphur-rich inclusions contain highly variable volumetric ratios of solid phases and compressed gas. The globule assemblage (Fig. 1) consists of predominantly sulphates and subordinate carbonate and silicate phases. Aphthitalite ( $K_3Na(SO_4)_2$ ), cesanite ( $Ca_2Na_3[(OH)(SO_4)_3]$ ), thenardite ( $Na_2(SO_4)$ ) and an unknown carbonate-sulphates are ubiquitous in polyphase inclusions. Calcites, dolomite and tetraferriphlogopite were found episodically in globules from outer layers of concentrically zoned rounded xenoliths. Additional components: langbeinite ( $K_2Mg_2(SO_4)_3$ ),  $MgSO_4$ ,  $CaSO_4$ ,  $SrSO_4$ , tychite  $Na_6Mg_2(CO_3)_4(SO_3)$ ,  $MgCO_3$  were identified in the peripheral part of the angular xenoliths. Carbonate-sulphate exsolution lamellae in the host aphthitalite extend to the edges of the inclusions, indicating that the entrapment of the globules preceded exsolution.

According to Raman spectroscopy analysis spatially associated gas inclusions evolved from pure  $CO_2$  in halite-1 to  $H_2$ -hydrocarbon-bearing inclusions in halite-2. Detection of  $CH_4$ - $H_2$ -bearing gas inclusions has suggested that thermal decomposition of buried organic material or serpentinisation of olivine may be the gas source. GC-MS analysis revealed more complex composition of volatiles in halite-2: hydrocarbons and their derivatives, sulphur-bearing compounds (carbon disulphide ( $CS_2$ ), and dimethyl disulphide

( $C_2H_6S_2$ ), which are characteristic for oil-bearing sediments of Siberian salt deposits (Kontorovich et al., 1997).

Origin of chloride xenoliths is highly debated (Abersteiner et al., 2018).

Evolution of gas composition from  $CO_2$  at the centre of xenoliths to complex hydrocarbons- $H_2$ -bearing at the rims may be best explain by flash alteration of xenoliths rather than differentiation of kimberlite melt.

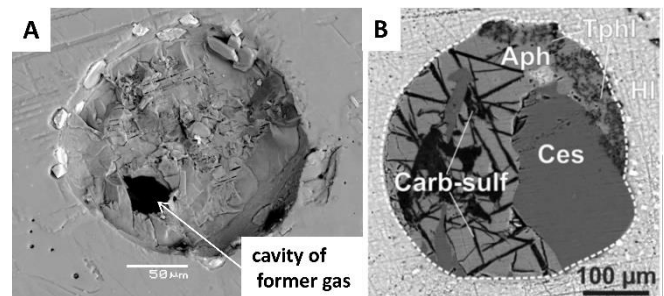


**Fig. 1.** A) BSE image of exposed sulphate inclusion in halite-2; B) polished surface of cut sulphate-rich inclusion. SEM images showing morphology and composition of sulphate-rich inclusions in halite-2: Aph-aphthitalite, Ces-cesanite, Tphl-tetraferriphlogopite, HI-halite.

## Acknowledgement

This work is partly supported by Russian Foundation for Basic Research (grant 18-05-00682).

## References

- Abersteiner A. et al. (2018) J. Petrol. 59:1467-1492.
- Grishina S. et al. (1992) Eur. J. Mineral. 4:1187-1202.
- Kontorovich A. et al. (1997) Petrol. Geosci. 3:359-369.
- Lowenstein T. K. et al. (2016) Geol. Soc. Am. Bull. 128:1555-1568.

# Mikheevskoe porphyry copper deposit: conditions of ore formation; insights from fluid inclusion study and alteration mineralogy

Groznova, E.<sup>1,2\*</sup>, Abramov, S.<sup>2</sup>, Plotinskaia, O.<sup>2</sup> & Bocharov, V.N.<sup>3</sup>

<sup>1</sup>Institute of Experimental Mineralogy, Russian Academy of Sciences (IEM RAS), Russia; <sup>2</sup>Institute of Geology of Ore Deposits, Petrography, Mineralogy and Geochemistry, Russian Academy of Sciences (IGEM RAS), Russia; <sup>3</sup>St Petersburg University, Russia; \*grozelena@yandex.ru

Mikheevskoe Cu-Au-Mo deposit (South Ural, Chelyabinsk region) is associated with porphyritic magmatism of diorite composition. The deposit is confined to the belt of dikes of quartz diorites and their porphyry differences, which is stretched submeridionally between two large diorite bodies.

Porphyry-style mineralisation is represented by bornite-chalcopyrite association in the central part, to chalcopyrite, pyrite-chalcopyrite and then pyrite mineralisation in the outer parts (Plotinskaia et al., 2018). The wall-rock alteration minerals associated with porphyry ore mineralisation (biotite, hornblende, early chlorite) have been replaced by metamorphic minerals: epidote, prehnite, pumpellyite, chlorite (Abramov et al., 2016). Therefore, it can be assumed that a part of the ore mineralisation was also recrystallised (metamorphosed) at prehnite- pumpellyite facies conditions.

Microthermometric measurements were carried out using a THMSG-600 (Linkam) microscope heating-freezing stage installed on a BX-41 "Olympus" microscope (lens 50x) at the Institute of Experimental Mineralogy of Russian Academy of Sciences (IEM RAS), Chernogolovka. The homogenisation temperatures ( $T_{\text{hom}}$ ) were determined from the point of transition of gas into the solution. The salt composition of the fluids was determined from the eutectic temperature ( $T_e$ ). The concentration of salts (in wt% - eq. NaCl.) was calculated from the melting point ( $T_{\text{melt}}$ ) of the last ice crystal of dissolution of the solid phase. The compositions of the gas phases of fluid inclusions (FI) were studied by the Raman spectroscopy method (LabRAM-HR800) in the RC Geomodel, St.Petersburg University.

Most of the studied FI contain two phases (vapour + liquid) in different ratios. Inclusions with three phases (gas+liquid+halite) were determined only in two samples.  $T_{\text{hom}}$  of all studied FI vary from 165 to 350 °C, but in most cases does not exceed 250 °C (Fig. 1).

The salinity varies mainly from 3 to 15 wt%, NaCl eq.; chloride brines (31–33 wt%, NaCl eq.) were found only in one sample. Most FI studied have a Na-chloride composition ( $T_e = -23.5$  to  $-36$  °C), in three samples inclusions containing solutions of the composition Mg, Na-Cl and Ca(Mg, Na)-Cl were identified. The fluid density is 0.9 – 1.1 g/cm<sup>3</sup>. In the vapour phase of several FI, carbon dioxide was detected by Raman spectroscopy, but freezing did not occur during cryometry, which indicates a low fluid density.

The study of FI in minerals of ore associations (Groznova et al., 2015) showed that in most samples fluid inclusions corresponding to the porphyry stage of the Miheevskoe deposit were not preserved. The temperature range of  $T_{\text{hom}}$  agrees with the estimates of the temperatures of metamorphic recrystallisation the rocks of the deposits (170-350 °C) (Abramov et al., 2016).

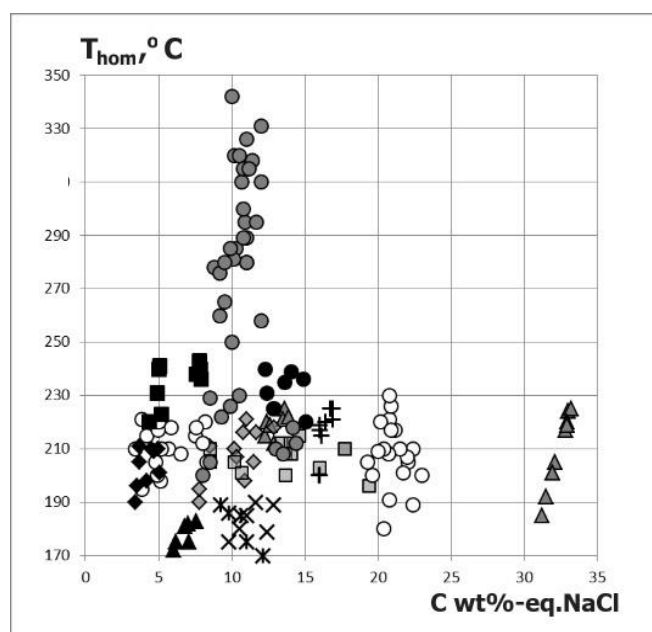


Fig. 1. Homogenisation temperatures and concentrations of fluid inclusions in quartz from various associations (black and grey symbols) of the Mikheevskoe deposit. White circles - epithermal precious metal mineralisation.

## Acknowledgement

Supported by RFBR projects ##19-05-005245 and 19-05-00476.

## References

- Abramov S.S. et al. (2016) in: Proceedings of the International Scientific Conference dedicated to the 300<sup>th</sup> anniversary of the Mineralogical Museum. RAS, Moscow, 2016, 3-4.
- Groznova E.O. et al. (2015) in: ECROFI 2015:70-71.
- Plotinskaya O.Y. et al. (2018) Ore Geol. Rev. 94:239-260.

## Natrocarbonatites: a product of three-phase immiscibility

**Guzmics, T.<sup>1\*</sup>, Berkesi, M.<sup>1</sup> & Szabó, Cs.<sup>1</sup>**

<sup>1</sup>Lithosphere Fluid Research Lab, Institute of Geography and Earth Sciences, Eötvös Loránd University, Hungary;  
\*tiber.guzmics@gmail.com

The origin of natrocarbonatites has been debated for decades by petrologists because experimental results and natural observations do not come to an agreement. Experimental work (Weidendorfer et al., 2017) and observations on Kerimasi (KER) melt inclusions (Guzmics et al., 2012) show evidence for the formation of Na-rich carbonate melt by progressive crystallisation of calcite and F-apatite from a Ca-rich carbonate melt, in the absence of silicate melt. Such a magmatic process would generate a significant amount of calciocarbonatite rocks, but such lithologies have not been found at Oldoinyo Lengai (OL). Furthermore, the coexistence of silicate and carbonate melts is visible from nepheline-hosted melt inclusions hosted in nephelinite rocks at OL. In addition, formation of natrocarbonatite melt by unmixing from nephelinite melt is unlikely based on experimental results (Kjarsgaard et al., 1995) indicating that natrocarbonatite and nephelinite rocks form immiscible melts 150-450 °C above the eruption temperatures of OL natrocarbonatite melts. The lack of agreement between experimental results and natural observations led to theories that OL natrocarbonatites formed as a condensate from hydrous carbonate fluids that unmixed from nephelinite melt (Nielsen and Veksler, 2002).

The melt and fluid inclusions provide previously unavailable data as carbonate melt and the fluid condensate described by previous models (Veksler and Keppler, 2000) are not preserved in fossil rocks due to their high reactivity at surface conditions, including contact with moist air.

Here, we present a model (Guzmics et al., 2019) of natrocarbonatite formation that explains discrepancies between experimental results and natural observations. We show evidence for the presence of coexisting nephelinite melt, F-rich carbonate melt and alkali carbonate fluid (Fig. 1). Compositions of these phases differ from the composition of OL natrocarbonatites, therefore, it is unlikely that natrocarbonatites formed directly from one of these phases. On the other hand, mixing of the outgassing alkali carbonate fluid and the F-rich carbonate melt can yield natrocarbonatite compositions at temperatures close to subsolidus temperatures of the nephelinite (<630-650 °C).

Moreover, we show that fluorine concentrations of up to 14 wt% in the carbonate melt leads to significant suppression of the calcite liquidus, preventing calcite precipitation during nepheline crystallisation. In addition, the observed low H<sub>2</sub>O (<4 wt%) content of the alkali carbonate fluid phase

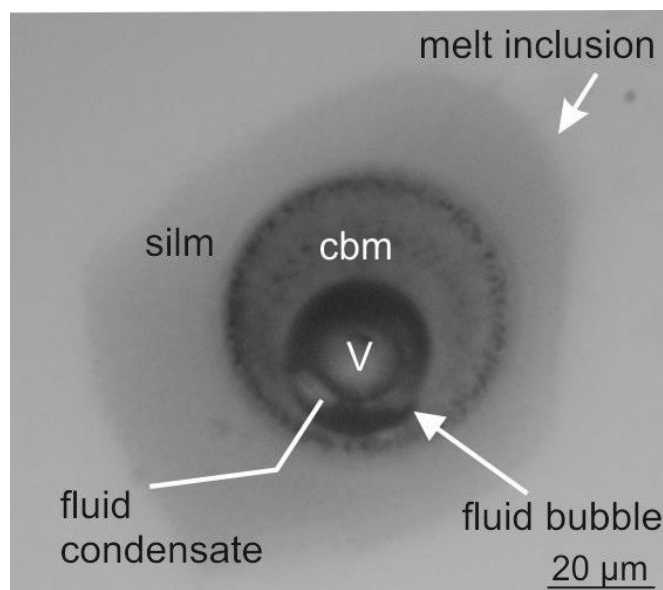


**Fig. 1.** Photomicrograph of run product in nepheline-hosted melt inclusion quenched from 850 °C, containing quenched silicate melt (silim), carbonate melt (cbm), and a fluid bubble. v—vapour CO<sub>2</sub>; fluid condensate—natrite<sub>ss</sub> + nahcolite, where natrite<sub>ss</sub> is natrite solid solution.

shows that a water-rich environment is not required for the generation of natrocarbonatites as suggested by previous models. Our model is consistent with the observation that natrocarbonatites are associated with nephelinite rocks, as occurs at OL, rather than with calciocarbonatites.

### Acknowledgement

This study was supported by the project NKFI K-119535.

### References

- Guzmics T. et al. (2012) *Contrib. Mineral. Petr.* 164:101-122.
- Guzmics T. et al. (2019) *Geology* 47:527-530.
- Kjarsgaard et al. (1995) in: *IAVCEI Proceedings in Volcanology* 4:163-190.
- Nielsen T.F.D. and Veksler I.V. (2002) *Contrib. Mineral. Petr.* 142:425-435.
- Veksler I.V and Keppler H. (2000) *Contrib. Mineral. Petr.* 138:27-34.
- Weidendorfer D. et al. (2017) *Geology* 45:507-510.

# Sulphur isotope and microthermometric characteristics of the carbonate-replacement type (CRD) Altinoluk Pb-Zn-Cu±Au±Ag deposit, NW Turkey

Hanilçı, N.<sup>1\*</sup>, Kasapçı, C.<sup>1</sup> & Öztürk, H.<sup>1</sup>

<sup>1</sup>Department of Geological Engineering, Avcılar Campus, Istanbul University-Cerrahpaşa, Turkey;

\*nurullah@istanbul.edu.tr

The Altinoluk Pb-Zn-Cu±Au±Ag deposit is located at the Biga Peninsula in NW Turkey. The Eocene and Miocene magmatic rocks, which are extensively exposed in the Biga Peninsula, are associated with a large number of porphyry type Au-Cu-Mo, skarn-type Pb-Zn±Cu and epithermal Au mineralisations in the region.

The Altinoluk Pb-Zn-Cu±Au±Ag deposit occurs within the Paleozoic rocks of the Kazdağ Massif. The deposit formed along marble and amphibole schist contacts as banded and lens-shaped zones that lie parallel to the foliation in the amphibole schist, dipping 7-18°. The orientation of the ore zones is approximately N-S. Vein thicknesses range between 30 and 150 cm, and have lengths in the direction of inclination varying between 100 and 150 m. Although the ore mostly shows a banded structure, breccia fill and vuggy structure is also defined. Banded, comb, feathery and stockwork textures are observed in the quartz.

The ore assemblage consists of galena, sphalerite, chalcopryrite, pyrite, chalcocite, covellite, quartz and calcite.

Stable sulphur isotope analysis was carried out on 12 samples (7 galena and 5 sphalerite). The  $\delta^{34}\text{S}_{\text{VCDT}}$  values of both minerals ranges between 3.34 and 7.48 ‰. The average  $\delta^{34}\text{S}_{\text{VCDT}}$  values of sulphide minerals is 5.08 ‰. The narrow range of  $\delta^{34}\text{S}$  values indicates a homogeneous sulphur source. Sulphur isotope data indicates that sulphur in sulphides was most probably derived from a magmatic system.

Microthermometric data was obtained from fluid inclusions in quartz and sphalerite. The fluid inclusions are regular in shape and have sizes varying from 5 to 50  $\mu\text{m}$  (Fig.1 a, b). All data was obtained from primary fluid inclusions. The homogenisation temperature ( $T_h$ ) varies between 167 and 268 °C in quartz and between 179 and 225 °C in sphalerite. The average  $T_h$  in quartz and sphalerite is 216 °C ( $n=87$ ) and 197 °C ( $n=8$ ), respectively. The average calculated salinity of fluid inclusions is 5.2 and 5.5 wt% NaCl equivalent in quartz and sphalerite, respectively (Fig.1c).

Two intrusives, Narlı-Şelale and Altinoluk, are located 1.5 km away from the Altinoluk deposit. The deposit occurs between the amphibole schist and marble, and no skarn minerals have been observed.

The mean  $T_h$  of the fluids responsible for the mineralisation is 214 °C and salinity is 5.26 wt% NaCl equivalent. The sulphur isotope data, moderate  $T_h$  and relatively low salinity of the fluids indicates that the Altinoluk deposit was formed

related to magmatic activity, as a carbonate replacement type (CRD) mineralisation.

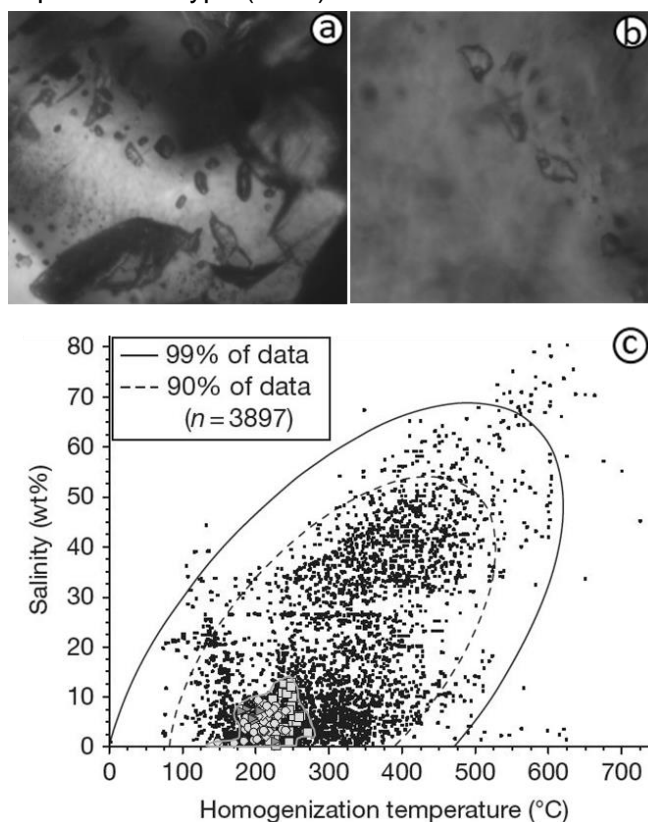


**Fig. 1.** Two-phase liquid-rich fluid inclusions in A) sphalerite and B) quartz in Altinoluk Pb-Zn-Cu±Au±Ag. and C) fluid inclusion homogenisation temperature-salinity pairs from 3897 individual fluid inclusions from skarn deposits (after Bodnar et al., 2014) and distribution of  $T_h$  vs. salinity for quartz and sphalerite from the Altinoluk Pb-Zn-Cu±Au±Ag deposit (gray area).

## References

Bodnar R.J. et al. (2014) in: Treatise on Geochemistry 2<sup>nd</sup> ed. 13:119-142.

# Fluid inclusion evidence for the role of marine (evaporitic) brines during the formation of volcanic-hosted Cu deposits in the Neoproterozoic Caledonian Highlands, New Brunswick, Canada

Hanley, J.<sup>1\*</sup>, Tweedale, F.<sup>1</sup>, Zajacz, Z.<sup>2</sup>, Tsay, A.<sup>2</sup>, Sharpe, R.<sup>3</sup> & Fayek, M.<sup>3</sup>

<sup>1</sup>Dept. of Geology, Saint Mary's University, Canada; <sup>2</sup>Dept. of Earth Sciences, University of Toronto, Canada; <sup>3</sup>Dept. of Geological Sciences, University of Manitoba, Canada; \*jacob.hanley@smu.ca

Vein-hosted Cu (-Au-Ag-Bi) mineralisation in the Neoproterozoic Caledonian Highlands, southern NB, Canada, occurs within quartz-carbonate-rich shear zones cross cutting felsic lithic tuffs, minor sandstones, intermediate intrusives, and interbedded felsic and mafic flows of the Neoproterozoic Broad River Group (~ 620 Ma). Mineralisation in the quartz-carbonate veins consists of chalcopyrite in deep veins and bornite-chalcocite-hematite in shallower veins (Fig. 1A), with later supergene alteration of the ores to cuprite-malachite. Precious metal and accessory phases consist of electrum and bismuthinite. Wall-rock alteration is characterised by sericitisation, albitisation, and paragonitisation. Replacement of chalcopyrite by bornite and by chalcocite-hematite (Fig. 1B) indicates changes in fluid redox to more oxidising conditions as mineralisation progressed. Sulphide mineralisation is coeval with carbonate precipitation, infilling fractures and dissolution cavities/vugs in the quartz.

Fluid inclusions in quartz are two-phase liquid-vapour at room temperature (Fig. 1C). Homogenisation occurs by vapour bubble disappearance between 150-270 °C (n=70); however, individual assemblages show relatively narrow ranges (e.g., 173-191 °C, n=22). Bulk salinities from final ice melting range from 4 to 13 wt% NaCl eq. (narrower for individual assemblages). Later assemblages of hypersaline, Ca-rich brine inclusions (Fig. 1D-E) in vein infilling carbonate have fluid composition (LA-ICPMS) consistent with evaporated seawater (Ca/Na>4.5; 10<sup>3</sup> ppm of Mg-K-Sr-Pb-Zn-Ba) and are Cu-bearing (20-70 ppm), whereas earlier quartz-hosted inclusions show elevated B-Cs-As consistent with magmatic vapour. Stable isotope data for pre-ore quartz ( $\delta^{18}\text{O}_{\text{bulk}} = 15.1\text{‰}$ ;  $\delta^{18}\text{O}_{\text{SIMS-qtz}} = 11.8 \pm 1.5\text{‰}$ , 1s, n=40) and chlorite ( $\delta^{18}\text{O}_{\text{bulk}} = 6.9\text{‰}$ ;  $\delta\text{D}_{\text{bulk}} = -60.1\text{‰}$ ) and post-ore calcite ( $\delta^{18}\text{O}_{\text{bulk}} = 13.7\text{--}17.2\text{‰}$ ;  $\delta^{13}\text{C}_{\text{bulk}} = -5.3$  to  $-4.4\text{‰}$ ) combined with Sr isotope data (calcite:  $^{87}\text{Sr}/^{86}\text{Sr}_0 = 0.70743\text{--}0.70902$ ), LA-ICPMS and microthermometric data suggest that the metal-precipitating fluids were mixtures of magmatic fluid and evaporated seawater (estimated  $\delta^{18}\text{O}_{\text{fluid}} \sim 1$  to 6 ‰). Values of  $\delta^{18}\text{O}$  decrease from early euhedral quartz to quartz adjacent to, or enclosed entirely within, bornite-chalcocite by ~ 4‰, due to the incursion of evaporated seawater.

The host setting, vein assemblages and paragenesis, and fluid inclusion and isotope systematics are very similar to Cu sulphide

deposits that overprint basalts in the well-known Keweenawan Cu district (e.g., Mamainse Point, Ontario; Houghton, Michigan; Richards and Spooner, 1989) but involved mixing of metalliferous magmatic fluids with bittern brines rather than meteoric waters. No evaporitic basins existed in the area within the Neoproterozoic. However, Carboniferous-age (~347-331 Ma) evaporitic basins (Visean Windsor group) are a likely bittern source. Therefore, mineralisation *postdates* the host volcano-sedimentary sequence by at least ~200 Ma.

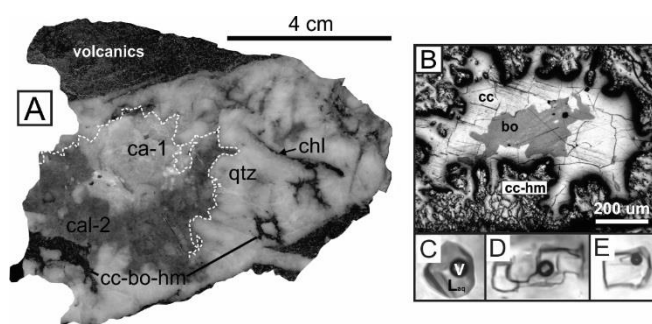


**Fig. 1.** A) Polished slab of a sulphide-quartz-carbonate vein hosted in mafic volcanics (cal=calcite; qtz=quartz; cc-bo-hm=chalcocite-bornite-hematite; chl=chlorite). B) Reflected light (PPL) image of cc-hm replacing cc replacing bo. C) Two-phase (20 °C) moderate salinity fluid inclusion in early quartz. D) Two-phase (20 °C) brine inclusions in late carbonate. E) Two-phase (20 °C) brine inclusions in late carbonate. Fields of view for C-E are 20 µm high.

## Acknowledgement

NSERC (Gov. Canada), Government of New Brunswick

## References

Richards J. and Spooner E. (1984) *Econ. Geol.* 89:360-385.

# Polymetallic U-Ag-Ni-Co-Bi vein deposits in the Northwest Territories, Canada: the product of heating and oxidation of marine evaporite brines and metal-enriched hydrocarbons within crystalline basement

Hanley, J.<sup>1\*</sup>, Trottier, C.<sup>1</sup>, Burke, J.<sup>1</sup>, Ootes, L.<sup>2</sup>, Zajacz, Z.<sup>3</sup>, Tsay, A.<sup>3</sup> & Fayek, M.<sup>4</sup>

<sup>1</sup>Dept. of Geology, Saint Mary's University, Canada; <sup>2</sup>British Columbia Geological Survey, Canada; <sup>3</sup>Dept. of Earth Sciences, University of Toronto, Canada; <sup>4</sup>Dept. of Geological Sciences, University of Manitoba, Canada; \*jacob.hanley@smu.ca

Polymetallic, uranium-bearing “five-metals” type hydrothermal vein systems in the Northwest Territories of Canada, formed in the Proterozoic, show widely contrasting grade and tonnage characteristics from one deposit district to another. The results presented here represent a 4-year study comparing sub-economic, poorly mineralised examples hosted in the Great Slave Lake area (Great Slave Supergroup, and Slave Province) with a historically world-class deposit in the Port Radium area (Eldorado deposit, Great Bear Lake: ~13 Moz Ag; 6000 t U<sub>3</sub>O<sub>8</sub>).

Integration of a variety of microanalytical methods (fluid inclusion microthermometry, SIMS, single fluid inclusion analysis by LA-ICPMS, hot CL, Raman spectroscopy, SEM-EDS) has focused on characterising processes responsible for U-Ni-Co-As-Ag-Bi co-precipitation. Pre-mineralisation fluids were comprised of heated basement brines (rich in Ca-Na-Sr-Ba; ~20-30 wt% CaCl<sub>2</sub> eq.). The onset of mineralisation was associated with the introduction of immiscible hydrocarbon fluid and marine evaporite brine (rich in Ca-Na-Mg-Pb-Zn; 20-35 wt% CaCl<sub>2</sub> eq.), and a shift in brine δ<sup>18</sup>O<sub>VSMOW</sub> by +10 ‰ (Fig. 1A-C).

Notably, whereas basement and basinal brines containing only sub-ppm and low-ppm concentrations of ore metals, respectively, co-trapped (immiscible bitumen (now solid hydrocarbon) inclusions, in contrast, are metal enriched, containing thousands of ppm of U-Ni-Co-Bi-Ag-Sb-As-Mo-Cu (Fig. 1D). Integration of all data types strongly suggests that the precipitation of metals and bitumen was triggered by mixing of heated, oxidising <sup>18</sup>O-depleted crystalline basement brine (metal-poor) with <sup>18</sup>O-enriched basinal-type brines and metal-rich bitumen or oil droplets. Oxidation and heating of the hydrocarbon phase resulted in rapid and efficient metal precipitation at P<0.5 kbar and ~200 °C, constrained by the intersection of brine and carbonic fluid isochores.

The brines and metal-rich hydrocarbons were likely sourced from black shale units in former overlying intracratonic basins (e.g., Hornby Bay, Thelon, Athabasca) that outcrop ~100-700 km away from the study areas. The cation composition (Fig. 1E) of brine inclusions can be used to differentiate small, sub-economic deposits that formed deeper in the basement rocks, farther from overlying sedimentary metal sources from shallower, much larger economic deposits that

formed immediately below mature basin sequences. Importantly, high-grade polymetallic vein systems of this variety may be linked to the protracted metallogenic evolution of previously overlying intracratonic sedimentary basins rather than the basement rocks in which the deposits are hosted. This work provides unambiguous support from the fluid inclusion record for the involvement of basinal ore fluids (c.f. Gandhi et al., 2018; Markl et al., 2016; Burisch et al., 2017).

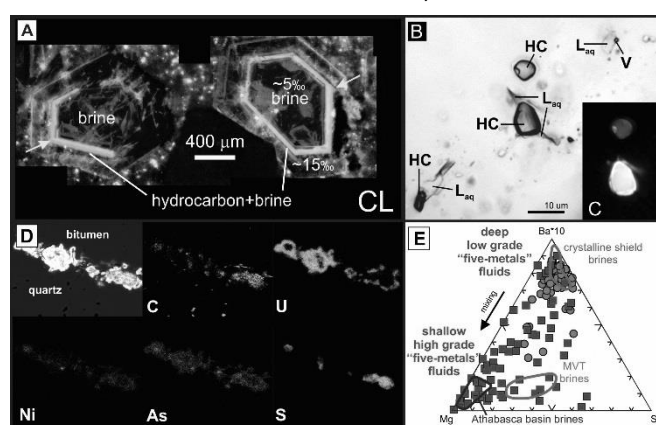


**Fig. 1.** A) Hot CL images showing zoned quartz in arsenide veins. Cores contain brine inclusions, rims have immiscible hydrocarbon-brine. B) Transmitted light (PPL) image of immiscible brine-hydrocarbon fluids. C) Fluorescence of co-trapped hydrocarbons. D) SEM-BSE/X-ray maps of bitumen showing metal enrichment. E) Brine Ba-Mg-Sr ternary (LA-ICPMS) differentiating deep, low-grade, small deposits and shallow, high-grade, large deposits across a mixing trend.

## Acknowledgement

GNWT and GSC Targeted Geoscience Initiative 5.

## References

- Burisch M. et al. (2017) Ore Geol. Rev. 81:42-61.
- Gandhi S. et al. (2018) Ore Geol. Rev. 96:28-47.
- Markl G. et al. (2016) Miner. Deposita 51:703-712.

# Fluid inclusion characteristics of gem quality crystal diaspore, Milas, SW Turkey

**Hepvidinli, B.<sup>1\*</sup> & Hanilçi, N.<sup>1</sup>**

<sup>1</sup>Istanbul University-Cerrahpaşa, Turkey; \*bihterhepvidinli@gmail.com

Turkey is characterised by bauxite deposits located in eight different provinces. Six of which are located in the Anatolide-Tauride belt, one in the Arabian Platform and other one in the Pontides (Hanilçi, 2019). The gem quality diaspore crystals occurred in Küçükçamlik (KC) bauxite, located in Milas-Yatağan province.

Küçükçamlik bauxite experienced low grade metamorphism. This metabauxite occurs between Triassic schist and Jurassic marble. The KC bauxite consist of 61% Al<sub>2</sub>O<sub>3</sub>, 2.5% SiO<sub>2</sub>, 21% Fe<sub>2</sub>O<sub>3</sub> and 2.8% TiO<sub>2</sub>. The gem quality diaspore crystals occurred within the metabauxite zone as cross-cutting veins. According to Hatipoğlu et al. (2010a) the diaspore crystals occur in bauxite zone during the hydrothermal processes.

The Al and Fe rich minerals should have been dissolved in bauxite ore by the aqueous complex and recrystallised. The paragenesis of the veins mainly consists of diaspore, muscovite, hematite, ilmenite, chloritoid, minor quartz, goethite and clay minerals. Diaspore crystals are located within foliation plane, cracks, fractures, fold hinges and discordance of metabauxite (Hatipoğlu et al., 2010b).

The diaspore crystals (Fig. 1a) are transparent to pale-dark green colour in day to and colour-changed feature in incandescent light green, amber to lavender colour, perfect cleavage and V-shape twins.

Three types of primary fluid inclusions were recognised in diaspore crystals. The first type is represented by “liquid-rich” (LV-type) aqueous fluid inclusions, the second type by “liquid-CO<sub>2</sub> + vapour-CO<sub>2</sub>” (CV-type) inclusions the third type by “liquid-H<sub>2</sub>O+liquid-CO<sub>2</sub>+vapour-CO<sub>2</sub>” (LCV-type) inclusions.

The eutectic temperature ( $T_e$  °C) values of carbonic phase-bearing inclusions (LCV and CV types) ranges between -57.2 °C to -28.6 °C. Clathrate formation observed in all type of inclusions, and their clathrate melting temperature ( $T_{m-clth}$  °C) were between 6.1 °C and 17.8 °C.

Due to majority of melting temperature of clathrate higher than 10 °C, the salinity has not been calculated. Salinity calculation has done by using a few  $T_{m-clth}$  which below 10 °C as between 2 and 5 wt% NaCl equivalent.

The  $T_e$  values higher than -56.6 °C and the  $T_{m-clth}$  melting temperature higher than 10 °C of carbonic phase-bearing inclusions indicates the presence of an additional component, such as CH<sub>4</sub> and/or N<sub>2</sub>, in the solution system. The average homogenisation temperature of studied fluid inclusions is observed at 255 °C (between 216.9 °C and 311 °C).

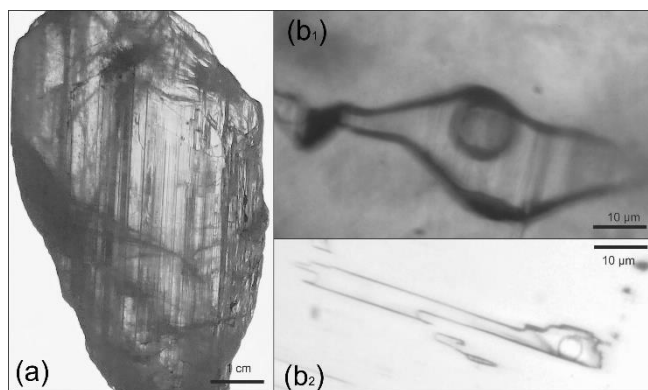


**Fig. 1.** A) Gem quality crystal diaspore and B1-2) LV-type inclusions observed in this sample.

Fluid inclusion phase behaviour during the low temperature and micro thermometric data indicate that the fluid responsible to diaspore formation should be metamorphic fluids. The existence of LCV and CV type inclusions as a primary, indicate that the diaspore precipitated from an immiscible fluid.

## Acknowledgement

This work was supported by Scientific Research Projects Coordination Unit of Istanbul University-Cerrahpaşa. Project number FYL-2018-29207.

## References

- Hanilçi N. (2019) Miner. Res. Turkey 681-730.
- Hatipoğlu M. et al. (2010a) Miner. Deposita 45:201–205.
- Hatipoğlu M. et al. (2010b) J. Asian Earth Sci. 39:359–370.

# Polymineralic silicate- and carbonate-rich inclusions in eclogite-facies metapelites: indication for immiscible melts in the subducted oceanic crust

Herms, P.<sup>1\*</sup>, Giehl, C.<sup>2</sup>, Rohrbach, A.<sup>3</sup>, Appel, P.<sup>1</sup>, Aradi, L.E.<sup>4</sup> & Raase, P.<sup>1</sup>

<sup>1</sup>Department of Geosciences, University of Kiel, Germany; <sup>2</sup>Anton Paar Germany GmbH, Ostfildern, Germany; <sup>3</sup>Department of Mineralogy, University of Münster, Germany; <sup>4</sup>Lithosphere Fluid Research Lab, Eötvös Loránd University, Hungary; \*petra.herms@ifg.uni-kiel.de

Polymineralic inclusions are investigated in garnet porphyroblasts of eclogite-facies metapelites from the Usagaran Belt, Tanzania. Metapelites intercalated with metabasites and carbonates represent an oceanic crust subducted to 60-70 km depth (Möller et al., 1995). Temperatures of about 900 °C are deduced from ternary feldspar compositions. Most metapelites have the mineral assemblage garnet–kyanite–two feldspars–quartz–biotite. Large grains of antiperthite occur, which are in part recrystallised to two feldspars. The garnet porphyroblasts contain two main types of polymineralic inclusions: Type I consisting of quartz + plagioclase + biotite ± kyanite + carbonates (<10 vol%); Type II consisting of dolomite (≤30 vol%) + quartz + kyanite.

Both types of inclusions have similar sizes between 10 and 50 µm with an average size of about 25-30 µm. In order to get information about the origin and bulk composition of the inclusions, piston cylinder experiments were aimed to rehomogenise the polymineralic inclusions by melting. Experiments were undertaken at 750 to 900 °C at 1.5 GPa and at 900 to 1050 °C at 2.5 GPa with a run duration of 24h. Backscatter images of the products show that, at 1.5 GPa, few Type I inclusions homogenised nearly completely only at 900 °C and others were only partly molten with interstitial glass between rounded quartz, plagioclase and biotite relics and an additional bubble. At 2.5 GPa, most of the Type I inclusions are completely molten at temperatures of 1000 and 1050 °C. In the TAS diagram, the melt composition of the homogenised inclusions plot in a relatively narrow range in the dacite-rhyolite field. This limited compositional range confirms that the Type I inclusions are not only mineral aggregates accidentally captured during garnet growth but represent true trapped melts. Type II carbonate-rich inclusions did not show evidence of melting during all the runs, although a distinct porosity developed. Polymineralic inclusions in garnet are

associated with pure CO<sub>2</sub> fluid inclusions containing daughter Ca/Mg-carbonate crystals (Herms, 2002). This points to the presence of Ca and Mg components in the original fluid. To shed more light into the origin of the polymineralic inclusions several observations can be consulted. Although most of the inclusions occur in an intermediate zone between core and rim of the garnets showing a prograde growth zonation, all type of inclusions can also occur within the core. The outermost rim is free of inclusions. Definitely, the garnet porphyroblasts did not form by peritectic growth. The occurrence of the inclusions in different growth zones could imply that a partial melt intruded the garnet along cracks and subsequently some melt is trapped by healing of the cracks. The similar size of Type I and II inclusions and their occurrence in the same cluster inside the garnet porphyroblasts further imply that they represent two immiscible melt phases, a silicate- and a carbonate-rich one. Raman 2D-spectral images on two euhedral carbonate-rich inclusions show a symplectitic intergrowth of quartz and kyanite, which could have been formed by a reaction of the carbonate melt with the garnet host. In both carbonate-rich inclusions a CO<sub>2</sub> fluid could be identified.

The investigation of the polymineralic inclusions indicate that there must have been partial melting in the subducted oceanic crust at high temperatures and pressures at least in the kyanite stability field. At these P-T conditions, a dacite-rhyolite melt could have been immiscible with a carbonate melt, which perhaps originated and liberated from subducted marine carbonates.

## Acknowledgement

DFG-funded project: number HE 1567/2-1

## References

- Herms P. (2002) *Eur. J. Mineral.* 14:361-373.  
Möller A. et al. (1995) *Geology* 23:1067-1070.

## Fluid inclusion characteristics of amethyst from Morocco

**Jarmołowicz-Szulc, K.<sup>1\*</sup>, Dumańska-Słowik, M.<sup>2</sup> & Toboła, T.<sup>2</sup>**

<sup>1</sup>Polish Geological Institute-National Research Institute, Poland; <sup>2</sup>AGH-The University of Science and Technology, Faculty of Geology, Geophysics and Environmental Protection, Poland; \*kjar@pgi.gov.pl

The recently studied gemstone crystal of amethyst from Boudi (Morocco) shows macroscopically a characteristic violet and colourless zonation and contains needle-like red solid inclusions perpendicular to the crystal face in non-coloured parts. Solid and fluid inclusions are seen in the micro scale and seem to lie in two cutting directions – parallel and perpendicular to the prism (Dumańska-Słowik et al., 2017). The following methods were applied in this research: petrographic FI analysis, fluorescence studies, microthermometry, Raman micro-spectroscopy.

In colourless fragments of the crystal, two-phase, liquid-vapour fluid inclusions occur in one plane. They form straight fluid inclusion assemblages (FIAs), which cross each other without any displacements. The liquid/vapour ratios are variable in the individual FIAs. They are accompanied by solid red inclusions, the composition of which corresponds to hematite. Fluid inclusions in this part of the crystal are often stretched and necked down.

The violet proportions of the crystal are relatively more abundant in fluid inclusions than the colourless parts. The majority of the inclusions, hosted in the violet proportions, are pseudo-secondary and contained two-phase (liquid and vapour) at room-T: liquid is predominant relative to vapour. Rarely, three-phase inclusions are also present (Fig. 1). Microthermometric measurements and Raman microspectroscopy in the two-phase (liquid-vapour) fluid inclusions revealed the presence of H<sub>2</sub>O, CO<sub>2</sub> and HSO<sub>4</sub><sup>-1</sup> (Frezzotti et al., 2012). Microthermometry in fluid inclusions hosted in the colourless amethyst showed lower homogenisation temperatures (154-218 °C) than those hosted in the violet crystal proportions (219-320 °C) (Dumańska-Słowik et al., 2017). In the colourless part, the fluid inclusions could be formed at least in two temperature intervals, i.e. 214–219 °C and 154-164 °C. In the violet proportions, two FIA generations could be distinguished, i.e. 210-230 °C and 290-330 °C. The eutectic temperatures (T<sub>e</sub>) in the colourless and violet parts are measured to be between -24 to -20 °C and -22.8 to -20.7 °C, respectively. This suggests a compositional difference between the fluid inclusions hosted in colourless and violet parts of the crystal.

Our results indicate a hydrothermal origin of the studied amethyst and reveal that NaCl and H<sub>2</sub>O could be the predominant components in the FIAs; CO<sub>2</sub> occasionally occurred. Carbon dioxide could have been derived from a decarbonatisation process (Van den Kerkhof and Hein, 2001) resulted in CO<sub>2</sub> from a reaction between

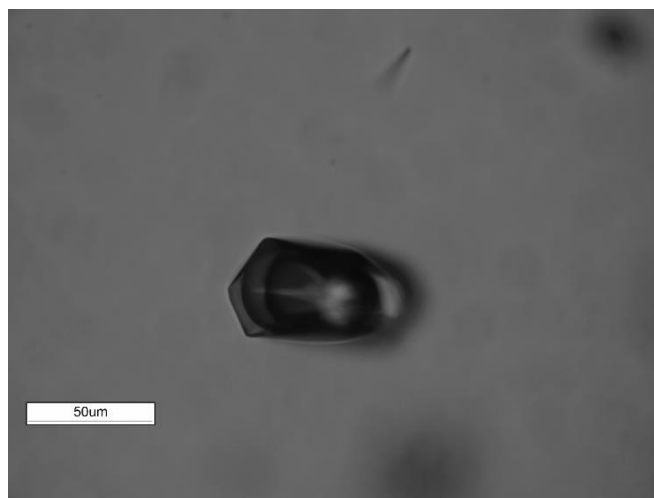


**Fig. 1.** Photomicrograph taken on a three-phase fluid inclusion hosted in violet part of the amethyst. Polarised light, 1N.

hydrothermal fluids and sedimentary rocks (Yang et al., 2001). The presence of the pseudo-secondary, secondary and necked down fluid inclusions may suggest a tectonic and metasomatic process after crystallisation of the studied amethyst.

### References

- Dumańska-Słowik M. et al. (2017) Spectrochim. Acta A. 187:156-162.
- Frezzotti M.L. et al. (2012) J. Geochem. Explor. 112:1-20.
- Van den Kerkhof A.M. and Hein U.P. (2001) Lithos 55:27-47.
- Yang K.H. et al. (2001) Mineral. Mag. 65:477-487.

# New data on the formation conditions of the Dyvok gold ore occurrence (South Yakutia, Russia)

**Kardashevskaya, V.N.<sup>1\*</sup>, Anisimova, G.S.<sup>1</sup> & Badanina, E.V.<sup>2</sup>**

<sup>1</sup>*Diamond and Precious Metal Geology Institute, SB RAS, Russia;* <sup>2</sup>*Saint-Petersburg State University, Russia;*  
*\*kardashevskaya92@mail.ru*

The Dyvok gold ore occurrence is located in the Neryungri district, Republic of Sakha (Yakutia), 300 km southeast of the city of Neryungri. In 2005, geologists of the YakutskGeologiya Mining and Geological Company carried out prospecting work in the Dyvok occurrence area and estimated the average gold grade in the ores at 3 g/t Au.

The Dyvok gold ore occurrence is confined to the zone of influence of the Tyrkanda deep fault (Kardashevskaya and Anisimova, 2018). The host rocks include K-feldspar-quartz metasomatites and beresitised and argillised rocks. The three most productive orebodies of the occurrence consist of quartz veins and veinlets.

Four mineral associations are recognised at the occurrence: gold-arsenopyrite-pyrite-quartz, gold-chalcopryrite-sphalerite, quartz-boulangerite, and quartz-telluride.

Primary fluid inclusions (FI) from quartz veins were studied by methods of microthermometry, (Laboratory of the Department of Geology, North-Eastern Federal University), and Raman spectroscopy (analyst V.N. Bocharov, GeoModel Resource Center, St. Petersburg State University).

Quartz from the auriferous ore bodies is light-grey in colour, massive, locally drusy, and mostly oxidised. Quartz contains three groups of fluid inclusions: 1: monophasic (mostly gas), 2: diphasic (gas+liquid), and 3: three-phase (gas+liquid phase+liquid carbon dioxide) (Fig. 1). They have irregular or rounded form, and a size range from 1 to 50 µm. FI data suggest the formation of the early auriferous mineral association (arsenopyrite-pyrite-quartz) at temperatures of 270-335 °C and a pressure of 0.7 kbar. Studies of quartz from the middle gold-chalcopryrite-sphalerite association showed homogenisation temperatures of 186-219 °C. No FI were found in quartz from the quartz-boulangerite association. The latest quartz-telluride association is characterised by an average

homogenisation temperature of 199 °C. For the middle and late associations, the trapping pressure was not determined because of the lack of co-existing three-phase FI.

The composition of the inclusion gas phase was analysed with Raman spectroscopy. For these Raman experiments we chose syngenetic primary FI. It was found that inclusions from the gold-arsenopyrite-pyrite-quartz and gold-chalcopryrite-sphalerite associations mostly contain CO<sub>2</sub> and very rarely CH<sub>4</sub>. Solid phases in fluid inclusions from the early association include dawsonite and native sulphur. The carbonate ion is consistently observed in the aqueous solution. FI from quartz from the late association are dominated by carbon dioxide. CH<sub>4</sub> and N<sub>2</sub> are present in trace amounts.

The results of the study show that the early and middle mineral associations were formed at shallow- and mid-depth conditions, respectively, with the involvement of deeper sources for the ore constituents. The presence of carbonate in solution indicates oxidising conditions. The late mineral association was deposited at a temperature of at least 199 °C, with an important role of methane and nitrogen.

## Acknowledgement

The reported research was funded by Russian Foundation for Basic Research and the government of the region of the Russian Federation, grant № «18-45-140045» and according to Diamond and Precious Metal Geology Institute, Siberian Branch, Russian Academy of Sciences research activities plan, project 0381-2019-0004

## References

Kardashevskaya V.N. and Anisimova G.S. (2018) XIX. International Multidisciplinary Scientific Geo Conference 18:259-264.

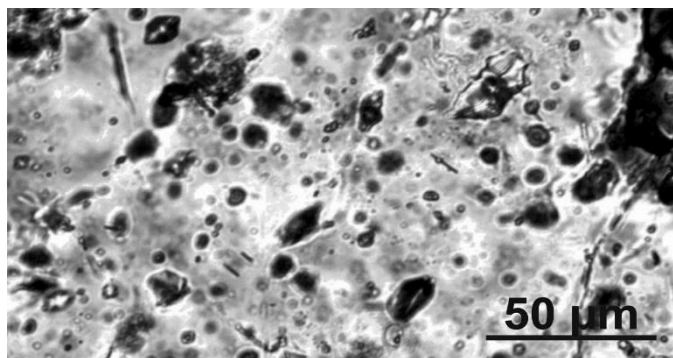


**Fig. 1.** Types of fluid inclusions in quartz from the Dyvok gold ore occurrence.

# Fluid inclusion and microtextural evidence for efficient gold precipitation from Au-undersaturated fluids via coupled redox-pH change

Kerr, M.J.<sup>1,2\*</sup>, Hanley, J.J.<sup>1</sup>, Kontak, D.J.<sup>2</sup>, Ramlochund, P.<sup>1</sup> & Zajacz, Z.<sup>3</sup>

<sup>1</sup>Department of Geology, Saint Mary's University, Canada; <sup>2</sup>Harquail School of Earth Sciences, Laurentian University, Canada; <sup>3</sup>Department of Earth Sciences, University of Toronto, Canada; \*mitchell.kerr@smu.ca

The ~380 Ma metasediment-hosted Dufferin gold deposit in the Meguma Terrane, Nova Scotia, Canada, hosts several stacked, mineralised saddle-reef-type quartz veins along lithological contacts between meta-sandstones and black slates (rich in carbonaceous material 'CM') in the tightly folded Crown Reserve Anticline. The saddle-reef veins record multiple generations of veining, with early gold-poor laminated veins cut or incorporated into later gold-mineralised massive quartz. Locally, vugs in the late massive quartz contain undeformed euhedral quartz crystals that host two fluid inclusion types, confirmed by cathodoluminescence imaging to be both of secondary origin: (i) Type 1 – 3-phase, aqueous-carbonic (H<sub>2</sub>O-NaCl-CO<sub>2</sub>+N<sub>2</sub>+CH<sub>4</sub>), 1.3 ± 0.4 wt% eq. NaCl fluid inclusions (Fig. 1a), and (ii) Type 2 – 2-phase, aqueous-dominated (H<sub>2</sub>O-NaCl+CO<sub>2</sub>+N<sub>2</sub>+CH<sub>4</sub>) 3.2 ± 1.0 wt% eq. NaCl fluid inclusions. Type 1 fluid inclusions are gold-bearing, but gold-undersaturated (i.e., 0.045 ± 0.024 ppm [n=58] versus a calculated concentration of 0.1 – 2 ppm at 300°C; 70% above the LOD) and also contain moderate concentrations of As (67.1 ± 50.1 ppm; n=80) and Sb (31.6 ± 20.4 ppm; n=80). Type 2 fluid inclusions have lower average gold contents (0.025 ± 0.012 ppm; n=7; 22% above LOD), as well as As (9.24 ± 8.28 ppm; n=24), and Sb (5.66 ± 5.64 ppm; n=23).

CM is ubiquitous as coatings on quartz in mineralised saddle veins within the cavities and along mineral grain boundaries adjacent to vein laminations and vein margins. The occurrence of micro-inclusions (≤ 2 μm) of gold in CM-filled cavities strongly suggests the gold mineralisation and CM are genetically-related (Fig. 1b). Based on an integrated, microanalytical petrographic study (SEM, confocal laser Raman microspectroscopy, microthermometry, fluid inclusion LA-ICP-MS analysis, SIMS δ<sup>18</sup>O<sub>VSMOW</sub> and δ<sup>13</sup>C<sub>VBPDP</sub>, cathodoluminescence), we propose that late gold mineralisation at Dufferin proceeded through a coupled mechanism involving fluid reduction (via interaction with authigenic CM) and pH increase. This led to the destabilisation of soluble gold bisulphide complexes and highly efficient gold precipitation from the type 1 gold-undersaturated aqueous-carbonic fluids. This conclusion is based on the following key observations: (i) the decrease in concentration of Au and redox-sensitive elements (As, Sb), and the increase in concentration of elements inherited through wall rock interaction (Mg, K, Ca, Sr, Fe) between the aqueous-carbonic (type 1) and aqueous (type 2)

fluids, respectively; (ii) the decrease in CO<sub>2</sub> abundance between type 1 (X<sub>CO<sub>2</sub></sub> = 0.15) and type 2 (X<sub>CO<sub>2</sub></sub> = 0.02) fluids corresponding with CO<sub>2</sub> removal via reduction/respeciation and late carbonate precipitation; and (iii) the occurrence of native gold within CM-filled cavities and fractures.

This work improves existing genetic models for metasediment-hosted "orogenic" gold systems in the Meguma Terrane and elsewhere by providing direct insight into the mechanisms responsible for at least some of the observed gold: i.e., gold precipitation via fluid reduction and pH increase through fluid interaction with CM-bearing material.

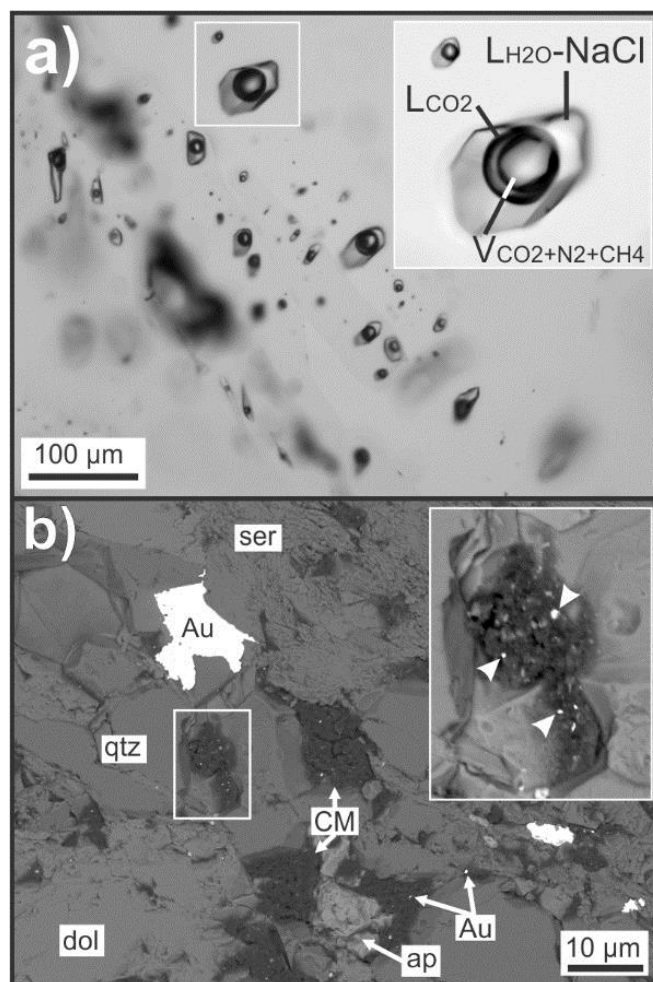


**Fig. 1.** A) A Type 1, gold-bearing aqueous-carbonic fluid inclusion assemblage of secondary origin. B) micro-inclusions of Au (arrow heads in inset) in CM-filled cavities.

# Critical homogenisation of low-salinity fluid inclusions: modeling, heating experiments, and oddities

**Klyukin, Y.I.<sup>1\*</sup>, Steele-MacInnis, M.<sup>1</sup>, Tutolo, B.<sup>2</sup>, Pujatti, S.<sup>2</sup>, Lecumberri-Sanchez, P.<sup>1</sup> & Bodnar, R.J.<sup>3</sup>**

<sup>1</sup>Department of Earth and Atmospheric Sciences, University of Alberta, Canada; <sup>2</sup>Department of Geoscience, University of Calgary, Canada; <sup>3</sup>Department of Geosciences, Virginia Tech, USA; \*klyukin@ualberta.ca

Fluid inclusions of the critical density for a given composition (here, termed "critical FI") will homogenise by fading of the meniscus between liquid and vapour. Many previous studies have noted that such inclusions may show chaotic appearance of "boiling" as they approach the critical homogenisation temperature.

For a single component system, such as pure H<sub>2</sub>O, the densities of the liquid and vapour control the evolving volumetric ratios of phases as an inclusion is heated towards homogenisation. In the case of critical FI containing pure H<sub>2</sub>O, because the densities of each phase will approach the critical density, and because the critical density is intermediate between liquid and vapour, the volumetric phase ratios of liquid to vapour will be similar at the moment of critical homogenisation. This has sometimes been referred to as the "50/50 rule" for critical homogenisation (Oakes et al., 1994).

Behaviour of the multicomponent systems, on the other hand, is more complex. In addition to the density constraints, the volumetric phase ratios are also controlled by partitioning of the components between liquid and vapour. So for example, in the case of saline aqueous inclusions, the evolving salinities of liquid and vapour during heating towards critical homogenisation must also be taken into account. As shown here, this leads to some unexpected consequences.

In the present study, we modelled the pressure-temperature path of the critical FI of H<sub>2</sub>O-NaCl with different salinities. We used the equations of Driesner and Heinrich (2007) and Driesner (2007). FI are treated as closed, isochoric systems. We calculated the internal pressures, compositions, densities and volumetric phase ratios of liquid and vapour as the inclusions are heated towards critical homogenisation.

We show that the inclusions show monotonous decrease in volume fraction of the vapour as the temperature increases from 100 °C up to the temperature of ~350 °C. Above this temperature, critical FIs exhibit a large variation in volumetric fraction of vapour, which is most notable for FIs with salinity below ~7 wt% NaCl (Fig. 1).

Interestingly, these critical FIs tend to mimic the homogenisation to liquid phase, in that the bubble first shrinks to quite small volume fractions before fading of the meniscus. Hence, for hydrothermal systems in which critical phenomena are expected, critical FI may be misidentified as showing homogenisation to liquid phase.

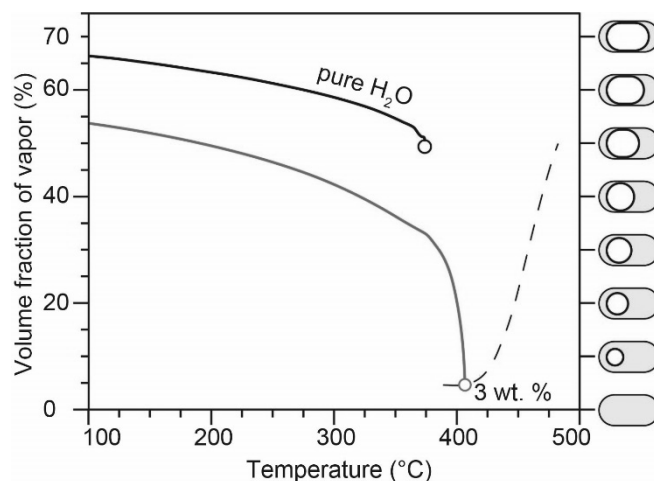


**Fig. 1.** Calculated volume fraction for the fluid inclusions with pure H<sub>2</sub>O (black solid line) and 3 wt% NaCl (gray). Dashed line indicates endpoints for salinity in range from 1 to 10 wt% NaCl.

Mid-ocean ridge hydrothermal systems represent one potential setting where critical FI are reasonably expected, yet rarely or never reported. Phase separation in the roots of such systems is expected to occur routinely along the liquid + vapour phase boundary near or at the critical point of seawater. In this work, we explore the possibility that critical FI may be more common in this setting than previously realised, owing to these inclusions imitating the behaviour of FIs homogenising to the liquid.

## References

- Driesner T. and Heinrich C.A. (2007) *Geochim. Cosmochim. Ac.* 71:4880-4901.
- Driesner T. (2007) *Geochim. Cosmochim. Ac.* 71:4902-4919.
- Oakes C.S. et. al. (1994) *Geochim. Cosmochim. Ac.* 58:2421-2431.

# Fluid properties of an unusual epithermal gold deposit hosted by a shear zone, Banská Hodruša, Slovakia

**Koděra, P.<sup>1\*</sup>, Kubač, A.<sup>1</sup>, Uhlík, P.<sup>1</sup>, Laurent, O.<sup>2</sup>, Fallick, A.E.<sup>3</sup> & Milovský, R.<sup>4</sup>**

<sup>1</sup>Department of Economic Geology, Faculty of Natural Sciences, Slovakia; <sup>2</sup>Earth Science Institute ETH Zürich, Switzerland; <sup>3</sup>Scottish Universities Environmental Research Centre, UK; <sup>4</sup>Slovak Academy of Sciences, Slovakia; \*koder1@uniba.sk

The intermediate-sulphidation Au-Ag-Pb-Zn-Cu deposit Banská Hodruša occurs at the Rozália mine, 400-650 m below the surface. It is hosted by a low-angle shear zone in the centre of the Neogene Štiavnica stratovolcano in the Central Slovakia Volcanic Field. The shear zone is related to processes of exhumation of a subvolcanic granodiorite pluton, probably accompanied by a sector collapse of the hosting stratovolcano (Kubač et al., 2018). The deposit developed during five mineralisation stages and two stages of shear zone evolution.

Fluid inclusions from quartz, sphalerite and carbonates from the gold mineralisation are of low salinity (~1–3 wt% NaCl eq.) and moderate homogenisation temperatures (Th; ~250–310 °C) with frequent evidence of boiling. A similar temperature (270–290 °C) was determined from the illite crystallinity (KI ~0.4 to 0.6) from the wall-rock alteration. No apparent differences occur among individual stages, except Stage 1 silicites with slightly higher Th values (up to 330 °C), and sphalerite from various stages with slightly lower Th values (~250–280 °C). The fluid pressures calculated from boiling fluid inclusion populations were ~85 bars for Stage 1 inclusions, while the Stage 2 and 3 inclusions showed variable pressures (45–80 bars). The high pressures correspond to initial opening of host fractures, when the hydrothermal system was governed by suprahydrostatic conditions. The likely paleodepth (550 ± 100 m) was derived from the lowest fluid pressure value (Koděra et al., 2005).

LA-ICPMS analyses of fluid inclusions systematically detected the same set of elements (Na, B, Cl, K, As, Rb, Sr, Sb, Cs ± Fe, Cu, Zn, Au, Pb) showing fairly similar ratios to Na. This suggests a common, long-lasting fluid source throughout the entire hydrothermal process. High B/Rb, B/Sr and As/Rb ratios indicate that contracted magmatic vapour was the dominant source of fluids (c.f. Large et al., 2016). Fluids in pre-mineralisation stages (1 and 2a) had probably a higher proportion of the contracted magmatic vapour, as indicated by their relatively higher B, As, Sb contents, Na/K values and lower Cl, Rb contents than later stages. This can be explained by preferential accumulation of B, As and Sb in vapour, while Rb and K are affiliated to magmatic brines (Pokrovski et al., 2002). Gold content in fluids typically ranges from 0.2 to 2 ppm in all gold bearing stages; but some individual inclusions

have sometimes up to 50 ppm Au. Ag/Au ratio was similar to most ores at the deposit, i.e. close to 10.

Isotope data from vein quartz and illites showed a relatively narrow range of  $\delta^{18}\text{O}_{\text{fluid}}$  values (-2 to 1‰) for all stages of veins. Fluids in equilibrium with illite also have homogeneous hydrogen isotope ratio (-50 to -69‰  $\delta\text{D}_{\text{fluid}}$ ). The isotopic composition suggests that both magmatic and meteoric components were present in the fluids. The magmatic component was vapour escaping from the parental magma chamber. Vapour has contracted to liquid before mixing with a deep-convecting meteoric fluid, which occurred outside of the deposit. Some admixed proportion of brine could be also associated. Enrichment in gold resulted from the ability of vapour to transport gold, and due to the degassing of a mafic magma that has penetrated the parental magma chamber. Precipitation of ore mineralisation was triggered by pressure decrease from suprahydrostatic to hydrostatic conditions, boiling and cooling rather mixing of fluids. Ore mineralisation is related to focusing of fluids in areas with a dense network of dilatational structures, while the argillised upper boundary of the shear zone was a collector of hydrothermal fluids and boiling-derived gases.

## Acknowledgement

This work was supported by the grant APVV-15-0083 and the company Slovenská banská, spol. Ltd.

## References

- Koděra P. et al. (2005) *Miner. Deposita* 39:921-943.
- Kubač A. et al. (2018) *Miner. Petrol.* 112:705-731.
- Large S.J.E. et al. (2016) *Geology* 44:1015-1018.
- Pokrovski G.S. et al. (2002) *Geochim. Cosmochim. Ac.* 66:3453-3480.

## Javorieite – the type mineral of shallow porphyry gold systems, hosted by salt melt inclusions

**Koděra, P.<sup>1\*</sup>, Takács, A.<sup>2</sup>, Racek, M.<sup>3</sup>, Šimko, F.<sup>4</sup>, Luptáková, J.<sup>5</sup>, Váczi, T.<sup>2,6</sup> & Antal, P.<sup>7</sup>**

<sup>1</sup>Comenius University, Faculty of Natural Sciences, Department of Economic Geology, Slovakia; <sup>2</sup>Eötvös Loránd University, Department of Mineralogy, Hungary; <sup>3</sup>Charles University in Prague, Faculty of Science, Institute of Petrology and Structural Geology, Czech Republic; <sup>4</sup>Slovak Academy of Sciences, Institute of Inorganic Chemistry, Slovakia; <sup>5</sup>Earth Science Institute, Slovak Academy of Sciences, Slovakia; <sup>6</sup>Hungarian Academy of Sciences, Institute of Solid State Physics and Optics, Hungary; <sup>7</sup> Department of Inorganic Chemistry Faculty of Science, Palacký University, Czech Republic; \*koder1@uniba.sk

Javorieite,  $\text{KFeCl}_3$ , is a new mineral, commonly hosted by salt melt inclusions enclosed in vein quartz in the Biely Vrch porphyry gold deposit and several other porphyry gold systems in the Central Slovakia Volcanic Field in the Western Carpathians (Koděra et al., 2015, 2017). Salt melt inclusions represent a rare type of fluid inclusions, which have trapped a hypersaline liquid at high temperature. The generation of the water-free salt melt with high concentrations of Fe and K is the result of quick expansion and cooling of magmatic fluids during their ascent from associated Fe-rich dioritic magma emplaced at shallow depth (Koděra et al., 2014). At room temperature salt melt inclusions do not contain any visible liquid phase, and the entire volume of the inclusions is occupied by several salt crystals and a distorted vapour bubble. Salt melt inclusions are found in shallow magmatic-hydrothermal systems, typically associated with Cu-Au porphyry mineralisation (e.g. Rottier et al., 2016). The mineral name refers to the Javorie stratovolcano, which hosts most porphyry gold systems in this volcanic field.

Within the inclusions, javorieite occurs in the form of small (up to 15  $\mu\text{m}$ ) green anhedral crystals with high relief. It is extremely hygroscopic and readily oxidised if exposed to the air. It is accompanied by several other daughter minerals, especially halite ( $\text{NaCl}$ ), rinneite ( $\text{NaK}_3\text{FeCl}_6$ ), chlorocalcite ( $\text{KCaCl}_3$ ), hibbingite,  $\text{Fe}_2(\text{OH})_3\text{Cl}$ , unknown  $\text{FeCl}_2$  hydrate, fluorite, molybdenite and scheelite. The javorieite, as well as most of the other daughter minerals, were identified through comparison with the Raman spectra of the synthetic analogue, and through data obtained with the FIB-SEM-EBSD analytical technique. The combination of several independent analytical tools on three different inclusions proved the match in chemistry and crystallography of javorieite with synthetic  $\text{KFeCl}_3$ . Javorieite is orthorhombic, the unit-cell parameters are  $a = 8.715(6) \text{ \AA}$ ,  $b = 3.845(8) \text{ \AA}$ ,  $c = 14.15(3) \text{ \AA}$ ,  $V = 474.16(3) \text{ \AA}^3$ ,  $Z = 4$ . Furthermore, the experimental data in the  $\text{NaCl-KCl-FeCl}_2$  system agree with the microthermometric behaviour of javorieite.  $\text{KFeCl}_3$  (javorieite) and  $\text{FeCl}_2$  are the last phases in this system undergoing eutectic crystallisation at 309 °C or 319 °C (Robelin et al.,

2004), which corresponds to typical temperatures of first melting of the studied salt melt inclusions (320-338 °C). The presence of javorieite in three other localities in this volcanic field was confirmed by Raman spectroscopy. The distinctive Raman spectrum of javorieite (main bands at 66-69, 108-109, 119-120, 134-135, 235-237  $\text{cm}^{-1}$ ) can help in future studies of salt melt inclusions worldwide, including a quick recognition of shallow porphyry systems that can be potentially enriched in gold.

### Acknowledgement

This work was supported by the grants APVV-0537-10 VEGA-1/0560/15 and ITMS: 26220120064.

### References

- Koděra P. et al. (2014) *Geology* 42:495-498.
- Koděra P. et al. (2015) in: *ECROFI* 2015:86-87.
- Koděra P. et al. (2017) *Eur. J. Mineral.* 29:965-1004.
- Robelin C. et al. (2004) *Thermodyn.* 36:809-828.
- Rottier B. et al. (2016) *Chem. Geol.* 447:93-116.

## How warm? An intercalibration of novel geothermometry methods for calcite

**Koltai, G.<sup>1\*</sup>, Krüger, Y.<sup>2</sup>, Kluge, T.<sup>3</sup>, Leél-Össy, Sz.<sup>4</sup>, Spötl, C.<sup>1</sup> & Dublyansky, Y.<sup>1</sup>**

<sup>1</sup>Institute of Geology, University of Innsbruck, Austria; <sup>2</sup>Department of Earth Science, University of Bergen, Norway; <sup>3</sup>Institute of Environmental Physics, University of Heidelberg, Germany; <sup>4</sup>Department of Physical and Applied Geology, Eötvös Loránd University; \*gabriella.koltai@uibk.ac.at

Temperatures below ~55 °C represent a “blind spot” in classical paleo-geothermometry given the lack of available methods for measuring them. Yet, such temperatures are common in many subsurface environments including thermal groundwaters and shallow basinal fluids. Minerals crystallising from such waters may trap tiny amounts of them as fluid inclusions.

For several decades, the only available method to constrain the paleo-fluid’s temperature has been measurements of the liquid-vapour homogenisation temperature of primary fluid inclusions. Since two-phase inclusions mostly form when the entrapment temperature is ~55 °C or higher, assessing formation temperatures for minerals formed from cooler fluids has remained a challenge until recently, when a technological break-through has made it possible to measure homogenisation temperatures also in originally monophasic fluid inclusions by laser-induced bubble nucleation (Krüger et al., 2007; Krüger et al., 2011).

During the last decade another novel method, clumped isotope thermometry of calcite, has been developed which offers high potential as a palaeo-thermometre over a wide temperature range (Affek et al., 2008; Kluge et al., 2015). As most of the current knowledge on clumped isotope systematics is based on theoretical and experimental studies of synthetic calcite, the intercalibration with other methods on natural samples is important (Came et al., 2017; Manganot et al., 2017).

The aim of this study is to compare these two state-of-the-art analytical methods and investigate how well they compare for low-temperature environments. To this end, we collected hypogene calcite samples from different thermal karst areas of the Pannonian basin, where an earlier study demonstrated that the temperature of speleogenetic hydrothermal fluids varied between 35 and 95 °C (Dublyansky, 1995).

Optical microscopy shows that two-phase inclusions are present in the calcite samples from the Buda thermal karst area, while monophasic liquid inclusions prevail in samples from Bükk Mts. and Aggtelek Mts. The first results of clumped isotope thermometry indicate paleo-water temperatures of 10 to 100 °C for these calcite crystals. At this point, the results are preliminary and the analytical uncertainty may be as high as 10 °C.

So far, homogenisation temperatures have been measured on six monophasic fluid inclusion assemblages after bubbles had been created by

femtosecond laser pulses. These results indicate that mineral crystallisation happened in the range of 10 to 34 °C. Clumped isotope analyses of the same calcite crystals yielded similar paleo-temperatures between 10 (±10) and 35 (±10) °C. These initial results yielded by the two novel methods are comparable for all but one sample.

### Acknowledgement

This project has been funded by the University of Innsbruck.

### References

- Affek H.P. et al. (2008) *Geochim. Cosmochim. Ac.* 72:5351-5360.
- Came R.E. et al. (2017) *Geochim. Cosmochim. Ac.* 199:31-47.
- Dublyansky Y.V. et al. (1995) *Environ. Geol.* 25:24-35.
- Kluge T. et al. (2015) *Geochim. Cosmochim. Ac.* 157:213-227.
- Krüger Y. et al. (2007) *Eur. J. Mineral.* 19:693-706.
- Krüger Y. et al. (2011) *Chem. Geol.* 289:39-47.
- Manganot X. et al. (2017) *Chem. Geol.* 472:44-57.

## Formation conditions of U-Ti-Metagel mineralisation in the Elkon Deposit (Yakut region, Russia)

**Komarova, M.M.<sup>1\*</sup>, Aleshin, A.P.<sup>1</sup>, Komarov, V.I.B.<sup>1</sup> & Krylova, T.L.<sup>1</sup>**

<sup>1</sup>*Institute of Geology of Ore Deposits, Petrography, Mineralogy and Geochemistry, Russian Academy of Sciences, Russia; \*ivanchenko.marija@gmail.com*

The Elkon Au-U deposits are the most important reserve source of natural uranium in Russia. The Elkon Horst, hosting all uranium deposits of this region, extends to 60 km in the northeast direction with a width of 30 km.

The most productive for uranium is the Southern zone of the Proterozoic origination, was rejuvenated by the Mesozoic tectonic-magmatic activation (TMA). It controls five large-scale deposits (from NW to SE: Elkon, Elkon Plateau, Kurung, Neprohodimoe, Druzhnoe). The deposits are traced for 25 km along the Southern zone; the lower boundary of the mineralisation is not outlined down to the depth of 2 km. The mineralisation is complex with Au and Mo in some parts.

As it was reported before (Miguta, 2001) the ores are mainly composed of brannerite (U<sub>2</sub>Ti<sub>2</sub>O<sub>6</sub>). However, fulfilled by authors study of uranium mineralisation under optical and scanning electron microscope showed that the bulk of the ore located in the Southern zone is composed an unknown amorphous polyphase U-Ti-metagel (UTM). Consistent formation of phases with different U/Ti ratio indicates the primary nature of U-Ti-metagel, rather than the result of the metamict decomposition of brannerite. Crystalline brannerite was revealed in insignificant quantities formed simultaneously with UTM. It was suggested that the reason for the deposition of U minerals in both amorphous and crystalline forms is a wide temperature range of the hydrothermal process.

The fluid inclusions (FI) of pre-ore and post-ore stages have been studied. The pre-ore stage is represented by quartz, the post-ore – quartz and zonal veinlets of quartz, carbonate and fluorite.

Four types of the primary inclusions (5-20 μm) have been recognised at room temperature (21 °C). Type I is two-phase liquid-vapour aqueous inclusions. Type II is two-phase FI with vapour CO<sub>2</sub>. Type III is 3-phase FIs with liquid H<sub>2</sub>O, liquid CO<sub>2</sub> and gas CO<sub>2</sub> phases. Type IV contains phases from type III and solid phase.

A wide range of homogenisation temperatures (T<sub>h</sub>) of hydrothermal fluid (430-103 °C) has been revealed in the result of microthermometric study of FIs in minerals of pre-ore and post-ore stages.

T<sub>hom</sub> of FIs in the pre-ore quartz veins ranges 380-150 °C, and salinity matches 10-11 wt% eq. NaCl without CO<sub>2</sub> and other gas admixture.

Parameters of the post-ore stage are more variable. Quartz T<sub>hom</sub> ranges 430-103 °C, high-temperature carbonate I T<sub>hom</sub> is 380-107 °C, late carbonate II T<sub>hom</sub> is <180 °C.

Microthermometric study of zonal quartz-carbonate-fluorite vein exhibits local temperature variations. The casing of vein is represented by quartz with T<sub>hom</sub><sup>avg</sup> 233 °C (240-170 °C); the middle part with T<sub>hom</sub><sup>avg</sup> 291 °C (380-197 °C) is made of carbonate; violet fluorite overlap carbonate in the central part and shows T<sub>hom</sub><sup>avg</sup> 228 °C (424-140 °C).

FIs of the type III, IV are characterised by presence of crystalline hydrates up to 8.8 – 5.6 °C. It is also possible to preserve the presence of a small amount of other gases, possibly CH<sub>4</sub>, which amount does not exceed 1-2 mol%.

Average temperatures, as well as temperature variation are similar for both pre-ore and post-ore stages. It allows to determine surely temperatures of uranium ore formation as 400-120 °C. Fluids possessed Na-chloride, rarely Na-chloride-carbonate composition and moderate salinity (6-16 wt% eq. NaCl). The wide range of temperatures confirms an assumption made before that various temperatures were the reason of formation of uranium mineralisation both in the form of predominantly amorphous phase (U-Ti-metagel), as well as in rarely crystalline form (brannerite). Abrupt temperature decrease was apparently the main factor of ore deposition.

### Acknowledgement

This study was supported by program no.0136-2018-0017.

### References

Miguta A.K. (2001). *Geol. Ore Deposit* 43:117-135.

## The 'pargasosphere' concept: the fluid-solid 'ping-pong' along major discontinuities of the shallow upper mantle and its bearing on global plate tectonics

**Kovács, I.<sup>1,2\*</sup>, Berkesi, M.<sup>1,3</sup>, Liptai, N.<sup>1</sup>, Pálos, Zs.<sup>1,3</sup>, Lange, T.P.<sup>1,3</sup>, Szabó, Cs.<sup>3</sup>, Szanyi, Gy.<sup>1</sup>, Gráczner, Z.<sup>1</sup>, Wéber, Z.<sup>1</sup>, Novák, A.<sup>1</sup>, Süle, B.<sup>1</sup>, Timkó, M.<sup>1</sup>, Czifra, T.<sup>1</sup>, Molnár, Cs.<sup>1</sup>, Patkó, L.<sup>3</sup>, Aradi, L.E.<sup>3</sup>, Szűcs, E.<sup>1</sup> & Wesztergom, V.<sup>1</sup>**

<sup>1</sup>MTA CSFK Lendület Pannon Lith<sub>2</sub>Oscope Research Group, Hungary; <sup>2</sup>MTA CSFK Geodetic and Geophysical Institute, Hungary; <sup>3</sup>Lithosphere Fluid Research Lab, Eötvös Loránd University, Hungary;

\*kovacs.istvan.janos@csfk.mta.hu

Water is an essential component of life, but also a vital one for making Earth a geologically 'living' planet. The principle of plate tectonics is that the Earth's rigid outer shell, the lithosphere, 'floats' on the underlying less viscous asthenosphere. The reasons for their distinct physical properties are still unclear, therefore, the refined understanding of the lithosphere-asthenosphere boundary (LAB) and mid lithosphere discontinuities (MLDs) remains an important endeavor for the whole Earth Science community. The new 'pargasosphere' concept may offer an alternative model why minute amount of 'water' and its constitution in the Earth's shallow upper mantle accounts for the changes in physical and geochemical properties at the LAB under young extensional basins and oceanic plates and at MLDs under older continental plates in ~100 km depth (Green et al., 2010; Kovács et al., 2017). The postulate of the idea is that the 'water' is stored in hydrous phases such as amphibole (pargasite) and nominally anhydrous minerals (NAMs) where pargasite is stable at temperatures less than ~1100 °C and at pressures less than ~ 3 GPa (~100 km). In contrast, at temperatures and pressures exceeding these thresholds 'water' is usually present in NAMs and/or free fluid/melt phases. Consequently 'water' changes its constitution in the upper mantle either being present in solid or fluid components of the upper mantle depending on the P-T conditions. This 'ping-pong' of 'water' in the P-T space of the upper mantle has a dramatic rheological impact. This is because 'water' in the stability field of pargasite is locked only in solid phases making the upper mantle rheologically stronger (i.e. Berkesi et al., 2019). In contrast where pargasitic amphibole is not stable 'water' is either present in the fluid phase or higher concentration in NAMs as structurally bound hydroxyl. This means that the upper mantle beyond the stability field of amphibole (pargasite) is less viscous and can be more easily deformable. We present micro- and nanoscale results how the 'water' hops in and off between solid and fluid states and how it may offer an alternative way to look at global plate tectonics.

### Acknowledgement

This presentation was supported by the MTA CSFK Lendület Pannon Lith<sub>2</sub>Oscope project.

### References

Berkesi et al. (2019) Chem. Geol. 508:182-196.

Green D.H. et al. (2010) Nature 467:448-451.

Kovács I. et al. (2017) Acta Geod. Geophys. 52:183-204.

## Study of quartz xenocrysts and mafic enclaves from the “Laleaua Alba” (“White Tulip”) composite dacite dome, Gutai Mts., Romania

**Kővágó, Á.<sup>1\*</sup>, Kovács, I.<sup>2</sup>, Józsa, S.<sup>1</sup>, Kovacs, M.<sup>3</sup>, Szabó, Cs.<sup>1</sup>, Kovács, Z.<sup>1</sup> & Kesjár, D.<sup>4</sup>**

<sup>1</sup>Department of Petrology and Geochemistry, Eötvös Loránd University, <sup>2</sup>Geodetic and Geophysical Institute Research Centre for Astronomy and Earth Sciences Hungarian Academy of Sciences, Hungary; <sup>3</sup>Tech. Univ. Cluj-Napoca, North Univ. Centre Baia Mare, Romania; <sup>4</sup>Institute for Geological and Geochemical Research Research Centre for Astronomy and Earth Sciences Hungarian Academy of Sciences, Hungary; \*kovago.akos@gmail.com

The Laleaua Alba composite dacite dome is located above the Dragoş, Vodă deep-seated fault system (Tischler et al., 2007) in the Gutai Mts. (Romania). The dacite is 8.5-8.0 My old (Kovacs, 2002) and contains numerous magmatic enclaves.

Based on mafic phenocrysts content, the enclaves are classified into two groups. The amphibole-bearing group has diktytaxitic texture without vesicular glassy groundmass. The amphibole- and clinopyroxene-bearing group shows panidiomorphic texture, which suggests having a slower cooling rate relative to amphibole-bearing group. The enclaves likely crystallised when a hot mafic melt cooled during either underplating or at the magma chamber walls (Miller et al., 1999).

Quartz xenocrysts having a clinopyroxene corona occur in both groups of mafic enclaves. This unique texture may record different stages of magma evolution (Kovacs et al., 2017). The quartz crystals are abundant in negative crystal shaped silicate melt inclusions (SMI). The size of the SMIs are in the range of 10-40 µm and, consisting of Si-glass and bubble (Fig. 1).

We analysed major and trace element compositions of the minerals. To complete the petrographic observations. FTIR (Fourier Transform Infrared) and Raman spectroscopy were used to determine the structural hydroxyl content of the NAM's (nominally anhydrous minerals) and the volatile content of silicate melt inclusions to better understand the volatile composition during the crystallisation of the enclaves and the pyroxene corona.

The mineral compositions and bulk rock chemistry of the enclaves suggest a basaltic parental melt. FTIR measurements showed an increase in hydroxyl content of the minerals from the quartz xenocryst to the enclave. We suggest that the enclaves crystallised from a basaltic melt. The quartz crystals were incorporated into the basaltic melt before the complete crystallisation of the enclaves. In the basaltic melt the clinopyroxene corona protected the quartz from further dissolution. The melt inclusions may represent the ‘in situ’ melt of the quartz based on their moderate hydroxyl and alkali contents.

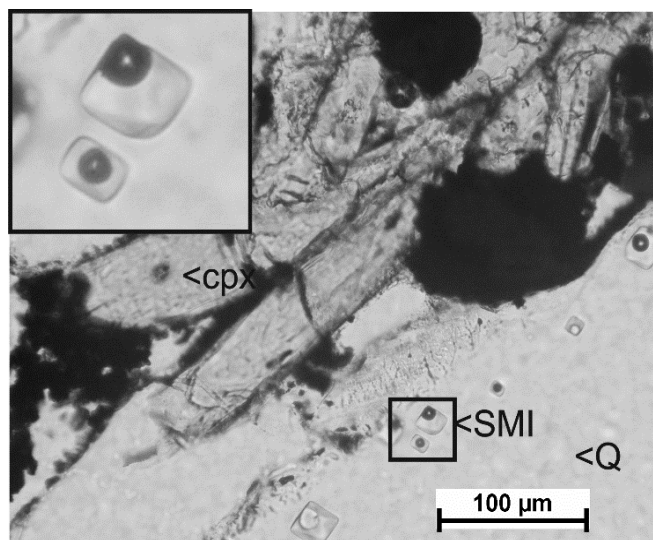


**Fig. 1.** Photomicrographs on silicate melt inclusions (SMI) in the edge of the quartz (Q) xenocryst and clinopyroxene (cpx) corona around the quartz.

### References

- Kovacs M. (2002) Editura Dacia Cluj-Napoca 201 p. (in Romanian).
- Kovacs M. et al. (2017) *Lithos* 294-295:304-318.
- Miller T.P. et al. (1999) *Japan J. Volcanol. Geoth. Res.* 89:275-301.
- Tischler M. et al. (2007) *Int. J. Earth Sci.* 96:473-496.

# Factors of high productivity of the Bystrinsky skarn-porphyry Cu-Au Deposit fluid-magmatic system (Eastern Transbaikalia, Russia): constraints from Fluid inclusions

**Kovalenker, V.A.<sup>1\*</sup>, Krylova, T.L.<sup>1\*</sup>, Luptáková, J.<sup>2</sup>, Kiseleva, G.D.<sup>1</sup> & Yazykova, Y.I.<sup>1</sup>**

<sup>1</sup>*Institute of Geology of Ore deposits, Petrography, Mineralogy and Geochemistry Russian Academy of Science (IGEM RAS), Moscow, Russia;* <sup>2</sup>*Earth Science Institute, Slovak Academy of Sciences (ESI SAS);*

\**VladKov2007@yandex.ru, t-krylova@yandex.ru*

The large Bystrinsky Cu-Au skarn-porphyry world class deposit is located in southeast part of Eastern Transbaikalia. In this territory the collisional and post-collisional magmatic processes occurred in close spatiotemporal relations. Geological structure, features of magmatism, mineralogy and geochemistry were discussed earlier (Kovalenker et al., 2016). It was found that the formation of a multicomponent (Cu-Au-Ag-W-Mo) ore was associated with subvolcanic intrusions of porphyry granitoids. This process caused a hydrothermal (retrograde) alteration of the early (prograde) anhydrous skarns and deposition of gold-copper-sulphide ores. It also found certain similarities with porphyry-skarn deposits of NE China (Pirajno and Zhou, 2015). However, the reasons of the high productivity of the magmatic-hydrothermal system remained unclear.

We believe that the reason of this may be the composition and properties of mineral-forming fluids in the transition from the magmatic to the hydrothermal stage of the process. New results from the fluid inclusion studies in minerals formed in different stages during the formation of ore can contribute to the identification of factors that influenced the productivity of the ore-forming system.

Crystal-fluid (mineral inclusions that trapped the liquid or liquid-vapour fluid) and fluid inclusions in pre-ore quartz trapped early postmagmatic fluids, as well as fluid inclusions (FI) in quartz, scheelite, apatite, characterising the hydrothermal fluids of different periods of mineral formation were studied by microthermometry (Linkam THSMG-600, IGEM RAS) and Raman spectroscopy (Lab RAM-HR800, ESI SAS) methods.

Our study showed that the porphyry mineralisation in the early (pre-ore) period was formed at the temperatures >530 °C from low-density aqueous or aqueous-carbon dioxide fluids and from brines with salinity up to 38-47 wt% NaCl eq. The mineral-forming system was periodically heterogeneous. Crystal-fluid inclusions of anhydrite, quartz, calcite and the same daughter minerals inside fluid inclusions in pre-ore quartz suggest that the post-magmatic fluids contained silicic acid, Cl<sup>-</sup>, SO<sub>4</sub><sup>2-</sup>, possibly some CO<sub>3</sub><sup>2-</sup> and HCO<sub>3</sub><sup>-</sup> ions. The cationic composition was dominated by Ca<sup>2+</sup>, Mg<sup>2+</sup>, Na<sup>+</sup>, there was a significant amount of Fe and other ore components. The presence of hematite in the matrix of pre-ore quartz, as well as daughter crystals of hematite, sometimes together with

magnetite inside FI in this quartz, indicate the oxidised nature of fluids.

The early molybdenite was formed at T>500 °C from Na-Ca-K-(Mg?)-Cl-(SO<sub>4</sub>) liquids with a significant amount of ore components (e.g., Fe).

Fluid inclusions from the late ore associations showed that low-density aqueous or aqueous-carbon dioxide fluid and chloride-sulphate brines were replaced by typical hydrothermal more neutral fluids of different salinity as the temperature decreased. Significant amounts of N<sub>2</sub>, CH<sub>4</sub>, and H<sub>2</sub> appear in substantially aqueous or aqueous-carbon dioxide gas phase either periodically or in different areas of the field. The amount of CO<sub>2</sub> in the fluid composition increased as the mineral-forming process developed.

Our data show that during separation from the magmatic chamber, the ore-forming fluids could be characterised by oxidative conditions and acidic pH, which determined their ability to contain and carry significant amounts of ore elements, including Fe, Au, Ag, Cu, Pb, Zn, Mo, W, REE etc. This might be one of the main factor that contributed to the high productivity of the mineral system of Bystrinsky deposit.

## Acknowledgement

This work was supported by RFBR, projects 18-05-00673 and 19-05-00476.

## References

- Kovalenker et al. (2016) Dokl. Earth Sci. 468:566-570.  
Pirajno F. and Zhou T. (2015) Econ. Geol. 110:603-629.

# Fluid inclusion chemostratigraphy on the Eocene Kosd Formation (Central Hungary)

**Körmös, S.<sup>1\*</sup>, Steinbach, G.<sup>2</sup> & Schubert, F.<sup>1</sup>**

<sup>1</sup>University of Szeged, Department of Mineralogy, Geochemistry and Petrology; <sup>2</sup>Hungarian Academy of Science, Biological Research Centre; \*krmssandor@gmail.com

Outcrops of Kosd Formation (KF) are located in the Bükk Mountains, the Left Side Blocks of Danube and the Buda Hills as small spots. The current research is based on an area, where the KF was encountered by wellbores, drilled in early 2000s by MOL Plc. The research area is located at the northern part of central Hungary. The KF unconformably overlies the Mesozoic basement and represents the beginning of sedimentation during the Eocene. It is set up by two parts, the lower one contains terrigenous, while the upper one consists of shallow marine, lagoonal sediments. The KF often hosts hydrocarbon reservoir rocks and coal seams. Therefore, the KF was chosen for fluid inclusion (FI) studies performed on drill cuttings and drill cores. Drill cuttings were used for a robust analysis throughout the stratigraphic column, using mass spectrometry in order to get chemostratigraphic insights of the paleo-fluid system. During the evaluation of mass spectrometric data we have considered organic and inorganic molecule ions and fragments, but focused on volatile hydrocarbon compounds. Based on the results of chemostratigraphy, drill cores were selected for detailed FI studies in order to reveal the diagenetic evolution.

The FI chemostratigraphy of digested drill cuttings suggests the presence of hydrocarbons. Methane is dominant throughout the investigated section of 400 m. There are compounds representing liquid hydrocarbons, such as nonane and decane. Furthermore, aromatic- and polycyclic hydrocarbons are present at high response level. Hydrocarbon compounds containing higher number of carbon atoms prevail a relatively narrow, approximately 80 m interval. Moreover, using the ratios of dedicated hydrocarbon species, we have determined the paleo-fluid regimes. In addition, we conclude the presumable extent of hydrocarbon migration.

Detailed FI analyses were carried out on authigenic minerals of the sandstone and siltstone members of KF, which are located in 150 m apart from each other. Aqueous fluid inclusion (AI) assemblages were found in centimetre-sized grown-up calcite (Cal<sub>GU</sub>) crystals in oversized pores, in dolomite (Dol) and along dust rims of quartz overgrowths (Qtz<sub>OG</sub>) in the sandstone member. Petroleum (PI) and AI assemblages were found in sparry calcite (Cal<sub>SP</sub>) filling bioclasts and in pore-filling quartz (Qtz<sub>PF</sub>) in the siltstone member.

The AI assemblages are primary in origin and contain 2–10 µm, locally up to 40 µm of size, two-phase, liquid-dominant (liquid+vapour) FIs. Raman

microspectroscopy of AIs proved the presence of methane in the vapour phase. The PIs appear to be primary in Cal<sub>SP</sub>, while those in Qtz<sub>PF</sub> form primary or secondary assemblages. PI assemblages consist one-phase liquid, two-phase liquid-dominant (liquid+vapour) and three-phase liquid-dominant (liquid+vapour+solid) FIs, which are 2–10 µm of size. The fluorescence colour of PIs shows a blue shift from the yellowish towards the bluish colours under UV excitation. The range of homogenisation ( $T_h$ ) and final ice melting temperatures ( $T_{mICE}$ ) are shown in Table 1. Nevertheless, the determination of  $T_{mICE}$  in case of Qtz<sub>OG</sub> was often prevented by the absence of vapour phase during ice melting.

FIA	$T_h$ [°C]			$T_{mICE}$ [°C]			Member of KF
	min	max	n	min	max	n	
<i>AI</i>							
Cal <sub>GU</sub>	126	137	83	-2.5	-3.4	94	Sandstone
Dol	105	142	33	-0.6	-5.5	21	
Qtz <sub>OG</sub>	100	146	93	-0.2	-3.4	15	
<i>PI + AI</i>							
Cal <sub>SP</sub>	105	170	21				Siltstone
Cal <sub>SP</sub>	115	146	11	-1.6	-5.2	15	
Qtz <sub>PF</sub>	117	189	15				
Qtz <sub>PF</sub>	120	129	5	-0.9	-2.2	3	

**Table 1.** Summary of minimum (min) and maximum (max) values of  $T_h$  and  $T_{mICE}$  measurements, and the number (n) of FIs measured.

Summarising our observations, we could conclude the variation of chemical composition throughout the studied section of KF using FI chemostratigraphy. Furthermore, these results were supported by detailed FI studies and provided essential information about the diagenetic evolution of investigated formation. Moreover, we could draw a rough estimation about the physico-chemical properties and relative timing of hydrocarbon emplacement.

## Acknowledgement

Authors express their gratitude to MOL Plc. for handing over rock samples and the permission of publishing the results. This project was supported by NTP-NFTÖ-18-B-0384 (Hungary).

## New experiments on Fe<sup>3+</sup>/Fe<sup>2+</sup> re-equilibration in olivine-hosted melt inclusions

**Krasheninnikov, S.P.<sup>1\*</sup>, Portnyagin, M.V.<sup>1,2</sup>, Botcharnikov, R.E.<sup>3</sup>, Wilke, M.<sup>4</sup>, Klimm, K.<sup>5</sup>, Garrevoet, J.<sup>6</sup>, Buhre, S.<sup>3</sup>, Groschopf, N.<sup>3</sup>, Scherbakov, V.D.<sup>7</sup> & Mironov, N.L.<sup>1</sup>**

<sup>1</sup>Vernadsky Institute, Russia; <sup>2</sup>GEOMAR, Germany; <sup>3</sup>Institute of Geosciences, Johannes Gutenberg University, Germany; <sup>4</sup>University of Potsdam, Germany; <sup>5</sup>Goethe University Frankfurt, Germany; <sup>6</sup>Photon Science, DESY, Germany; <sup>7</sup>Moscow State University, Russia; \*[spkrash09@gmail.com](mailto:spkrash09@gmail.com)

Melt inclusions and their host olivine provide important information on the composition of parental melts and their fractionation precursory to volcanic eruptions (Sobolev, 1996; Danyushevsky et al., 2002; Gaetani et al., 2002). New methods for studying melt inclusions also allow assessing the timing of magma fractionation and transport to the surface (Colin et al., 2012; Newcombe et al., 2014). However, some aspects of the interpretation of melt inclusion data remain controversial. In particular, the time scales of redox state re-equilibration between inclusions, olivine and host magma are not well understood.

In this work, we have conducted kinetic experiments aimed at quantification of the time-scales of  $fO_2$  re-equilibration in melt inclusions. We studied inclusions in olivine phenocrysts from the glassy margin of a pillow-lava from Loihi volcano (Hawaii, USA) and a magnesian basalt of Kluchevskoy volcano (Kamchatka, Russia). Thirty-two experiments were carried out in a Nabertherm<sup>®</sup> tube furnace at GEOKHI RAS (Krasheninnikov et al., 2017) at temperatures of 1180, 1230, and 1280 °C at 1 atm. Redox conditions for the experiments were set using Ar-H<sub>2</sub>-CO<sub>2</sub> gas mixtures corresponding to FMQ-1, FMQ+1 and FMQ+3 (in log units relative to the Fayalite-Magnetite-Quartz oxygen buffer). The olivine crystals with melt inclusions were exposed to different redox conditions for various times ranging from 5 minutes to 12 hours and quenched in water.

Major element composition of 100 melt inclusions and their host olivines were studied by microprobe (JGU and MSU). For 28 melt inclusions, the valence state of Fe in the glass was determined by XANES spectroscopy (DESY). Unheated inclusions have Fe<sup>3+</sup>/Fe<sup>2+</sup> = 0.25. The value of Fe<sup>3+</sup>/Fe<sup>2+</sup> in experimentally treated inclusions changed significantly (up to 25 rel%) already after 1 hour of experiment and shifted towards the values expected at  $fO_2$  of experiments. In general, the redox conditions in the inclusions re-equilibrated completely with the ambient gas within 5-12 hours of experimental treatments.

The results testify that the valence state of iron in melt inclusions in olivine reflects the oxidation state of magma only on the latest stage of its fractionation. Information about the initial conditions can be lost as a result of inclusion re-equilibration with evolved magma. However, possible instantaneous and late-stage variations in the magma redox state, e.g., during degassing or

cooling on magma ascent, can be preserved by Fe<sup>3+</sup>/Fe<sup>2+</sup> in rapidly quenched melt inclusions.

### Acknowledgement

The research supported by RFBR grant №18-35-00497 (to S.K.), DESY project №I-20170875 and DFG №Bo2941/4-1 (both to R.B.). We acknowledge DESY (Hamburg, Germany), a member of the Helmholtz Association HGF, for the provision of experimental facilities. Parts of this research were carried out at Petra III.

### References

- Colin A. et al. (2012) *Contrib. Mineral. Petr.* 164:677-691.  
Danyushevsky L.V. et al. (2002) *Chem. Geol.* 183:5-24.  
Gaetani G.A. and Watson E.B. (2002) *Chem. Geol.* 183:25-41.  
Krasheninnikov S.P. et al. (2017) *Dokl. Earth. Sci.* 475:919-922.  
Newcombe M. et al. (2014) *Contrib. Mineral. Petr.* 168:1030.  
Sobolev A.V. (1996) *Petrology* 4:209-220.

# Structural hydroxyl content of nominally anhydrous minerals and their relation to fluid inclusions in peridotite xenoliths (Perşani Mountains Volcanic Field, Transylvanian Basin, Romania)

**Lange, T.P.<sup>1,2</sup>, Liptai, N.<sup>1,2,3</sup>, Patkó, L.<sup>1,2,4</sup>, Berkesi, M.<sup>1,2</sup>, Kesjár, D.<sup>5</sup>, Szabó, Cs.<sup>1,3</sup> & Kovács, I.J.<sup>1,2,3\*</sup>**

<sup>1</sup>Lithosphere Fluid Research Lab, Institute of Geography and Earth Sciences, Eötvös Loránd University, Hungary; <sup>2</sup>Lendület Pannon LitH<sub>2</sub>Oscope Research Group, CSFK, MTA, Hungary; <sup>3</sup>Geodetic and Geophysical Institute, CSFK, MTA, Hungary; <sup>4</sup>Isotope Climatology and Environmental Research Centre, Institute for Nuclear Research, MTA, Hungary; <sup>5</sup> Institution of Geological and Geochemical Research, CSFK, MTA, Hungary; \*kovacs.istvan.janos@csfk.mta.hu

Hydrogen incorporation into nominally anhydrous minerals (NAMs, e.g., olivine and pyroxene) can drastically change the melting temperature, rheology and geophysical properties of the lithospheric mantle. At mantle conditions, H<sup>+</sup> can also be present in the form of H<sub>2</sub>O as fluid and incorporated as “OH” in hydrous minerals (amphibole, phlogopite).

In this study, we focus on mantle xenoliths collected from the Perşani Mountains Volcanic Field, presenting structural hydroxyl information to figure out how the hydroxyl content and fluid inclusions in the NAMs can affect the deformation mechanism of peridotites. Selected mantle xenoliths are slightly to strongly deformed (showing equigranular to protomylonitic texture), lineation is defined by spinel. Olivin always, ortho- and clinopyroxene porphyroclasts sometimes show deformation signatures.

Primary (Fig. 1) fluid inclusions within orthopyroxene occur randomly, have an average size of 10 µm, show negative crystal shape and have vapour and fluid phases at room temperature. Secondary fluid inclusions within orthopyroxene are elongated, have an average size of 30 µm, are found along fractures and have two phases, a vapour and a fluid one. Fluid inclusions in orthopyroxene are enclosed generally parallel to clinopyroxene and amphibole lamellae. Fluid inclusions within olivin and clinopyroxene are dominantly considered as secondary fluid inclusions.

We conclude that lamellae in mantle minerals contribute to fluid migration, helping the deformation rate of the mantle wedge underneath the study area. Diffusion of H<sub>2</sub>O from fluid inclusions into host pyroxene can result in amphibole lamellae formation as observed by Berkesi et al. (2019). Diffused H<sup>+</sup> can incorporate in vacancy changing the rheology of the host mineral.

## Acknowledgement

Measurements of this study was financially supported by the Lendület Research Grant to the MTA CSFK Lendület Pannon LitH<sub>2</sub>Oscope Research group. The conference participation is subsidised by the Talent Support Council of Eötvös Loránd University, Budapest. This work was also supported by the ÚNKP-18-3 New National Excellence Program of the Ministry of Human Capacities.

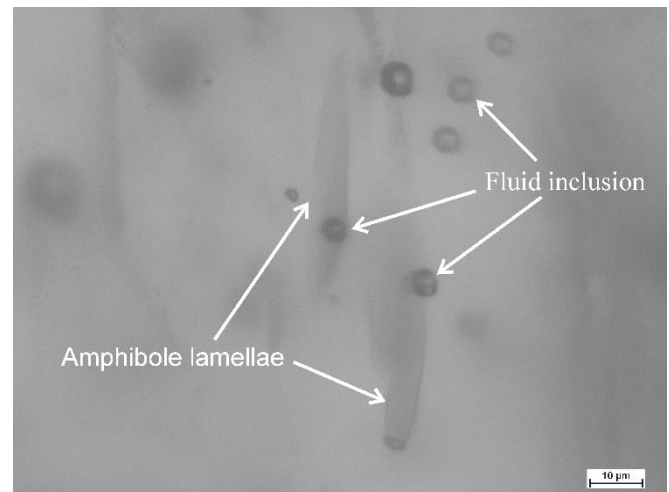


**Fig. 1.** Primary fluid inclusions occurring together with amphibole lamellae in orthopyroxene (PGR-I-0345).

## References

Berkesi M. et al. (2019) Chem. Geol. 508:182-196.

# Determination of composition, pressure and density of CO<sub>2</sub>-CH<sub>4</sub> gas mixtures by Raman spectroscopy. Application to natural fluid inclusions from the Central Alps, Switzerland

Le, V.H.<sup>1\*</sup>, Caumon, M.C.<sup>2</sup>, Tarantola, A.<sup>1</sup>, Randi, A.<sup>1</sup>, Robert, P.<sup>1</sup> & Mullis, J.<sup>2</sup>

<sup>1</sup> GeoResources Laboratory, CNRS, Université de Lorraine, France; <sup>2</sup>Mineralogisch-Petrographisches Institut, Switzerland; \*van-hoan.le@univ-lorraine.fr

Raman spectroscopy is widely used since the 1970s as an alternative method to microthermometry to analyse fluid inclusions (Frezzotti et al., 2012). Quantitative Raman measurements are generally based on relative Raman scattering cross-section (RRSCS) and the variation of spectral features (peak position, peak area/intensity) as a function of composition, pressure or density. However, most of the published data were established at low density and without evaluating the effect of composition (Burke, 2001). This can lead to important error when applied to geological fluids containing generally several substances at elevated pressure. CO<sub>2</sub> and CH<sub>4</sub> are among the dominant gas species within a large variety of geological fluids (Mullis et al., 1994). The experimental data of Seitz et al. (1996) revealed variation trends of different Raman spectral parameters of CO<sub>2</sub> and CH<sub>4</sub> but no calibration was given because the results themselves were quite scattered.

The first aim of this study is to verify the effect of composition and density on the RRSCS of CO<sub>2</sub> and CH<sub>4</sub> (to N<sub>2</sub>) by renewing these data using modern performance instruments for better accuracy. The second aim is to establish new calibration data for quantitative measurements of CO<sub>2</sub>-CH<sub>4</sub> gas mixtures over a pressure range of 5 to 600 bars. Herein, binary gas mixtures of CO<sub>2</sub> and/or CH<sub>4</sub> and/or N<sub>2</sub> were prepared at different proportions (from 10 to 90 mol%). A high-pressure optical cell system (HPOC) (Chou et al., 2012) with a transparent microcapillary (Caumon et al., 2014) containing the prepared gas mixtures placed on a heating-cooling stage (Linkam CAP500®) were used for Raman in-situ analyses at controlled PTX conditions (Fig. 1).

Our experimental results show that RRSCS of CO<sub>2</sub> and CH<sub>4</sub> remain constant with varying composition and pressure and are close to published data. The results are nevertheless presented here with better accuracy. Thus, it can be used for determining the composition of gas mixtures. The Fermi diad splitting of CO<sub>2</sub> and the peak area/intensity ratio of CH<sub>4</sub> band were demonstrated to be sensitive to pressure (density) and composition. New polynomial equations are derived from our experimental data for pressure and density determination. The latter results are then applied to natural fluid inclusions hosted in quartz from the Central Alps, Switzerland (Mullis et al., 1994). The Raman results are compared with those obtained from microthermometry for validation.

## References

- Burke E. (2001) *Lithos* 55:139-158.  
Chou I. M. et al. (2012) in: *EMU Notes* 12:227-247.  
Caumon M.C. et al. (2014) *Chem. Geol.* 378-379:52-61.  
Frezzotti M.L. et al. (2012) *Geochem. Explor.* 112:1-20.  
Mullis J. et al. (1994) *Geochim. Cosmochim. Ac.* 58:2239-2267.  
Seitz J. et al. (1996) *Am. J. Sci.* 296:577-600.

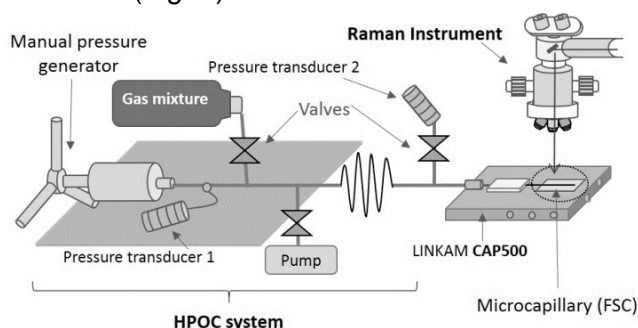


Fig. 1. Sketch of the experimental setup

Thereby, the behaviours of CO<sub>2</sub> and CH<sub>4</sub> Raman spectra could be investigated to figure out the most reliable quantitative parameter for pressure and density determination.

## Evolution of mineralizing fluids at the Cantung W-Cu skarn deposit, Northwest Territories, Canada

**Legros, H.<sup>1\*</sup>, Elongo, V.<sup>1</sup>, Lecumberri-Sanchez, P.<sup>1</sup>, Falck, H.<sup>2</sup> & Adlakha, E.<sup>3</sup>**

<sup>1</sup>Earth and Atmospheric Sciences, University of Alberta, Canada; <sup>2</sup>NWT Geological Survey, Canada; <sup>3</sup>Department of Geology, Saint Mary's University, Canada; \*hlegros@ualberta.ca

The Cantung deposit, located in the Canadian Cordillera (southwest corner of the Northwest Territories), is a world-class W-Cu skarn deposit. Since 1962, ~7.68 Mt of ore has been extracted at a grade of ~1.4 % WO<sub>3</sub>. The Cantung deposit is hosted in the carbonate units of the Cambrian Sekwi Formation, which are part of the Selwyn Basin. The skarn is spatially associated with monzogranite intrusions from the Tungsten plutonic suite (94 to 98 Ma). At Cantung, the main pluton is a sub-alkaline biotite monzogranite called the Mine Stock (Rasmussen et al., 2011).

Tungsten is hosted in scheelite (CaWO<sub>4</sub>), which is mostly disseminated or present in veins in the two ore bodies of the Cantung deposit: the Open Pit and the E-Zone. The main site of mineralisation is the E-Zone ore body, which is hosted in Lower Cambrian to Devonian marble near its contact with the Mine Stock pluton (Zaw, 1976; Mathieson and Clark, 1984).

We aim to determine the nature and evolution of fluids involved in the formation of the Cantung deposit through an integrated, microanalytical fluid inclusion study. Samples from the Mine Stock pluton below the E-zone deposit as well as from the orebody itself have been collected. Fluid inclusions have been petrographically characterised and range in paragenesis from the early magmatic fluid, to the ore-forming fluid, and finally the late post-mineralising fluid.

The least modified magmatic fluid samples are those from barren quartz in greisenized Mine Stock below the ore body. This fluid is preserved as assemblages of primary, two-phase aqueous fluid inclusions hosted along growth zones in quartz. Salinity of this fluid as well as homogenisation temperature are low (less than 6 wt% equiv. NaCl and 150-250 °C).

Scheelite contains fluid inclusions likely representing the ore fluid. Scheelite have very complex fluid inclusions which are not yet completely characterised. All fluid inclusions in scheelite have homogenisation temperatures higher than 250 °C and are unique to the scheelite hosted fluid inclusions.

The quartz veins crosscutting the skarn show two types of fluid inclusions: CH<sub>4</sub>-rich one-phase inclusions and two-phase aqueous inclusions. Both (non-Scheelite) types are secondary fluid inclusions and are observed in the quartz associated with late stage garnet, and have a wide range of salinity. In contrast, when associated with tourmaline, quartz hosts two-phase aqueous inclusions and CO<sub>2</sub>-rich inclusions with low salinity,

comparable to the fluid observed in the greisen quartz. The latter fluid inclusion types observed in the quartz associated with tourmaline are consistent with those described by Yuwan et al. (2007).

Characterisation of the multiple generations of fluid inclusions will take place using microthermometry, Raman spectroscopy, and LA-ICPMS.

### References

- Mathieson G.A. and Clark A.H. (1984) *Econ. Geol.* 79: 883-901.
- Rasmussen K.L. et al. (2011) *Ore Geol. Rev.* 41:75-111.
- Yuwan J. et al. (2007) in: *Mineral and Energy Resource Assessment of the Greater Nahanni Ecosystem Under Consideration for the Expansion of the Nahanni National Park Reserve, Northwest Territories* 5344:177-190.
- Zaw K. (1976) MSc thesis, Queen's University, Canada.

# Characteristics and implications of fluid inclusions in cretaceous siliceous sandstone, Ri-qing-wei Basin, China

Li, G.H.<sup>1\*</sup>, Chen, Y.<sup>1</sup>, Chen, L.S.<sup>1,2</sup> & Zhou, Z.Z.<sup>3</sup>

<sup>1</sup>School of Geosciences, China University of Petroleum, China; <sup>2</sup>School of International Business, The Southwestern University of Finance and Economics, China; <sup>3</sup>College of Earth Science and Engineering, Shandong University of Science and Technology, China; \*chinaliguanhua@gmail.com

The Ri-qing-wei Basin is located between the southeast part of the Wulian-Rongcheng fault and the northwest of the Qianliyan fault. It is a narrow and long rift basin with a NE-SW orientation. The basin contains Cretaceous deep-water turbidites associated often to other siliceous rocks. The presence of Ri-qing-wei is recently recognised; its formation mechanism has not been known precisely, yet. In this study, siliceous rocks and their siliceous strips were the main research objects. The characteristics of siliceous rock samples were studied petrographically under polarisation microscope. The fluid inclusions in the cement quartz from siliceous rocks have been selected for a detailed fluid inclusion (FI, Fig. 1) study. We carried out Raman spectroscopic, microthermoemtric and cathodoluminescence measurements.

Under cathodoluminescence microscope, we found fluid inclusions, located to a distinct boundary within the quartz particles, have different colours. The microthermometry of the fluid inclusions showed a temperature range for homogenisation between 292.6 °C and 297.6 °C. Late Mesozoic lithosphere has undergone extensive magmatic activity induced by extensive thinning of the lithosphere in the east China (Charles et al., 2013). Therefore, it is considered that the formation of the siliceous rocks might be affected by a hydrothermal activity originated from the surrounding magmatic rocks.

## Acknowledgement

This work was supported by the National Natural Science Foundation of China (No. U1762108) and the Key Research Projects of Shandong Province (No. 2017CXGC1608 and 2017CXGC1602).

## References

Charles N. et al. (2013) Gondwana Res. 24:412-428.

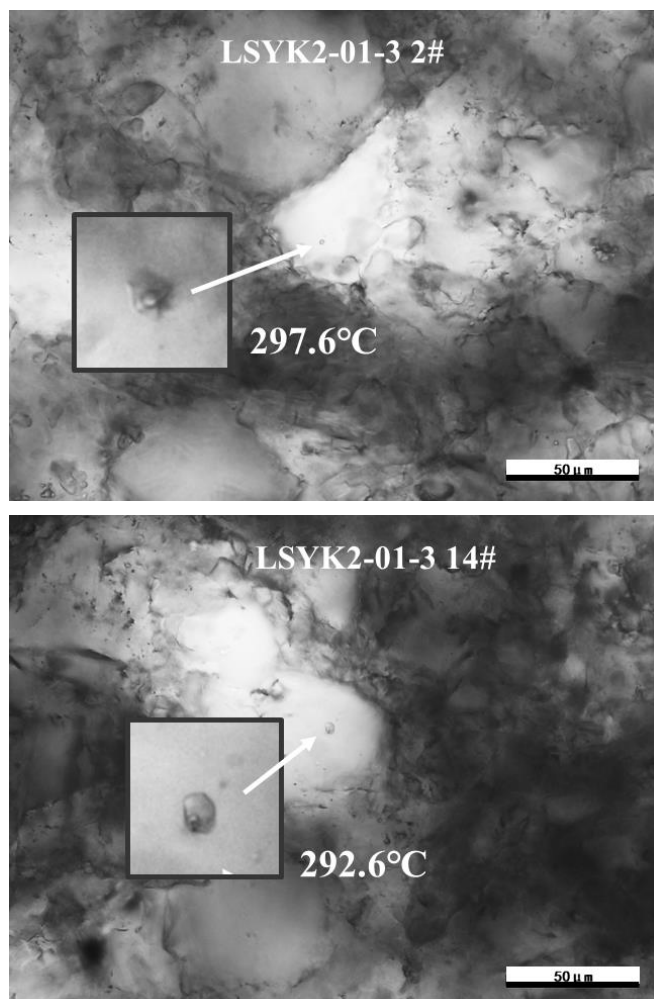


**Fig. 1.** Representative photos of quartz-hosted fluid inclusions at room-T taken under polarisation microscope. Homogenisation temperatures are also indicated.

# Combined application of Raman spectroscopy and focused ion beam – scanning electron microscopy on silicate melt inclusions to track metasomatism in spinel peridotite xenoliths

Liptai, N.<sup>1,2\*</sup>, Berkesi, M.<sup>1,3</sup>, Patkó, L.<sup>1,3</sup>, Griffin, W.L.<sup>4</sup>, O'Reilly, S.Y.<sup>4</sup> & Szabó, Cs.<sup>1,3</sup>

<sup>1</sup>MTA CSFK Lendület Pannon LitH<sub>2</sub>Oscope Research Group, Hungary; <sup>2</sup>MTA CSFK Geodesic and Geophysical Institute; <sup>3</sup>Lithosphere Fluid Research Lab, Eötvös Loránd University, Hungary; <sup>4</sup>ARC Centre of Excellence for Core to Crust Fluid Systems (CCFS) and GEMOC, Macquarie University, Australia; \*liptai.nora@csfk.mta.hu

Silicate melt inclusions (SMIs) play a key role in mantle research as their composition represents characteristics of the melt present in the mantle at the time of entrapment, therefore they can preserve valuable information about metasomatic processes. There are several methods to study SMIs, but the combination of Raman spectroscopy with focused ion beam – scanning electron microscopy (FIB-SEM) provides an exceptional opportunity to identify daughter phases, obtain their major element compositions and reconstruct a 3D model of the inclusion.

In this study we present analyses on partially crystallised primary SMIs hosted in clinopyroxene in a metasomatised spinel peridotite xenolith from the Nógrád-Gömör Volcanic Field, located in the northern part of the Pannonian Basin in Central Europe. Xenoliths from this locality have been affected by several different metasomatic events prior to entrainment by the host basalt (Liptai et al., 2017). The youngest of these events is a melt-rock reaction which transformed the lherzolite wallrock into wehrlite (Patkó et al., 2013). Based on the petrology of the xenolith featured in this study, the analysed SMIs have trapped the melt which can be linked to this metasomatism.

Raman spectroscopy and imaging revealed the presence of apatite, clinopyroxene, sulphates (anhydrite and barite) and amphibole within the inclusions. The volatile bubble is composed of CO<sub>2</sub>. Slicing with FIB-SEM revealed additional phases such as spinel, sulphide and mica (Fig. 1). Geochemical analyses and 3D reconstruction of the inclusions allowed the calculation of the bulk major element composition of the SMIs, and LA-ICP-MS analyses on other inclusions of the same host clinopyroxene grain provided trace-element concentrations as well.

Based on the obtained bulk geochemistry, the melt trapped in the inclusions is enriched in Fe and has OIB-type characteristics. This is in agreement with the metasomatic process related to the formation of the wehrlites, which is inferred to have been caused by an intraplate mafic melt, similar to the host basalt of the xenoliths. Pre-entrapment evolution and reaction with the lherzolite wallrock resulted in intermedier melt composition. Petrogenetic modeling showed that the melt was generated with a very small degree of partial melting of a garnet lherzolite source. Following the entrapment and partial crystallisation, a volatile bubble exsolved from the residual glass during

ascent at shallow depths, as suggested by homogeneous CO<sub>2</sub>-densities. Small crystals such as sulphates and mica, formed probably in a late stage at the boundary of the bubble and the glass, indicate the presence of S and possibly water in the original bubble composition.

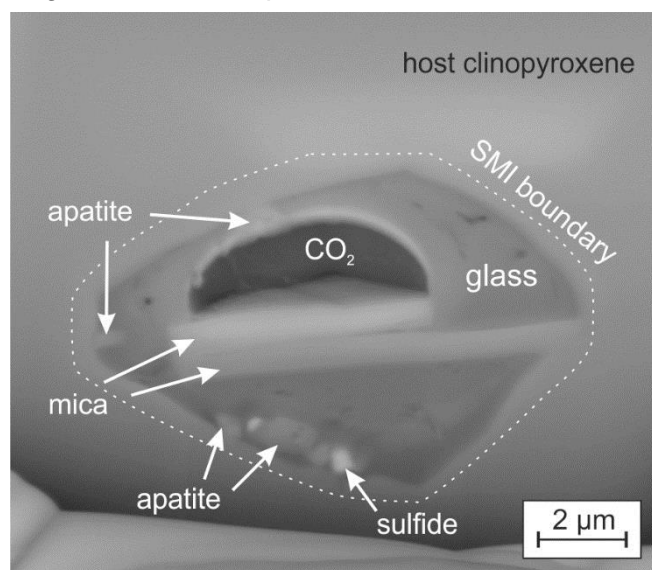


**Fig. 1.** Backscattered electron image of an SMI slice obtained during FIB-SEM analyses.

## Acknowledgement

This study was supported by a PhD scholarship of Macquarie University (Australia) and Eötvös Loránd University (Hungary) to N. Liptai, a Bolyai János Postdoctoral Research Fellowship of the Hungarian Academy of Sciences to M. Berkesi, and the Lendület Pannon LitH<sub>2</sub>Oscope Research Group.

## References

- Liptai N. et al. (2017) *J. Petrol.* 58:1107-1144.
- Patkó L. et al. (2013) *Mineral. Mag.* 77:1934.

# Multiple stages of oil filling in Archean buried hill reservoir in the Bozhong depression, Bohai Bay basin, eastern China: evidence from fluid inclusions

Liu, T.Y.<sup>1\*</sup> & Chen, Y.<sup>1</sup>

<sup>1</sup>School of Geosciences, China University of Petroleum, China; \*gracetingyu@outlook.com

One of the most important oil-bearing fault basins in eastern China is the Bohai Bay. The basin has undergone complex tectonic evolution. Industrial petroleum pool had been found in Archean buried hill of the Bozhong depression, Bohai Bay basin. The Bozhong depression is located in the northern section of the Tanlu Fault Zone, which has gone through strong stretching and extension. Lithologically the anticline is composed of gneiss, which is overlain by the Paleogene of the Dongying formation the Shahejie formation and the Kongdian formation. The third member (Es<sub>3</sub>) of Shahejie formation is the most important source rock, whereas the mudstone carbonate of Dongying and Shahejie formation are the reservoir rocks. Hydrocarbon generation of Es<sub>3</sub> began around 24 Mya and reached its peak around 12 Mya (Xue et al., 2018). The generated oil and gas entered the Archean reservoir through fractures on both sides of the anticline. We collected Archean rock samples to study quartz-hosted fluid inclusions related to oil accumulation. We carried out microscopic observations and micro-thermometric analysis on the fluid inclusions. Two main oil-filling stages were confirmed by our fluid inclusions study. In order to understand the oil filling and migration period and reservoir controlling factors in this area, we collected Archean core samples to study fluid inclusions related to oil accumulation by microscopic observation and micro-thermometry analysis. The results show hydrocarbon migrations in the metamorphosed reservoir.

The first generation (early) of hydrocarbon inclusions in secondary trails of quartz has blue-green fluorescence liquid phase (Fig. 1a) and showed homogenisation temperatures in the range of 117.6-121.7 °C. These inclusions are considered to be formed in quartz fractures initially, then the fractures healed, causing inclusions isolated.

The second generation (late) of secondary hydrocarbon inclusions found in quartz. The later formed hydrocarbon inclusions distributed along fractures cutting through quartz grains and have blue-white fluorescence (Fig. 1b). Their homogenisation temperatures are measured to be between 94.7 and 166.3 °C. Here we found coeval aqueous fluid inclusions, which showed a range for homogenisation temperatures in 130.0-155.6 °C and a salinity between 11.70 and 20.97 eq., NaCl wt%. The hydrocarbon inclusions in the second generation show higher maturity than those on the first generation.

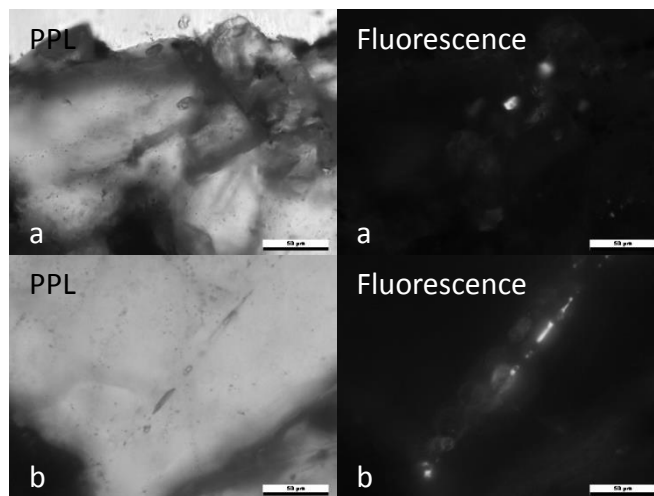


**Fig. 1.** Quartz-hosted secondary hydrocarbon inclusions. A) first generation, B) second generation. Photomicrographs under visible light (left), under fluorescent light (right).

## References

Xue Y. et al. (2018) China offshore oil and gas. 30:1-9 (Chinese with English abstract).

# Fluid inclusion, stable and noble gas isotope study of hydrothermal Cu-mineralisations in the Mirdita Zone, Albania: implications for their genesis

Lovász, A.<sup>1\*</sup>, B. Kiss, G.<sup>1</sup>, Czuppon, Gy.<sup>2</sup>, Molnár, K.<sup>3,4</sup> & Benkó, Zs.<sup>3</sup>

<sup>1</sup>Department of Mineralogy, Eötvös Loránd University Hungary; <sup>2</sup>Institute for Geological and Geochemical Research, HAS, Hungary; <sup>3</sup>Institute for Nuclear Physics, HAS, Hungary; <sup>4</sup>Department of Petrology and Geochemistry, Eötvös Loránd University, Hungary; \*lovasz.a0@gmail.com

The Mirdita Zone is an ophiolitic unit of the Dinarides in Albania, where ocean floor remnants of the Jurassic Neotethys are preserved. Two geotectonic units can be distinguished in this zone: MOR-type in the western and SSZ-type in the eastern parts. The investigated hydrothermal mineralisations are gabbro-hosted, quartz-sulphide vein type copper deposits, namely Puka-Kçira in the Western (MOR-type) and Thirra in the Eastern (SSZ-type) Ophiolite Belts (Robertson and Shallo, 2000). The genesis of the Jurassic gabbro-hosted mineralisations is unclear and the deposit type was also not defined. Therefore, our goal is to determine the nature and origin of the ore-forming fluids and to contribute to the modelling of the deposit formation processes.

Based on our field observations, petrographical and mineralogical studies as well as the geological background, the deposits may have formed during regional metamorphism by metamorphic-hydrothermal fluids or by a local submarine hydrothermal event, i.e. as feeder zones of volcanogenic massive sulphide (VMS) deposits. Although the mineral chemistry favours the latter possibility, fluid inclusion microthermometry and stable- as well as noble gas isotope analyses were conducted constrain the origin of the studied copper deposits

Quartz and calcite containing fluid inclusions are present in both deposits (Fig. 1), providing a great opportunity to define the geochemical character of the forming fluids and processes which played a key role during their formations. Fluid inclusion petrography suggests homogenous parent fluids in every case. The minimum formation temperature of the late-stage calcite is 180–260 °C at both locations, while the minimum ore-forming temperature is 275–356 °C at Puka-Kçira and 330–389 °C at Thirra, as suggested by inclusions of coeval quartz. The appearance of two quartz generations as well as late calcite, together with the wide temperature ranges, suggest multiple hydrothermal events and dynamically changing conditions. Cryoscopic measurements combined with Raman spectroscopy show the NaCl–H<sub>2</sub>O system (salinities of 2.4–7.2 NaCl equiv. wt%) and minor methane content. Combining He, Ne and Ar noble gas isotope as well as H stable isotope analyses of the fluid inclusions, the fluid source can be traced. The noble gas systematics and H isotope compositions of the quartz- and sulphide-hosted fluid inclusions as well as the C–O isotope compositions of late-stage calcite indicate that the

ore-forming fluid has seawater origin which evolved by fluid–rock interactions within the crust and admixture of minor amount of magmatic fluid.

Based on these results, the metamorphic origin can be excluded while the VMS origin is confirmed.

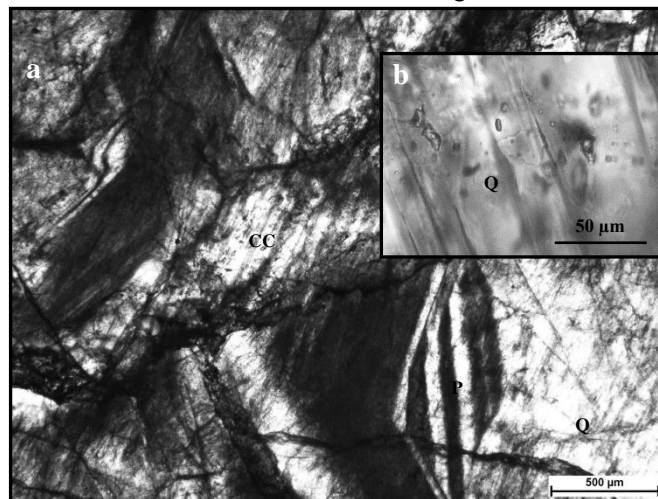


**Fig. 1.** A) Early generation of quartz (Q) containing primary inclusions (P) with later stage calcite (cc). B) Two-phase S- and I-type FIs in calcite.

## Acknowledgement

The research was supported by the ÚNKP-16-2, New National Excellence Program of the Ministry of Human Capacities (to A. Lovász), the OTKA PD 112580 (to G. B. Kiss), the Bolyai Scholarship (to Zs. Benkó) and the ENERAG project (funding from the European Union's Horizon 2020 research and innovation programme under Grant Agreement No. 810980).

## References

Robertson A.H.F. and Shallo M. (2000) *Tectonophysics*. 316:197-214.

## Seafloor hydrothermal systems control seawater chemistry: evidence from fluid inclusions in halite

**Lowenstein, T.K.<sup>1\*</sup>, Weldeghebriel, M.F.<sup>1</sup>, García-Veigas, J.<sup>2</sup>, Demicco, R.V.<sup>1</sup>, Cendón, D.I.<sup>3</sup>, Graney, J.<sup>1</sup>, Bodnar, R.J.<sup>4</sup> & Sendula, E.<sup>4</sup>**

<sup>1</sup>Department of Geological Sciences and Environmental Studies, Binghamton University, USA; <sup>2</sup>Scientific and Technological Centers, Universitat de Barcelona, Spain; <sup>3</sup>Australian Nuclear Science and Technology Organisation, Australia; <sup>4</sup>Department of Geosciences, Virginia Polytechnic Institute and State University, USA; \*lowenst@binghamton.edu

The major ion chemistry ( $Mg^{2+}$ ,  $Ca^{2+}$ ,  $Na^+$ ,  $SO_4^{2-}$ ,  $Cl^-$ ,  $HCO_3^-$ ) and isotopic composition ( $\delta^7Li$ ,  $\delta^{11}B$ ,  $^{87}Sr/^{86}Sr$ ) of seawater have varied in the Phanerozoic. Changes in the  $Mg^{2+}$  and  $Ca^{2+}$  concentration of ancient seawater (Fig. 1) influenced the evolution of marine shell-building organisms because the  $Mg/Ca$  ratio of seawater controls which carbonate, calcite or aragonite, is favored to precipitate (Ries, 2010). Secular changes in the  $Ca^{2+}$ ,  $Mg^{2+}$ , and  $SO_4^{2-}$  concentration in Phanerozoic seawater controlled the mineralogy of marine potash evaporites such that  $MgSO_4$  evaporites occur in phase with aragonite seas and  $KCl$  evaporites occur with calcite seas (Hardie, 1996). Long-term changes in the major ion chemistry of seawater also parallel sea level fluctuations, icehouse-greenhouse climates, and variations in atmospheric  $CO_2$ .

Fluid inclusions in marine halite are direct samples of ancient evaporated seawater. Chemical analyses of seawater fluid inclusions were used to document the major ion chemistry of the Phanerozoic oceans (Lowenstein et al., 2001), but there is disagreement over which global-scale processes were most directly responsible for the observed variations. First order controls on the temporal changes in seawater chemistry include variations in the rates of: (1) seafloor spreading and midocean ridge hydrothermal discharge (Demicco et al., 2005), (2) continental weathering, for example, Cenozoic uplift of the Himalayas (Edmond, 1992), (3) deposition of marine carbonates and dolomitisation (Broecker, 2013), and (4) low-temperature weathering of seafloor basalt and incorporation into marine sediments (Demicco et al., 2005).

Recent analytical advances using Laser ablation ICP MS now allow quantitative measurement of minor and trace elements in fluid inclusions in halite. Lithium, for example, has undergone significant variations in concentration in Phanerozoic seawater. Li is a conservative element that is not incorporated to any significant degree in minerals precipitated from seawater, such as calcite, aragonite, gypsum or halite, so there is no  $Li^+$  loss as seawater evolves during progressive evaporation. Li today is largely supplied to the oceans by mid-ocean ridge hydrothermal brines (72% of modern  $Li^+$  inflow to

the oceans) at concentrations three orders of magnitude higher than river water sources of Li, so past variations in the  $Li^+$  concentration of seawater may be related to fluctuations in mid-ocean ridge hydrothermal activity. Here, we present a 350 Ma record of seawater  $Li^+$  concentrations from direct measurement of primary fluid inclusions in marine halite and show from modeling that seafloor hydrothermal systems have controlled the  $Li^+$  composition of seawater over geologic time. The modeling results apply to other elements whose past concentrations mirror that of  $Li^+$ , most notably  $Ca^{2+}$  and  $Sr^{2+}$ .

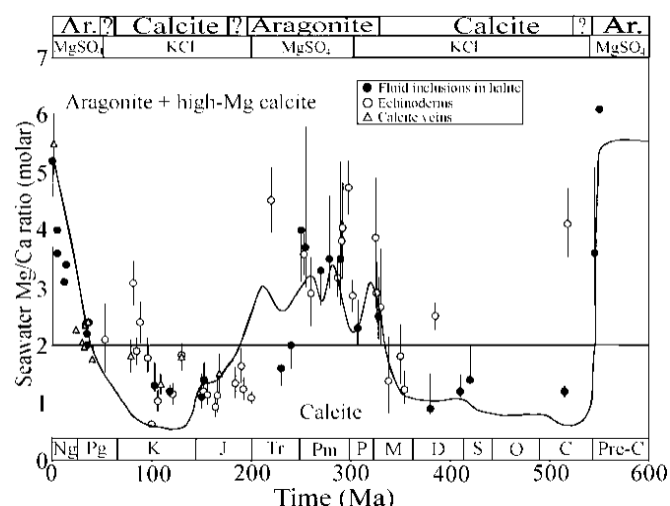


**Fig. 1.** Secular variation in the  $Mg^{2+}/Ca^{2+}$  ratio of seawater during the Phanerozoic (modified from Holt et al., 2014).

### Acknowledgement

David Collins is thanked for his help using the LA ICP MS. Zoltan Zajacz and Marcel Guillong provided invaluable advice on the operation of the LA ICP MS.

### References

- Broecker W. (2013) *Am. J. Sci.* 313:776-789.
- Demicco R.V. et al. (2005) *Geology* 33:877-880.
- Edmond J. M. (1992) *Science* 258:1594-1597.
- Hardie L.A. (1996) *Geology* 24:279-283.
- Holt N.M. et al. (2014) *Geochim. Cosmochim. Ac.* 134:317-334.
- Lowenstein T.K. et al. (2001) *Science* 294:1086-1088.
- Ries J.B. (2010) *Biogeosciences* 7:2795-2849.

# Preliminary results on UHP fluid inclusions preserved in UHP marbles from the Dora-Maira Massif (Italian Western Alps)

Maffeis, A.<sup>1\*</sup>, Ferrando, S.<sup>1</sup>, Castelli, D.<sup>1</sup> & Frezzotti, M.L.<sup>2</sup>

<sup>1</sup>Department of Earth Sciences, Università degli Studi di Torino, Italy; <sup>2</sup>Department of Earth and Environmental Sciences, Università degli Studi di Milano-Bicocca, Italy; \*andrea.maffeis@unito.it

The direct study of the fluids that circulated during active subduction of continental crust at sub-arc depth is fundamental to understand the Deep Carbon Cycle (Kelemen and Manning, 2015). The investigation of metamorphic and fluid evolution of UHP impure marbles is promising to follow the fate of carbonates during deep subduction.

In the UHP Brossasco-Isasca Unit (BIU) of the Dora-Maira Massif, there are some hectometre-scale lenses of impure marbles that experienced peak metamorphic conditions at ~4.0 GPa and ~730 °C (Castelli et al., 2007). Some marbles preserve evidence for multiple events of dissolution-precipitation of Dol (all mineral abbreviations after Whitney and Evans, 2010) occurred during UHP prograde to early-retrograde evolution in presence of a complex, solute-rich aqueous fluid (Ferrando et al., 2017).

An impure marble, consisting in the simple peak mineral assemblage Cc (ex Arg) + Dol + Di + Ol, has been selected to assess both the composition and evolution of the fluid phase during exhumation. A detailed petrographic investigation allowed distinguishing five main groups of synchronous inclusions within zoned Di:

- Group I: large (5-25 µm) primary bi-phase multisolid aqueous inclusions (liquid + different kinds of solids) within the UHP core of porphyroblastic Di; (Fig. 1);
- Group II: small (<1-8 µm) primary, within the mantle of porphyroblastic Di, bi-phase aqueous inclusions containing liquid and vapour (L+V) [L/(L+V)~80-90%];
- Group III: small (<1-6 µm) secondary intragranular (grain internal), bi-phase aqueous inclusions containing liquid and vapour (L+V) [L/(L+V)~60-80%];
- Group IV: small (<1-8 µm) secondary (intragranular, grain boundary → grain boundary) tri-phase aqueous inclusions containing a liquid, a vapour bubble and a cubic solid (probably a salt; L+V+S);
- Group V: variable sized (<1-24 µm) secondary (intragranular: grain boundary → interior in Di bigger than 200-240 µm; grain boundary → grain boundary in Di smaller than 200-240 µm) bi-phase aqueous inclusions containing liquid and vapour (L+V) and characterised by a dominant vapour bubble [L/(L+V) ~30-40%].

Regarding the multiphase aqueous inclusions, micro-Raman analyses allowed to recognise the presence of Mg-Cc + Tlc + Tr ± Dol ± H<sub>2</sub>O<sub>liq</sub> ± a non-Raman active phase. Based on results from optical

microscopy, the latter phase can be a cubic daughter mineral (i.e. a salt). SEM-EDS analysis on open inclusions, revealed appreciable Cl content in Tr and Tlc (Ferrando et al., 2017). This finding points to a solute-rich aqueous COH fluid, containing Ca, Mg, Si, CO<sub>3</sub><sup>2-</sup> and Cl. This solute-rich fluid may be responsible for the UHP dissolution-precipitation of carbonates during subduction. The subsequent evolution during exhumation occurred in presence of more diluted aqueous fluids characterised by distinct salinities and by the lack of dissolved Si and CO<sub>3</sub><sup>2-</sup>.

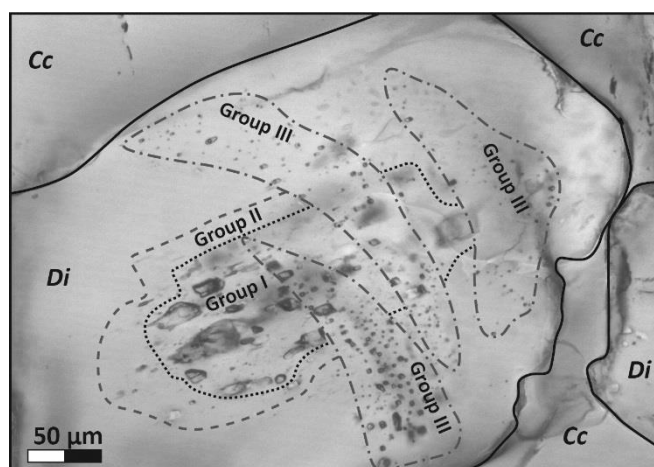


**Fig. 1.** Typical microstructural relationships between diopside-hosted, primary Group I bi-phase multisolid aqueous and primary Group II and secondary Group III aqueous inclusions. Stacked microphotographs (50X), from 0 to 6 µm of depth in the crystal.

## References

- Ferrando S. et al. (2017) *Am. Mineral.* 102:42-60.  
Castelli D. et al. (2007): *J. Metamorph. Geol.* 25:587-603.  
Kelemen P.B. and Manning C.E. (2015) *P. Natl. Acad. Sci. USA* 112:E3997-E4006.  
Whitney D.L. and Evans B.W. (2010) *Am. Mineral.* 95:185-187.

# Fluid constraints in the Miguel Vacas Cu deposit (Ossa-Morena Zone, Portugal)

Maia, M.<sup>1,2\*</sup>, Moreira, N.<sup>1,2</sup>, Mirão, J.<sup>1,3</sup>, Noronha, F.<sup>2,4</sup> & Nogueira, P.<sup>1,2</sup>

<sup>1</sup>University of Évora, Faculty of Sciences and Technology, Portugal; <sup>2</sup>Institute of Earth Sciences, Portugal; <sup>3</sup>HERCULES Laboratory, University of Évora, Portugal; <sup>4</sup>University of Porto, Faculty of Sciences, Portugal; \*mcmaiageo@gmail.com

The ancient *Miguel Vacas* copper mine belongs to a cluster of ancient Cu mines and occurrences in the Ossa-Morena Zone, specifically in the *Sousel-Barrancos* metallogenic belt (SBMB), such as *Mociços*, *Ferrarias* and *Bugalho*. This deposit is characterised by an anastomosing vein structure mainly composed of quartz + carbonate + sulphides that extends over 2 km in length with an NNW-SSE direction. Chalcopyrite is the main primary Cu mineralisation; strong supergene enrichment is evidenced by the mineral assemblage of libethenite, malachite, bornite and digenite. Prospects in the area also reveal the presence of arsenopyrite. An epigenetic epithermal model for the Cu mineralisation is proposed for *Miguel Vacas*, as well as for other SBMB deposits (Mateus et al., 2003). This study aims to the characterisation of the fluids related with the mineralising processes. Sampling was done in a borehole at different depths (eight samples from 53 to 188 m). This study allowed identifying three different FI types regarding their composition.

LVS<sub>1-3</sub> where L and V is H<sub>2</sub>O, S<sub>1</sub> corresponds to halite, S<sub>2</sub> is a carbonate and S<sub>3</sub> an opaque phase; most of the inclusions contain a halite crystal. LV consists of two-phase inclusions where L and V are H<sub>2</sub>O. L<sub>1-2</sub>V where L<sub>1</sub> is H<sub>2</sub>O; L<sub>2</sub> and V are CO<sub>2</sub>. *Miguel Vacas* fluids studied in mineralised veins show a wide range of homogenisation temperatures ( $T_h = [62.8 - 350 \text{ }^\circ\text{C}]$ ;  $\bar{x} = 181 \text{ }^\circ\text{C}$ ) and salinities ( $[0.35 - 30.9]$ ;  $\bar{x} = 17.89 \text{ wt\% NaCl equiv.}$ ). First ice melting temperatures ( $T_e = [-68 - -14 \text{ }^\circ\text{C}]$ ;  $\bar{x} = -46 \text{ }^\circ\text{C}$ ) suggest the presence of solutes such as CaCl<sub>2</sub> and MgCl<sub>2</sub>.

LV microthermometry data allowed to differentiate between two major groups (LV-a and LV-b), enhancing that even though these inclusions are gathered in the same FI assemblage they belong to a different fluid pulse. LVS<sub>1-3</sub> and LV-a inclusions were studied in quartz + calcite ore-bearing veins, with comb-zoned textures, where these fluids coexist. Figure 1 suggests mixing between high salinity (LVS<sub>1-3</sub>) and lower salinity fluids (LV-a) (arrow trend), which may indicate different fluid sources present in the system. It should be emphasised that halite-bearing FI's show  $T_{h(L+V \rightarrow L)}$  at lower temperatures than halite melting ( $T_{mHal} = [83.1 - 181.4 \text{ }^\circ\text{C}]$ ;  $\bar{x} = 144.7 \text{ }^\circ\text{C}$ ). LV-b FI's are found in shallower milky quartz samples (53 and 65 m), close to a dolerite intrusion and are distributed in cluster assemblages. LV-b thermometric data advocate for a much different fluid source, perhaps related with the dolerite intrusion. Petrographic evidence

suggests that this quartz crystallised earlier than the quartz + calcite + sulphides paragenetic sequence.

The fluid inclusions from the *Miguel Vacas*, as well as from the *Mociços* Cu deposit, suggest that Cu ore-bearing fluids in SBMB ancient mines share a similar source with an important contribution of magmatic fluids.

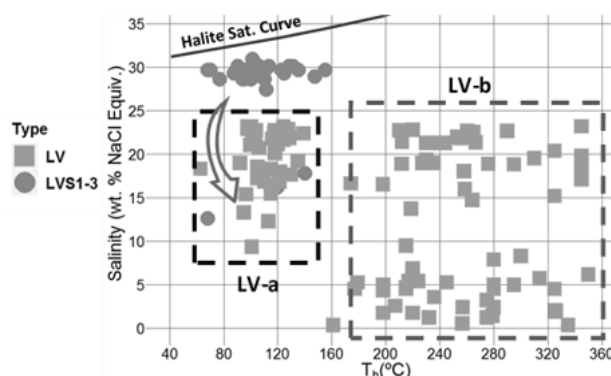


Fig. 1. Salinity (wt% NaCl equiv.) versus  $T_h$  from the obtained data from the different Types of fluid inclusions.

## Acknowledgement

To HERCULES Laboratory of the University of Évora for Raman Spectroscopy equipment usage and to the Institute of Earth Sciences. This work is a contribution to the project "ZOM-3D Metallogenic Modelling of Ossa-Morena Zone: Valorisation of the Alentejo Mineral Resources" (ALT20-03-0145-FEDER-000028), funded by Alentejo 2020 (Regional Operational Program of Alentejo) through the FEDER / FSE / FEEL. M.

## References

Mateus A. et al. (2003) in: VI Congresso Nacional de Geologia, Lisboa (Portugal), Ciências da Terra (UNL), Lisboa, nº esp. V, CD-ROM, F90-F93.

## Fluid constraints in the Mociços Cu deposit (Ossa-Morena Zone, Portugal)

Maia, M.<sup>1,2\*</sup>, Moreira, N.<sup>1,2</sup>, Vicente, S.<sup>1,2</sup>, Mirão, J.<sup>1,3</sup>, Noronha, F.<sup>2,4</sup> & Nogueira, P.<sup>1,2</sup>

<sup>1</sup>University of Évora, Faculty of Sciences and Technology, Portugal; <sup>2</sup>Institute of Earth Sciences, Portugal; <sup>3</sup>HERCULES Laboratory, University of Évora, Portugal; <sup>4</sup>University of Porto, Faculty of Sciences, Portugal; \*mcmiaigeo@gmail.com

The Mociços copper deposit is located in the Ossa-Morena Zone, at the Sousel-Barrancos metallogenic belt (SBMB) and belongs to a cluster of ancient Cu mines and occurrences, such as Miguel Vacas, Ferrarias and Bugalho. This deposit is characterised by a main sulphide assemblage of chalcopyrite + pyrite in a quartz + carbonate decametric lode, with an NNW-SSE general trend, which cross-cuts metasedimentary Paleozoic successions with circa 1 km length.

The model proposal for SBMB deposits (Mateus et al., 2003) states that the Cu contents were remobilised from metasedimentary host rocks by low to moderate salinity and temperature fluids. The study of more than 200 fluid inclusions (FI's) allowed identifying four main FI types. LVS<sub>1-3</sub> where L and V are H<sub>2</sub>O, S<sub>1</sub> is halite, S<sub>2</sub> is a carbonate and S<sub>3</sub> is an opaque. Most of these inclusions contain a halite crystal. L<sub>1-2</sub>VS<sub>1-2</sub> each phase representing L<sub>1</sub> is H<sub>2</sub>O, L<sub>2</sub> and V are CO<sub>2</sub>, S<sub>1</sub> is halite and S<sub>2</sub> is a carbonate or opaque. L<sub>1-2</sub>V where L<sub>1</sub> is H<sub>2</sub>O, L<sub>2</sub> and V are CO<sub>2</sub>. LV consists of two-phase inclusions where L and V are H<sub>2</sub>O. In addition, CO<sub>2</sub>-rich biphasic FI's (L and V are CO<sub>2</sub>) were studied in milky deformed quartz. These inclusions suggest a metamorphic fluid circulation with possible CO<sub>2</sub> devolatilisation from the metasedimentary host rocks.

Figure 1 plots  $T_h$  versus salinity for all the studied FI assemblages. A two-stage fluid circulation model is suggested by the presence of a high-salinity and a relatively lower salinity fluid (NaCl range= [0.18 – 44.3 wt% NaCl equiv.];  $\bar{x}$  = 21.85 wt% NaCl equiv.) (see arrow). The high salinity FI's are almost exclusively halite-bearing, aligning in the halite saturation curve. These high salinity fluids may be related to brines of magmatic origin, contributing with hot ore-bearing fluids which are progressively replaced with meteoric fluids ( $T_h$  range= [68 – 420 °C];  $\bar{x}$ =182.8 °C).

The majority of the halite-bearing FI's ( $T_{mHal}$  range [138.3 – 370 °C];  $\bar{x}$ =242 °C) show a behaviour where  $T_{h(L+V \rightarrow L)} < T_{mHal}$ , corresponding to a pressure of  $\approx$  50-100 MPa. This inclusion behaviour has been reported for several magmatic-hydrothermal ore deposits (Becker et al., 2008). Several carbonates and daughter minerals were identified by Raman spectroscopy. First ice melting temperatures ([-5 – -70 °C];  $\bar{x}$ = -48.4 °C) indicate the presence of solutes other than NaCl, like CaCl<sub>2</sub> and MgCl<sub>2</sub> as suggested by the presence of the carbonates. Fluid inclusion data from the Mociços deposit suggests that a more complex and deeper

fluid circulating system must be present and further studies will be carried out.

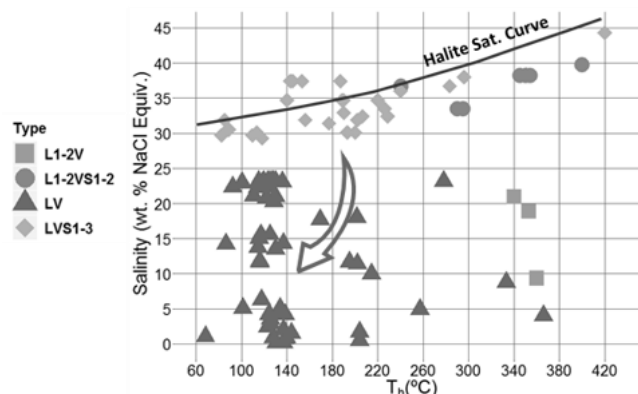


Fig. 1. Salinity (wt% NaCl equiv.) versus  $T_h$  from the obtained data for the different fluid inclusions Types.

### Acknowledgement

To HERCULES Laboratory of the University of Évora for usage of Raman Spectroscopy equipment and to the Institute of Earth Sciences. This work is a contribution to the project "ZOM-3D Metallogenic Modelling of Ossa-Morena Zone: Valorisation of the Alentejo Mineral Resources" (ALT20-03-0145-FEDER-000028), funded by Alentejo 2020 (Regional Operational Program of Alentejo) through the FEDER / FSE / FEEI. M.

### References

- Becker S.P. et al. (2008) Econ. Geol. 103:539-554.
- Mateus A. et al. (2003) In: VI Congresso Nacional de Geologia, Lisboa (Portugal), Ciências da Terra (UNL), Lisboa, nº esp. V, CD-ROM, F90-F93.

# Fluid inclusion study of Cu-rich deposits from the Sousel-Barrancos metallogenic belt (Ossa-Morena Zone, Portugal)

Maia, M.<sup>1,2\*</sup>, Moreira, N.<sup>1,2</sup>, Mirão, J.<sup>1,3</sup>, Noronha, F.<sup>2,4</sup> & Nogueira, P.<sup>1,2</sup>

<sup>1</sup>University of Évora, Faculty of Sciences and Technology, Portugal; <sup>2</sup>Institute of Earth Sciences, Portugal; <sup>3</sup>HERCULES Laboratory, University of Évora, Portugal; <sup>4</sup>University of Porto, Faculty of Sciences, Portugal; \*mcmiaigeo@gmail.com

The physical and chemical properties of mineralising fluids may provide important input for the metallogenic modelling of a particular deposit. The purpose of this study is to characterise the fluids involved with Cu mineralisation in the *Miguel Vacas* and *Mociços* ancient mines, as well as the *Ferrarias* occurrence, located in the Portuguese Ossa-Morena Zone (OMZ), in the denominated Sousel-Barrancos metallogenic belt (SBMB). These deposits are characterised by quartz + carbonate veins with main sulphide mineral assemblages of chalcopyrite + pyrite and bornite ± digenite in the supergene enrichment zone. In *Ferrarias*, sphalerite and galena were also identified, whereas arsenopyrite was found in the *Miguel Vacas* deposit. The evaluation of relative ages and spatial distribution of fluid inclusions is essential for establishing a metallogenic model for these Cu-rich deposits. Twenty bipolished thick sections were prepared from borehole and surface samples, and over 400 fluid inclusions (FI's) were studied using microthermometry and Raman spectroscopy.

FI's were classified regarding their composition as LVS<sub>1-3</sub>, where L and V are H<sub>2</sub>O, S<sub>1</sub> is halite, S<sub>2</sub> is a carbonate and S<sub>3</sub> is an opaque phase; Most of these inclusions contain a halite crystal. L<sub>1-2</sub>VS<sub>1-2</sub>, where L<sub>1</sub> is H<sub>2</sub>O, L<sub>2</sub> and V are CO<sub>2</sub>, S<sub>1</sub> is halite and S<sub>2</sub> is a carbonate or an opaque phase. L<sub>1-2</sub>V, where L<sub>1</sub> is H<sub>2</sub>O, L<sub>2</sub> and V are CO<sub>2</sub>. LV consists of two-phase inclusions, where L and V are H<sub>2</sub>O. Besides these fluids, several two-phase LV FI's (where L and V are CO<sub>2</sub>) were studied in deformed milky quartz, hosted in the metasedimentary units from the *Mociços* deposit.

The wide range of salinities [0.18 – 44.3;  $\bar{x}$  = 17.6 wt%, NaCl equiv.] and homogenisation temperatures [62.8 – 420 °C;  $\bar{x}$  = 211.3 °C] found for the FI's from these deposits reveal a two-stage fluid-circulation model. The data shows a high-salinity fluid with variable T<sub>h</sub> values, along with a trend towards lower salinities, suggesting different sources for the fluids trapped. The presence of several daughter minerals such as Ca-Mg-carbonates and opaque minerals, combined with first ice melting temperatures ranging between -5 and -80 °C ( $\bar{x}$  = -39.3 °C) suggest that high-temperature fluids were rich in solutes like NaCl, MgCl<sub>2</sub> and CaCl<sub>2</sub>. The correlation between Cu mineral phases and carbonates suggests that these fluids may have been the carrier of Cu during mobilisation and deposition. CO<sub>2</sub>-bearing FI's microthermometry data (T<sub>mCO<sub>2</sub></sub> = [-60.5 °C - -56.4

°C;  $\bar{x}$  = -57.5 °C] and T<sub>hCO<sub>2</sub></sub> = [7.1 – 30.5 °C;  $\bar{x}$  = 20.4 °C]) suggest that a magmatic source also provided some CO<sub>2</sub>. Alternatively, CO<sub>2</sub> with minor CH<sub>4</sub> (< 5 mol%) may have formed by the devolatilisation of organic matter in the Paleozoic host rock.

FI data suggest that Cu mobilisation and precipitation was controlled by high-salinity fluids with variable CO<sub>2</sub> contents, which evolved to lower salinity fluids, due to mixing with meteoric water. The high-salinity fluids (LVS<sub>1-3</sub>, L<sub>1-2</sub>VS<sub>1-2</sub>) show features that are comparable with those found in Cu deposits with a strong magmatic signature. Several plutonic to sub-volcanic calc-alkaline bodies near the SBMB (e.g. *Sta. Eulália* Plutonic Complex) are considered possible sources. These magmatic bodies suggest porphyry-like conditions during the geodynamic evolution of the OMZ (see also *Baleizão* porphyries). The FI's may provide evidence for the presence of deep-seated magmatic intrusions related to Cu mineralisation in the SBMB, in fact, positive magnetic anomalies were found near the *Mociços* area (Silva et al., 2000) corroborating this hypothesis.

## Acknowledgement

To HERCULES Laboratory of the University of Évora for Raman Spectroscopy equipment usage and to the Institute of Earth Sciences. This work is a contribution to the project "ZOM-3D Metallogenic Modelling of Ossa-Morena Zone: Valorisation of the Alentejo Mineral Resources" (ALT20-03-0145-FEDER-000028), funded by Alentejo 2020 (Regional Operational Program of Alentejo) through the FEDER / FSE / FEEI. M.

## References

Silva E.A. et al. (2000) Tectonophys. 321:57-71.

# Clumped isotope composition of CH<sub>4</sub> released by crushing methods from quartz of the external part of the Central Alps (Val d'Illicez, Switzerland)

Mangenot, X.<sup>1\*</sup>, Tarantola, A.<sup>2</sup>, Chailan, O.<sup>3</sup> Girard, J-P.<sup>3</sup>, Mullis, J.<sup>4</sup> & Eiler, J.M.<sup>1</sup>

<sup>1</sup>Caltech, Geological and Planetary Sciences, Pasadena, CA, USA; <sup>2</sup>Université de Lorraine, CNRS, GeoReSSources Laboratory, Vandoeuvre-lès-Nancy, France; <sup>3</sup>Total, EP / R&D, Pau, France; <sup>4</sup>Departement of Environmental Sciences, Institute of Mineralogy and Petrography, Switzerland; \*xmang@caltech.edu.

Hydrocarbon-bearing fluids trapped as inclusions can be regarded as time capsules of geofluids and are invaluable for understanding the evolution and migration of petroleum in sedimentary basins. These fluid inclusions can be studied using microthermometric methods to approximate the minimum inclusion trapping temperature and pressure and the gross composition of included petroleum can be derived by confocal microscopy and pressure-volume-temperature (PVT) simulation. Additional crushing or thermal decrepitation techniques can be used to release the petroleum (oil or gas) in fluid inclusions and analyse its molecular and isotopic compositions (e.g.  $\delta^{13}\text{C}$ ,  $\delta\text{D}$ ).

Here we propose a new methodology consisting in the measure of multiply substituted ("clumped") isotope composition of the methane trapped in fluid inclusions. Indeed, recent analytical development in isotopic ratio mass spectrometry - IRMS (Eiler et al., 2013) now permits to quantify the abundance of both  $^{13}\text{CH}_3\text{D}$  and  $^{12}\text{CH}_2\text{D}_2$ , i.e. two isotopologues of interest of methane, with sufficient precision for direct thermometry applications. In a CH<sub>4</sub> isotopically equilibrated system,  $\Delta^{12}\text{CH}_2\text{D}_2$  and  $\Delta^{13}\text{CH}_3\text{D}$  values are a direct function of the methane generation temperature (Young et al., 2017) (Fig. 1), and thus can be used as a new isotopic thermometer. This new tool can be applied in various geological environments (surface, diagenetic and/or metamorphic), covering virtually a temperature range from 0 to >500 °C. As part of this study, an offline crusher has been developed, and connected to a vacuum cryogenic-system, to extract and purify the required quantity of CH<sub>4</sub> (~40 h IRMS integration time = i.e. 60 to 120  $\mu\text{moles}$  of CH<sub>4</sub>).

We present here preliminary clumped isotope thermometry results from 2 generations of CH<sub>4</sub>-bearing fluid inclusions occurring in authigenic fissure quartz from Val d'Illicez in the external part of the Central Alps, Switzerland. In this methane-saturated environment, fluid immiscibility led to coexisting methane-dominated and methane bearing water-rich fluid inclusions where the homogenisation temperatures directly reveal inclusion formation temperatures.  $\delta^{13}\text{C}$  and  $\delta\text{D}$  composition indicate that CH<sub>4</sub> was generated by thermogenic cracking at high maturity (Tarantola et al., 2007). The methane released by crushing in three of these samples (to date; April 2019) display  $\Delta^{12}\text{CH}_2\text{D}_2$  and  $\Delta^{13}\text{CH}_3\text{D}$  clumped isotope composition both (1) in thermodynamic equilibrium

between each other and (2) in very good agreement with the fluid inclusion homogenisation temperatures measured independently (c.f. 230-260 °C; Mullis et al. 1975). Such isotopic results may be explained by two possible scenarios: (1) the methane preserved its initial formation temperature and has been generated near the fluid entrapment site from organic matter-rich flysch, or (2) the CH<sub>4</sub> has been isotopically re-equilibrated with the H<sub>2</sub>O, meaning that the clumped isotope temperature reflects an equilibrium temperature.

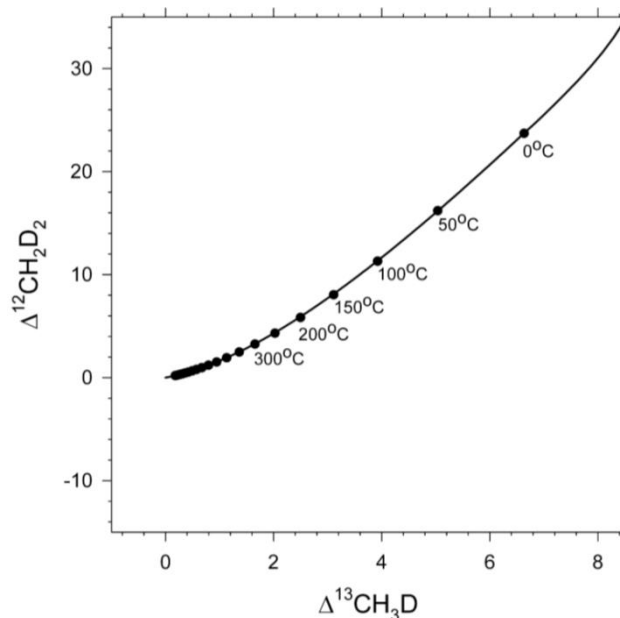


**Fig. 1.** Clumped isotope thermodynamic equilibrium curve in  $\Delta^{12}\text{CH}_2\text{D}_2$  and  $\Delta^{13}\text{CH}_3\text{D}$  space. Both axes are in per mil. From Young et al., 2017

## References

- Eiler J.M. et al. (2013) *Int. J. Mass Spectrom.* 335:45-56.
- Mullis J. et al. (1975) *Bull. Suisse Min. Pét.* 55.
- Tarantola A. et al. (2007) *Chem. Geol.* 237:329-357.
- Young E.D. et al. (2017) *Geochim. Cosmochim. Ac.* 203:235-264.

# Fluid inclusion evidence for gold deposition during boiling at shallow-water depths in initially deep-water volcanogenic massive sulphide systems: a potential evolutionary link between marine and epithermal gold systems

Marshall, D.<sup>1\*</sup>, Nicol, C.A.<sup>1</sup> & Greene, R.<sup>2</sup>

<sup>1</sup>Earth Sciences, Simon Fraser University, Canada; <sup>2</sup>Mining Engineering, University of British Columbia, Canada; \*marshall@sfu.ca

Gold, present as electrum, in the Battle Gap, Ridge North-West, HW, and Price deposits at the Myra Falls (MF) mine on Northern Vancouver Island, Canada occurs in late veinlets cutting the earlier volcanogenic massive sulphide (VMS) lithologies. MF is a typical Kuroko-type VMS deposit. The ore mineral assemblage containing the gold comprises dominantly galena, tennantite, bornite, sphalerite, chalcopryrite, pyrite, and rarely stromeyerite, and it is defined as an Au-Zn-Pb-As-Sb association. The gangue is comprised of barite, quartz, and minor feldspathic volcanogenic sedimentary rocks and clay minerals.

The deposition of gold as electrum in the baritic upper portions of the VMS sulphide mineralisation occurs at relatively shallow water depths and beneath the sea floor. Primary, pseudosecondary, and secondary fluid inclusions, petrographically related to gold (Fig. 1), show boiling fluid inclusion assemblages in the range of 123 to 173 °C, with compositions and eutectic melt temperatures consistent with seawater at approximately 3.2 wt% NaCl equivalent. Earlier detailed volcanogenic stratigraphic studies (Jones et al., 2006 and references within) indicate the main phases of VMS mineralisation at MF occurred at water depths below storm wave base (<200 m) and most likely much deeper water depths due to the observed lack of vesicles in the volcanic rocks. Kuroko-type VMS systems are typical of Island-arcs, gold enriched and span a broad range of water depths. The fluid inclusion assemblages and homogenisation temperatures are consistent with boiling seawater corresponding to water depths ranging from 15 to 125 m. Additionally, the observed slightly more dilute brines corresponding to salinities of approximately 1 wt % NaCl indicate that there is input from very low-salinity brines, which could represent a transition from subaqueous VMS precious metal enrichment (Hannington et al., 1999) to more terrestrial epithermal-like conditions for precious metal deposition.

## References

- Hannington et al. (1999) Econ. Geol. Mon. Ser. 10:43-70.  
Jones S. et al. (2006) Econ. Geol. 101:555-584.  
Marshall D. et al. (2018) Geosci. J. 8:422.

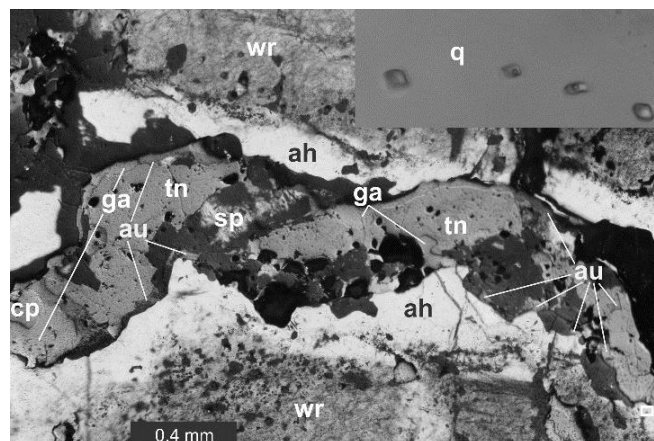


**Fig. 1.** Composite photomicrographs of the alteration halo surrounding the gold-bearing veinlets and fluid inclusions. The main image, taken under simultaneous plane-polarised transmitted and reflected light, shows the barite-rich wall rock (wr) and quartz dominated alteration halo (ah) surrounding the veinlet. The veinlet assemblage comprises tennantite (tn), galena (ga), sphalerite (sp), chalcopryrite (cp), and gold/electrum (au). The inset image shows the magnified region delineated by the white rectangle, in plane-polarised light, comprising a trail of "boiling" pseudosecondary two phase (liquid + vapour) fluid inclusions hosted within a quartz (q) crystal lining the walls of the veinlet. The two central fluid inclusions represent the liquid portion of the boiling fluid, while the two outer fluid inclusions represent the conjugate vapour inclusions of the boiling system. Inset field of view is approximately 50 microns. After Marshall et al. (2018).

# Primary volatiles in the Northern Limb of the Bushveld Complex and their effect on PGE mineralisation

McFall, K.A.<sup>1\*</sup>, McDonald, I.<sup>1</sup> & Tattitch, B.<sup>2</sup>

<sup>1</sup>School of Earth and Ocean Science, Cardiff University, U.K.; <sup>2</sup>University of Bristol, U.K.; \*McFallK@cardiff.ac.uk

High-temperature 'primary' volatiles have been suggested to have an important influence on the development of platinum-group element (PGE) mineralisation in layered intrusions (Boudreau and McCallum, 1992), however the source(s), abundance and role of fluids in mineralisation are still highly debated. In order to address this question we have searched for and identified fluid inclusions in primary magmatic silicates from magmatic sulphide Ni-Cu-PGE deposits across the Northern Limb of the Bushveld Complex.

One of these is the Aurora Ni-Cu-PGE deposit which shows evidence of dolomite assimilation, hydrothermal influence and modification. Base metal sulphides (BMS) have low PGE concentrations, with PGE grade controlled by platinum group minerals (PGM). 75 area % of PGMs are hosted in hydrothermal alteration minerals, with 52% spatially removed from BMS (McFall et al., 2019).

Plagioclase and orthopyroxene crystals at Aurora contain primary aqueous brine inclusions, vapour-liquid inclusions (>80% vapour) and rare salt melt inclusions (Fig. 1). Laser Raman analysis shows the vapour-liquid inclusions to be CO<sub>2</sub>-CH<sub>4</sub> vapour with a thin film of liquid CO<sub>2</sub>. The brine inclusions contain liquid and vapour H<sub>2</sub>O, halite daughter minerals and commonly sylvite, Ca/Mg carbonate and FeCl<sub>2</sub> daughter minerals. Rare inclusions also contain hematite crystals.

Primary brine inclusions in cumulus feldspar have a mean homogenisation temperature of 922 °C (n=19, σ=95), with a range of 683 – 1100 °C, and a mean salinity of 68.6 wt% NaCl (σ=18.8). Primary brine inclusions in inter-cumulus orthopyroxene have a mean homogenisation temperature of 849 °C (n=47, σ=24), with a range of 819 – 880 °C, and a mean salinity of 66.6 wt% NaCl (σ=2.1). Primary vapour-liquid inclusions in cumulus feldspar have a mean homogenisation temperature of 820 °C (n=20, σ=109) with a range of 698 – 1055 °C, while those in inter-cumulus orthopyroxene have a mean homogenisation temperature of 802 °C (n=14, σ=95) with a range of 549 – 859 °C.

The range of homogenisation temperatures recorded here are greater than suggested by previous studies of inclusions in primary silicates from layered ultramafic intrusion-hosted PGE deposits (Hanley et al., 2008). The highest values are above the solidus of their host minerals, indicating that volatiles were present while the system was at least partially molten. These volatiles included an oxidised, acidic and highly saline aqueous fluid, preserved as brine inclusions;

similar to the fluids invoked for hydrothermal transport of PGEs on experimental grounds (Xiong and Wood, 2000). The PGE grade in Aurora is predominately associated with hydrothermal alteration hosted PGMs, rather than with magmatic sulphides. Assimilation of dolomite would have released water and CO<sub>2</sub>, creating a volatile phase with the potential to dissolve and/or remobilise PGEs from any early BMS liquid (Holwell and McDonald, 2007).

Follow-up studies are ongoing to establish whether similar fluids are present in other PGE deposits (e.g. Waterberg, Platreef) across the northern Bushveld. If these exist more widely, it implies that the presence of volatiles may be a relatively common occurrence, with important implications for PGE mineralisation and geometallurgy in magmatic sulphide deposits which intrude reactive wall rocks.

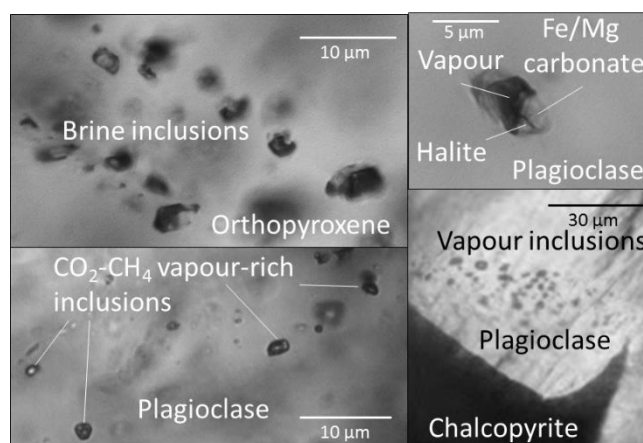


**Fig. 1.** Fluid inclusions in primary magmatic silicates (cumulus plagioclase and inter-cumulus orthopyroxene) in the Aurora Ni-Cu-PGE deposit.

## References

- Boudreau A. and McCallum I. (1992) *Econ. Geol.* 87:1830-1848.  
Hanley J.J. et al. (2008) *J. Petrol.* 49:1133-1160.  
Holwell D. and McDonald I. (2007) *Contrib. Mineral. Petr.* 154:171-190.  
McFall K. et al. (2019) *Ore Geol. Rev.* 106:403-422.  
Xiong Y. and Wood S. (2000) *Miner. Petrol.* 68:1-28.

# Using melt inclusions to evaluate magmatic contributions to gold-bearing hydrothermal systems, Doyon-Bousquet-LaRonde district, Abitibi greenstone belt, Québec, Canada

Meagher, D.<sup>1</sup>, Hanley, J.J.<sup>1</sup>, Zajacz, Z.<sup>2</sup>, Tsay, A.<sup>2</sup> & Mercier-Langevin, P.<sup>3</sup>

<sup>1</sup>Department of Geology, Saint Mary's University, Canada; <sup>2</sup>Department of Earth Sciences, University of Toronto, Canada; <sup>3</sup>Geological Survey of Canada, Canada; \*daniel.meagher32@gmail.com

This study represents the first comprehensive silicate melt inclusion (SMI) microanalytical investigation in an Archean terrane.

The Mooshla Intrusive Complex (MIC) in the Doyon-Bousquet-LaRonde (DBL) mining camp, Abitibi greenstone belt, Québec, Canada may be one of only a few examples, globally, of magmatic systems directly genetically-linked to numerous Au-rich VMS, orogenic- and sub-seafloor epithermal-style gold deposits. The current research aims to determine if Au-enriched magmatic volatiles were supplied to the hydrothermal ore-forming systems during emplacement, crystallisation, and degassing of the spatially associated intrusives/volcanics. In particular, addressing this question quantitatively is critical in explaining the anomalously high Au content in VMS deposits in the DBL mining camp.

Previous studies (Galley and Lafrance, 2014 and references therein) have suggested a link between the MIC and the deposits in the area based on geochronology, mapping/field relations, petrography, and litho-geochemistry. However, using bulk rock analyses to constrain the metal budget of the MIC is not appropriate because of the deformational, metamorphic, and alteration events that have occurred in the area, which can modify the metal chemistry of bulk rocks and mask evidence of degassing and fluid-melt partitioning. This is an ongoing issue when documenting the possible relationships between intrusions and Au metallogenesis in Archean terranes because of the overlapping nature of multiphase deformation and regional metamorphic episodes (Galley & Lafrance, 2014).

The analysis of SMI preserved in phenocryst quartz and other inert host minerals (e.g., apatite, titanite, zircon) provides a means to determine the original metal tenor of the system because their compositions may be unaffected by post-solidus processes. Additionally, integrating SMI petrography and geochemical analysis will allow the temporal evolution of the melt to be evaluated at different stages in the magmatic-hydrothermal evolution of this environment.

LA-ICP-MS analyses on SMI in volcanic units was performed and the ore metals Au-Ag-Cu-Mo-Sn-Sb-W were quantified, in addition to a range of other compatible and incompatible trace elements (LILE, REE, HFSE). The petrography and mineralogy of the melt inclusions, combined with their chemistry allows the differentiation of melt inclusions from trapped enclaves of altered wall rock. The LA-ICP-MS analyses of SMI show that

the melts were highly and variably enriched in Au ( $\sim 69 \pm 110$  ppb;  $n = 24$ ), Ag ( $\sim 950 \pm 2295$  ppb;  $n = 63$ ), Cu ( $\sim 84 \pm 311$  ppm;  $n = 40$ ), Mo ( $\sim 1.4 \pm 0.7$  ppm;  $n = 127$ ), Sn ( $\sim 3.6 \pm 3.9$  ppm;  $n = 98$ ), Sb ( $\sim 0.75 \pm 0.74$ ;  $n = 49$ ), and W ( $\sim 0.49 \pm 0.43$ ;  $n = 122$ ).

In addition to SMI, quartz phenocrysts also trapped apatite microcrysts that were growing as primary phases as the system evolved. There appears to be fairly distinct bulk compositional differences between the quartz-hosted apatite grains of various volcanic units of the Bousquet Formation. The apatite chemistry evidently implies that the stage of liquid evolution that crystallised apatites of unit 2.0 (felsic sill) is very different than unit 5.3 (rhyolite). The one thing shared by the apatites of both units is a strong negative Eu anomaly. However, unit 2.0 apatites have a larger Eu anomaly than most of the granites and some of the other lithologies (although there is quite a bit of overlap). The apatite chemistry, combined with SMI fractionation trends, indicates extensive plagioclase crystallisation at depth.

The depth of SMI entrapment cannot be constrained from major and trace element chemistry. To do this, other factors (volatile content, evidence for coeval fluid-melt entrapment) must be considered. Both homogenised and unhomogenised primary melt inclusions contain a dark bubble/s. Petrography and laser Raman analysis of bubbles in homogenised SMI indicate that they are composed of CO<sub>2</sub> liquid, implying a very high P of entrapment. Importantly, the carbonic phase was not observed in every inclusion and the phase proportion of carbonic: melt phases is variable from inclusion to inclusion which indicates that the melt was saturated in CO<sub>2</sub> at the time of entrapment. Deep-seated exsolution of this carbonic fluid could have contributed to metal removal from the melt.

## Acknowledgement

TGI-4 (Natural Resources Canada), Gov. of Canada

## References

Galley A. and Lafrance B. (2014) *Econ. Geol.* 109:205-229.

# Genetic constraints inferred from mineral paragenetic sequence and fluid inclusions of the Beni H'midane fluorite-barite-stibnite deposit in Constantine (Algeria)

Meddane, S.<sup>1,3\*</sup>, Kolli, O.<sup>1,3</sup>, Sami, L.<sup>2,3</sup>, Bakelli, A.<sup>1,3</sup> & Bouabalou, S.<sup>4</sup>

<sup>1</sup>University of Sciences and Technology Houari Boumediene (FSTGAT/ Geology, Algeria); <sup>2</sup>University of Mouloud Mammeri Tizi Ouzou (Geology, Algeria); <sup>3</sup>Laboratoire de Métallogénie et Magmatisme de l'Algérie (FSTGAT/ Geology, Algeria); <sup>4</sup>Agence du Service Géologique de l'Algérie (ASGA, Algeria); \*smeddane@usthb.dz

The Beni H'midane fluorite-barite-stibnite mineralisation is situated in the northeastern part of Algeria not far from the city of Constantine. This mineralisation occurs in two stratigraphic units: 1) The Constantinian neritic unit, containing an Aptien limestone with orbitolines and a Cenomanian limestone with rudists; 2) The Mio-Pliocene post-nappe unit, represented by a detrital formation and versicolor marl series, with interbedded lacustrine limestones.

This region has suffered a polyphased tectonic event which is directly related to the mineralisation.

The mineralisation is controlled by thrust and normal fault trending E-W to NW-SE, conjugated to another set of faults directed N-S to NE-SW which controls the circulation of fluids.

The mineralisation appeared as vein, veinlets, breccia, and stockworks in the neritic carbonate, and in Mio-Pliocene limestone as paleokarst feelings. The host rocks are affected by different alterations such as silicification, ferrugination, kaolinisation, carbonatation and decarbonatation.

The mineralisation is mainly composed of fluorite, barite, and calcite. The subordinate components are stibnite, quartz, stibiconite, kaolinite, pyrite and iron oxides. Petrographic observations show two types of fluorites: (i) an early fluorite and (ii) a late fluorite.

The fluid inclusions hosted in fluorites were classified by the criteria of (Roedder, 1984); three types of fluid inclusions (FIs) have been distinguished: (i) pure-liquid single-phase (PL-type), (ii) liquid-rich two-phase (L-Type), and (iii) vapour-rich two-phase (V-type).

In the early fluorite types (colourless, purple and black), (FIs) are liquid-rich two-phase (L-Type), found parallel to the growth zones and annealed fractures plane in the crystals core (Fig. 1). In the late fluorite types (colourless, honey, and greenish), (FIs) are mainly pure-liquid single-phase (PL-type), concentrated parallel to the growth zones, and rarely liquid-rich two-phase (L-Type) in crystal planes.

Microthermometric measurements were performed on primary two-phase (L-type, V-type) FIs in the early and late fluorite:

The FIs hosted in the early-stage fluorite type were homogenised at 110–280 °C (mainly 160 °C, 260 °C); their  $T_m$  (ice) range from -17.1 °C to -22.8 °C. The FIs hosted in the late-stage fluorite yield slightly lower homogenisation temperatures of 104–140 °C (peaking at 110 °C), which correspond to  $T_m$  (ice) of -0.1 °C to -2.5 °C.

Microthermometric data shows that the temperature and salinity during mineralisation of the fluorite, in the early stage was higher than in the late stage. Therefore, we can suggest that mineralisation was deposited from solution generated by mixing of different fluids.

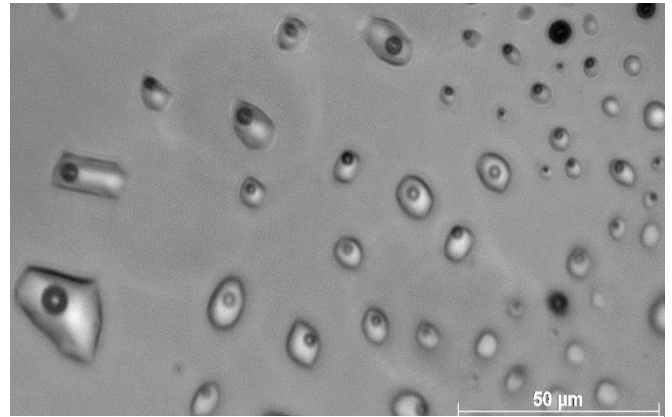


**Fig. 1.** Photomicrograph of primary liquid-rich two-phase (L-Type) fluid inclusions on annealed fractures plane in the early fluorite.

## Acknowledgement

We wish to express our special thanks to Associate Pr. Kotaro Yonezu, Dr. Morad Cherbal and the whole team of the Department of Earth Resources Engineering, Kyushu University in Japan for their kind support.

## References

Roedder E. (1984) in: Rev. Mineral. 12:644 p.

# Hydrocarbon accumulation characteristics in the deep reservoirs of Yingxiongling area in the Qaidam Basin, western China

Meng, Q.Y.<sup>1\*</sup> & Yu, Z.C.<sup>1</sup>

<sup>1</sup>Research Institute of Petroleum Exploration and Development, State Key Laboratory of Enhanced Oil Recovery, China; \*mqy5948@petrochina.com.cn

The Yingxiongling area of the Qaidam Basin is the most productive block, which is mainly controlled by the widely distributed limestone reservoir and high-quality salt cap rock. The study area is located in the Cenozoic source rock development area of the Qaidam Basin, and the deep layers have the inherent advantages of near-source. A combination of techniques, such as polarisation microscope, quantitative grain fluorescence (QGF), fluorescence spectroscopy, and microthermometry have been used to characterise the episode of the oil emplacement. The results show that yellow and light blue fluorescent inclusions are well developed in reservoir. Combined with the burial and thermal history, it is concluded that the deep layers of the Yingxiongling area mainly experienced the low-maturity oil charging in the late Lower Youshashan Formation (15 Ma), and the mature-highly matured oil charging in the late Upper Youshashan Formation (7 Ma). In addition, because of the influence of the late stage of Himalayan tectonic movement, the middle and deep reservoirs have experienced the process of oil charging and migrating to overlying layers.

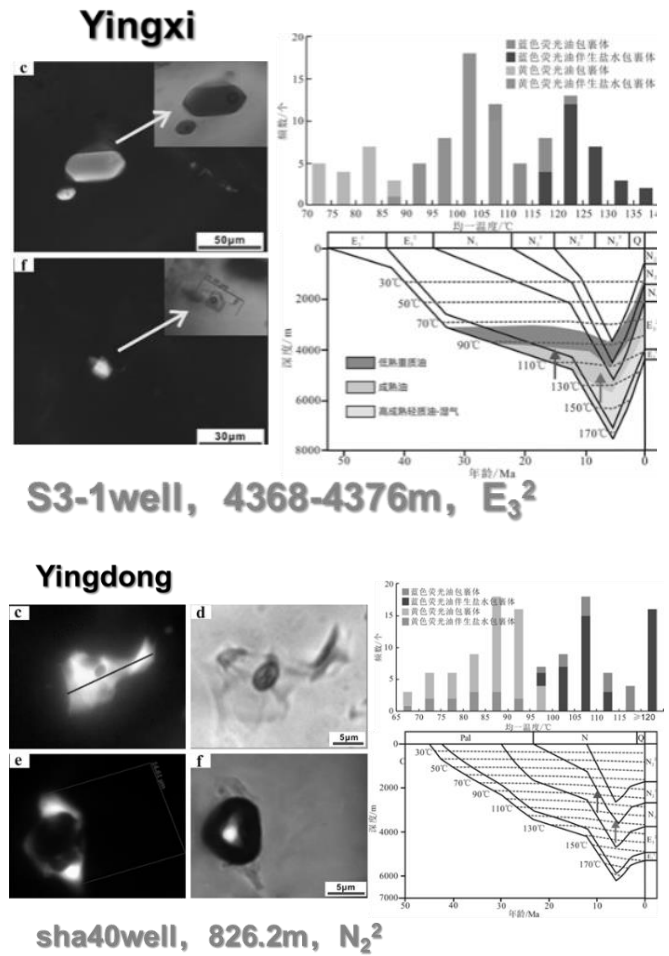


Fig. 1. Characteristic photomicrographs of oil inclusions in the west (Yingxi) and east (Yingdong) Yingxiongling Area.

## LA-ICP-MS for fluid inclusion analysis: current capabilities and application cases

**Mercadier, J.<sup>1\*</sup>**

<sup>1</sup>GeoRessources Lab, CNRS, Université de Lorraine, CREGU, France; \*julien.mercadier@univ-lorraine.fr

Laser Ablation (LA) coupled to ICP-MS is a booming technique since the last 25 years in Earth Sciences, with many major contributions concerning the chemical analysis of minerals and fluid inclusions since the pioneer publications by Jackson et al. (1992) and Günther et al. (1998). For the field of fluid inclusions, the application of LA-ICP-MS has currently allowed a deep understanding of the chemistry of geological fluids, whether for the analysis of major (e.g. %) to trace (ppbs) elements, including metals of economic interest (Audétat et al., 1998; Richard et al., 2012; Richter et al., 2018) and for the measurements of halogens and isotopic ratios to trace geological processes (Leisen et al., 2012, Fusswinkel et al., 2018, Pettke et al., 2004).

Given the possibilities that multiple generations of different fluids of various age and chemistry may be trapped through time in a single mineral phase, the high sensitivity and spatial resolution capabilities of LA-ICP-MS to selectively sample and analyse individual fluid inclusion appeared like a revolution in the understanding of fluid-driven mass transfer in the Earth's crust. Determining the chemical composition of geological fluids trapped in fluid inclusions by LA-ICP-MS, however, remains currently an analytical challenge. Indeed, fluid inclusions represent micro-cavities of generally 10-100 µm in diameter, which contain small quantities of liquids (pl to nl) with variable compositions and concentrations of chemical elements (Heinrich et al., 2003; Allan et al., 2005; Pettke et al., 2012; Wagner et al., 2016).

The application of LA-ICP-MS to fluid inclusions generates short transient signals, typically of several seconds. Such a short duration, coupled to the fact that each fluid inclusion can be only analysed once, represents one of the major analytical limits for their analysis by LA-ICP-MS. This is particularly the case for small fluid inclusions (< 10 µm) and/or containing low-salinity fluid, which in fact represent most of fluid inclusions found in nature compared to the large and high-salinity fluid inclusions encountered in some ore deposits. Such limitations have led to the fact that the detailed chemistry of many geological fluids is not yet known.

Quadrupole (Q) ICP-MS remains today the most widespread technique for the analysis of fluid inclusions due to its high sensitivity, speed, and multi-element capabilities. New developments, like cryo-cell (Albrecht et al., 2014) or triple Q-based ICP-MS configuration coupled to reaction cell, pave the way for new analytical opportunities and detection of elements sensible to isobaric

interferences. Sector-field (SF) and time-of-flight (TOF) ICP-MS have recently proven improvements for fluid inclusion analysis with higher sensitivities, higher speed of acquisition, quasi-simultaneous detection of all elements, and/or lower limits of detection (Wälle and Heinrich 2014; Harlaux et al., 2015). These new generations of ICP-MS reveal to be highly promising for analysing fluid inclusions, but their contribution to the understanding of geological fluids remains largely to be explored. Some examples based on the use these technologies will be presented to bring new data to this field of research.

### Acknowledgement

J.M. thanks researchers and students from GeoRessources lab and Günther Group (ETH Zurich), and TOFWERK, Agilent and Nu.

### References

- Albrecht M. et al. (2014) *J. Anal. Atom. Spectrom.* 29:1034-1041.
- Allan M.M. et al. (2005) *Am. Mineral.* 90:1767-1775.
- Audétat A. et al. (1998) *Science* 279: 2091-2094.
- Jackson S.E et al. (1992) *Can. Mineral* 30:1049-1064.
- Fusswinkel T. et al. (2018) *J. Anal. Atom. Spectrom.* 33:768-783.
- Günther D. et al. (1998) *J. Anal. Atom. Spectrom.* 13:263-270.
- Harlaux M. et al. (2015) *J. Anal. Atom. Spectrom.* 30:1945-1969.
- Heinrich C. et al. (2003) *Geochim. Cosmochim. Ac.* 18:3473-3497.
- Leisen M. et al. (2012) *Chem. Geol.* 330-331:197-206.
- Pettke T. et al. (2004) *Earth Planet. Sc. Lett.* 296:267-277.
- Pettke T. et al. (2012) *Ore Geol. Rev.* 44:10-38.
- Richard A. et al. (2012) *Nat. Geosci.* 5:142-146.
- Richter L. et al. (2018) *Geology* 46:263-266.
- Wagner T. et al. (2016) *Elements* 12:323-328.
- Wälle M. and Heinrich C. (2014) *J. Anal. Atom. Spectrom.* 29:1052-1057.

# Initial CO<sub>2</sub> content of parental arc magmas of Karymsky volcano (Kamchatka) inferred from study of olivine-hosted melt inclusions

Mironov, N.L.<sup>1\*</sup>, Portnyagin, M.V.<sup>2,1</sup>, Tobelko, D.P.<sup>1</sup>, Smirnov, S.Z.<sup>3</sup>,  
Krasheninnikov, S.P.<sup>1</sup> & Gurenko, A.<sup>4</sup>

<sup>1</sup>Vernadsky Institute, GEOKHI RAS, Russia; <sup>2</sup>GEOMAR, Germany; <sup>3</sup>IGM SB RAS, Russia; <sup>4</sup>CRPG, France; \*nmironov@geokhi.ru

We present new data on CO<sub>2</sub> content in melt inclusions (MIs) from Karymsky volcano estimated using micro-Raman spectroscopic data on CO<sub>2</sub> density of fluid bubbles and volume proportions of glass and fluid inside inclusions (e.g., Moore et al., 2015). This study was focused on further development of this technique, in particular on the ways of simple and precise quantification of 3-D MIs size.

We studied sixteen partially crystallised MIs in olivine (Fo<sub>77-89</sub>). Before Raman analysis, they were reheated during 5 min at 1170 °C and quenched. The quenched MIs were consisting of glass and bubbles of vapour-CO<sub>2</sub>. The bubbles were measured for their density in IGM SB RAS, Novosibirsk, using Horiba LabRam HR800 (532 nm, 1800g). CO<sub>2</sub> density ranged from 0.03 to 0.21 g/cm<sup>3</sup> (Mironov et al., 2019) (Fig. 1). Sizes of MIs and bubbles were measured using optical methods. MI thickness, which is usually not reported in MI studies, was quantified in two ways. First, it was measured with built-in microscope micrometre and further corrected for the refractory index of olivine of 1.68 (average value of olivine Fo<sub>80-90</sub> refractory indices, e.g. Troeger, 1979). Independently from the first method, the 3-D size was measured using two orthogonal sections of olivine grains (Fig. 1). Both methods yielded comparable results for the same inclusions. The maximum difference for the estimated relative volume of fluid bubble did not exceed 0.8 %. Based on our measurements, the bubble shows 3.0-5.7 vol%, (4.1 vol% in average) in the MIs (Fig. 1). None of the MIs has bubble volume exceeding critical value of 6-8% suggested for originally homogeneous MIs (e.g. Aster et al., 2016; Frezzotti et al., 2001).

Based on mass-balance calculation (e.g. Moore et al., 2015; 2018) (Fig. 1), we estimated the minimum CO<sub>2</sub> concentrations in the MIs, assuming the presence of CO<sub>2</sub> only in the bubbles (Fig. 1) at room-T. The concentrations range from 0.05 to 0.45 wt% and likely represent melts degassed in variable extents and originated from an initial primitive magma enriched in CO<sub>2</sub> (≥0.45 wt%). Note that the using of a less precise estimation for MIs volume (e.g., assuming elongated ellipsoid shape with two equal dimensions) is not accurate in many cases and resulted in highly under- or overestimation of the CO<sub>2</sub> content in the MIs (Fig. 1b).

SIMS analyses of CO<sub>2</sub> and H<sub>2</sub>O in the quenched glasses of MIs are currently in progress. The data

will be considered to use to calculate the total amount of CO<sub>2</sub> in MIs and show at the meeting to discuss possible crystallisation depths of parental arc magmas and sources of CO<sub>2</sub>.

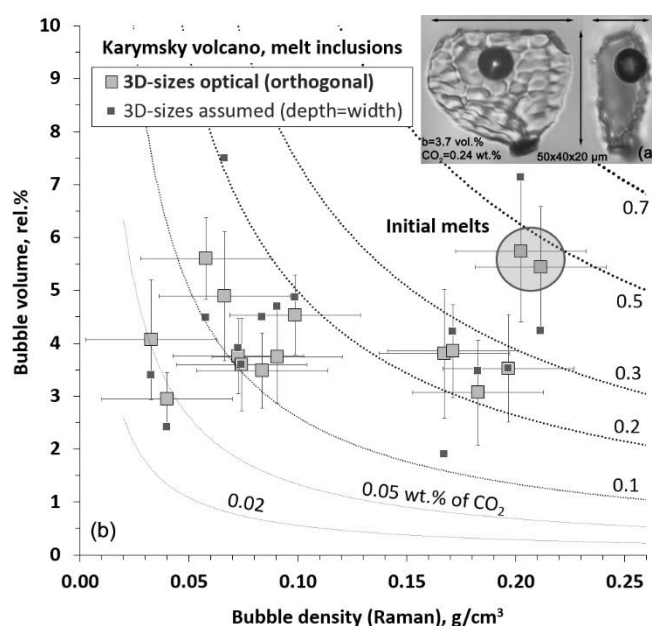


**Fig. 1.** Minimum CO<sub>2</sub> content in Karymsky melt inclusions. Larger symbols show data for 3D MI/bubble sizes measured optically. The lines indicate CO<sub>2</sub> contents in melts obtained by mass-balance calculation (Mironov et al., 2019)

## Acknowledgement

This work has been supported by Russian Foundation for Basic Research, grant 19-05-00934.

## References

- Aster E.M. et al. (2016) J. Volcanol. Geoth. Res. 323:148-162.
- Frezzotti M.L. (2001) Lithos 55:273-299.
- Mironov et al. (2019) Russ. Geol. Geophys+ (submitted).
- Moore L.R. et al. (2015) Am. Mineral. 100:806-823.
- Moore L.R. et al. (2018) J. Volcanol. Geoth. Res. 358:124-131.

# Noble gas geochemistry of the phenocrysts from the Ciomadul volcanic complex (Eastern Carpathians): a pilot study

**Molnár, K.<sup>1,2\*</sup>, Czuppon, Gy.<sup>3</sup>, Palcsu, L.<sup>1</sup>, Benkó, Zs.<sup>1</sup>, Tóth, Á.<sup>4</sup>, Németh, B.<sup>4</sup>, Kis, B-M.<sup>1,4,5</sup>, Lukács, R.<sup>4</sup> & Harangi, Sz.<sup>2,4</sup>**

<sup>1</sup>Isotope Climatology and Environmental Research Centre, Institute for Nuclear Research, Hungarian Academy of Sciences, Hungary; <sup>2</sup>Department of Petrology and Geochemistry, Eötvös Loránd University, Hungary; <sup>3</sup>Institute for Geological and Geochemical Research, RCAES, Hungarian Academy of Sciences, Hungary; <sup>4</sup>MTA-ELTE Volcanology Research Group, Hungary; <sup>5</sup>Faculty of Biology and Geology, Babeş-Bolyai University, Romania; \*molnar.kata@atomki.mta.hu

Different geochemical reservoirs (e.g. crust, mantle, air) have distinct noble gas signatures (Ozima and Podosek, 2004). Therefore, elemental and isotopic composition of noble gases from well gases, water samples and, fluid- and melt inclusions in different mineral phases can reveal important information about the origin of the fluids, which formed the minerals. Noble gas isotopes are often utilised in subduction-related volcanic systems also to constrain the origin of hot springs, fumaroles, mofettes and bubbling pools (e.g. Kis et al., 2017; Daskalopoulou et al., 2018). Moreover, it is less common to measure the noble gas elemental and isotopic compositions in phenocryst-hosted inclusions in volcanic rocks though they can help to constrain the evolution of the magma and better understand the magmatic processes within the lithosphere. The goal of this study is to determine the noble gas compositions of phenocrysts in the Ciomadul volcanic complex (Eastern Carpathians).

The Ciomadul volcanic complex is a tightly-packed lava dome complex truncated by two deep explosion craters (Szakács and Seghedi, 1995). It is situated at the southeastern end of the andesitic-dacitic Călimani-Gurghiu-Harghita volcanic chain in the Eastern Carpathians (Romania), in a subduction-related post-collisional geodynamic setting (Seghedi et al., 2011). The volcanic complex formed between ca. 160 and 30 ka (e.g. Harangi et al., 2015; Molnár et al., 2019). The noble gas signatures of the present-day gas discharges (i.e. dry mofettes, bubbling pools, CO<sub>2</sub> bubbling peat bogs) of Ciomadul revealed the presence of a mantle-derived component (Kis et al., 2017).

The studied sites are two pyroclastic outcrops (Băile Tuşnad and Bixad; Tf and Bx, respectively; Vinkler et al., 2007). Products of these outcrops is considered to be the last phase of explosive activity of Ciomadul (Vinkler et al., 2007). Since the Ciomadul dacite contain only small amount of pyroxene and olivine crystals; plagioclases and amphiboles were separated (ca. 1.5 g) from the pumices for the noble gas measurements. Noble gas was extracted from the plagioclase- and amphibole-hosted fluid inclusions by vacuum crushing (single step: 150 strokes). In the extraction, the He concentrations vary between  $9.7 \times 10^{-10}$  and  $3 \times 10^{-8}$  ccSTP/g, with an  $R/R_A$  value between 0.12 and 5.56 where R is the corrected

<sup>3</sup>He/<sup>4</sup>He ratio of the sample and  $R_A$  is the atmospheric value ( $(1.382 \pm 0.005) \times 10^{-6}$ ; Sano et al., 2013). The Ne content ranges between  $3.4 \times 10^{-10}$  and  $5.1 \times 10^{-9}$  ccSTP/g, whereas the <sup>40</sup>Ar/<sup>36</sup>Ar ratios are between 295.5 and 303.9. Although the Ne and Ar content and the above ratios show the effect of air contamination, based on the He isotopic signature, the presence of a mantle-derived component ( $R/R_A > 1$ ) can be detected.

## Acknowledgement

The research was financed by the European Regional Development Fund in the project of GINOP-2.3.2-15-2016-00009, by the Hungarian National Research, Development and Innovation Fund (NKFIH) within No. K116528 project and supported by the ÚNKP-18-3-II-ELTE-377 scholarship.

## References

- Daskalopoulou K. et al. (2018) J. Volcanol. Geoth. Res. 365:13-22.  
Harangi Sz. et al. (2015) J. Volcanol. Geoth. Res. 301:66-80.  
Kis B-M. et al. (2017) J. Volcanol. Geoth. Res. 341:119-130.  
Marty B. et al. (1994) Earth Planet. Sc. Lett. 126:23-39.  
Molnár K. et al. (2019) J. Volcanol. Geoth. Res. 373:133-147.  
Ozima M. and Podosek F.A. (2004) in: Noble Gas Geochemistry 217-280.  
Sano et al. (2013) in: Adv. in Isotope Geochem 11-31.  
Seghedi I. et al. (2011) Tectonophys. 502:145-157.  
Szakács A. and Seghedi I. (1995) Acta Vulc. 7:145-153.  
Vinkler A-P. et al. (2007) Földt. Közl. 137:103-128.

# Limited thermochemical sulphate reduction in hot, anhydritic, sour gas carbonate reservoirs: the Upper Jurassic Arab Formation, United Arab Emirates

Morad, S.<sup>1\*</sup>, Morad, D.<sup>2</sup>, Nader, F.H.<sup>3</sup>, Rossi, C.<sup>4</sup> & Gasparini, G.<sup>3</sup>

<sup>1</sup>Department of Earth Sciences, Khalifa University of Science and Technology, United Arab Emirates; <sup>2</sup>Department of Geosciences, University of Oslo, Norway; <sup>3</sup>IFP Energies Nouvelles, France; <sup>4</sup>Departamento de Petrología y Geoquímica, Universidad Complutense, Spain; \*sadoon.morad@ku.ac.ae

Thermochemical sulphate reduction (TSR) in hot and anhydrite-rich sour gas reservoir carbonates of the Arab Formation (Upper Jurassic) has been constrained using petrography, stable isotopes and fluid inclusion microthermometry and spectroscopy. Limited TSR, despite the established perfect conditions for this reaction, is manifested by rare calcitisation of anhydrite with slightly lower  $\delta^{13}\text{C}_{\text{VPDB}}$  values ( $-3.2$  to  $-0.1$  ‰) than calcite precipitated in equilibrium with Late Jurassic seawater. Fluid inclusion microthermometry and spectroscopy of calcite (Fig. 1) that has replaced anhydrite indicates that TSR occurred between 140 and 155 °C in the presence of geochemically evolved ( $\delta^{18}\text{O}_{\text{SMOW}} = +9.2$  to  $+14.5$  ‰), highly saline (20.3 and 22.5 wt% NaCl eq.), NaCl-CaCl<sub>2</sub>-MgCl<sub>2</sub> dominated brines. The lack of evidence for extensive TSR, despite the suitable current temperatures and abundant sulphates in the gas reservoir, coupled with the relatively more common TSR-related calcite in the flanks (water zone) than crest (gas zone), indicate that: (1) gas emplacement while the reservoir was buried at shallower depth slowed down or inhibited TSR in the crest even when it subsequently reached depths where extensive TSR would occur, and (2) H<sub>2</sub>S (up to 38 vol%) has migrated from the underlying Permo-Triassic and/or Jurassic sulphate-bearing carbonate deposits. This study demonstrates that constraining the timing of hydrocarbon emplacement within the context of burial-thermal history is crucial for a better understanding of the origin and distribution of H<sub>2</sub>S in hot, anhydrite-rich, sour gas reservoirs.

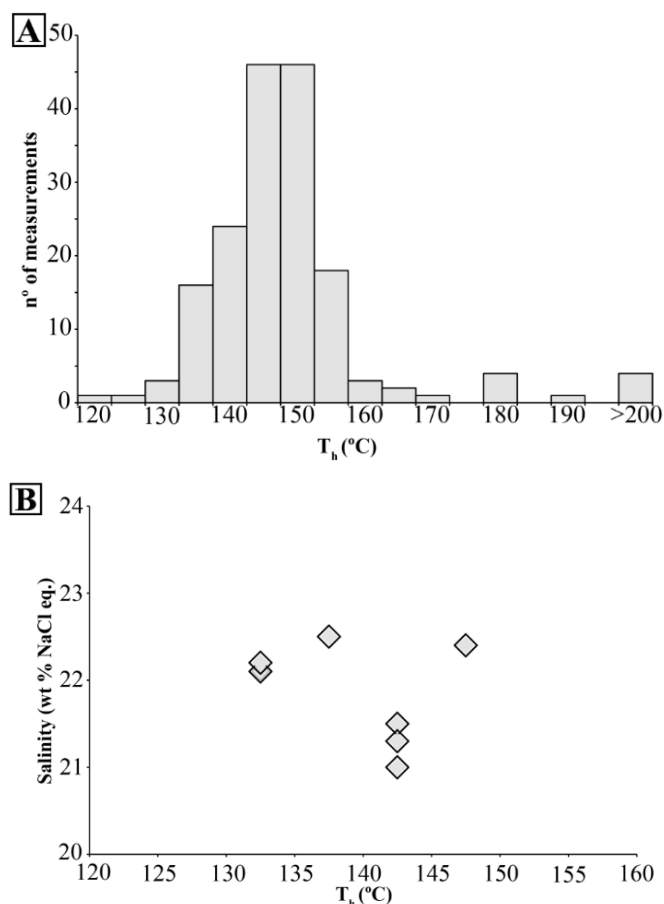


**Fig. 1.** Homogenisation temperatures ( $T_h$ ) and salinity data of aqueous, presumably primary fluid inclusions in nodular and tabular calcite obtained from the Arab Formation. A) Histogram for all measured aqueous and presumably primary fluid inclusions. Most  $T_h$  values range between 135 and 155 °C. B) Cross-plot showing that there is no correlation between  $T_h$  and salinity.

# Composition of fluid inclusions in quartz of gold ore deposit Mnogovershinnoye (Russia)

Morozova, K.A.<sup>1\*</sup>, Prokofiev, V.Y.<sup>1</sup> & Petrov, V.A.<sup>1</sup>

<sup>1</sup>Institute of Geology of Ore Deposits, Petrography, Mineralogy, and Geochemistry, Ras, Russia;

\*vladarus99@gmail.com

Gold deposit Mnogovershinnoye is located in Nikolaevskii district of Khabarovskii krai, Russia. The deposit is primary, refers to the geological and industrial type of gold silver deposits in magmatic zones. The Deposit consists of a group of converging steep-falling complex structure of gold-quartz veins and quartz mineralisation zones, forming ore zones, concentrated in the band of faults of the North-Eastern strike.

A total of 5 samples from mineralised quartz veins were investigated. Only three samples were suitable for microthermometric studies of fluid inclusions. There were distinguished primary, primary-secondary and secondary fluid inclusions according to the criteria (Roedder, 1984). Uniformly distributed in the mineral-owner or confined to the area of crystal growth fluid inclusions has been attributed to the primary fluid inclusions. Inclusions confined to the secant host mineral cracks were considered secondary. Primary-secondary fluid inclusions are confined to cracks that do not reach the outer boundaries of crystals and grains, and in phase filling they are similar to primary inclusions. Two main types of fluid inclusions were allocated to the phase composition (Fig. 1): 1) two-phase gas-liquid inclusions of water-salt solutions (type 1); 2) essentially gas-rich inclusions (type 2).

Fluid inclusions evenly distributed over the volume of individual quartz grains and assigned to primary inclusions were selected for thermo- and cryometric studies. However, the parameters of phase transitions were also obtained for primary-secondary and secondary inclusions.

The chemical composition of the fluid captured in the inclusions was evaluated by measurements of phase transitions and transformations occurring during heating and cooling of the preparations. The accuracy of temperature measurement is 0.2 °C in the temperature range from -20 to +20 °C and decreases at higher and lower temperatures. The composition of salts prevailing in aqueous solutions of fluid inclusions was estimated by the results of eutectic melting temperature measurements. The total salt concentration in two-phase fluid inclusions was estimated from ice melting temperatures on the basis of experimental data for the NaCl-H<sub>2</sub>O system (Bodnar and Vityk, 1994). Fluid pressure was calculated for heterogeneous fluids as water vapour pressure. Salt concentrations, densities and fluid pressures were estimated using the FLINCOR program.

The study was conducted more than 300 individual fluid inclusions in quartz from the mineralised veins of the deposit

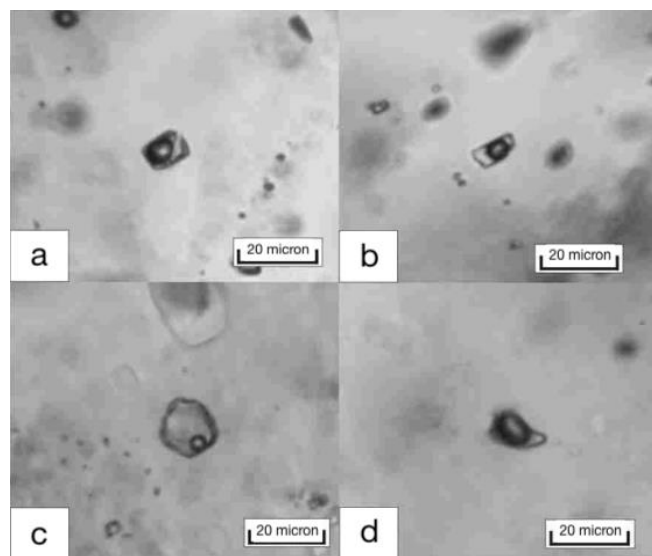


Fig. 1. Types of fluid inclusions in quartz of mineralised veins of the Mnogovershinnoye Deposit A-C) two-phase inclusions of water-salt solutions of type 1; D) gas inclusion of type 2.

Mnogovershinnoye. Ore-forming fluid of mineralised veins of the deposit Mnogovershinnoye contained chlorides Na, Mg and K. This is evidenced by chloride eutectic solutions of inclusions (from -23 to -34 °C). Two-phase gas-liquid fluid inclusions in quartz are homogenised into liquid at temperatures from 485 to 126 °C, the salt concentration varies from 12.2 to 0.2 wt% NaCl<sub>eq</sub>, the fluid density is 0.47-0.95 g/cm<sup>3</sup>.

In some cases the inclusion of type 1 were captured along with gas inclusions of type 2, which indicates the heterogeneous state of fluid. Deep cooling of gas inclusions to temperatures of -180 °C did not reveal condensation of any phases, which indicates that gas inclusions are filled only with low-density water vapour. Water vapour pressure varied from 570 to 180 bar at temperatures from 485 to 360 °C. Hydrothermal fluids of the Mnogovershinnoye Deposit detect the development of high-, medium- and low-temperature fluids whose salinity varies from moderate to low and do not correspond to the fluids of epithermal deposits in these parameters (Simmons et al., 2005). Perhaps they are associated with subvolcanic magmatism level.

## References

- Bodnar R.J. and Vityk M.O. (1994) in: Fluid Inclusions in Minerals. Methods and Applications 117-130.
- Roedder E. (1984) in: Rev. Mineral. 12:644 p.
- Simmons F.A. et al. (2005) Econ. Geol. 100<sup>th</sup> Ann. Vol.:485-522.

# The nature and reactivation of the silicic crystal mush body beneath the Late Pleistocene Ciomadul volcano: a fluid and melt inclusion study

**Németh, B.<sup>1\*</sup>, Bali, E.<sup>2</sup>, Lukács, R.<sup>1</sup>, Guðfinnsson, G.H.<sup>2</sup> & Harangi, Sz.<sup>1,3</sup>**

<sup>1</sup>MTA-ELTE Volcanology Research Group, Budapest, Hungary; <sup>2</sup>NordVulk, Institute of Earth Sciences, University of Iceland, Reykjavík, Iceland; <sup>3</sup>Department of Petrology and Geochemistry, Eötvös Loránd University, Hungary; \*bianca.nemeth@gmail.com

The last volcanic eruptions in the Carpathian-Pannonian Region (CPR) happened around 30 ka at Ciomadul volcano, eastern-central Europe (Molnár et al., 2019). The Ciomadul is part of a long-lived dacitic volcanic system, where eruptions started at 1 Ma (Molnár et al., 2018). The active phases, which lead to mostly K-rich calc-alkaline dacites and smaller amount of shoshonitic rocks, were divided by long repose times (Molnár et al., 2018). Beneath Ciomadul, based on the presence of an anomalous seismic zone (Popa et al., 2012) and electrical conductivity (Harangi et al., 2015), Kiss et al. (2014) inferred the presence of a low-T (700–750 °C) silicic crystal mush body.

We studied fluid inclusions (FI) and silicate melt inclusions (SMI) hosted in the macrocrysts and crystal clots from four outcrops of the Ciomadul in order to characterise better the silicic crystal mush body and reveal the processes of reactivation, which triggered the volcanic eruptions.

The studied high-K and crystal-rich dacite samples are dominantly composed of plagioclase (Pl), amphibole (Amph), biotite (Bt), clinopyroxene, quartz and K-feldspar macrocrysts together with apatite, titanite, zircon and allanite accessories (Kiss et al., 2014). Overall two types of crystal clots were observed in Ciomadul dacite:

- a) felsic, that consists of low-T mineral association derived from a silicic crystal mush and,
- b) mafic, that could be derived from primitive basaltic magmas intruded into the crystal mush.

In the studied occurrences we found only felsic clots referring to nature of the crystal mush. Our geothermobarometric calculations suggest a polybaric magma storage between 8 and 15 km at temperatures around 700–750 °C. Crystallisation were likely taken place over a range of redox conditions ( $\Delta\log f_{O_2}$ , NNO) from ~ 0 to +1.3.

The presence of a large number of neighboring FIs and SMIs in the felsic clots and in the macrocrysts (Pl, Bt and Amph) indicate the coexistence of a fluid and a melt phase at the time of crystallisation of host minerals. Furthermore, the FIs and SMIs were entrapped in host minerals in several steps, which suggests the existence of a long-lived crystal mush. The primary FIs contain one phase at room temperature and are dark-coloured. The majority of the SMIs contain glass  $\pm$  bubble(s). Some of the observed SMIs hosted in plagioclase from the lava dome samples additionally have colourless polycrystalline part, which contains cristobalite and plagioclase daughter phases. The composition of the fluid

inclusions and the bubbles of the silicate melt inclusions was determined by Raman spectroscopy. They contain CO<sub>2</sub>  $\pm$  N<sub>2</sub> (up to 3.2 mol%), whereas water was not detected at room temperature.

Glasses of the silicate melt inclusions are rhyolitic, showing small compositional variation. SMIs could represent the melt fraction coexisted with the crystal mush at the temperatures corresponding to the cotectic, or at larger depth the eutectic, point of the system. The groundmass glass of one of the studied pumice samples is also rhyolitic. Our mass balance calculations suggest a remelting of felsic phases at the minimum point. The mixing between the remelted phases and the intercrystal rhyolitic melt yielded an eruptible melt fraction.

The fact that both the FIs and the bubbles of the SMIs are dominated by CO<sub>2</sub> indicates that the partial melting of the crystal mush happened in the presence of a CO<sub>2</sub>-bearing COH fluid. This suggests that effective reactivation of a crystal mush, responsible to the volcanic eruption, is possible without the physical interaction between mafic magma and felsic crystal mush.

## Acknowledgement

This research belongs to the OTKA-NKFIH K116528 project. The Tempus Public Foundation and the Norway Grants with the Scholarship Program of EEA Financial Mechanism 2009-2014 supported the joint work between the Hungarian and Icelandic partners.

## References

- Harangi et al. (2015) *J. Volcanol. Geoth. Res.* 290:82-96.  
Kiss et al. (2014) *Contrib. Mineral. Petr.* 167:1-27.  
Molnár et al. (2018) *J. Volcanol. Geoth. Res.* 354:39-56.  
Molnár et al. (2019) *J. Volcanol. Geoth. Res.* 373:133-147.  
Popa et al. (2012) *Pure Appl. Geophys.* 169:1557-1573.

# Constraints on magma metal fertility from silicate and sulphide melt inclusions in mineralised volcanic and intrusive rocks in the northeastern Cobequid Highlands, Nova Scotia, Canada

**Neyedley, K.<sup>1,2\*</sup>, Hanley, J.J.<sup>1</sup>, MacHattie, T.<sup>2</sup>, Zajacz, Z.<sup>3</sup>, & Tsay, A.<sup>3</sup>**

<sup>1</sup>Department of Geology, Saint Mary's University, Canada <sup>2</sup>Department of Energy and Mines, Nova Scotia Geological Survey Branch, Canada <sup>3</sup>Department of Earth Sciences, University of Toronto, Canada;  
\*kevinneyedley@gmail.com

In the northeastern Cobequid Highlands, Nova Scotia, Canada, bedrock mapping, and bulk rock and stream sediment geochemical surveying by the Nova Scotia Department of Energy and Mines has identified a potentially large epithermal Au system in a thick sequence of Late Devonian to Early Carboniferous bimodal volcanics along the Cobequid-Chetabucto Fault zone, a major crustal transform that juxtaposed the Meguma and Avalonia terranes in the Paleozoic. Two Au occurrences have been reported and comprise zones of silicified and sulphidised volcanic rocks with up to 660 ppb Au reported and grains of native gold have been recovered in stream sediments in the area. Highly anomalous bulk rock concentrations of As (~4500 ppm), Sb (~50 ppm), Se (~2.5 ppm), and Hg (up to 600 ppb) are reported at or nearby the location of elevated Au. Metal associations, gangue textures, alteration and fluid inclusion systematics are consistent with a very shallow (<250 m), transiently boiling, low-sulphidation epithermal environment. Melt inclusions (sulphide and silicate melt) are abundant in accessory zircon within both volcanic and broadly coeval intrusive phases.

Electron microprobe analyses of exposed, homogenised silicate melt inclusions from five volcanic (n=40) and eight intrusive (n=66) phases indicate the magma was subalkaline ( $\text{Na}_2\text{O}+\text{K}_2\text{O} \sim 4\text{-}8$  wt%;  $\text{SiO}_2 \sim 67\text{-}80$  wt%). Volatile concentrations are variable across all phases with  $\text{H}_2\text{O}$  concentrations of  $4.5 \pm 3.0$  wt%, Cl  $730 \pm 460$  ppm, and F  $1120 \pm 580$  ppm. The highest Cl concentrations are present in melts from a hybrid porphyry unit (i.e., fragments of mafic rock in felsic matrix suggesting mixing) that contains coevally entrapped silicate and sulphide melt inclusions and Cl concentrations are  $1140 \pm 310$  ppm and have  $\text{H}_2\text{O}$  contents of  $4.8 \pm 2.5$  wt%, consistent with the typically higher Cl/ $\text{H}_2\text{O}$  of mafic magma contributions.

Preliminary LA-ICP-MS analyses of silicate melt inclusions show that the melts are generally poor in As (< 10 ppm) and Sb (< 1.5 ppm) but are variably enriched in Cu (up to 1 wt%;  $1130 \pm 2190$  ppm; n = 93), Mo ( $5.2 \pm 2.9$  ppm; n = 55), and W ( $2.4 \pm 2$  ppm; n = 85). It is important to note, that only some lithologies, but both volcanic and intrusive, have elevated Cu concentrations that are not consistent across all lithologies. No systematic correlations are present between metal concentrations and age of the host phases. A

positive correlation is present between Cs and Mo concentration suggesting Mo is likely concentrated in the magma due to melt fractionation. However, Cu does not show any correlation with Cs indicating Cu has likely been lost by fluid exsolution. LA-ICP-MS analyses of sulphide melt inclusions from the hybrid porphyry are modestly enriched in Cu ( $2.04 \pm 0.57$  wt%; n=19), Co ( $700 \pm 270$  ppm; n=19), Ni ( $740 \pm 190$  ppm; n=14), and Mo ( $94 \pm 51$  ppm; n=19), comparable to sulphide melt inclusions reported in other barren and mineralised magmatic-hydrothermal systems globally. Other elements of notable enrichment include Se, Bi, and Te. Arsenic was only above detection in one inclusion (2.71 ppm) and Sb was always below detection with a minimum detection limit of 0.57 ppm.

The anomalously high concentrations of Cu in some silicate melt inclusions could either represent the coentrapment of a sulphide melt or a saturated Cu-enriched volatile phase, the latter being consistent with the large range of volatile concentrations recorded in homogenised silicate melt inclusions. The As- and Sb-poor nature of the silicate and sulphide melts could indicate that a metal-enriched volatile phase exsolved from the magma prior to silicate melt entrapment and/or sulphide saturation or the intrusive phases studied were not the source of As and Sb enrichment (and by association Au) observed in the volcanic units.

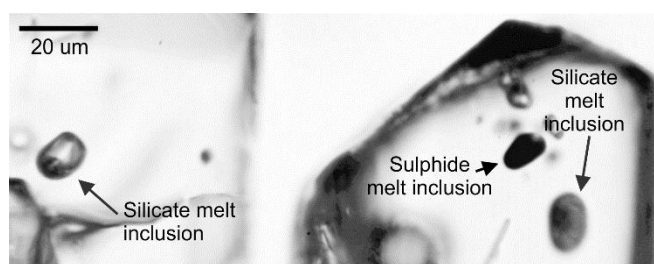


**Fig. 1.** Representative zircon-hosted silicate and sulphide melt inclusions from a hybrid porphyry, northeastern, Cobequid Highlands, Nova Scotia, Canada.

# Heterogeneous deep source versus shallow crustal imprints in the petrogenesis of kamafugites from San Venanzo volcano, Italy

Nikogosian, I.K.<sup>1\*</sup>, Bracco Gartner, A.J.J.<sup>1</sup>, Ersoy, Ö.<sup>2</sup> & Van Bergen, M.J.<sup>2</sup>

<sup>1</sup>Vrije Universiteit Amsterdam, The Netherlands; <sup>2</sup>Utrecht University, The Netherlands; \*i.nikogosian@vu.nl

Within the wide compositional spectrum of potassium-rich magmatism in Central Italy, kamafugitic rocks in the Intra-Appennine Volcanic Province constitute the most alkalic and silica-undersaturated end-member, showing the highest enrichment in many incompatible trace elements. A close association with carbonatitic rocks has posed questions concerning the ambiguous origin of carbon, which may have been derived from the mantle source or from interaction with Mesozoic carbonates residing in the crust. We explored the crystallisation history of olivines and their melt inclusions (MI), separated from a representative rock specimen from San Venanzo, which enabled us to (1) determine the primary composition(s) of mantle-derived kamafugite melts and (2) trace the effects of crustal interaction on melt composition and magma evolution. Complex textures of olivine phenocrysts and their trace element compositions provide a framework for the sequence in which melt evolved within a single magmatic plumbing system.

Olivine crystals in the studied kamafugite show complex textures between core and rim parts. There are strong indications of drastic late-stage changes in the crystallisation regime, including irregular and patchy compositional zoning and increasing amounts of inclusions in the rims, as well as rare primary melt inclusions in pristine parts of the olivines (Fig. 1).

Pristine core parts, characterised by high Fo (93–90 mol%), low CaO (0.2–0.3 wt%) and Cr-spinel inclusions (Cr# ~0.7), are considered to have crystallised from a primary, mantle-derived melt. Compositions of homogenised melt inclusions in these core parts are consistent with derivation from high-MgO melts, but span a continuous range for K<sub>2</sub>O, Na<sub>2</sub>O, P<sub>2</sub>O<sub>5</sub>, TiO<sub>2</sub> and CaO content.

Contrastingly, the rim parts show a strong compositional gradient of decreasing forsterite (down to Fo<sub>70</sub>) and increasing CaO (up to 1.8 wt%). Profiles of phosphorous contents in the olivines point to steep increases in the rim parts, indicating that they originated as rapid overgrowths onto phenocryst cores.

Homogenised MI from the rim parts are compositionally close to evolved carbonate-bearing volcanic products, natural skarns and glasses generated in carbonate assimilation experiments. These combined signatures suggest that the rim parts crystallised from an evolved melt that was contaminated through interaction with carbonate-rich lithologies. Fluid inclusions in the rim parts indicate that this interaction occurred at relatively shallow crustal levels (2–10 km; Fig. 1).

From the major and trace element content of core-hosted MI we infer that the kamafugite represents an assembly of primary melts with different compositions, controlled by low-degree melt extraction from a mantle source with mineralogical variations. Both the major and trace element content of core-trapped MI furthermore demonstrate an important role for apatite in the mantle source during primary melt generation of the San Venanzo kamafugites. Our observations are consistent with a mantle source affected by siliceous K<sub>2</sub>O-rich and carbonate/apatite-rich metasomatic agents derived from subducted carbonate-bearing metapelites.

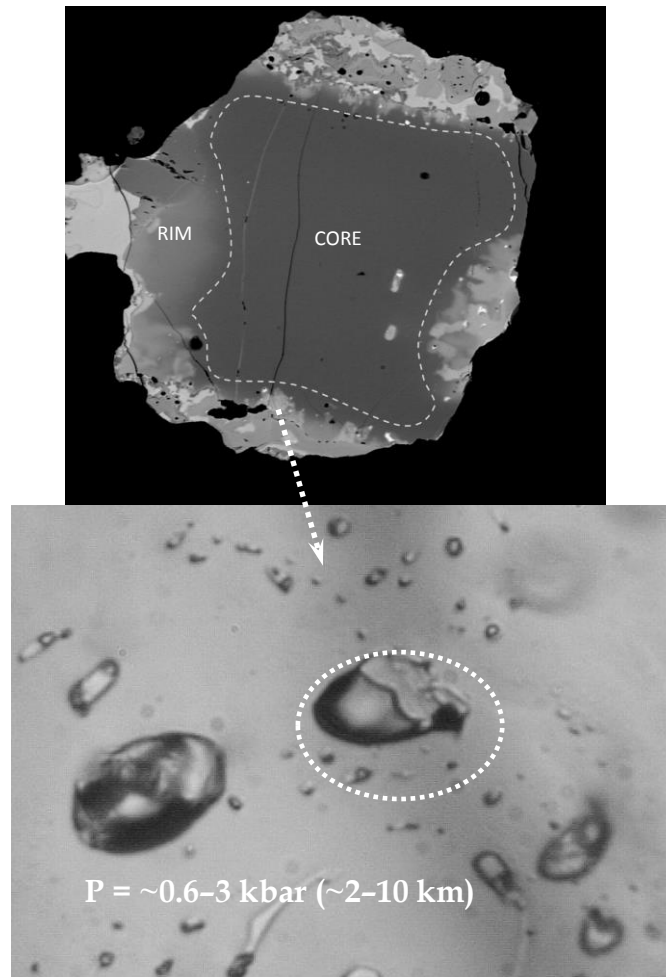


Fig. 1. Typical texture of the studied olivines and fluid inclusions in the rim parts.

## Fluid inclusion studies of pegmatites from parts of southwestern Nigeria

**Oyedokun, M.O.<sup>1\*</sup> & Okunlola, O.A.<sup>1</sup>**

<sup>1</sup>Department of Geology, University of Ibadan, Ibadan Nigeria; \*trustoyee@yahoo.co.uk

Geochemical assessment of fluid inclusions in minerals has been successfully used in the description of genesis and characteristics of different ore-forming fluids. However, there are few reported applications of fluid inclusion studies in the delineation and characterisation of ore-forming fluids in pegmatites from southwestern Nigeria. This study was designed to determine the type, origin and characteristics of fluids involved in the genesis of pegmatites from parts of southwestern Nigeria.

Systematic geological mapping was carried out in the Olode, Komu and Idiyen areas. Samples of pegmatite were obtained and a fluid inclusion study was carried out on pegmatitic quartz using microthermometry.

Three types (I, II and III) of aqueous, primary to pseudo-secondary inclusions were observed. Type I are two-phase LV inclusions of ~2–100  $\mu\text{m}$  occurring as isolated inclusions, clusters and trails (Fig. 1). Type II inclusions are three-phase LVS, ~2–15  $\mu\text{m}$  and they occur as isolated individuals and in trails. Type III are monophasic (liquid) and occur as isolated inclusions, clusters and in trails that also contain types I and II. Type I inclusions have salinity of 0.7–21.9 wt%  $\text{NaCl}_{\text{eq}}$ . All inclusions homogenised into the liquid phase at ( $T_h$ ) of 80–335  $^{\circ}\text{C}$ . Temperature-pressure modeling revealed type II inclusions with  $T_h$  of 350  $^{\circ}\text{C}$  as the earliest fluid trapped and were associated with late magmatic hydrothermal fluids. Type II inclusions were trapped at 250  $^{\circ}\text{C}$ . Type I inclusions were trapped at 160–250  $^{\circ}\text{C}$ , indicating dilution and interaction of ore-forming fluid with meteoric water while Type III inclusions were trapped at a much lower temperature of <50  $^{\circ}\text{C}$  based on  $T_h$  values.

The pegmatites of Southwestern Nigeria are characterised by aqueous fluid inclusions of primary and pseudo-secondary types and they are of magmatic to meteoric origins.

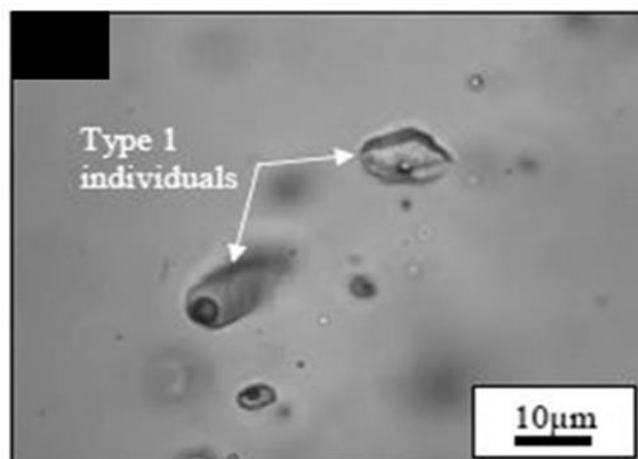


**Fig. 1.** Type I (Liquid-Vapour) inclusions. Photomicrograph.

# Geology, geochemistry and microthermometric characteristics of the Tuztaşı Au mineralisation (NW Turkey): primary results

Özbaş, F.<sup>1\*</sup> & Hanilçı, N.<sup>1</sup>

<sup>1</sup>Department of Geological Engineering, Istanbul University-Cerrahpaşa, Avcılar Campus, Turkey;  
\*faith.ozbas@istanbul.edu.tr

The Tuztaşı (Çanakkale-Ayvacık) Au mineralisation is located at the Biga Peninsula in NW Turkey. The Biga Peninsula hosts a variety of epithermal Au-Ag (e.g. Agi Dagi, Kirazli, Kisacik, Sahinli, Koru, Madendag), porphyry Au-Cu-Mo (e.g. Halilaga, Tepeoba), Pb-Zn±Cu skarns (e.g. Handeresi, Bagirkacdere, Culfacukuru) deposits and is one of the most actively mining area in Turkey. The Peninsula can be tectonically subdivided into three zones. These are; (i) the Ezine zone (Permian meta-sedimentary and Permo-Triassic ophiolitic rocks), (ii) the Ayvacık-Karabiga zone (eclogite-bearing ophiolitic mélangé and Late Triassic limestone blocks) and (iii) the Sakarya zone (Permian metamorphic rocks of the Kazdağ Group and Permo-Triassic sedimentary and magmatic rocks of the Karakaya Complex). Cenozoic volcanic and plutonic rocks cover extensive areas. (Okay et al., 1991).

There are four stratigraphic units in the study area. From old to young; (i) Lower Carboniferous Sutuvén Formations includes gneiss, amphibole schist, marble, (ii) Late Cretaceous Çetmi Ophiolitic Melange includes serpentine, diabase, gabbro, shale, sandstone and limestone, (iii) Oligo-Miocene Evciler Pluton represented by granodiorite, and (iv) Late Miocene İlyasbaşı Formation includes conglomerate, sandstone and mudstones.

The Tuztaşı Au mineralisation is located in Paleozoic gneiss and schist of Kazdağ Massif. The Au-bearing quartz vein is 5 km long, trending to N20E, dipping to NW as 60-80°, has 2 to 10 m thickness and up to 500 m long. Silicic and argillic alteration has developed in around the vein. The quartz veins display different filling textures through the vein such as vugs, breccia, feathery, cockade and comb, and rare colloform and crustiform texture. The quartz veins include very rare pyrite and its oxidation product goethite and hematite. Pyrites are euhedral, and fine grained. Au content of the quartz vein varies between 0.09 ppm and 4.02 ppm, and the average is 1 ppm.

Microthermometric data has obtained from the fluid inclusions which are hosted by medium to fine crystalline quartz, saccharoidal and colloform bands. Only two-phase liquid rich inclusions, vapour (V) and liquid (L), containing ranging 20 to 30 vol% vapour and 70 to 80 vol% liquid (Fig. 1) were recognised. The inclusions are typically 20-30 µm in size but the most of the inclusions are 10 µm or less. All data obtained from primary fluid inclusions. Two FIA's have been observed due to their L/V ratio, size and microthermometric results,

and both are markedly different. The homogenisation temperature of first FIA's ranging from 240 to 265 °C and their salinities are between 1 and 2 wt% equiv. NaCl. The homogenisation temperature of second FIA's ranging from 160 to 205 °C and their salinities are almost as same as the first assemblages.

Alteration type, quartz textures and

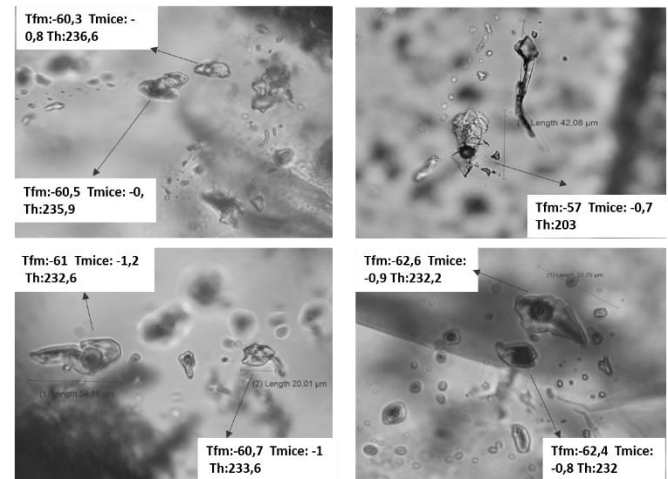


**Fig. 1.** Two-phase liquid rich inclusions, vapour (V) and liquid (L) and their microthermometric results.

microthermometric data suggest that the Tuztaşı Au mineralisation is an epithermal mineralisation. The gold may have precipitated due to boiling represented by feathery, colloform, crustiform textures. The very variable Au values along the vein should be related to the variation in the degree of boiling along the vein.

## Acknowledgement

This study is a part of Ph.D. thesis that was prepared in the Institute of Graduate Education of Istanbul University-Cerrahpaşa and was supported by The Scientific Research Projects Coordination Unit of Istanbul University-Cerrahpaşa, project number 25927.

## References

Okay A. et al. (1991) Bull. Tech. Uni. Istanbul 44:191-255.

# Investigation of alteration and hydrothermal fluid properties of the Latala, epithermal base and precious metal deposit, northern Miduk (Iran)

**Padyar, F.<sup>1\*</sup>, Rahgoshay, M.<sup>1</sup>, Tarantola, A.<sup>2</sup>, Pourmoafi, M.<sup>1</sup>, Vanderhaeghe, O.<sup>3</sup> & Caumon, M.C.<sup>2</sup>**

<sup>1</sup>Faculty of Earth Sciences, Shahid Beheshti University, Geological Survey of Iran, Iran; <sup>2</sup>Université de Lorraine, CNRS, CREGU, GeoRessources Nancy, France; <sup>3</sup>France Université de Toulouse GET, CNRS, IRD, UPS, CNES (Toulouse), France; \*padyar@geologist.com

The study area is located north of the Miduk porphyry and east of the Sarah intrusives central Iran. During Oligocene-Miocene, porphyry intrusives such as Miduk, Sarah, as well as the injection of subsequent dykes into the volcanic rocks series, resulted in the precipitation of silica veins bearing base and precious metal mineralisation associated with porphyry and alteration zones. Hydrothermal alteration is distinguished by a proximal potassic assemblage, dominated by hydrothermal zircons, secondary biotite and K-feldspar, grading outward and upward into a phyllic assemblage. A propylitic halo, distinguished by the occurrence of chlorite, epidote, and carbonates, is well developed in the enclosing volcanic rocks. In Latala, wall rocks are strongly altered by hydrothermal solutions. Alteration in the wall rocks varies from a proximal silicic to distal argillic to advanced argillic assemblage. Alteration in the veins is composed of siliciclastic and oxide zones grading outwardly into argillic and propylitic zones. There are lesser amounts of jarosite and goethite. Wall-rock reactions and evolution of magmatic fluid would lead to Fe-rich fluids (Heinrich, 2005; Rahfeld et al., 2015). In Latala area two assemblages are observed: 1) quartz-kaolinite 2) quartz-adularia. Smoky quartz and kaolinite assemblage represents argillic alteration in Latala deposit. The presence of quartz-adularia is dominated by boiling up of CO<sub>2</sub> and alkaline-rich fluid. The mafic and felsic volcanic rocks in the host sequences are high-K calc-alkaline and shoshonitic basalts. Smith et al. (2017) demonstrated that mineral assemblage during alteration affected by the host lithology and mineral buffers. Petrography and Raman spectrometry studies indicate the presence of phyllosilicates (presumably muscovite and illite), chlorite, quartz and natrocarbonate minerals such as dawsonite in fluid inclusions (Padyar, 2017).

For the Latala vein type base and precious metals deposit, homogenisation temperatures and salinity vary between 131 and 380 °C and 0.17 and 10.6 wt% NaCl equiv. respectively. Fluid inclusion temperature and petrography as well as alteration indexes calculated based on chemical analyses document the nature of the hydrothermal fluid.

Alteration and mineralisation in Latala deposit attributes to intensity of alteration host rock and existence minerals. Alteration products such as mckinstryite, jarosite and goethite indicate the presence a supergene copper-bearing fluid with a

low-salinity, forming of fluid with  $f_{H_2} - f_{S_2}$  at a low temperature.

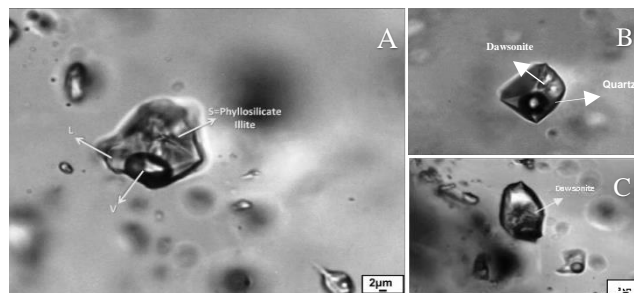


**Fig. 1.** A) The fluid inclusion bearing phyllosilicates such as illite. B-C) The fluid inclusion bearing natrocarbonate such as dawsonite.

## Acknowledgement

This work was supported by a grant from Ministry of Science, Research and Technology of Iran and benefited from support of the CNRS-TRIGGER program. We would like to thank authorities in the Shahid Beheshti University, the Geological Survey & Mineral Exploration of Iran, Miduk copper mine and GeoRessources lab of the University de Lorraine (France).

## References

- Heinrich C.A. (2005) *Miner. Deposita* 39:864-889.
- Padyar F. (2017) Ph.D. thesis. University of Shahed Beheshti, Tehran 220.
- Rahfeld A. et al. (2015) SGA meeting. Nancy, France, book. 1:339-342
- Smith D.J. et al. (2017) *Ore Geol. Rev.* 89:772-779.

# Water content in quartz-hosted silicate melt inclusions from a Plinian fall layer, Bükkalja Volcanic Field

**Pálos, Zs.<sup>1,2\*</sup>, Biró, T.<sup>3</sup>, Kovács, I.J.<sup>2</sup>, Aradi, L.E.<sup>1</sup>, Kesjár, D.<sup>4</sup>, Fehér, K.<sup>3</sup>, Berkesi, M.<sup>1</sup> & Szabó, Cs.<sup>1</sup>**

<sup>1</sup>Lithosphere Fluid Research Lab, Eötvös Loránd University, Hungary; <sup>2</sup>MTA CSFK Geodetic and Geophysical Institute, Hungary; <sup>3</sup>Eötvös Loránd University, Institute of Geography and Earth Sciences, Hungary; <sup>4</sup>MTA CSFK Institute for Geological and Geochemical Research, Hungary; \*paloszsofia@gmail.com

Volatiles in magmatic systems play a key role in determining the eruptive behaviour of rhyolitic systems. However, the accurate measurement of magmatic volatiles dissolved in the melts is challenging, hence the study of silicate melt inclusions (SMIs) became a common practice in the last decades.

The objectives of this research were i) to measure the 'water' content of quartz-hosted melt inclusions in a specific rapidly cooled, rhyolitic Plinian fall tuff layer from the Carpathian Pannonian Region's (CPR) Bükkalja Volcanic field, ii) elaborate a suitable method for the thickness determination of unexposed silicate melt inclusions by using Fourier Transform Infrared spectroscopy (FTIR) and thus iii) make an estimation on the partition coefficient of water between quartz and rhyolitic melt.

Sixty-one doubly polished quartz grains bearing glassy and negative crystal-shaped SMIs (>50 µm on their longer extent) were measured by FTIR and Raman spectroscopy. On selected SMI-bearing crystals, FTIR-FPA (Focal Plane Array) imaging was carried out to shed light on possible 'water' concentration gradient around the SMIs.

The mean structural OH<sup>-</sup> content of quartz grains (12.7 ± 2.9 wt. ppm) showed a good agreement with the 12.8 ± 3.2 wt. ppm average value presented by Biró et al. (2017) from the same layer. Bulk 'water' content in the studied SMIs fall in the range of 0.03 – 5.66 wt%, OH<sup>-</sup> content range is 0.00 – 3.89 wt%, H<sub>2</sub>O contents range is 0.00 – 11.75 wt% (FTIR) and 0.91 – 2.96 wt% (Raman), respectively. The thickness of SMIs for FTIR quantification was determined from the contribution of the SMI to the Si-O absorbance region (1441–2100 cm<sup>-1</sup>) by subtracting the "inclusion-free" spectra from the spectra from the "SMI-bearing" one (Fig. 1).

FPA images showed no concentration gradient of OH<sup>-</sup> in quartz around the SMIs.

The glassy nature and negative crystal shape of the SMIs imply a rapid quenching during or after the eruption. The rapid cooling is further supported by the absence of diffusion profiles around the SMIs, which suggests that no significant dehydration happened after the emplacement of the rhyolite. Despite the fact that SMIs are from a rapidly quenched deposit, their OH<sup>-</sup>/H<sub>2</sub>O ratio indicates nonequilibrium condition (e.g., at ~1 wt% bulk water content of the melt, the ratio is ~0.7 / ~0.3 wt%, Ihinger et al., 1999). A pre-eruptive

degassing in a shallow magma storage system probably may cause the diffusional loss of OH<sup>-</sup> and a "virtual" enrichment of H<sub>2</sub>O in the melt (which is in correspondence with the relative diffusivities of the two species; Kronenberg et al., 1986). Considering the degassed pre-eruptive conditions, a  $D^{\text{quartz/melt}}=0.0004$  partition coefficient was calculated.

The present results and methodology is promising to be routinely applied for SMI water content investigation, independently from other methods, with little cost and demand on sample preparation.

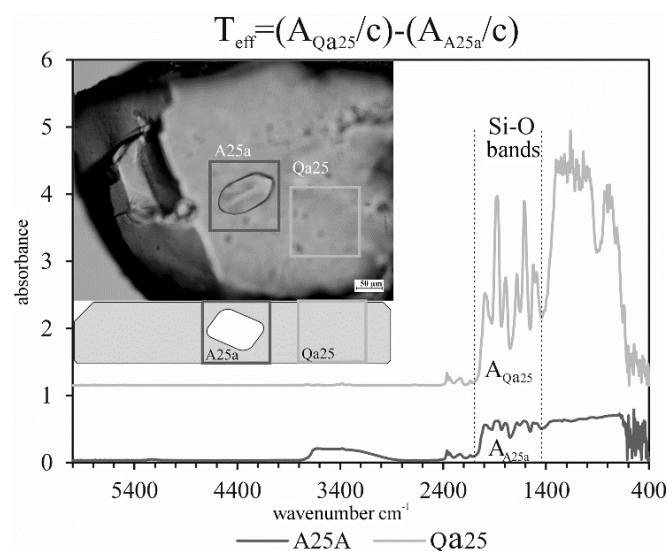


**Fig. 1.** Petrographic picture and the technique of effective thickness estimation on SMIs after the method of Biró et al. (2016), where  $c$  is a constant,  $c=3.3089$  1/µm and  $A_{xy}$  is the integrated area of Si-O bands.

## References

- Biró T. et al. (2016). *Eur. J. Mineral.* 28:313-327.
- Biró T. et al. (2017). *Am. Mineral.* 102:1187-1201.
- Ihinger P.D. et al. (1999) *Geochim. Cosmochim. Ac.* 63:3567–3578.
- Kronenberg A.K. et al. (1986) *J. Geophys. Res. B: Solid Earth* 91:12723-12741.

# The characteristics of wehrlite forming mantle metasomatism - a silicate melt inclusion study in upper mantle xenoliths from Mediterranean Region

**Patkó, L.<sup>1,2,3\*</sup>, Hidas, K.<sup>4</sup>, Sendula, E.<sup>5</sup>, Liptai, N.<sup>1,3</sup>, Aradi, L.E.<sup>1</sup>, Berkesi, M.<sup>1,3</sup>, Bodnar, R.J.<sup>5</sup>, Garrido, C.J.<sup>4</sup> & Szabó, Cs.<sup>1,3</sup>**

<sup>1</sup>Lithosphere Fluid Research Lab, Institute of Geography and Earth Sciences, Eötvös Loránd University, Hungary;

<sup>2</sup>Isotope Climatology and Environmental Research Centre, Institute for Nuclear Research, MTA, Hungary;

<sup>3</sup>Lendület Pannon Lith<sub>2</sub>Oscope Research Group, Geodetic and Geophysical Institute, MTA CSFK, Sopron, Hungary;

<sup>4</sup>Instituto Andaluz de Ciencias de la Tierra, CSIC and UGR, Spain; <sup>5</sup>Department of Geosciences, Virginia Tech, USA; \*[levente.patko@ttk.elte.hu](mailto:levente.patko@ttk.elte.hu)

In the subcontinental lithospheric mantle, beside the dominant lherzolites, clinopyroxene-rich peridotites (wehrlites) also appear. Interaction between a mafic silicate melt and a lherzolite wallrock is the most commonly considered way to form wehrlites.

In this research, we studied upper mantle wehrlite xenoliths collected from the Mediterranean Region such as Nógrád-Gömör Volcanic Field (NGVF; Hungary-Slovakia), Oran Volcanic Field (OVF; Algeria) and South East Iberian Volcanic Province (SEIVP; Spain). Based on the detailed geochemical investigations of the rock forming phases, the xenoliths can be considered as metasomatic products (Patkó et al., 2011; Hidas et al., 2016).

We studied primary silicate melt inclusions (SMIs) hosted by newly-formed clinopyroxenes and olivines, and by orthopyroxene remnants in wehrlite xenoliths from all the studied localities. Our aim was to have a better understanding on the behaviour of trace and major elements during metasomatic processes.

The distribution of the SMIs is similar in all localities. SMIs are occurring dominantly in clusters, however individual inclusions are also appearing rarely.

The clinopyroxene-hosted SMIs are in between 5 and 60 µm. They have negative crystal shapes and contain clinopyroxene, spinel, amphibole ± mica and ± apatite daughter minerals. The latter are in the range of 1-5 µm. Bubble could also be observed in the SMIs.

The olivine-hosted SMIs are 5-50 µm large and show spherical shapes. They are dominated by Si-glass together with minor amounts of clinopyroxene and spinel daughter minerals. A small (1-3 µm in diameter) bubble also occur. The orthopyroxene-hosted SMIs have similar nature to that of SMIs in olivines.

In all SMIs the bubbles contain CO<sub>2</sub>-dominated fluid phase, based on Raman spectroscopy.

In order to obtain better understanding on the role of trace elements during mantle metasomatism, representative SMIs were selected for a detailed LA-ICP-MS study. The results revealed enrichment in incompatible trace elements, especially in LILE (e.g. Ba, Sr, Pb) and HFSE (e.g. Nb, Ta, Zr) compared to the host clinopyroxene.

With the combined use of above analytical tools, we could constrain the compositional change of the melt agent during the metasomatic process (i.e. wehrlite formation).

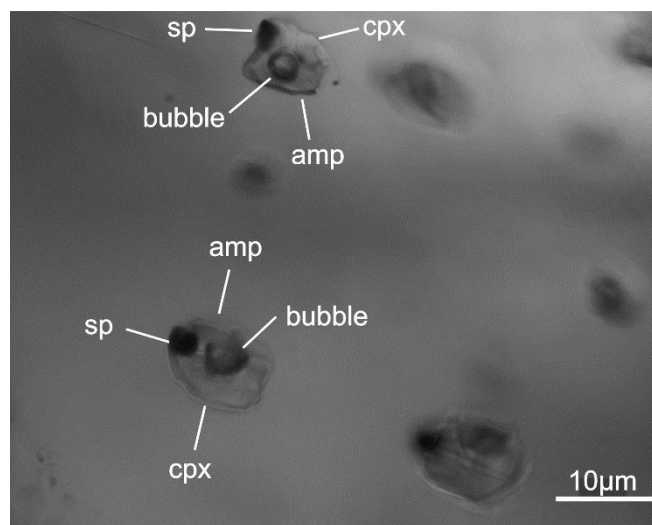


**Fig. 1.** Photomicrograph on the silicate melt inclusions hosted in clinopyroxene, Nógrád-Gömör Volcanic Field (xenolith NME1129D). Daughter minerals: cpx – clinopyroxene, sp – spinel, amp – amphibole.

## Acknowledgement

This research was financially supported by the grant of the Hungarian Scientific Research Found [grant number 78425] to Szabó.

## References

- Hidas K. et al. (2016) *Tectonics* 35:2657-2676.  
Patkó L. et al. (2011) *Astro. J.* 743:L23.

# Fluid inclusions in sedimentary basins: coupling to basin modeling for time and overpressure estimates

Pironon, J.<sup>1\*</sup>

<sup>1</sup>GeoRessources lab, CNRS, CREGU, Université de Lorraine, France; \*jacques.pironon@univ-lorraine.fr

The main objective of fluid inclusion research in sedimentary basins is to build P-T scenarios. Careful petrographic observations can lead to chronologies of fluid inclusions (i.e. fluid events) included in paragenetic sequences. In rare cases, data obtained by radioisotopes may allow obtaining absolute ages for some minerals. But in many cases fluid inclusion studies remain highly frustrating. It is clear that P-T data deduced from fluid inclusions could tell us more about geodynamics! For example, fluid inclusion results can be placed in a P-T diagram and crosschecked with the hydrostatic and lithostatic thermal gradients built using a basin modeling software (Petromod, Temisflow...) (Ungerer et al., 1990; Hantschel and Kauerauf, 2009). These tools include the modeling of burial, thermal history, oil and gas generation and migration processes, and were developed for oil and gas applications. They allow 1D, 2D or 3D views of the basin in time and space. The P-T evolution is calculated taking into account the lithology of the log profiles deduced from wells or outcrops. The present day heat flow and the temperature and pressure at the bottom hole, in addition to temperature data obtained from PRV or other geothermometers complete the input. By consequence, for each profile, the temperature gradient is calculated from different surface heat flow scenarios, related to crust thinning, with respect to geodynamical evolution since sediment deposit. The heat flow could vary by a factor 2 between a rift environment to a "cold" basin. The resulting lithostatic and hydrostatic thermal gradients are displayed on the P-T diagram of the virtual example of the Fig. 1. The evolution of the P-T gradients are therefore time dependent. The slope of the gradients in a P-T projection is linked to the heat flow regimes and is also due to the sedimentation and compaction rates and the rock properties (thermal conductivity, radiogenic heat production and heat capacity) which vary from layer to layer. The loops are due to erosion stages.

Fluid inclusion data are plotted in the same P-T projection as it is described in Bourdet et al. (2010). The technique of the double isochore is applied when coeval aqueous and oil inclusions are present and their relative homogenisation temperatures are measured. Because the inclusions are trapped together and filled by non-miscible fluids, the isochore intersection gives the true P-T conditions of fluid trapping (filled circle in Fig. 1).

From the inclusion data, the overpressure (i.e. the difference between pore pressure and hydrostatic pressure) can be determined to be

around 70 bar (dotted lines on Fig. 1). At the same time, by projection onto the litho- or hydro-static gradient, the trapping time can be estimated to be around 215 Ma.

The objective of this abstract is to demonstrate how inclusionists can enrich their conclusions by correlating fluid inclusion data and basin modeling. Estimate of the trapping time and the pressure regime is of first importance to understand fluid-rock interactions in specific geodynamical contexts.

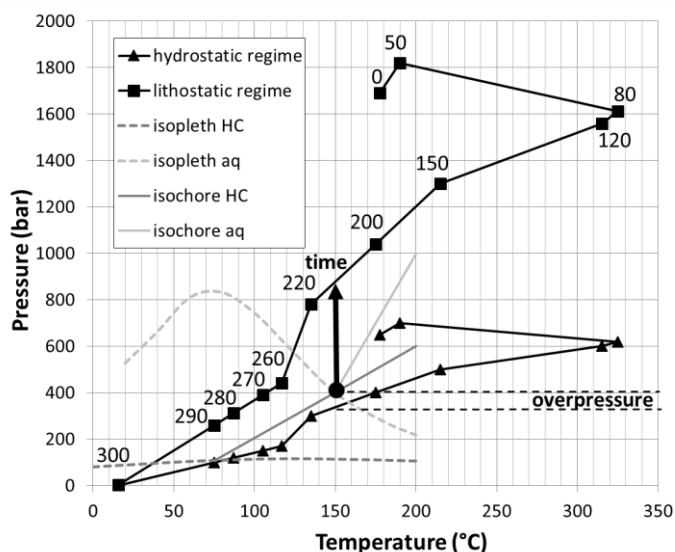


Fig. 1. Virtual P-T graph showing the hydro- and litho-static gradients, the isochores and isopleths for the coeval aqueous and oil inclusions. Times in Ma.

## References

- Bourdet J. et al. (2010) Mar. Petrol. Geol. 27:126–142.
- Hantschel T. and Kauerauf A.I. (2009) Fundamentals of Basin and Petroleum Systems Modeling p.476.
- Ungerer P. et al. (1990) A.A.P.G. Bull. 74:309-335.

**Recent advances in experimental studies with melt inclusions  
at controlled P-T-fO<sub>2</sub>-aH<sub>2</sub>O conditions**

**Portnyagin, M.V.<sup>1,2\*</sup>, Mironov, N.L.<sup>2</sup>, Botcharnikov, R.E.<sup>3</sup>, Almeev, R.A.<sup>4</sup>,  
Krasheninnikov, S.P.<sup>2</sup>, Tobelko, D.P.<sup>2</sup> & Holtz, F.<sup>4</sup>**

<sup>1</sup>GEOMAR, Germany; <sup>2</sup>Vernadsky Institute, Russia; <sup>3</sup>Institute of Geosciences, Johannes Gutenberg University, Germany; <sup>4</sup>Institute for Mineralogy, University of Hannover, Germany; \*mportnyagin@geomar.de

Melt inclusions in olivine are unique probes of primitive and evolved melts, providing insights into the composition and evolution of mantle-derived and crustal magmas (e.g., Roedder, 1984; Sobolev, 1996). The amount of published melt inclusion data is rapidly growing and has a significant impact on the current models of mantle magmatism and its sources in different geodynamic settings over the entire Earth's history. Interpretation of the melt inclusion data is, however, strongly relying on the assumption that the processes occurring in melt inclusions after their entrapment in host mineral are well understood and can be tracked using numerical modeling.

About ten years ago we initiated a systematic study of melt inclusions in olivine using experiments at precisely controlled P-T-fO<sub>2</sub> conditions and in presence of volatiles. The aim of these studies was two-fold: 1) to investigate whether melt inclusions are able to resist changing conditions in host magma (cooling, decompression, degassing, mixing) and preserve their initial composition, and, if not, 2) to reconstruct the initial composition of melt inclusions by forcing their re-equilibration at conditions of entrapment in olivine.

In this talk, we will give an overview of our published (Portnyagin et al., 2008; Mironov et al., 2015; Moore et al., 2018) and new results (Portnyagin et al., 2019; Krasheninnikov et al., 2019), and perspectives. In particular, we will summarise the data on kinetics and mechanism of hydrogen diffusion in olivine linked to the time scales of melt inclusion re-equilibration. We will show that hydrogen loss or gain is responsible for large changes in major element composition of melt inclusions. These changes go far beyond traditional olivine crystallisation and Fe-Mg exchange processes and up to now they were overlooked or misinterpreted in published studies. Our more recent data provide evidence that fluorine also can exchange rapidly, yet not as fast as hydrogen, between melt inclusions and external melt, causing decoupling of fluorine from other halogens and incompatible elements in inclusions. Redox conditions recorded by the Fe<sup>2+</sup>/Fe<sup>3+</sup> ratio in melt inclusions also change on the time-scale of a few hours in response of changing external conditions (Krasheninnikov et al., 2019).

The observations that melt inclusions in olivine can be easily modified after entrapment raises the question about reliable and robust method for the reconstruction of their initial composition. The existing numeric modelling techniques fail due to the complexity of changes occurring in melt inclusions after entrapment. Alternatively, we demonstrate that the reproduction of the initial H<sub>2</sub>O, CO<sub>2</sub>, S, major and trace element composition of inclusions can be successfully achieved in re-equilibration experiments with controlled P-T-fO<sub>2</sub>-aH<sub>2</sub>O conditions corresponding to that estimated from mineral thermo- and barometres.

In summary, recent experimental studies with melt inclusions revealed several re-equilibration phenomena, which change significantly our views on behaviour of melt inclusions after entrapment. As a rule, melt inclusions behave as semi-closed systems and do not preserve initial compositions. Experiments provide an efficient tool to recognise the post-entrapment changes and to reconstruct initial composition of inclusions.

**Acknowledgement**

This work has been supported by grants from the German Science Foundation and Russian Foundation for Basic Research. The current support from RFBR grants 19-05-00934 (to N.M.), 18-35-00497 (to S.K.) and 18-35-00529) to D.T. is kindly acknowledged.

**References**

- Krasheninnikov S.P. et al. (2019) ECROFI 2019 (this volume).
- Mironov N. et al. (2015) Earth Planet. Sc. Lett. 425:1-11.
- Moore L.R. et al. (2018) J. Volcanol. Geoth. Res. 358:124-131
- Portnyagin M. et al. (2008) Earth Planet. Sc. Lett. 272:541-552.
- Portnyagin M. et al. (submitted) Earth Planet. Sc. Lett.
- Roedder E. (1984) in: Rev. Mineral. 12:644 p.
- Sobolev A.V. (1996) Petrology 4:209-220.

## Exceptionally Au-rich fluid inclusions: detection of gold nanoparticles

**Prokofiev, V.<sup>1\*</sup>, Banks, D.<sup>2</sup>, Lobanov, K.<sup>1</sup>, Selektor, S.<sup>3</sup>, Milichko, V.<sup>4</sup>, Borovikov, A.<sup>5</sup>, Akinfiev, N.<sup>1</sup>, Lüders, V.<sup>6</sup> & Chicherov, M.<sup>1</sup>**

<sup>1</sup>*Institute of Geology of Ore Deposits, Petrography, Mineralogy, and Geochemistry, RAS, Russia;* <sup>2</sup> *School of Earth and Environment, University of Leeds, UK;* <sup>3</sup>*A.N. Frumkin Institute of Physical Chemistry and Electrochemistry RAS, Russian;* <sup>4</sup>*Department of Nano-Photonics and Metamaterials, The ITMO University, Russia;* <sup>5</sup>*Institute of Geology and Mineralogy, Sobolev V.S. RAS Russia;* <sup>6</sup>*GFZ German Research Centre for Geosciences, Germany;* \*vpr2004@rambler.ru

Mineralisation was detected in the deepest man-made hole on Earth, the Kola Superdeep drillhole (SG-3, 12262 m), drilled to provide information about rocks and processes in the deep zones of the continental crust of the Baltic Shield (Kola, 1998). The borehole was drilled in the Pechenga ore district of the Russian Federation where there is a greenstone belt of Proterozoic age with gold mineralisation at the present day surface. In drill-core from 9500-11000 m, a gold-bearing region with a vertical extension of about 1500 m occurs, in which the gold concentration varies from 0.01 to 6.7 ppm (INAA analyses). Gold, with up to 26 wt% Ag, is present as small flakes (up to 10 microns) and irregularly shaped grains located in biotite, hornblende, plagioclase, and quartz.

Fluid inclusions in quartz veins between 9052 to 10744 m can be divided into four types: 1) gas inclusions of dense CO<sub>2</sub>, 2) vapour-liquid two-phase aqueous inclusions, 3) three-phase inclusions with NaCl daughter crystals, and 4) CO<sub>2</sub>-aqueous inclusions.

The LA-ICP-MS data, revealed the presence of high concentrations of gold in individual fluid inclusions of all 4 types from above mentioned depths region. Gold concentration in type 1 fluid inclusions varies from 0.7 to 326 ppm (average 56 ppm, n=64), in type 2 from 4.8 to 691 ppm (average 261 ppm, n=15), in type 3 from 3.0 to 6483 ppm (average 754 ppm, n=57), and in type 4 inclusions from 5 to 8081 ppm (average 919 ppm, n=38).

The ablation of fluid inclusions in quartz, shows that the appearance of the gold coincides with the appearance of the K and Na signals from the inclusion fluids. The presence of gold was not detected during the ablation of quartz around type 1 to 3 fluid inclusions, which indicates that gold is located only inside the fluid inclusions. The gold signal is not the continuous smooth asymmetric curve observed from elements in solution, but is a series of spikes. Such a signal indicates the gold is present as a number of particles and is not in solution.

Type 4 CO<sub>2</sub> inclusions are an exception as only very small signals for Na or K are present. During ablation of the enclosing quartz, gold was found in concentrations ranging from 4 to 52200 ppm. However, no gold particles were detected in this quartz, either by optical microscope or by SEM.

Oblique illumination of the fluid inclusions by a laser beam shows intense scattering of the light in the L-V-S inclusions. In normal (unassociated with this project) aqueous only inclusions the laser beam is only weakly scattered at interfaces. This clearly indicates dispersed gold nanoparticles particles in the inclusions.

Definitive proof of the presence of gold nanoparticles in the fluid inclusions was obtained from recording the confocal UV-Vis absorption spectra in different areas of fluid inclusions. For the type 3 and 4 inclusions, spectra recorded near the bubble/solution interface exhibit a pronounced absorbance band in the region of about 500 nm. This band is characteristic for the plasmonic absorbance by spherical gold nanoparticles of 18-20 nm in diameter (Link and El-Sayed, 2000). The presence in some cases of an additional red-shifted band at 610-630 nm can be reasonably attributed to aggregates of the nanoparticles.

The  $\delta^{13}\text{C}_{\text{PDB}}$  of these inclusions ranged from -5.3 to -5.4 ‰, which corresponds to a juvenile source of CO<sub>2</sub> (Hoefs, 2009). Therefore, we surmise the presence of a juvenile, predominantly CO<sub>2</sub> fluids rising from deep in the earth.

The discovery of gold nanoparticles in such fluids at high concentrations, requires a new look at the scale of the migration of gold and the ratio of the mass of the fluid relative to the metal carried by it.

### Acknowledgement

This work was financially supported by Russian Foundation for Basic Research (Grant no. 18-05-70001).

### References

- Hoefs J. (2009) *Stable Isotope Geochemistry*, Springer.  
Kola superdeep (1998) *Scientific results and research experience*. Moscow 260 (in Russian).  
Link S. and El-Sayed M.A. (2000) *Int. Rev. Phys. Chem.* 19:409-453.

# Generation of CO<sub>2</sub> - SO<sub>2</sub> fluxes in the lithospheric mantle beneath El Hierro (Canary Islands) on metasomatic reactions of carbonate-rich silicate melts

Remigi, S.<sup>1\*</sup>, Frezzotti, M.L.<sup>1\*\*</sup> & Ferrando, S.<sup>2</sup>

<sup>1</sup>Department of Earth and Environmental Sciences, Università di Milano - Bicocca, Italy; <sup>2</sup>Department of Earth Sciences, Università di Torino, Italy; \*s.remigi@campus.unimib.it; \*\*maria.frezzotti@unimib.it

At the Canary Islands, chemical heterogeneities in the lithospheric mantle are result from infiltration of a volatile-rich metasomatic agent having a debated nature (Frezzotti et al., 1994; 2002a, 2002b; Neumann et al., 2002). Melt and fluid inclusions preserved in mantle xenoliths can reveal the nature of metasomatic agents and processes. We studied a peridotite xenolith suite from El Julan Cliff (El Hierro, Canary Islands) comprising 1 spinel Ol(olivine)-orthopyroxenite, 3 spinel lherzolites, and 5 spinel harzburgites. The Ol-orthopyroxenite consists of Ol porphyroclasts, up to 61 vol% of poikilitic Opx (orthopyroxene) grains, and minor Sp (spinel). Harzburgites and lherzolites (protogranular textures) consist of Ol and Opx porphyroclasts, and subordinate Cpx (clinopyroxene) and Sp. All rocks show evidence of modal and cryptic metasomatism, although hydrous phases are absent.

In peridotites, abundant glass microveins are present in Ol, and between Ol and Opx. Ol in contact with glass microveins is embayed, whereas Opx shows overgrowths. Microveins consist of colourless silicate glass and carbonate droplets. The silicate glass is trachytic and silica oversaturated (SiO<sub>2</sub> = 62.55-68.57, K<sub>2</sub>O + Na<sub>2</sub>O = 8.13-10.01, in wt%; Na<sub>2</sub>O/K<sub>2</sub>O = 1.0 - 1.6). Carbonate in droplets is calcite. In Ol, glass microveins are associated with melt and fluid inclusions. Melt inclusions consist of Anh, Cc, and subordinate sulphide aggregates. Two distinct types of fluid inclusions (FI) are observed associated with microveins and melt inclusions: a) FI1's (≤3-15 μm in size) contain CO<sub>2</sub>+N<sub>2</sub> (N<sub>2</sub> ≤18 mol%) and are present as intragranular trails. They have densities ≤1.19 g/cm<sup>3</sup>, corresponding to 1.8±0.02 GPa at 950 °C (Oglialoro et al., 2017); b) large FI2 (20-50 μm in size), present in the same trails, which contain CO<sub>2</sub>±N<sub>2</sub> (N<sub>2</sub> ≤0.3 mol%) and more than 70 vol% daughter minerals, including Anh, Mg-Cc, Dol, hydrated Mg-sulph., Shl, Ap, Sp, Mag, and Tlc. In metasomatic Opx, FI3 (≤3-10 μm in size) present with a primary distribution and negative-crystal shapes, which contain CO<sub>2</sub>±N<sub>2</sub>±SO<sub>2</sub> (N<sub>2</sub> 0.01-0.03 mol%; SO<sub>2</sub> 0.6-1.30 mol%; d = 1.10-0.99 g/cm<sup>3</sup>). When SO<sub>2</sub> is present, S<sub>0</sub> is detected.

FI4 are late pure CO<sub>2</sub> fluids (3-40 μm in size; d = 1.11-0.65 g/cm<sup>3</sup>) along intragranular trails in all main mineral phases, originated by magma degassing on ascent (Oglialoro et al., 2017).

Data show infiltration of a volatile-rich carbonate - silicate melt, enriched in SO<sub>3</sub>, P, Cl, and N<sub>2</sub>, at the base of the oceanic lithosphere beneath the

Canary Islands. Similar metasomatic melts react with Ol to form Opx (e.g., Ol-orthopyroxenite). As reactions proceed, the silicate component in the melt decreases whereas the carbonate component increases to form Cpx±Ol from Opx. At this stage, evidence for immiscibility between volatile-saturated carbonate, sulphate and silicate melts could be preserved by coeval sulphate-, carbonate-rich inclusions, and FI. CO<sub>2</sub>-N<sub>2</sub>-H<sub>2</sub>O-salt fluids could be generated and unmix to form coexisting CO<sub>2</sub>±N<sub>2</sub>±SO<sub>2</sub>-rich fluids (FI1 and FI3) and high density (CO<sub>2</sub>-N<sub>2</sub>) saline melts (FI2).

The geochemical nature of the metasomatic melt (e.g., silica oversaturation, high K<sub>2</sub>O, and Na<sub>2</sub>O; high SO<sub>3</sub>, CO<sub>3</sub><sup>2-</sup>, Cl, and N<sub>2</sub>) points to a possible origin by partial melting of crustal mafic rocks (Rosenthal et al., 2014) at asthenospheric depths, as predicted to explain the HIMU signature of Canary Island magmatism (Day et al., 2011). High fluxes of CO<sub>2</sub> and SO<sub>2</sub> are generated on metasomatic reactions. These will ascend through the lithosphere feeding the magmas of El Hierro, which are known to degas significant amounts of CO<sub>2</sub> and SO<sub>2</sub> (about 1.3-2.1 Mt CO<sub>2</sub> and 1.8-2.9 Mt S, Longpré et al., 2017).

## Acknowledgment

Study funded by MIUR-Dipartimenti Eccellenza 2018-2022. Authors thank C. Tiraboschi for microprobe analyses.

## References

- Day J.M. et al. (2011) Earth Planet. Sc. Lett. 305:226-234.
- Frezzotti M.L. et al. (1994) Eur. J. Mineral. 6:805-818.
- Frezzotti M.L. et al. (2002a) Eur. J. Mineral. 14:891-904.
- Frezzotti M.L. et al. (2002b) Lithos 64:77-96.
- Longpré M.-A. et al. (2017) Earth Planet. Sc. Lett. 460:268-280.
- Neumann E.-R. et al. (2002) J. Petrol. 43:825-857.
- Oglialoro E. et al. (2017) B. Volcanol. 79:70.
- Rosenthal A. et al. (2014) Sci. Rep. 4:6099.

# The composition of magma-derived fluids in the oceanic crust

Richter, L.<sup>1\*</sup>, Diamond, L.W.<sup>1</sup> & Pettke, T.<sup>1</sup>

<sup>1</sup>Institute of Geological Sciences, University of Bern, Switzerland; \*lisa.richter@geo.unibe.ch

Fluid–rock interaction in the oceanic crust is mostly attributed to circulation of seawater, including the formation of seafloor volcanogenic massive sulphide (VMS) deposits. However, some studies have proposed that crystallising magmas may also contribute metal-bearing hydrothermal fluids to VMS systems (Yang and Scott, 1996). In order to explore this idea further, we have characterised the magmatic-hydrothermal fluids evolved by oceanic plagiogranites that have intruded the volcanic sequence of the Semail ophiolite, Oman.

The sampled plagiogranites contain miarolitic cavities, which indicate that they reached fluid saturation during their final crystallisation. Euhedral quartz crystals in the cavities show growth zonation. Early magmatic zones contain primary devitrified silicate-melt inclusions, whereas later magmatic–hydrothermal quartz overgrowths contain abundant liquid–vapour–halite (LVH) and coexisting vapour (V) inclusions. Similar inclusions have been found in plagiogranites in the Troodos ophiolite in Cyprus (Kelley et al., 1992).

Upon heating, individual assemblages of LVH inclusions show halite melting over small  $T$  ranges ( $\leq 10$  degrees), followed by homogenisation via vapour disappearance over similarly narrow  $T$  ranges. Taking all the analysed assemblages together, halite melting ( $T_m(\text{HLV} \rightarrow \text{LV})$ ) occurs over the range 210–285 °C, implying salinities from 32–38 wt%  $\text{NaCl}_{\text{eq}}$ , and homogenisation ( $T_h(\text{LV} \rightarrow \text{L})$ ) occurs at 380–410 °C. Vapour-rich inclusions homogenise into the V phase and final ice-melting temperatures ( $T_m(\text{Ice})$ ) vary from -2.2 to -1.4 °C, implying 2.4–3.7 wt%  $\text{NaCl}_{\text{eq}}$ .

Laser-ablation-ICP-MS analyses of individual LVH inclusions yield compositions that resemble typical magma-derived fluids (e.g. elevated Na, K, Fe, Zn; low Mg, Ca), such as in Cu-porphyry deposits (Fig. 1). These hypersaline brines contrast with the compositions of modified seawater in the oceanic crust – such as the fluids that induce spilite or epidosite alteration (Richter and Diamond, 2019). In particular, the cation ratios show that the hyper-saline brines cannot be the product of boiling of modified seawater. They thus represent magmatic–hydrothermal fluids, in accord with their petrographic setting.

In conclusion, we have demonstrated that fluids exsolved from plagiogranites are present as hypersaline brines + vapours in the upper oceanic crust of the Semail ophiolite, and that they differ strongly in composition from other hydrothermal fluids in the oceanic system. Metal contents in the magma-derived hypersaline brines are very high, but whether they contributed to seafloor VMS

deposits remains unclear. Since plagiogranites constitute only a small portion (~8 vol%) of the Semail oceanic crust and since they release only a few vol%  $\text{H}_2\text{O}$  upon crystallisation, it seems unlikely that the hypersaline brines are a significant source of metals for VMS deposits.

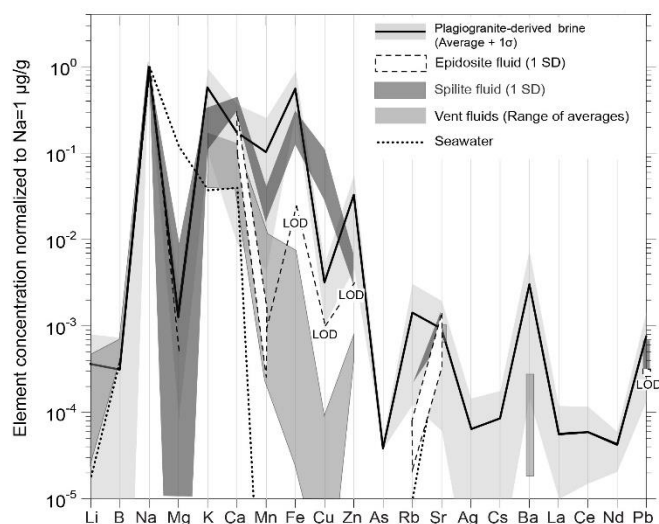


**Fig. 1.** Multi-element plot of magma-derived brines from plagiogranites in comparison to I-type (Landtwing et al., 2010) and S-type melt-derived fluids (Audétat et al., 2000). Note that element concentrations are normalised to 1 µg/g Na.

## References

- Audétat A. et al. (2000) *Econ. Geol.* 95:1563-1581.
- Kelley D.S. et al. (1992) *J. Geophys. Res.* 97:9307-9322.
- Landtwing M.R. et al. (2005) *Earth Planet. Sc. Lett.* 235:229-243.
- Richter L. and Diamond L.W. (2019) in: *ECROFI 2019* (this volume).
- Yang K. and Scott S.D. (1996) *Nature* 383:420-423.

## Trace element behaviour during evaporation of seawater

**Sendula, E.<sup>1\*</sup>, Gill, B.C.<sup>1</sup>, Weldeghebriel, M.F.<sup>2</sup>, Lowenstein, T.K.<sup>2</sup> & Bodnar, R.J.<sup>1</sup>**

<sup>1</sup>Department of Geosciences, Virginia Polytechnic Institute and State University, USA; <sup>2</sup>Department of Geological Sciences and Environmental Studies, Binghamton University, USA; \*seszter1@vt.edu

It has been known since the late 1970's that the major element concentration of paleo-seawater ( $Mg^{2+}$ ,  $Ca^{2+}$ ,  $K^+$ ,  $Na^+$ ,  $SO_4^{2-}$ ,  $Cl^-$ ,  $HCO_3^-$ ) has varied during Earth's history and that changes coincide with periods of preferential precipitation of calcite or aragonite as a function of  $Mg^{2+}/Ca^{2+}$  ratios in seawater. Data obtained from fluid inclusions in halite have contributed enormously to our understanding of these chemical changes (Lowenstein et al., 2014), which is possible only because the behaviour of major elements during evaporation of seawater is well known (McCaffrey et al., 1987). Seawater preserved in fluid inclusions in halite is concentrated at least ten times, and some of the original  $Ca^{2+}$ ,  $HCO_3^-$ , and  $SO_4^{2-}$  has been lost as a result of calcite and gypsum precipitation prior the halite, therefore, the actual, non-evaporated seawater concentrations have to be calculated from these measurements.

While the major element evolution of paleo-seawater is relatively well understood, our knowledge of how the minor and trace element composition of ancient seawater has varied during the evolution of Earth is still deficient. Attempts have been made recently by our group to use fluid inclusions in halite to reconstruct trace element concentrations as a proxy for redox conditions of paleo-seawater. However, interpretation of trace element data can be difficult due to the lack of experimental data and appropriate geochemical models describing the behaviour of trace elements during evaporation of seawater. The goal of this study is to fill this gap and provide experimental data on this subject, and investigate the preservation of trace elements in evaporite-hosted fluid inclusions by evaporating seawater in a controlled laboratory setting.

The seawater sample used in our preliminary laboratory evaporation experiment was collected from the coast of North Carolina in the summer of 2018. Twenty liters of seawater was placed under heating lamps in an HDPE tray and natural evaporation conditions were simulated by switching the lamps on and off each day. When halite started to precipitate, the water (~2L) was transferred into a small glass baking tray. Water samples collected at different stages of evaporation (up to 28 times more concentrated than seawater) and have been analysed with ICP-MS. Halite was sampled at the time of each water sampling, and fluid inclusions (Fig. 1) were analysed with LA-ICP-MS at Virginia Tech.

Our preliminary results indicate that some of the measured elements behave conservatively during evaporation of seawater (e.g. Li, K, Rb, Se, Cs, Mo,

U) as observed by comparing trace element concentrations to Mg, which was assumed to behave conservatively. Non-conservative behaviour was observed for Sr, Ba, Zn and Fe and is likely connected to co-precipitation with calcite and gypsum. Vanadium seems to behave conservatively during early stages of evaporation, and deviates from this trend when halite starts to precipitate.

When comparing the composition of the evaporating seawater to the analysed fluid inclusion compositions, measurements of fluid inclusions in halite successfully reproduced concentrations reported for corresponding water samples for K, Ca, Sr, Li, Rb, Mo, Ba and U. Concentrations of V, Fe and Cu obtained from fluid inclusion measurements were significantly lower than concentrations in the water samples. The disagreement is most likely due to differences in interlaboratory analytical procedures.



**Fig. 1.** Fluid inclusions in halite precipitated during experiments of evaporation of seawater.

### References

- Lowenstein T.K. et al. (2014) Treatise on Geochem. 2<sup>nd</sup> Ed. 569-622.  
McCaffrey M.A. et al. (1987) J. Sediment. Petrol. 57:928-937.

# Melt composition and magma storage conditions of oceanic tholeiites from the Bouvet triple junction (South Atlantic) obtained from chilled glasses and melt inclusions in phenocrysts

**Shishkina, T.A.<sup>1\*</sup>, Migdisova, N.A.<sup>1</sup>, Sushchevskaya, N.M.<sup>1</sup> & Krasheninnikov, S.P.<sup>1</sup>**

<sup>1</sup>GEOKHI RAS, Russia; \*t.shishkina@geokhi.ru

The Bouvet triple junction (BTJ) in South Atlantic connects the Mid-Atlantic (MAR), American-Antarctic (AAR) and Southwest Indian (SWIR) ridges. BTJ tholeiites originate from heterogeneously enriched magma sources, which reflect the complex geological history of this region. BTJ magmatism has been influenced by hotspots (Bouvet, Shona), jumping of ridge axes and involvement of continental lithosphere in melting processes (Le Roex et al., 1983; Migdisova et al., 2017).

A representative collection of quenched glasses and melt inclusions (MIs) in olivine and plagioclase phenocrysts from different segments of BTJ was studied with an aim to determine concentrations of main, trace and volatile components in melts and estimate magma storage conditions. Most of the samples are quenched glassy crusts of pillow lavas erupted under water. They were dredged from the ocean floor during cruises S18 of the R/V Akademik Nikolai Strakhov and G96 of the R/V Gelendzhik-96 in different parts of BTJ (MAR and SWIR segments adjacent to BTJ and Spiess ridge). Several samples were collected directly on the Bouvet Island. These basaltic lavas were erupted in subaerial conditions and therefore have crystallised ground mass with phenocrysts. MIs in pillow lavas are presented by naturally quenched brown glass droplets with sizes up to 200 µm. MIs in phenocrysts from on-island basalts are fully crystallised and therefore were experimentally rehomogenised at  $T=1150$  °C. All melt inclusions contain shrinkage bubbles. Concentrations of major, trace and volatile elements in glasses and minerals were analysed by various analytical methods: EMPA, LA-ICP-MS, SIMS, Raman spectroscopy.

The studied quenched glasses represent a wide range of melt compositions from basalts to dacites (47-59 wt% SiO<sub>2</sub>; 8.5-1.5 wt% MgO) while olivine-trapped melt inclusions are only basalts (49-52 wt% SiO<sub>2</sub>, 3.5-7.5 wt% MgO). Compositions of host olivines vary from Fo<sub>79</sub> to Fo<sub>89</sub>. Sometimes this range of olivine compositions can be observed within a single sample. Concentrations of major elements in glasses show regular melt evolution trends: SiO<sub>2</sub>, Na<sub>2</sub>O and K<sub>2</sub>O constantly increase, Al<sub>2</sub>O<sub>3</sub> and CaO – decrease, while FeO and TiO<sub>2</sub> have the typical maximum at about 4.5 wt% MgO reflecting the appearance of magnetite.

Water contents in the quenched glasses vary between 0.2 and 1.2 wt% H<sub>2</sub>O. There is no correlation between H<sub>2</sub>O content and the depth of lava eruption (400 – 2750 m) while there is a

certain trend of H<sub>2</sub>O increase in the course of melt evolution. In general H<sub>2</sub>O concentrations in MIs are the same as in quenched glasses surrounding host-minerals.

The temperatures of mineral – melt equilibrium were found to be in range of about 1050–1150 °C based on Fe-Mg and Y/Sc olivine-melt equilibrium (Danyushevsky, 2001; Mallmann and O'Neill, 2013). The redox conditions for BTJ samples were estimated with different methods and surprisingly give quite controversial results. An oxybarometre based on the distribution of vanadium between olivine and melt (Shishkina et al., 2018) and olivine-spinel equilibrium (Ballhaus et al., 1991) give the range between QFM+1.3 and QFM+1.9, while Fe<sup>2+</sup>/Fe<sup>3+</sup> ratio in melt inclusions gives much more reduced conditions: QFM-0.9 to QFM+0.5 (Lebedeva et al., 2001; Borisov et al., 2018). The discrepancy in the redox estimations may reflect the post-magmatic changes in valent state or distribution of elements and requires further investigation.

The crystallisation trends of BTJ magmas are typical for ocean tholeiites and can be reproduced at temperature range 1100-1300 °C and pressures between 2 and 5 kbars.

## Acknowledgement

The work was financially supported by RFBR grant №: 19-05-00990.

## References

- Ballhaus C. et al. (1991) *Contrib. Mineral. Petr.* 107:27-40.
- Borisov A. et al. (2018) *Contrib. Mineral. Petr.* 173:98.
- Danyushevsky L.V. (2001) *J. Volcanol. Geoth. Res.* 110:265-280.
- Le Roex A.P. et al. (1983) *J. Petrol.* 24:267-318.
- Lebedeva S.M. et al. (2001) *U. Min. Coll.* 11:270-281.
- Mallmann G. and O'Neill H. (2013) *J. Petrol.* 54:933-949.
- Migdisova N.A. et al. (2017) *Rus. Geol. Geophys.* 58:1289-1304.
- Shishkina T.A. et al. (2018) *Am. Mineral.* 103:369-383.

# P–T parameters and trace element characteristics of the highly magnesian parental melt of the Uitkomst layered massif (Bushveld Complex)

Solovova, I.P.<sup>1\*</sup>, Yudovskaya, M.A.<sup>1,2</sup>, Zinovieva, N.G.<sup>3</sup> & Averin, A.A.<sup>4</sup>

<sup>1</sup>Institute of Geology of Ore Deposits, Petrography, Mineralogy, and Geochemistry, RAS, Russia; <sup>2</sup>School of Geosciences, University of Witwatersrand, South Africa; <sup>3</sup>Department of Geology, Moscow State University, Russia; <sup>4</sup>Frumkin Institute of Physical Chemistry and Electrochemistry, RAS, Russia; \*solovova@igem.ru

The Bushveld Complex is one of the largest layered mafic intrusions on Earth. However, the composition and genesis of parental Bushveld magmas are still under discussion. We studied inclusions in cumulus olivine (Fo<sub>91</sub>) from ultramafic rocks of the Uitkomst massif, which is genetically related to the Bushveld Complex.

Crystallised primary melt inclusions (Fig. 1) contain daughter olivine and orthopyroxene. Complete homogenisation of the inclusions was not achieved even upon heating up to 1430 °C.

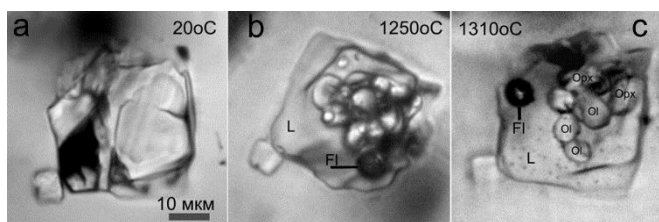


**Fig. 1.** Photomicrographs of primary inclusion in olivine: A) at 20 °C, B) at 1250 °C and C) at 1310 °C. L - melt, Fl – fluid, Ol and Opx – daughter olivine and orthopyroxene.

The compositions of melt inclusions recalculated to equilibrium with the host olivine (Fo<sub>91</sub>) have 53–57 wt% SiO<sub>2</sub>, <4.3 wt% CaO, and up to 2.9 wt% Na<sub>2</sub>O+K<sub>2</sub>O. The most primitive melts contain 20.5% MgO and 12% FeO.

Trace and volatile elements were analysed in the melt inclusions by SIMS. Glasses from heated melt inclusions contain 30–430 ppm H<sub>2</sub>O. Melts with the highest MgO contents are characterised by low heavy rare earth element (REE) contents, a steep REE distribution pattern (La<sub>PM</sub>/Yb<sub>PM</sub> up to 35.5), and the absence of a Eu anomaly. The low heavy REE contents indicate the retention of garnet in the residue. The relatively low contents of fluid-mobile large-ion lithophile elements (Ba 280 ppm, Sr 230 ppm, Th 4 ppm) are consistent with the low content of volatile components in the parental magma and the absence of primary fluid inclusions in minerals. The high-MgO magma is strongly enriched in Ni and V, which is of particular importance for determining the source of ore components. The correlation of Th/Zr with Nb/Zr indicates the occurrence of aqueous fluid metasomatism at the early stages of magma generation (Yu et al., 2019).

The conditions of magma formation in the mantle were estimated using the olivine-orthopyroxene-melt thermobarometre of Girnis (2003). The obtained conditions of high-MgO melt formation are 1520 °C and 1.8 GPa. The estimated composition and P-T parameters of melt generation indicate that the primary cumulus

assemblage of the massif crystallised from a komatiite-like melt (Wilson, 2012).

In addition to the high-MgO inclusions, there are primary melt inclusions with 14–16 wt% MgO. These inclusions exhibit a negative Eu anomaly and high contents of H<sub>2</sub>O (up to 2300 ppm) and fluid-mobile elements (Ba, Sr and Th). The strong correlation of (La/Nb)<sub>PM</sub> and (Th/Ta)<sub>PM</sub> indicates that the melt underwent mid-crustal contamination (Yu et al., 2019). This is supported by the presence of xenoliths of multiminerals inclusions up to 200 μm in size in olivine. Their mineral assemblage includes hydrous and Cl-bearing minerals. Sometimes these xenoliths are partly decrepitated and surrounded by haloes of tiny secondary CH<sub>4</sub>-bearing fluid inclusions. They are interpreted as altered xenoliths of crustal rocks.

The parental high-MgO melt is characterised by low CaO, TiO<sub>2</sub>, and H<sub>2</sub>O and high SiO<sub>2</sub> and REE contents with LREE>HREE. This supports the hypothesis of a depleted harzburgitic source pre-enriched with metasomatic fluids. More evolved magmas (MgO<16 wt%) were affected by crustal contamination, which resulted in their enrichment in Na, Ca, H<sub>2</sub>O and Cl.

## Acknowledgement

This study was supported by the Russian Foundation for Basic Research (18-05-00291) and Moscow State University (Program of Development).

## References

- Girnis A.V. (2003) *Petrology* 11:101-113.
- Yu L. et al. (2019) *Lithos* 326-327:158-173.
- Wilson A. (2012) *J. Petrol.* 53:1123-1168.

# Ferropyrosmalite-bearing fluid inclusions in the North Patagonian Andes metasedimentary basement, Argentina: a record of post-metamorphic metasomatism

Sosa, G.<sup>1\*</sup>, Van den Kerkhof, A.M.<sup>1</sup> & Oriolo, S.<sup>2</sup>

<sup>1</sup>Geoscience Centre, University of Göttingen, Germany; <sup>2</sup>IGEBA - University of Buenos Aires- CONICET, Argentina; \*gsosa@gwdg.de

The Paleozoic basement of the North Patagonian Andes, south of the Nahuel Huapi Lake, comprises paragneisses and schists with subordinate intercalations of amphibolites, meta-rhyolites, felsic orthogneisses and foliated intrusions. The timing of metamorphism is constrained at ca. 390-300 Ma by EPMA Th-U-Pb monazite ages. Besides the basement, large Mesozoic and Cenozoic granitoid intrusions and volcano-sedimentary rocks occur.

The paragneisses are characterised by a S<sub>2</sub> schistosity, comprising mica domains and microlithons of quartz. Folded quartz segregations commonly show rootless hinges of F<sub>2</sub>. White mica and retrograde chlorite show shape-preferred orientation parallel to S<sub>2</sub>, which is locally affected by crenulation and microkinking (F<sub>3</sub>). In addition, S<sub>2</sub> is cross-cut by randomly-oriented fine-grained aggregates of chlorite + white mica + opaque minerals ± epidote, ± apatite, which overprint all aforementioned microstructural features. In few cases, actinolite is present as well.

Under cathodoluminescence (CL) the quartz in the microlithons shows short-lived bright blue colours (changing to red), presumably induced by post-metamorphic heating. The quartz grains show diffusional zoning pointing at fluid migration along grain boundaries.

Fluid inclusions were studied in the mirrored fluid plates of the CL-sections. Multiphase highly saline fluid inclusions occur in clusters or are isolated. They typically contain L+V with 0.1-0.4 water volume fractions and several solid phases. Halite and sylvite are common daughter phases together with a number of Raman-active crystals. The latter could be identified as ferropyrosmalite Fe<sub>8</sub>Si<sub>6</sub>O<sub>15</sub>[(OH)<sub>6</sub>,Cl<sub>4</sub>] and hematite (Fig. 1a), or sometimes magnetite. The bubble may contain CO<sub>2</sub> with occasionally traces of nitrogen or H<sub>2</sub>S. Eutectic melting was observed between -58 and -54 °C indicating the presence of significant Ca<sup>2+</sup> (±Mg<sup>2+</sup>) concentrations in the brine. The inclusions have salinities of 27-43 wt% NaCl eq. During heating experiments, LV-homogenisation was observed between 430 and 520 °C. Halite dissolves between 290 and 580 °C and shortly after ferropyrosmalite also dissolves, accompanied by the simultaneous growth of a new mineral between 550 and 570 °C. The latter phase could be identified by Raman analysis as clinopyroxene (Fig. 1b), though sometimes also actinolite formed. As a result of heating several inclusions contain detectable amounts of hydrogen.

It is assumed that clinopyroxene and amphibole must have been present in the inclusions at high

temperatures and that ferropyrosmalite formed as a result of the reaction of these minerals with the brine. This retrograde reaction implies the uptake of FeCl<sub>2</sub> and H<sub>2</sub>O, and the enrichment of Ca<sup>2+</sup> in the brine (Kodera et al., 2003).

Secondary inclusions in short trails show varying water volume fractions between 0.1 and 0.8 have salinities of up to 5 wt% NaCl. Total homogenisation temperatures are between 250 and 390 °C. These inclusions probably represent the late magmatic fluid trapped along microfractures.

The ferropyrosmalite-bearing inclusions are

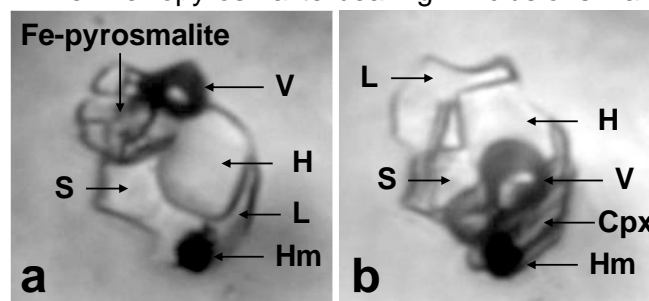


**Fig. 1.** A) Multiphase fluid inclusion at room temperature containing L+V, Fe-pyrosmalite, hematite (Hm), halite (H) and sylvite (S). B) After heating up to 552 °C a new greenish clinopyroxene (Cpx) crystal formed, whereas Fe-pyrosmalite was dissolved.

assumed to represent the fluids originated from the post-metamorphic Mesozoic magmatism, represented by widespread granitoids intruding the basement. This would be in agreement with monazite ages of 170-80 Ma found in the paragneisses. During these magmatic events, the metamorphic basement was largely overprinted by metasomatism.

## References

Kodera P. et al. (2003) Am. Mineral. 88:51-158.

# Subduction-related fluids in the high-pressure assemblage of the Cabo Ortegal Complex (NW-Spain) – a multisolid gaseous inclusion study

Spránitz, T.<sup>1\*</sup>, Berkesi, M.<sup>1</sup>, Józsa, S.<sup>2</sup> & Szabó, Cs.<sup>1</sup>

<sup>1</sup>Lithosphere Fluid Research Lab, Department of Petrology and Geochemistry, Eötvös Loránd University, Hungary;

<sup>2</sup> Department of Petrology and Geochemistry, Eötvös Loránd University, Hungary; \*spratom@caesar.elte.hu

The Cabo Ortegal Complex (COC, NW-Spain), the study area, is thought to have undergone through a complex tectonothermal history as a result of subduction and exhumation with peak metamorphic conditions at 1.6–1.8 GPa and 780–900 °C (Henry et al., 2017). Although the COC is a well-studied region, including comprehensive petrologic, geochemical and structural papers (e.g. Ibaraguchi et al., 1990), the knowledge about fluids, present during different stages of P-T evolution, is poorly constrained.

This study focuses on primary multisolid inclusions (as defined by Frezzotti and Ferrando, 2015) containing also gaseous phases, hosted in garnet porphyroblasts of eclogites and granulites. Our aim is to better understand deep fluid-mediated processes in a former subduction zone. HP eclogites and granulites are interpreted as two structural units in the COC, separated by thrust contacts (Ibaraguchi et al., 1990).

The studied eclogites of the COC are composed of garnet, omphacite, quartz, zoisite, and rutile characterised by coarse grain size along with moderate foliation. Granulites show various modal proportions of garnet, clinopyroxene and plagioclase. Although the studied rocks show textural evidences of overprinting at amphibolite and greenschist facies retrograde metamorphism (e.g. abundant amphiboles, zoisite symplectites), MSI have likely trapped fluids at prograde-to-peak stage. MSIs present in significant amounts in garnets together with oriented needle-shape rutile and euhedral quartz inclusions along growth zones (Fig. 1).

They appear in sizes of 3 to 40 µm with irregular or sub-rounded shapes (Fig. 1). At room temperature the inclusions consist of aggregates of micron-submicron sized solid and fluid phases. According to Raman imaging of unexposed and SEM-EDS of exposed inclusions, the following solids have been identified: carbonates (ankerite, siderite, dolomite, Mg-calcite) and white mica as dominant phases, whereas lesser amounts of disordered carbonaceous material, ± apatite, ± rutile, ± quartz. Fluid phases are ubiquitous and contain CO<sub>2</sub>, N<sub>2</sub>, ± CH<sub>4</sub>. These fluids appear between the aggregates of solids and around the wall of the inclusions. Comparing the characteristics of multiphase inclusions in eclogites and granulites, the main difference is that only eclogites contain disordered carbonaceous material together with CH<sub>4</sub> in great volume. Gaseous phase composition in the studied inclusions of eclogites is the following: CH<sub>4</sub> 25-60

mol%, CO<sub>2</sub> 20-60 mol%, N<sub>2</sub> 15-30 mol%, whereas in granulites carbon-dioxide is predominant (CO<sub>2</sub> 75-85 mol%, N<sub>2</sub> 15-25 mol%).

Consistency of major petrographic features and composition of primary multisolid gaseous inclusions in eclogites and granulites of the COC may indicate a large-scale fluid flux during subduction-related metamorphism with similar chemistry but at possibly different conditions of pressure-temperature-redox states. Furthermore, the studied multisolid inclusions with well-preserved fluid phases might serve as exceptional records of deep fluids trapped at subduction zone conditions.

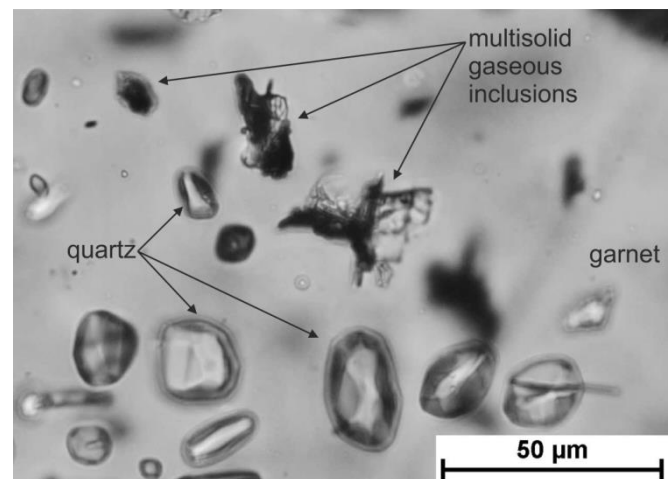


**Fig. 1.** Photomicrograph of the textural layout of the studied multisolid gaseous inclusion hosted by eclogitic garnet from the COC.

## References

- Frezzotti M.L. and Ferrando S. (2015) *Am. Mineral.* 100:352-377.  
Henry H. et al. (2017) *Earth Planet. Sc. Lett.* 472:174-185.  
Ibaraguchi J.I.G. et al. (1990) *Lithos* 25:133-162.

## Solubilities of minerals in hydrothermal saline fluids

Steele-MacInnis, M.<sup>1\*</sup> & Brooks, H.L.<sup>1</sup><sup>1</sup>University of Alberta, Canada; \*steelema@ualberta.ca

Transport of heat and materials, as well as chemical reactions in geologic systems, are driven and controlled by fluids. Current approaches to thermodynamic modeling of fluid-driven processes typically invoke only simple, dilute fluids, approximated by pure H<sub>2</sub>O (Dolejš and Manning, 2010). However, this approach has significant shortcomings, when compared to data on natural fluid inclusions. Natural geologic fluids are commonly rich in both non-electrolyte (e.g. CO<sub>2</sub>, CH<sub>4</sub>, N<sub>2</sub>), and electrolyte solutes (e.g. Na<sup>+</sup>, K<sup>+</sup>, Fe<sup>2+</sup>, Cl<sup>-</sup>). Fluid-inclusion studies reveal that highly saline fluids are common in many environments including subduction zones, metamorphic complexes, and magmatic-hydrothermal ore-forming systems – indicating that fluids are significantly more complex and contain high concentrations of various solutes. High salinities strongly affect activity-composition relationships in thermodynamic modeling, and mixing high salt contents with gas-rich fluids (i.e., containing CO<sub>2</sub> and other volatiles) expands the pressure-temperature limits of fluid phase immiscibility which partitions solutes and affects mineral stability relations. Thus, thermodynamic models accounting for multi-component, multi-phase fluids are needed for robust modeling of reactions and mass/energy transport in natural systems.

The only mineral whose solubility has been successfully and comprehensively modeled at high salinities, temperatures and pressures is quartz (Akinfiev and Diamond, 2009). The results of that modeling show that salinity exerts a major control on quartz solubility, which has major impacts on transport and precipitation in hydrothermal settings, such as in porphyry copper deposits (Monecke et al., 2018).

In this study, we combine successful elements from previous modeling of various minerals in H<sub>2</sub>O (Dolejš and Manning, 2010), with elements of quartz solubility modeling in multicomponent fluids (Akinfiev and Diamond, 2009), and new additions to account for speciation reactions involving sodium and/or chloride, to develop a new generic model for the solubilities of minerals in saline geologic fluids. We present a comprehensive model for solubilities of quartz, calcite, corundum, fluorapatite, fluorite, portlandite, and rutile, that simultaneously captures the full effects of pressure, temperature, and salinity across wide ranges of conditions (Fig. 1). Our approach represents fluid-rock reactions involving multiple components over wide ranges of bulk salinity, ranging from subduction zones and high-grade metamorphic environments to crustal hydrothermal

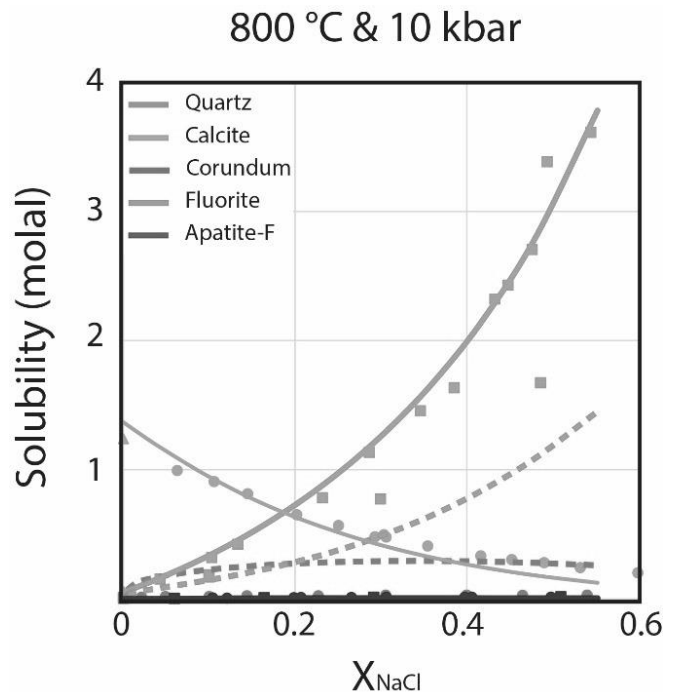


**Fig. 1.** Solubilities of minerals in saline aqueous fluids at 800 °C and 10 kbar, calculated using the model presented here.

systems. We present new calculations showing how these factors interact to give rise to mineral zonation in a variety of settings, including effects of phase separation and segregation. This new model thus allows investigation of hydrothermal mineralization that can be applied in future studies of hydrothermal processes.

## References

- Akinfiev N.N. and Diamond L.W. (2009) *Geochim. Cosmochim. Ac.* 73:1597-1608.  
 Dolejš D. and Manning C.E. (2010) *Geofluids* 10:20-40.  
 Monecke T. et al. (2018) *Econ. Geol.* 5:1007-1046.

# Raman-based N<sub>2</sub>, CH<sub>4</sub>, and CO<sub>2</sub> densimetres and barometres from the liquid-vapour curve to elevated temperatures and pressures

**Sublett, D.M.<sup>1\*</sup>, Sendula, E.<sup>1</sup>, Lamadrid, H.<sup>2</sup>, Steele-MacInnis, M.<sup>3</sup>,  
Spiekermann, G.<sup>4</sup> & Bodnar, R.J.<sup>1</sup>**

<sup>1</sup>Dept. of Geosciences, Virginia Tech, USA; <sup>2</sup>Dept. of Geological Sciences, University of Missouri, USA; <sup>3</sup>Dept. of Earth & Atmospheric Sci., University of Alberta, Canada; <sup>4</sup>Institute of Earth and Environmental Sciences, University of Potsdam, Germany; \*dsublett@vt.edu

N<sub>2</sub>, CO<sub>2</sub>, and CH<sub>4</sub> are major constituents commonly found in fluids related to metamorphic environments, sedimentary basins, some ore forming environments, and the surfaces and atmospheres of some celestial bodies such as Titan, the icy moon of Saturn. Experimental measurements of the changes in spectral properties with changing pressure-temperature (PT) conditions via Raman spectroscopy aids in the characterisation and analysis of these natural fluid systems. Here, Raman spectra were collected for N<sub>2</sub>, CO<sub>2</sub>, and CH<sub>4</sub> over the pressure ranges of 10-400 bars, 10-500 bars, and 10-500 bars, respectively, and temperature ranges of -160-200 °C, 22-350 °C, and -100-450 °C, respectively, and used to develop densimetres and barometres for each gas species over the respective temperature ranges. Changes in the peak position, and thus the vibrational frequency, of a given gas with changing pressure and temperature (PT) are influenced by the attractive (dispersion forces) and repulsive (collisional) interactions between molecules. PT changes that result in dominance of attractive intermolecular interactions show negative shifts in the peak position whereas PT changes that result in dominance of repulsive intermolecular interactions show positive shifts in peak position (Schindler and Jonas, 1980). Under isothermal conditions, spectra show an initial decrease in peak position with increasing pressure from low pressures as the molecules are forced closer together and experience increasing dispersion forces. Repulsive forces increase with increasing pressure along an isotherm as well, ultimately leading to positive shifts in the peak position above an inflection pressure unique to each gas. Isochoric changes in temperature from low temperatures (near the critical temperature) to higher temperatures lead to an initial increase in the peak position caused by an increase in the collisional frequency resulting from the additional thermal energy. However, the isobaric increase in temperature results in an increase in volume which weakens the influence of the repulsive interactions on the peak position as the molecules become sufficiently spaced apart such that interactions between molecules become much less frequent and often show behaviour similar to an ideal gas. At temperatures above an inflection temperature unique to each gas, increasing temperature results in shift in peak position to lower wavenumbers as the effect of long-range dispersion forces on the

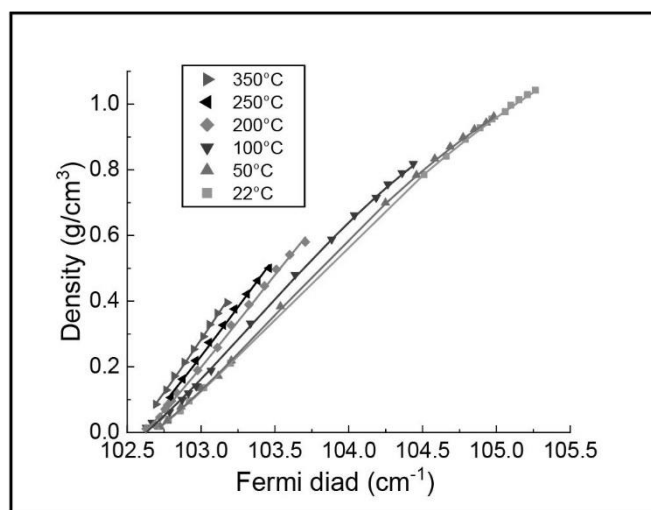


**Fig. 1.** Relationship between density and the Fermi diad of CO<sub>2</sub> from 22-350 °C. The symbols are the data collected in this study and the lines are the densimetre model developed in this study.

peak position exceeds the collisional effect. Isochoric changes in temperature from low temperatures near the critical temperature to higher temperatures lead to positive changes in the peak position of CH<sub>4</sub> and CO<sub>2</sub>, again likely resulting from increased intermolecular collisions. N<sub>2</sub> shows the opposite trend, for reasons that are unclear. We note here that, rather than peak position, the Fermi diad was used in the densimetre and barometre model for CO<sub>2</sub>. Fig. 1 shows the density-Fermi diad relationship of CO<sub>2</sub> over the temperature range studied.

## References

Schindler W. and Jonas J. (1980) J. Chem. Phys. 73:3547-3552.

# Amphibole-hosted fluid inclusion in mantle xenolith from the Eastern Transylvanian Basin

Szabó, Á.<sup>1\*</sup>, Berkesi, M.<sup>1</sup>, Aradi, L.E.<sup>1</sup> & Szabó, Cs.<sup>1</sup>

<sup>1</sup>Lithosphere Fluid Research Lab, Eötvös Loránd University, Hungary; \*abel.szabo@ttk.elte.hu

There are five major volcanic areas in the Carpathian–Pannonian Region (CPR) where basalt volcanoes, active during the Neogene–Quaternary period, brought large numbers of upper mantle xenoliths to the surface (e.g., Szabó et al., 2004). The easternmost and youngest alkaline basaltic volcanic field of CPR is developed in the Perşani Mountains (Eastern Transylvanian Basin, Romania) and provides, similarly to the Styrian Basin, amphibole-bearing xenoliths to this study.

The amphibole appears as <0.5 mm sized disseminated grains (<5 % in modal composition) in lherzolite or forms >1 cm wide hornblendite veins. The peridotite contains small amounts of interstitial amphibole, whereas the hornblendite contain occasionally other OH-bearing minerals such as apatite and phlogopite. The amphiboles in spinel lherzolites are depleted in incompatible trace (LRE and HFS) elements, whereas in hornblendites elevated incompatible trace element content is characteristic.

Several primary 5–30 µm sized fluid inclusions are observed in the amphiboles from the hornblendite vein. We selected a 20 µm sized intact fluid inclusion for this study. The amphibole is too weak to perform microthermometry measurements, therefore the fluid inclusion was studied at room temperature with Raman spectroscopy and FIB/SEM technique. Based on the Raman spectroscopy, the inclusion contains vapour CO<sub>2</sub> and multiple solid phases: amphibole (as a daughter phase; Raman band: 1001 cm<sup>-1</sup>), burbankite ((Na,Ca)<sub>3</sub>(Sr,Ba,Ce)<sub>3</sub>(CO<sub>3</sub>)<sub>5</sub>; 1076 cm<sup>-1</sup>), rutile (TiO<sub>2</sub>; 630 cm<sup>-1</sup>), sulphate (992 cm<sup>-1</sup>). The FIB/SEM exploration revealed that the fluid inclusion contains nahcolite, carbonate, quartz, Fe-bearing sulphate and different types of sulphides (Fe, Cu, Ni) (Fig. 1). The fluid is not related to brines, because the inclusion is not containing Cl, but the Na content is >5 wt%. Similar fluid composition was found (Aradi et al., 2019) in mantle xenoliths from the Styrian Basin (western part of the CPR).

These features indicate a complex volatile-rich melt-mantle interaction beneath the study area, which can be related to the subduction of the European plate beneath the Eastern Carpathians occurring in Neogene and supposedly causing extensive mantle metasomatism.

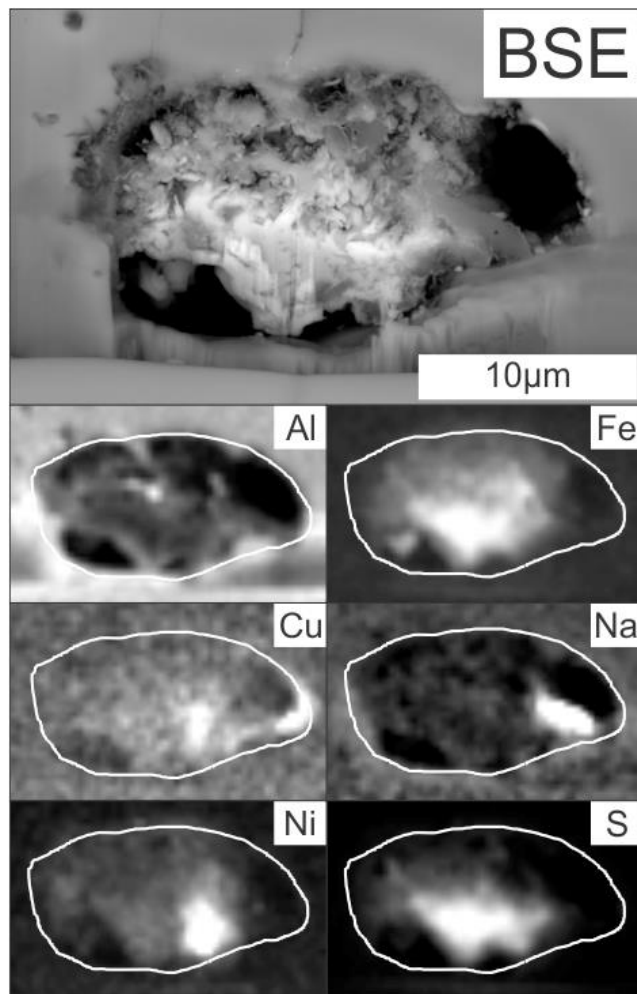


Fig. 1. BSE image and element maps of the studied fluid inclusion.

## Acknowledgement

This work was supported in the ELTE Institutional Excellence Program (1783-3/2018/FEKUTSRAT) supported by the Hungarian Ministry of Human Capacities. The study was also supported by Bolyai Postdoctoral Fellowship Program grant awarded to M. Berkesi.

## References

- Aradi et al. (2019) *Földt. Közl.* 149/1, 35–49.  
Szabó et al. (2004) *Tectonophys.* 393:119–137.

## TC-EA analysis of hydrogen isotopes in fluid inclusion water at the thick-section scale

**Tarantola, A.<sup>1\*</sup>, Rigaudier, T.<sup>2</sup> & Randi, A.<sup>1</sup>**

<sup>1</sup>Université de Lorraine, CNRS, GeoRessources, France; <sup>2</sup>CRPG-CNRS, Université de Lorraine, France;  
\*alexandre.tarantola@univ-lorraine.fr

The stable-isotopic signature (C, H and O) of fluid inclusions (FIs) complements *VX* data and constrains the origin of the main components (H<sub>2</sub>O, CO<sub>2</sub> and CH<sub>4</sub> essentially) and their possible exchanges or equilibration during fluid circulation. Because hydrogen and, to a lesser extent, oxygen strongly fractionate, fluid reservoirs have very specific isotopic signatures and the precision required for the analysis of fluid inclusion water is relatively low. The signature of the original fluid is possibly affected by fluid-rock interaction and partial or total equilibration during fluid circulation or even after fluid entrapment via equilibration with the host mineral. Thus, the oxygen isotopic composition of water is buffered in most oxygen-bearing host minerals (silicates, carbonates, etc.). As a consequence, the paleo- $\delta^{18}\text{O}$  value of water must be calculated from the  $\delta^{18}\text{O}$  value of the host-mineral using empirical fractionation coefficients as a function of temperature. Only the hydrogen isotopic composition of water (D/H or  $\delta\text{D}$ ) trapped in FIs is a direct measurement of the past circulating water.

The conventional technique of analysing water D/H of FIs has been used since decades because of its high reliability. It consists of (1) the extraction of the fluid contained within the inclusions by mechanical crushing (crush-leach) or thermal decrepitation, (2) the separation of the different chemical species by appropriate thermal traps, and (3) the analysis of pure gases by mass spectrometry (Dual-Inlet method; Dallai et al., 2004). This methodology becomes inappropriate, however, when several inclusion populations occur within a sample or if the amount of sample is too low. In favorable case studies, depending on fluid inclusion size and density, the amount of material should not be less than 1 gram in order to provide the minimum 10–20  $\mu\text{moles}$  required for accurate and reproducible isotopic values of hydrogen. This mass restriction is very high and so studies are generally restricted to samples containing only one fluid inclusion type.

$\delta\text{D}$  of hydrated minerals (<5 mg) are now commonly determined by using CF-IRMS techniques. Samples are combusted at high temperature on glassy carbon (1450 °C) leading to the reduction of hydroxyl groups to H<sub>2</sub>. After chromatographic separation, the recovered H<sub>2</sub> is analysed by IRMS (Sharp et al., 2001; Lupker et al., 2012). By coupling this technique to an evacuated sampler, a precision <0.5 ‰ can be obtained for  $\delta\text{D}$ , comparable to that of the classical Dual-Inlet.

The principle of continuous-flow analysis of water via high-temperature reduction on glassy carbon was adapted for the analysis of water isotopes from FIs in minerals (Dublyansky and Spötl, 2009). The modification entails connecting a custom-designed set of high-efficiency crushers and a cryo-focusing cell to the elemental analyser set-up. The water vapour transported by the carrier gas is trapped in a cryo-focusing cell at liquid N<sub>2</sub> temperature then released after flash-heating to 300 °C to the TC/EA high-temperature reactor as a single pulse. Only 0.1–0.2  $\mu\text{l}$  of water is required to achieve a precision <1.5 ‰ for  $\delta\text{D}$ .

In the present study, FIs trapped in quartz were directly decrepitated in the TC/EA carbon reactor at high temperature. The liberated water was automatically reduced to H<sub>2</sub>. This procedure allows a substantial reduction of the sample size (10–50 mg of quartz corresponding to 0.9–4.7  $\mu\text{mol}$  of water) compared to the 10–20  $\mu\text{moles}$  required for Dual-Inlet measurement.

We show the results of two experiments. The first one compares the  $\delta\text{D}$  values obtained on natural FIs trapped in quartz by conventional and direct TC/EA analyses with mass of samples from 1–4 g and 10–50 mg, respectively. For the two samples, the results are reproducible within the natural  $\delta\text{D}$  variation. In the second experiment, we have synthesised FIs with three different water solutions of known isotopic compositions. FIs were synthesised in a natural quartz crystal after decrepitation of natural FIs. TC/EA analyses of 10 to 50 mg of quartz samples containing synthetic FIs reproduce the values of the solutions used for the synthesis even though some of the initial inclusions were conserved. This methodology now yields analyses of good accuracy on 5x5 mm chips of selected areas from thick sections.

### References

- Dallai L. et al. (2004) in: Handbook of stable isotope analytical techniques 62-77.
- Dublyansky Y. and Spötl C. (2009) Rapid Commun. Mass Sp. 23:2605-2613.
- Lupker M. et al. (2012) Geochim. Cosmochim. Ac. 84:410-432.
- Sharp Z.D. et al. (2001) Chem. Geol. 178:197-210.

# Mantle melting conditions under the Eastern Volcanic Front of Kamchatka estimated from melt inclusions in olivine

**Tobelko, D.P.<sup>1\*</sup>, Portnyagin, M.V.<sup>1,2</sup> & Krasheninnikov, S.P.<sup>1</sup>**

<sup>1</sup>Vernadsky Institute of Geochemistry and Analytical Chemistry RAS, Russia; <sup>2</sup>GEOMAR Helmholtz Centre for Ocean Research Kiel, Germany; \*dariatobelko@gmail.com

Melt inclusions in high-Mg olivine provide unique constraints on the composition and origin of initially volatile-rich parental subduction-related magmas. Here we present new data on the composition of olivine phenocrysts, melt inclusions and inclusions of chromium spinel in olivine from high Mg# basalts of the Eastern Volcanic Front in Kamchatka.

We studied samples from Avachinsky, Gorely, Karymsky and Zavaritsky volcanoes containing olivine phenocrysts Fo80-91. The rocks studied were mostly lavas and volcanic bombs, which cooled slowly after eruption, and inclusions in olivine were significantly dehydrated. To estimate the initial H<sub>2</sub>O content in the melt inclusions, we used indirect method based on the significant influence of H<sub>2</sub>O in melt on the olivine liquidus temperature (e.g., Almeev et al., 2007). The method allows estimating H<sub>2</sub>O content by comparing independently determined “wet” and “dry” olivine crystallisation temperatures (Sobolev et al., 2016, Nazarova et al., 2017).

The “wet” crystallisation temperatures of 1090-1180 °C were estimated using Al-in-olivine thermometer (Coogan et al., 2014). The “dry” temperatures of 1100-1290 °C were estimated from the composition of melt inclusions using model of anhydrous olivine-melt equilibria (Ford et al., 1983). The calculated initial H<sub>2</sub>O content for primitive melts of the Eastern volcanic front was determined in the range from 1.7 (± 0.8) wt% for Gorely volcano to 4.4 (± 1.2) wt% for Karymsky volcano (Sobolev et al., 2016, Nazarova et al., 2017). The redox conditions of crystallisation were estimated from coexisting compositions of olivine and Cr-spinel (Ballhaus et al., 1990) at  $\Delta QFM=+1.3+2.1$ .

The melting conditions of the mantle source were estimated using geochemical thermometry (Portnyagin et al., 2007). According to the model, primary melts of the studied volcanoes can originate by 5-17 % partial melting (Fig. 1) of enriched MORB source (E-DMM). Using the estimated degrees of melting and H<sub>2</sub>O content in melts (corrected to equilibrium with olivine  $F_{O90}$ ), the mantle melting under the Eastern Volcanic front is estimated to occur near and up to 50 °C below the solidus of dry peridotite (Fig. 1). These estimates correspond to 1210-1270 °C at 1.5 GPa pressure.

Our new and recently published data (Mironov et al., 2015; Kamenetsky et al., 2017) suggests that the mantle melting temperatures under Kamchatka are likely lower and the H<sub>2</sub>O content in primary melts – higher than they have been estimated

earlier from partially dehydrated inclusions (Portnyagin et al., 2007). The mantle melting under Kamchatka seems to occur at low temperature conditions below the dry peridotite solidus.

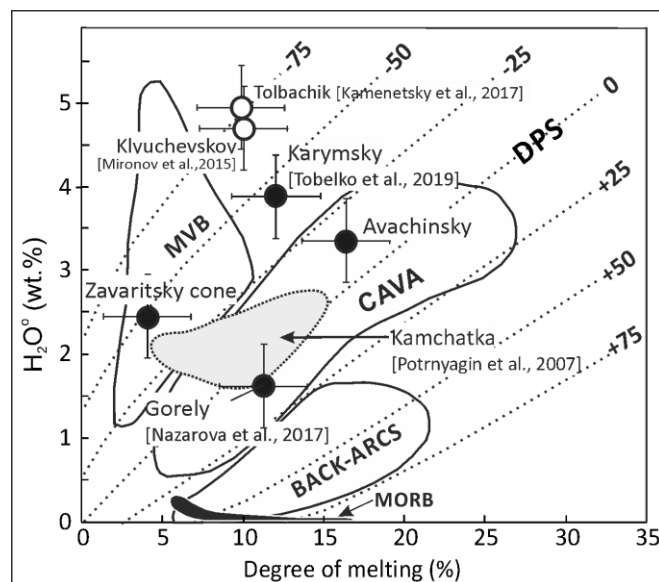


**Fig. 1.** Relationships between degrees of partial mantle melting and H<sub>2</sub>O contents in parental melts.

## Acknowledgement

This work has been supported by RFBR project №18-35-00529, №19-05-00934.

## References

- Almeev R.R et al. (2007) *Am. Mineral.* 92:670-674.
- Ballhaus C. et al. (1990) *Nature* 348:437-440.
- Coogan L.A. et al. (2014) *Chem. Geol.* 368:1-10.
- Ford C.E. et al. (1983) *J. Petrol.* 24:256-265.
- Kamenetsky V.S. et al. (2017) *Chem. Geol.* 471:92-110.
- Mironov N.L. et al. (2015) *Earth Planet. Sc. Lett.* 415:1-11.
- Nazarova D.P. et al. (2017) *Dokl. Earth Sci.* 472:311-314.
- Portnyagin M.V. et al. (2007) *Earth Planet. Sc. Lett.* 255: 53-69.
- Sobolev A. et al. (2016) *Nature* 531:628-632.

# Two types of melt inclusion in a 4200 years BP tephra from Ichinsky volcanic centre (Kamchatka)

Tolstykh, M.L.<sup>1</sup>, Naumov, V.B.<sup>1</sup>, Volynets, A.O.<sup>2</sup> & Pevzner, M.M.<sup>3</sup>

<sup>1</sup>Vernadsky Institute of geochemistry and analytical chemistry RAS, Russia; <sup>2</sup>Institute of volcanology and seismology FEB RAS, Russia; <sup>3</sup>Geological Institute RAS, Russia; \*mashtol@mail.ru

Ichinsky is the largest volcano in the Sredinny Range of Kamchatka. It is a complex, polygenetic Somma-Vesuvian type volcano. Ichinsky centre's Holocene deposits are represented mainly by dacitic tephra ( $\text{SiO}_2=65$ ,  $\text{MgO}=1.2-2$ ,  $\text{K}_2\text{O}=2.8-3.2$ , all in wt%)

We studied quenched melt inclusions (MI) hosted in Plagioclase (Pl), Clinopyroxene (Cpx), Orthopyroxene (Opx), Amphibole (Amph) and glass in tephra groundmass (GM) from Ichinsky volcano (ages of eruptions are determined by radiocarbon method and vary from 6500 to 4100 years before present, BP).

The tephra from one of the last eruptions contains two types of melt having different compositions (Fig. 1):

*Type1* MI in Opx, Cpx and Pl (An: 56-62),  $\text{SiO}_2=69-76$ ,  $\text{MgO}=0.3-0.6$ ,  $\text{K}_2\text{O}<2.5$  (all in wt%);

*Type2* MI in Amph and Pl (An:37-52),  $\text{SiO}_2=73-78$ ,  $\text{MgO}=0.1-0.2$ ,  $\text{K}_2\text{O}>3.5$  (all in wt%).

Low-potassium (low-K, Type1) melts showed enrichment of HREE and a decrease in LREE, Th and U relative to Type2 melts ( $\text{La/Yb} = 3-5$  to  $10-14$ , respectively). The low-K melts are characterised by low Nb concentrations (4–5 ppm as compared to 10–14 ppm in the other melts). These characteristics of low-K melts distinguish them from all other acid melts found in various eruptions of the Ichinsky volcano. However, low-K melts have similar characteristics to basaltic material from the monogenic centre Southern Cherpuk (Volynets et al., 2018). The latter formed at the southeast foot of Ichinsky volcano 6500 years BP.

We suggest that the low-K melts could be formed by an extended fractionation of basic Cherpuk melts. The formation of the GM of the 4200 years BP eruption may result from a magma mixing between a Type2 melts from the main magma chamber and differentiates of the 6500 years BP basic melts.

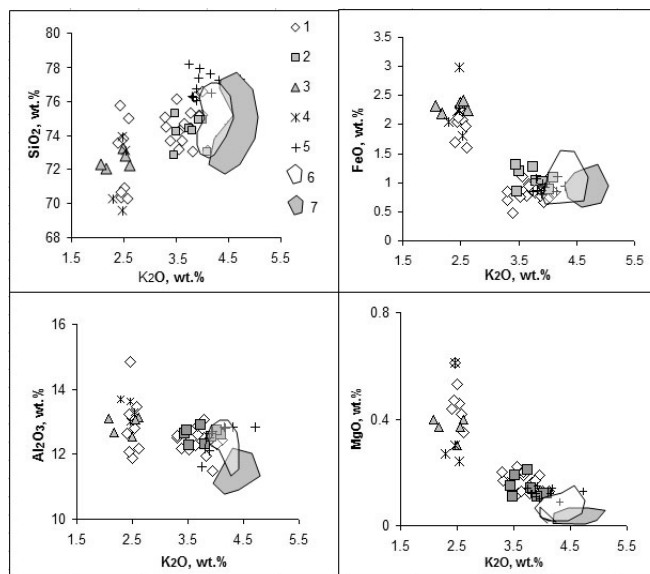


**Fig. 1.** Harker's diagrams for MI and GM of tephra 4200 years BP, 1,2,3,4 – MI in Pl, Amph, Cpx, Opx, respectively, 5 – Gm, 6 – MI in tephra of the eruption 6500 years BP, 7 – MI in tephra of the eruption 4100 years BP.

## Acknowledgement

This work is performed in accordance with research theme № 0137-2016-005 GEOKHI RAS, financial support by RFBR grants #17-05-00112, #18-05-00224a.

## References

Volynets A.O. et al. (2018) 7<sup>th</sup> International Maar Conference Abstract Volumes:112-114.

# Fluid inclusion and stable isotope geochemistry of rare-metal pegmatites, Sierra Grande de San Luis, Argentina

**Van den Kerkhof, A.M.<sup>1\*</sup>, Sosa, G.M.<sup>1</sup>, Lüders, V.<sup>2</sup>, Plessen, B.<sup>2</sup> & Montenegro, T.<sup>3</sup>**

<sup>1</sup>Georg-August University, Germany; <sup>2</sup>GeoForschungsZentrum, Germany; <sup>3</sup>Universidad Buenos Aires - CONICET, Argentina; \*akerkho@gwdg.de

In the Sierra Grande de San Luis, Nb-Ta-enriched pegmatites (398-411 Ma) outcrop in the eastern Conlara Metamorphic Complex, while 404-444 Ma Sn-enriched pegmatites (Sosa et al., 2002) outcrop in the more western Pringles Metamorphic Complex. The pegmatitic bodies are concordantly emplaced in fine-grained quartz-mica schist. The pegmatites represent the residual fluids of S-type syn-tectonic, meta- to peraluminous leucogranites of Famatinian age (Ortiz Suárez and Sosa, 1991; Galliski et al., 2019). The Nb-Ta-enriched pegmatites show a more complex mineralogy and contain beryl, spodumene and amblygonite, suggesting a higher internal fractionation, whereas the Sn-pegmatites are smaller and show a simpler mineralogy (principally Ab-Qtz, "albite-type").

Aqueous-carbonic inclusions (clusters) are typically trapped in cassiterite, plagioclase, beryl, apatite, tourmaline and quartz, whereas aqueous inclusions, trapped along healed fractures occur in columbite-tantalite, garnet, staurolite, quartz and in some cases also in plagioclase. Salinities in aqueous inclusions are usually very low, but aqueous-carbonic inclusions show mostly somewhat higher salinity (up to ca. 9 wt. NaCl-eq.), rarely 29-30 wt% NaCl-eq. total homogenisation temperatures for the aqueous-carbonic inclusions cluster in the 250-320 °C (quartz), 230-310 °C (cassiterite), and 310-350 °C (plagioclase) ranges; aqueous inclusions show much lower homogenisation temperatures in the range 110-160 °C.

The non-aqueous phase contains CO<sub>2</sub>, N<sub>2</sub>, CH<sub>4</sub> and sometimes traces of H<sub>2</sub>S, as measured by Raman analysis, with remarkable differences for each of the pegmatite minerals: beryl and tourmaline contain mainly H<sub>2</sub>O-CO<sub>2</sub>-N<sub>2</sub>, whereas cassiterite, plagioclase and quartz contain H<sub>2</sub>O-CO<sub>2</sub>-CH<sub>4</sub>-N<sub>2</sub> with variable amounts of CH<sub>4</sub> (up to pure CH<sub>4</sub>). Accordingly, fluid inclusions in minerals from Nb-Ta-pegmatites are normally free of CH<sub>4</sub> indicating more oxidizing conditions. Daughter crystals in fluid inclusions in beryl (Nb-Ta-pegmatite) are typically cristobalite as a metastable phase and sometimes also rhodochrosite or siderite with hematite or goethite.

The  $\delta^{13}\text{C}_{\text{VPDB}}$  values of CH<sub>4</sub> in cassiterite, plagioclase, quartz and tourmaline are always very negative (ca. -45 to -37 ‰), indicating organic origin. The CO<sub>2</sub> from the Sn-pegmatites (all minerals) shows lower  $\delta^{13}\text{C}_{\text{VPDB}}$  values (mainly -17 to -8 ‰) compared to the Nb-Ta-pegmatites (mainly -12 to 0 ‰), suggesting more extensive assimilation of organic material and therewith

lowering of the oxygen fugacity in the Sn-bearing fluids. This is in agreement with methane-bearing primary inclusions, which indicate reducing conditions with high mobility of Sn (Lehmann, 1990).

The  $\delta^{15}\text{N}$  values of N<sub>2</sub> range between 0 and +4 ‰ for fluids in cassiterite and quartz from the Sn-pegmatite and slightly higher (ca. +2 to +8 ‰) for quartz from the Nb-Ta-pegmatite, suggesting the mixing of magmatic and organogenic nitrogen.

We can distinguish between fluids with a more magmatic signature which correlate with Nb-Ta-pegmatite mineralisation, and fluids which changed composition due to interaction with the surrounding metasediments. Stable isotope signatures suggest that the pegmatitic fluids assimilated organic material from the metasedimentary country rocks particularly in the Pringles Metamorphic Complex. This agrees with the idea that the original magmatic fluids were regionally homogeneous, and that the pegmatite emplacement took place during or shortly after the peak of metamorphism in the Ordovician. The difference in ore mineral content can be explained by different oxygen fugacities. In the Sn-enriched pegmatite the oxygen fugacity was lowered due to the higher organic content in the original sediments. During crustal melting tin may have been leached from the Pringles Sn-enriched sediments and crystallised as cassiterite at increasing fO<sub>2</sub> and/or pH conditions at cooler deposition sites or as a result of interaction with meteoric water.

## References

- Galliski M.A. et al. (2019) *J. S. Am. Earth Sci.* 90:423-439.
- Lehmann B. (1990) *Lecture notes in Earth Sciences* 32.
- Ortiz Suárez A. and Sosa G.M. (1991) *Rev. As. Geol. Argentina*. Tomo XLVI (3-4):339-343.
- Sosa G.M. et al. (2002) *Eur. J. Mineral.* 14:627-636.

# Melt inclusions hosted in co-precipitated olivine, Cr-spinel and Al-spinel from Pohang basalt, Korea

Vetlényi, E.<sup>1\*</sup>, Zajacz, Z.<sup>2</sup>, Szabó, Cs.<sup>1</sup> & Guzmics, T.<sup>1</sup>

<sup>1</sup>Lithosphere Fluid Research Lab, Eötvös Loránd University, Hungary; <sup>2</sup>Department of Earth Sciences, University of Toronto, Canada; \*eniko.vetlanyi@gmail.com

We studied primary silicate melt inclusions (SMI) entrapped by coevally precipitating olivine and spinel phenocrysts from 2 million years old Pohang Basalt, South Korea. The basalt has porphyric texture and contains phenocrysts of forsteritic olivine (ol, mg#=0.84-0.88), Cr-bearing spinel (Cr-sp, cr#=0.15-0.24), Al-spinel (Al-sp, cr#<0.01), clinopyroxene (cpx) and anorthite-rich plagioclase (plg). The groundmass is consisting of cpx, ulvöspinel, plg and glass. Ol and spinel phenocrysts contain negative crystal and round shaped SMI sizing from 30 to 150 µm. Ol- and Cr-sp-hosted SMI contain each other's daughter phases and, Al-sp, cpx, sulphide-blebs, Si-glass and a fluid bubble (Fig. 1). Al-sp-hosted SMI contains cpx, sulphide-blebs, Si-glass and a fluid bubble.

Our microthermometry on the ol-hosted SMI suggested a melt entrapment at minimum temperature of 1250 °C. Applying our heating-quenching experimental methods in furnace, we produced homogenous glass inside the ol- and Cr-sp-hosted SMIs by quenching of the melt phases from 1250-1280 °C to room-T less than 3 s. Electron microprobe analyses were carried out on the quenched glasses, ol, Cr-sp and the daughter minerals, latter ones from the unheated SMI. For the melt entrapment in ol and Cr-sp (~min. 1250 °C), we calculated oxygen fugacity values to be between -0.8 and +0.6 relative to FMQ buffer.

LA-ICP-MS data from ol-, Cr-sp- and Al-sp-hosted SMI suggested that the concentrations of LREE, Nb, Ta and LILE are increased with its magma evolution. We calculated pressure value at cpx crystallisation, obtained from the compositions of phenocrysts-cpx from the basalt and daughter-cpx in unheated SMI hosted in ol and Cr-sp (Nimis and Ulmer, 1998). Cpx in ol-hosted SMIs shows a similar range for formation pressure (7.9-17.5 kbar) than cpx in Cr-sp-hosted SMI (8.2-12.8 kbar). These data are interpreted as minimum melt entrapping pressures. Cpx phenocrysts however, reveal significantly lower pressure (8-9 kbar) values. The high-P-entrapped (>15 kbar) SMI in ol and Cr-sp are representing a primitive melt, which could be modified by the fractionation in minor amount and, consequently, considered to be suitable to conclude on petrogenesis of the studied basalt.

Based on results from the SMI and phase diagrams developed by Presnall (1978), we reconstructed a crystallisation sequence as follows. At >17 kbar, ol and Cr-sp co-precipitated. The melt could have developed along the Cr-sp-ol

cotectic. Later on with decreasing the temperature, cpx started to be additionally precipitated when the melt composition reached the high pressure (15-20 kbar) peritectic point of the system. As the fractionation went on, the formation of Cr-sp might be replaced by that of Al-sp. During ascending of the host minerals with the basalt, the SMI preserved the major part of their entrapment pressure. This is suggested by the lack of plg in the SMI but the presence of this mineral together with cpx and spinel in the basalt groundmass. The melt outside the SMI could have precipitated pl+cpx+spinel at low pressure (5-10 kbar) eutectic point of the system. According to our calculations using trace element content of the SMI, the primitive melt could have been formed by a 12-14 % partial melting of a garnet lherzolite source rock.

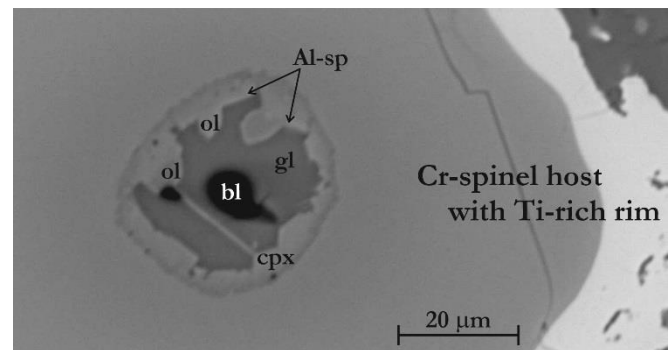


**Fig. 1.** BSE image of a Cr-spinel hosted SMI containing olivine (ol), Al-spinel (Al-sp), clinopyroxene (cpx), glass (gl) and bubble (bl) daughter phases, Pohang, S-Korea.

## Acknowledgement

This study was supported by the project NKFI K-119535.

## References

- Nimis P. and Ulmer P. (1998) *Contrib. Mineral. Petr.* 133:122-135.
- Presnall D.C. et al. (1978) *Contrib. Mineral. Petr.* 63: 203-220.

# Magmatic-related ore systems of volcanogenic massive sulphide deposits of the Urals, Russia: fluid inclusion and isotope data

**Vikentyev, I.V.<sup>1\*</sup>, Chugaev, A.V.<sup>1</sup>, Karpukhina, V.S.<sup>2</sup>, Simonov, V.A.<sup>3</sup>,  
Borisova, A.Y.<sup>4,5</sup> & Prokofiev, V.J.<sup>1</sup>**

<sup>1</sup>*Institute of Geology of Ore Deposits, RAS, Russia;* <sup>2</sup>*Institute of Geochemistry and Analytical Chemistry, RAS, Russia;* <sup>3</sup>*Institute of Geology and Mineralogy, Siberian Branch of RAS, Russia;* <sup>4</sup>*GET-OMP, Toulouse, France;* <sup>5</sup>*Geological Department, MSU, Russia;* \**viken@igem.ru*

Volcanogenic massive sulphide (VMS) deposits of the Urals are located inside the ensimatic paleo-arc Tagil-Magnitogorsk Megazone. Their formation was related to rhyolitic-basaltic Late Ordovician to Early Silurian volcanism of the Tagil zone and Middle Devonian one of Magnitogorsk zone. VMS deposits consist of thick lenses of semi-massive to massive sulphide underlain by minor discordant quartz-sulphide stockwork and quartz-phyllsilicate alteration.

Fluid inclusions (FIs) in minerals from ore bodies and altered host rocks, and melt inclusions (MIs) and FIs in quartz phenocrysts, as well as stable (S, O, C, H) and radiogenic (Sr, Pb) isotopes for rocks and ores were studied. Homogenised MIs were analysed for major elements and F, Cl by electron microprobe; REE and H<sub>2</sub>O were analysed using secondary ion mass spectrometry (SIMS). Trace and some major elements were analysed in MIs and FIs using near-infrared femtosecond laser ablation inductively-coupled plasma quadrupole mass spectrometry at GET, Toulouse.

Primary FIs in minerals in the ores (quartz, barite, sphalerite, carbonates) or secondary FIs in quartz phenocrysts do not exceed 10 µm in size. T<sub>h</sub> ranges from 375 to 97 °C (most commonly from 300 to 200 °C). The trapping pressure values range from 30 to 160 MPa, corresponding to buried, sub-seafloor conditions of ore genesis for major deposits. Sulphur and copper contents in fluids from vesicles range from 160 to 250 mg/l, and 0.3 to 1.2 g/kg of solution, respectively. The content of CO<sub>2</sub> can be up to 40 wt%. Bulk salinity ranges from 0.3 to 17 wt% NaCl eq. Minor phase separation occurred at deeper levels in some deposits. Na<sup>+</sup> and Mg<sup>2+</sup> (in some cases, also K<sup>+</sup> and Ca<sup>2+</sup>) dominate among cations in the fluid. For highly metamorphosed VMS deposits, the T<sub>h</sub> values of FIs are routinely higher (up to 440-465 °C), with trapping P=100-180 MPa, and bulk salinities between 1 and 18 wt% NaCl eq.

Primary magmatic FIs in quartz phenocrysts are 25 to 100 µm in size, with gas bubbles between 8 and 40 µm. Values of T<sub>h</sub> for FIs range from 124 to 245 °C with bulk salinities between 1.2 and 6.2 wt% NaCl eq. Micro-Raman investigations (LabRAM Raman microprobe: Dilor, G2R, Nancy) demonstrated only H<sub>2</sub>O in FIs. The magmatic fluids contained high concentrations (ppm) of B (40-2000), Cu (300-3700), Zn (80-3400), Pb (14-1000), Ba (20-2200), Sn (4-1600), Au (4-8) and Ag (4-11). MIs in quartz in felsic rocks (rhyolite-basalt bimodal

complex) correspond to tholeiitic series compositions. The concentrations of volatiles in the MIs are (in wt%) H<sub>2</sub>O up to 4.7, Cl up to 0.28, F up to 0.42, and an average S content of 0.025 wt%. Glassy MIs are significantly enriched in metals (ppm): Cu 1100, Zn 1400, Ag 40, Au 1.3. Chalcopyrite or bornite globule occurrences in MIs indicate elevated Cu content in the magmatic melts and provide evidence of an important role played by magmatic-derived metal components in ore formation.

The range in <sup>87</sup>Sr/<sup>88</sup>Sr<sub>0</sub> is 0.70597-0.70625 for carbonates, indicating less marine involvement and higher input of magmatic water characteristic for ores and host rocks. A deep-seated mantle source was the main source for Pb in galena. Stable isotope compositions of O and C of carbonates (δ<sup>18</sup>O<sub>VSMOW</sub>= +13 to +26.5 ‰, δ<sup>13</sup>C<sub>VPDB</sub>= -28 to +1 ‰ for massive ores; and δ<sup>18</sup>O<sub>VSMOW</sub>= +9 to +27 ‰, δ<sup>13</sup>C<sub>VPDB</sub>= -20 to -1 ‰ for altered igneous rocks) testify to the important addition of magma-derived components. Values of δ<sup>34</sup>S<sub>VCDT</sub> in ore sulphides range from -1 to +6 ‰ for majority of VMS deposits, confirming the dominant input of magmatic S to hydrothermal fluid, with a subordinate role of sea water SO<sub>4</sub><sup>2-</sup> and biogenic S. Data for the δD and δ<sup>18</sup>O of the fluid that deposited silicates of the Alexandrinskoe, Uzelga and Uchaly deposits lie between marine and magmatic values.

Our investigations of felsic volcanic rocks of the Uzelginsk ore field show a high likelihood of magmatic fluid and melt enrichment in metals (Cu, Zn, Au, etc.). Magmatic vapour was enriched in Cu, Se and Au relative to coexisting melt, suggesting a direct relationship between magmatic processes in the evolving arc sequences of the Urals and the origin of massive sulphide deposits.

## Acknowledgement

The authors thank V.B. Naumov and E.O. Dubinina for cooperation. This study was supported by Russian Foundation for Basic Research (project 18-05-70041).

## Contrasting fluids in the Svetlinsk gold-tellurium hydrothermal system, South Urals

**Vikent'eva, O.<sup>1\*</sup>, Prokofiev, V.<sup>1</sup>, Borovikov, A.<sup>2</sup>, Kryazhev S.<sup>3</sup>, Groznova E.<sup>1,4</sup>, Pritchinn, M.<sup>5</sup>, Vikentyev, I.<sup>1</sup> & Bortnikov, N.<sup>1</sup>**

<sup>1</sup>Institute of Geology of Ore Deposits, Petrography, Mineralogy and Geochemistry, RAS, Russia; <sup>2</sup>Sobolev Institute of Geology and Mineralogy, SB RAS, Russia; <sup>3</sup>Central Research Institute of Geological Prospecting for Base and Precious Metals, Russia; <sup>4</sup>Institute of Experimental Mineralogy, RAS, Russia; <sup>5</sup>Zavaritsky Institute of Geology and Geochemistry, UrB RAS, Russia, \*ovikenteva@rambler.ru

The large Svetlinsk gold-telluride deposit (54°17'35"N, 60°25'20"E) is located within deeply metamorphosed (up to amphibolite facies) volcano-sedimentary rocks (D-C) contacting with marble on the eastern flank. The gold ores can be divided into two types: (1) disseminated pyrite-pyrrhotite in the host rocks ( $C_{Au}$  up to 1 g/t); (2) sulphide-quartz veins and veinlets superimposed on the disseminated mineralisation (average  $C_{Au}$ =0.8-2.5 g/t). In marble the native gold is associated with quartz, topaz, fluorite and native sulphur. This deposit is a sample of "polygenic" and "polychronic" mineral system (Sazonov et al., 1989).

Fluid inclusions (FI) in quartz from different mineralisation stages were studied. New data were obtained using microthermometry, Raman spectroscopy, LA-ICP-MS and crush-leach analysis (including gas and ion chromatography, and ICP-MS). Four types of FI were revealed: (I)  $H_2O_L+CO_{2V}\pm CO_{2L}$ ; (II)  $CO_{2V}\pm CH_4, N_2$ ; (III)  $H_2O_L+H_2O_V$ ; (IV)  $CO_{2V}+CO_{2L}+S$ .

Additionally, a spherical native sulphur phase was detected in quartz from marble in aqueous-vapour,  $CO_2$ - $H_2S$ -bearing FI (Fig. 1). The gas phase of these FI contains  $CO_2$  (85.8 mol%),  $N_2$  (1.2 mol%) and  $H_2S$  (13 mol%). Multiphase FI contain halite and solid phases of complex composition (chalcoalumite group). Solid phases dissolve at temperature between 120-110 °C with the exception of the sulphur phase which dissolves between 205-210 °C. Homogenisation of FI occurs between 280-270 °C. Native sulphur in gaseous FI sublimates between 150-135 °C; these inclusions homogenise between 260-250 °C.

Mineralisation in marble was formed at 363-347 °C and 1.7-0.6 kbar from fluid with a bulk salinity of 21.3 wt% NaCl equiv. The assemblages of the quartz-pyrite-pyrrhotite stage were formed at 405-255 °C and 5-1 kbar from a fluid with a bulk salinity from 1.2 to 15.1 wt% NaCl equiv. Later assemblages (gold-telluride stage) were formed from fluids with a bulk salinity between 4.8-19.8 wt% NaCl equiv. at 320-130 °C.

Fluid composition was characterised using LA-ICP-MS with NaCl content as internal standard. FI of type I are enriched in (ppm) B (150), S (3970), K (370), Fe (18600), Zn (580), Au (190), whereas FI of type II contain B, Mg, K, Mn, Fe, Ni, Cu, Zn, As, Sr, Ba, W, Pb, Bi.

Temperatures estimated according to Na/K and Fe/Mn geothermometres (395-150 °C) are in agreement with microthermometry data.

Three fluids ( $H_2O$ -NaCl- $CO_2$ ,  $CO_2$ -[ $CH_4$ ,  $N_2$ ] and  $H_2O$ -NaCl) are observed in the Svetlinsk Au-Te hydrothermal system. Coexistence of  $CO_{2\pm}CH_{4\pm}N_2$  inclusions with  $H_2O$ - $CO_2$ -NaCl inclusions, displaying variable  $CO_2$  concentrations, can be explained by the entrapment of the heterogeneous aqueous and carbonic end-member fluids related to fluid immiscibility.

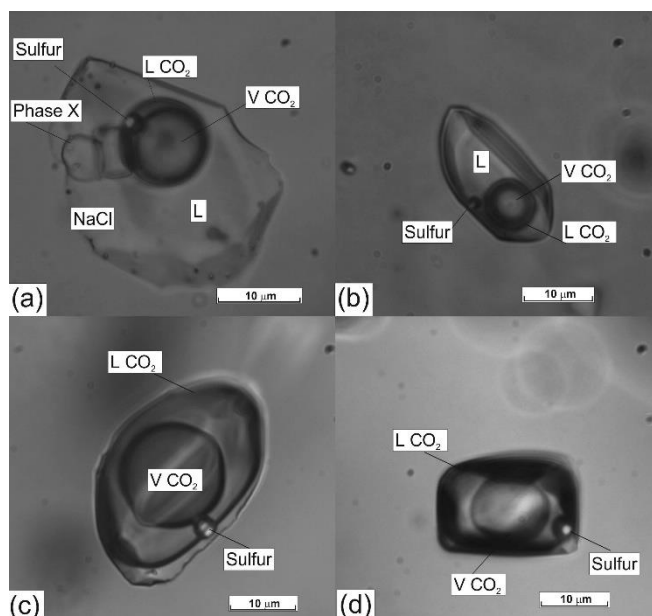


**Fig. 1.** Fluid inclusions (FI) with native sulphur in quartz from marble: A) multiphase FI, B) four-phase FI with  $CO_2$ , C-D) gaseous FI with dense  $CO_2$ . L – aqueous solution.

### Acknowledgement

Study was supported by Presidium of Russian Academy of Science.

### References

Sazonov V.N. et al. (1989) The mineralization of the salic blocks of the Uralian eugeosynclines.

# Fluid inclusions in quartz of ore vein of Valunistoye Au-Ag epithermal deposit (Northeast of Russia)

**Volkov, A.V.<sup>1\*</sup> & Prokofiev, V.Y.<sup>1</sup>**

<sup>1</sup>*Institute of Geology of Ore Deposits, Petrography, Mineralogy, and Geochemistry, RAS, Russia;*

*\*tma2105@yandex.ru*

The Valunistoye Au-Ag deposit is the third largest epithermal deposit of the Chukotka Peninsula. The deposit is situated in the north of the Okhotsk-Chukotka volcanogenic belt (OCVB) and is localised within a volcanic-domed elevation coinciding to the intersection of the northeast zone of the Kanchalan deep fault and the system of meridional disjunctive dislocations. Upper Cretaceous volcanic rocks are the host rocks for the Ag mineralisation. They consist of ignimbrites, lavas and tuffs which are rhyolitic to basaltic in composition, lenses and layers of sedimentary rocks, subvolcanic bodies and dikes of andesites, basalts and dacites. The deposit contains 12 vein zones, with a width of up to tens of metres. We have studied two of them, the vein zones Glavnaya and Novaya.

Veins with a width of up to 1 m prevail in these zones. The length of veins varies from 100 to 400 m. The Au and Ag content in the ores varies from 0-474 g/t, and 0-3794 g/t, respectively. The colloform-banded textures, often spatially related to brecciated textures, are widely developed. Ores are characterised by a Au/Ag ratio of 1:5-1:1, and a sulphide content of 0.5-5 vol%.

Microthermometric studies of fluid inclusions were done with a THMSG-600 heating-freezing stage (Linkam Scientific Instruments). Fluid inclusion salinity was assessed from final ice melting temperatures. Calculations of bulk salinity, and densities of the aqueous fluid were done with FLINCOR software (Brown, 1989).

The analysis of the fluid bulk composition was carried out using 0.5 g quartz samples (-0.5/+0.25 mm-size fractions) at the Central Research Institute for Geological Prospecting for Base and Precious Metals (analyst, Yu.V. Vasyuta) following the standard method (Kryazhev et al., 2006).

The primary two-phase fluid inclusions in quartz and calcite homogenised to liquid at temperatures between 174 and 284 °C. The bulk salinity varies from 0.2 to 0.7 wt % NaCl equiv., and the fluid density is in the range of 0.73-0.90 g/cm<sup>3</sup>.

A study of the fluid composition by bulk analysis of quartz monofractions of productive veins showed that among the anions there were bicarbonate ions (3.1 %), while the cations are K (2.3 %), Na (0.9 %), and Mg (0.04 %), consistent with eutectic temperature data. The fluid also contains carbon dioxide (5.4 %), methane (0.07 %), and a number of trace components (ppm): As (128), Li (18), B (42), Rb (1.1), Cs (0.2), Sr (4), Sb (22), Cu (3.2), Zn (27), Cd (0.02),

Pb (2.1), Bi (0.09), Ga (0.05), Ge (0.18), Mn (13), Fe (104), Co (1.35), V (0.09), Y (0.01), Sn (0.07), Ba (1.4), W (0.003), Tl (0.03), and REEs (0.05). The main indices of the fluid composition are CO<sub>2</sub>/CH<sub>4</sub> = 77, Na/K = 0.4, and K/Rb = 2055.

In general, ore-forming fluid parameters reported here for the Valunistoye deposit correspond to typical fluid parameters of epithermal deposits (Simmons et al., 2005).

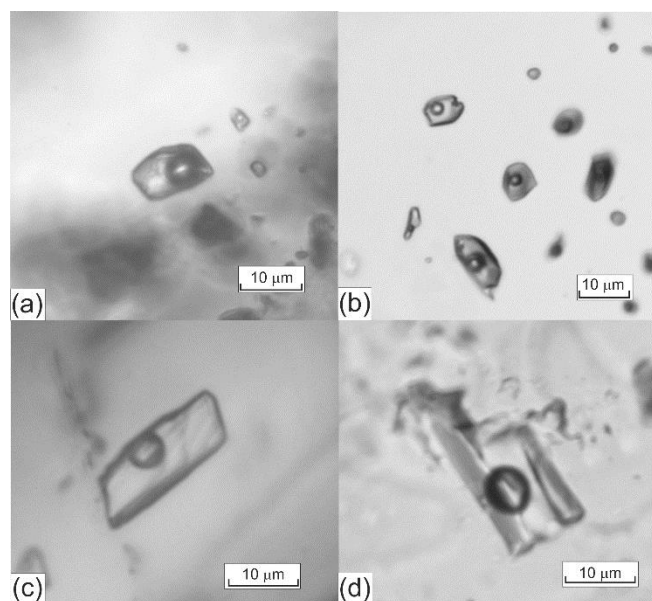


**Fig. 1.** Fluid inclusions in quartz A-B) and calcite C-D) of ore vein Valunistoye deposit. Scale bar 20 µm.

## Acknowledgement

This work was financially supported by Russian Foundation for Basic Research (Grant no. 18-05-70001).

## References

- Brown P. (1989) *Am. Mineral.* 74:1390-1393.
- Kryazhev S.G. et al. (2006) *Vestnik MGU. Ser. 4. Geologiya* 4:30-36.
- Simmons F.A. et al. (2005) *Econ. Geol.* 100:485-522.

# Characterisation of melt inclusions from the Mine Stock Pluton of the world-class Cantung W (Cu, Au, Bi) skarn deposit, Canadian Cordillera

Wagner, A.<sup>1</sup>, Adlakha, E.<sup>1\*</sup>, Hanley, J.J.<sup>1</sup>, Neyedley, K.<sup>1</sup>, Falck, H.<sup>2</sup> & Lecumberri-Sanchez, P.<sup>3</sup>

<sup>1</sup>Department of Geology, Saint Mary's University, Canada; <sup>2</sup>Northwest Territories Geological Survey, Canada; <sup>3</sup>Department of Earth and Atmospheric Sciences, University of Alberta, Canada; \*erin.adlakha@smu.ca

The Cantung W (Cu, Au, Bi) skarn deposit occurs in Cambrian carbonate units (Sekwi Formation) of the Selwyn Basin, Northwest Territories, Canada. The deposit is spatially associated with the peraluminous Mine Stock Pluton monzogranite of the Cretaceous Tungsten Plutonic Suite in the Canadian Cordillera. Although, mineralisation is spatially associated with the Mine Stock Pluton, recent work by Rasmussen et al. (2011) suggests mineralizing fluids were derived from a more fractionated melt sourced below the pluton, possibly associated with aplite dykes that crosscut the deposit. Reduced W skarn deposits such as Cantung are considered to form from W-rich, low salinity, fluids derived from evolved granitic magma below sites of mineralisation. Fractional crystallisation of granitic melts enrich residual magma in incompatible elements (i.e., W, Bi, Au and Cu), which are transferred to immiscible aqueous fluids when the melt reaches water-saturation. These fluids react with overlying carbonate, producing a zoned array of calc-silicate skarn endowed in scheelite (calcium-tungstate). Despite the connection between W skarn deposits and evolved granitic source melts, no studies have been completed on melt inclusions in skarn-related magmatic rocks.

Adlakha et al. (2018) reported both mafic and felsic melt inclusions hosted in apatite of the Mine Stock Pluton. Mafic inclusions (e.g., 56 wt% SiO<sub>2</sub>) occur at the cores of apatite (Fig. 1A). The apatite is zoned, recording a reaction rim of high Si+LREE. The contents of Si+LREE in apatite increase with Si content of the melt (Watson and Green, 1981). The presence of mafic inclusions and reaction rims suggest that the apatite is xenocrystic and likely crystallised in a mafic liquid before it was injected in a more felsic melt.

This project aims to constrain the composition and evolution of melts associated with the Cantung W skarn through melt inclusion microanalysis. Apatite-hosted melt inclusions occur predominately as crystallised (i.e., multi-phase inclusions), colourless and transparent inclusions, exhibiting a negative crystal shape, suggesting primary origin (Fig. 1B,C). Some inclusions contain coeval two- and three-phase fluid inclusions, indicating a water saturated melt. Major, trace, and metal concentrations of unhomogenised melt inclusions (n = 18) via LA-ICP-MS (Fig. 1D). Preliminary data indicate the inclusions are rhyolitic (ave. 71±3wt% SiO<sub>2</sub>) and highly fractionated (Ti/Zr = 1 to 3; Zr/Hf = 5 to 18),

similar to but slightly more evolved than the late stage aplite dykes (Ti/Zr = 3 to 13; Zr/Hf = 8 to 17; Rasmussen et al., 2011). The inclusions contain high contents of incompatible elements such as W (10 to 23 ppm), Sn (34 to 71 ppm), B (1000 to 3500 ppm), Cs (10 to 320 ppm), Nb (9 to 66 ppm) and Bi (6 to 19 ppm). The W content is at least an order of magnitude higher than continental crust (Palme and O'Neill, 2004). Both Au and Cu are below detection limits. Continued work includes further reduction of LA-ICP-MS data, homogenisation experiments, and quantification of major elements and volatiles via EPMA.

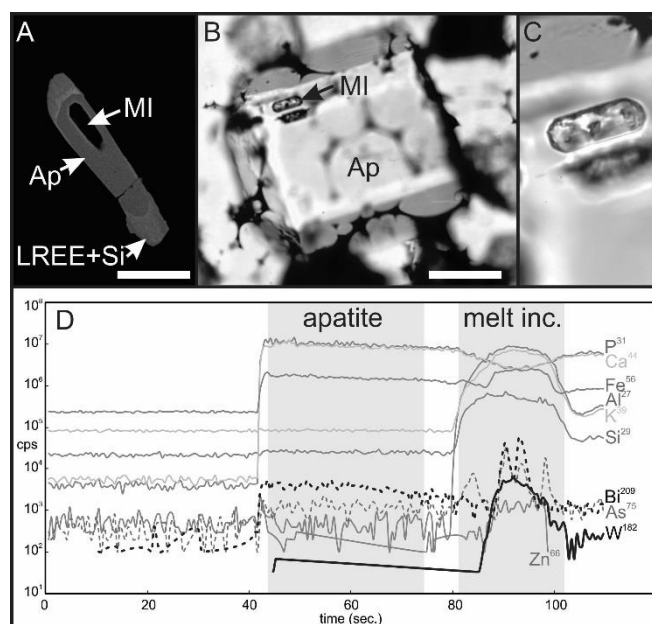


**Fig. 1.** A) Apatite (Ap) containing a mafic melt inclusion (MI) and exhibiting a Si-LREE reaction rim. B-C) Apatite separates containing a felsic melt inclusion that contains 22 ppm W. D) LA-ICP-MS spectra of the inclusion in C.

## Acknowledgement

NTGS for financial support.

## References

- Adlakha E. et al. (2018) *Eur. J. Mineral.* 30:1095-1113.  
Palme H. and O'Neill H. (2004) *Treat. Geoche.* 2:1-38.  
Rasmussen K. et al. (2011) *Ore Geol. Rev.* 41:75-111.  
Watson E.B. and Green T.H. (1981) *Earth Planet. Sc. Lett.* 56:405-421.

## Fluid evolution of iron-oxide copper gold mineralisation: Qibaoshan, China

Wang, M.<sup>1,2\*</sup>, Steele-MacInnis, M.<sup>2</sup>, Chen, Y.<sup>1</sup>, Liu, T.Y.<sup>1</sup> & Meng, F.C.<sup>1</sup>

<sup>1</sup>School of Geosciences, China University of Petroleum, China; <sup>2</sup>Department of Earth and Atmospheric Sciences, University of Alberta, Canada; \*miao5@ualberta.ca

The Qibaoshan deposit is an important polymetallic resource located in Wulian town, Shandong Province, China. The deposit is hosted by densely veined, brecciated porphyritic quartz diorite and granodiorite and has been previously described as a porphyry deposit (Yu et al., 2018). However, our field analysis of the current mining level (as of autumn 2018) revealed that the mineralised veins are composed almost invariably of coarse, specular hematite, quartz and carbonates with subordinate pyrite and chalcopyrite, suggesting that the deposit is more akin to the iron oxide-copper-gold family of deposits. In this study, we describe the paragenetic relationships and fluid evolution of this deposit.

According to field and petrographic criteria, we have identified four main paragenetic stages at Qibaoshan deposit. The veins commonly exhibit open space-filling textures with these four stages differentiated by stepwise, inward growth from the vein walls towards the vein centreline. The first stage is characterised by the formation of euhedral chlorite crystals and radiating aggregates, which commonly show well-developed growth oscillatory zoning. This open space-filling chlorite generally coats the outer vein wall, and grades outward into the chloritisation (alteration) of the adjacent host rocks (Fig. 1A). The second stage is primarily represented by specular hematite and quartz, which have also grown into open space, atop the earlier-formed euhedral chlorite. Hematite occurs as mm-sized tabular crystals (specularite) and radiating clusters (concentric overgrowths inward from vein walls) closely intergrown with quartz. Quartz too commonly occurs as prismatic, open-space filling columns, sometimes with well-developed pyramidal terminations pointing towards the vein centreline. The third stage is mainly composed of euhedral sulphide grains (pyrite and chalcopyrite) and quartz. The fourth and final stage is composed of euhedral, open space-filling carbonates (siderite and calcite) that show well developed growth zoning, and quartz. This final stage generally has the open space preserved (i.e., euhedral quartz and carbonate crystals are free standing).

Quartz precipitation occurred throughout the latter three paragenetic stages and the fluid inclusions in the euhedral quartz columns provide a record the fluid conditions and how these evolved during the three stages. In addition, the vein petrography shows that each paragenetic stage encompasses multiple fluid events, recorded by the sequence of fluid inclusion assemblages. Fluid inclusions in both the carbonate minerals, and both

hematite and pyrite analysed by infra-red light microscopy, provide additional constraints on these evolving conditions. The results show a transition from earlier fluids that were more enriched in CO<sub>2</sub> (Fig. 1B), towards highly saline brines (Fig. 1C) in the intermediate stages, and then towards less saline compositions in the latest stages. Thus, the Qibaoshan veins provide an excellent record of the complicated sequence of hydrothermal mineralisation in an iron oxide-copper-gold system.

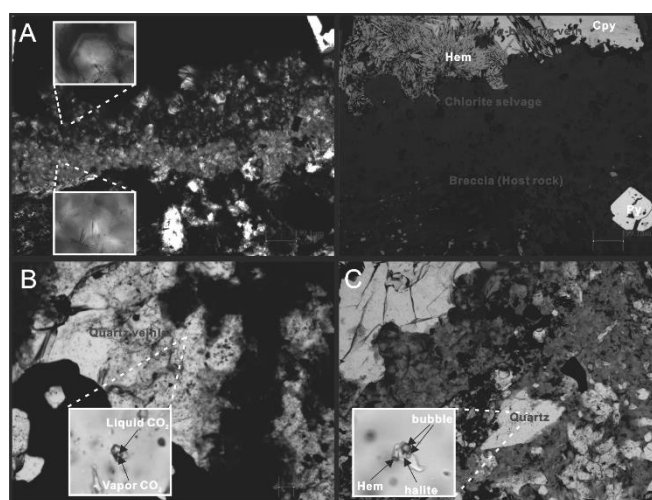


Fig. 1. A) Vein wall interface and chlorite selvage. B) CO<sub>2</sub>-bearing inclusion. C) daughter-phase bearing fluid inclusion.

### Acknowledgement

This work was supported by the Key Research Projects of Shandong Province (No. 2017CXGC1602 and 2017CXGC1608).

### References

Yu G.Y. et al. (2018) Geol. J. 1-16.

# Fluid inclusions in Eocene rock salt from the Dongying Depression, Bohai Bay Basin, eastern China: records on paleolake, paleoclimate and hydrocarbon associations

**Wang, X.T.<sup>1,2\*</sup>, Chen, Y.<sup>1</sup> & Zhou, Y.Q.<sup>1</sup>**

<sup>1</sup>*School of Geosciences, China University of Petroleum, China;* <sup>2</sup>*Department of Applied Geology, University of Goettingen, Germany;* \**xintaowang@s.upc.edu.cn*

Dongying Depression, a typical Paleogene halfgraben lacustrine basin with abundant hydrocarbon resources, is located in the southeastern Bohai Bay Basin and is filled with thick salt deposits (up to 900 m in thickness) in the Eocene Sha-4 member of Shahejie Formation (Es4). Over the past few decades, sedimentology and salt tectonics of these salt deposits have been investigated intensively. Unfortunately, very little attention was paid to studying their fluid-related features. As such, in this study the fluid inclusions (FIs) in the Eocene rock salt were systematically analysed and their implications to paleolake, paleoclimate, sealing capacity for hydrocarbon accumulation and salt deformation were discussed in detail, so as to improve the understandings about fluid-related features of salt deposits in the Dongying Depression.

Thick sections of rock salt samples were prepared with anhydrous ethanol for FI analysis. FIs were characterised by petrography, micro-fluorescence, microthermometry and Raman spectroscopy. (1) Primary FIs were mainly trapped in chevron textures formed by primary rock salt precipitation from evaporated lake brines or within salt crystals appearing in planar and alluvial fan-like arrangements. Most of individual primary inclusions are negative crystal shape. (2) Diagenetic FIs were principally trapped in healed microfractures inside salt grains, along grain boundaries, within primary salt crystals and rarely in clear rock salt cements. Most of single diagenetic inclusions are irregular and are bigger than individual primary inclusions. (3) The majority of these primary and diagenetic inclusions are two-phase (gas + liquid). (4) Anhydrite and leonhardtite ( $\text{MgSO}_4 \cdot 4\text{H}_2\text{O}$ ) identified by Raman are the two main daughter minerals in primary FIs. (5) Abundant hydrocarbon-bearing (HC-bearing) inclusions have been found as one kind of the important diagenetic FIs in rock salt, they can be further classified into two generations. The first generation mainly grew along intragranular healed micro-fractures and the liquid hydrocarbons inside appear yellow or yellow-green colour under UV light. The second generation presenting planar arrangement was trapped within salt crystals, the liquid hydrocarbons appear light blue colour in UV light. (6) These two generations of HC-bearing inclusions have a wide difference in amount, the first generation is major, the second one is minor. (7) The homogenisation temperatures ( $T_h$ ) of the first generation range from 83 to 106 °C (mean:

95.4 °C), while  $T_h$  of the second generation vary from 105.2 to 128 °C (mean: 115.7 °C).

Based on systematic analysis of FIs in the Eocene rock salt, their geological implications were discussed. (1) The occurrence of anhydrite and leonhardtite as two main daughter minerals in primary FIs indicates that salt lake brines in the Eocene must have just reached the early evapo-concentrated stage and rock salt was the main precipitate phase. The temperatures of lake brines that were deduced by phase equilibrium data of anhydrite and leonhardtite ranged from 37 to 61 °C. This implies that the climate was characterised by drought during the Eocene. (2) The presence of abundant HC-bearing inclusions demonstrates that rock salt has been permeable to hydrocarbon fluids during certain geological period. Based on HC-bearing inclusion analysis, combining with the burial and thermal history, two stages of hydrocarbon fluid activities in rock salt were determined. They occurred in the Late Oligocene and the Late Pliocene, respectively. The amount of the first generation HC-bearing inclusions is much higher than that of the second generation, so the first period hydrocarbon fluid activity was considered to be strong, indicating that certain regions of rock salt lost sealing capacity in the Late Oligocene. Whereas, the second period was relatively weak, the overall sealing capacity in the Late Pliocene was better than that in the Late Oligocene. (3) FIs presenting curving line arrangements that were trapped along grain boundaries are attributed to dynamic recrystallisation of salt crystals, they are typical deformation microstructures. FIs appearing in alluvial fan-like arrangements result from primary FI assemblages suffering from structural deformation, the extension direction of stretched FI is parallel to the minimum principal stress ( $\sigma_3$ ) and is perpendicular to the maximum principal stress ( $\sigma_1$ ). These two types of FI assemblages may provide the best tool available for assessing effects of fluids on salt deformation and could further improve the study of salt tectonics.

# Hydrocarbon-bearing fluid inclusions in the Upper Triassic tight sandstones, southwestern Ordos Basin, China: implications for oil migration and accumulation

**Wang, X.T.<sup>1,2\*</sup>, Chen, Y.<sup>1</sup>, Van den Kerkhof, A.M.<sup>2</sup>, Sosa, G.M.<sup>2</sup> & Zhou, Y.Q.<sup>1</sup>**

<sup>1</sup>*School of Geosciences, China University of Petroleum, China;* <sup>2</sup>*Department of Applied Geology, University of Goettingen, Germany;* \**xintaowang@s.upc.edu.cn*

The Ordos Basin is a large-scale residual Mesozoic intracratonic down-warped lacustrine basin, located in the western part of the North China Craton, and represents a gentle monocline with an east-west dip of less than 1°. In the southwestern Ordos Basin tight sandstones of the Upper Triassic Yanchang Formation developed calcite cement and have low permeability of ca. 0.85 mD in average and strong heterogeneity. These rocks represent the most important oil-bearing reservoirs in this basin. Here, abundant high-angle tectonic fractures developed.

The diagenesis, fractures, and petroleum geology of the Upper Triassic tight sandstones have been much studied in the literature. However, little attention has been paid to fluid inclusion planes (FIP) in the quartz particles, which can be directly related to hydrocarbon migration. So far it was not clear in how far the fracturing may be controlled by the forming of calcite cement. Furthermore, the question whether the reservoir densification predates or postdates hydrocarbon accumulation is unresolved. In the present study, thin section petrography, cathodoluminescence (CL), fluid inclusion (FI) analysis and paleomagnetic studies were applied.

Petrography and CL studies show different cement generations, namely calcite cement (Ca-I) showing orange-red CL in primary intergranular pores, and younger calcite cement (Ca-II) showing bright-yellow CL in residual intergranular pores. The amount of Ca-I is much higher than that of Ca-II. Furthermore, two quartz cement generations were distinguished: non-luminescent quartz overgrowths (Qtz-I), and younger microcrystalline authigenic quartz (Qtz-II) showing dark red luminescence in intergranular pores. Chlorite cement (Chl) occurs as pore-lining coatings around detrital grains.

Sandstone drill cores used in our FIP study were oriented by means of their paleomagnetic properties. Based on petrographic and UV-microscopic observations of orientated thick sections, only one generation of hydrocarbon (HC)-bearing inclusions was recognised. These inclusions are trapped along transgranular healed microfractures (FIP) in quartz, in calcite veins parallel to FIPs, and in Ca-II cement. Some HC-bearing inclusions are trapped in feldspar cleavage and in intragranular pores within quartz grains. HC-bearing inclusions are not found in Ca-I and quartz cement. The liquid hydrocarbons are yellow-green or yellow under UV light. The main orientation of HC-bearing FIP is NW-SE, corresponding to the

strike of the fractures formed during the Late Jurassic.

The same HC-bearing inclusions in calcite veins and Ca-II cement demonstrate that the calcite cement within the fractures is contemporaneous with the Ca-II infillings presented by the residual intergranular pores. The growth temperatures for calcite veins and Ca-II cement as determined by fluid inclusion microthermometry range from 98.1 to 130.0 °C with an average of 114.3 °C, while temperatures for Ca-I cement vary from 69.5 to 85.0 °C with an average of 77.0 °C. Combining these results with the burial and thermal history, we conclude that Ca-I cement formed during the Middle Jurassic, whereas calcite veins and Ca-II cements formed during the middle-late Early Cretaceous. This is also considered the major hydrocarbon accumulation period in the SW Ordos Basin.

Our study shows that Ca-I cement precipitated before the opening of NW-SE-oriented fractures and made the reservoir much more brittle. Ca-I cement also predates major hydrocarbon accumulation. Ca-I cement precipitation resulted in the massive loss of primary pore space. In conclusion the Yanchang Formation in the SW Ordos Basin is a typical example of a reservoir which underwent sandstone densification before oil accumulation. The NW-SE trending fractures and related micro-fractures served as important oil migration pathways, which controlled the position of "sweet spot".

## Acknowledgement

The research was co-funded by the National Natural Science Foundation of China (Grant No. 41172111, U1762108 and 41873070), the Fundamental Research Funds for the Central Universities (Grant No. 16CX06041A), and the Chinese Scholarship Council (No. 201606450054).

# Petrography, microthermometry and UV Raman spectroscopy of hydrocarbon-bearing inclusions in salt deposits: constraints on hydrocarbon compositions and sealing capacity of the Eocene rock salt in the Dongying Depression (China)

**Wang, X.T.<sup>1,2\*</sup>, Chen, Y.<sup>1</sup> & Zhou, Y.Q.<sup>1</sup>**

<sup>1</sup>*School of Geosciences, China University of Petroleum, China;* <sup>2</sup>*Department of Applied Geology, University of Goettingen, Germany;* \**xintaowang@s.upc.edu.cn*

Dongying Depression, a typical half-graben lacustrine basin with Mesozoic-Cenozoic strata, is located in the southeastern Bohai Bay Basin and is filled with thick salt deposits in Eocene Sha-4 member of Shahejie Formation (Es4). Rock salt is widely accepted as the best seal for hydrocarbon accumulations with respect to its three important physical properties: the near isotropic stress state, the low permeability at a burial depth of merely 70 m, and the good ductility in nature (Schoenherr et al., 2007). In this study, however, the presence of abundant hydrocarbon-bearing (HC-bearing) inclusions that are trapped in rock salt from Es4 in the Dongying Depression suggests otherwise.

HC-bearing inclusions were recognised by weak fluorescence under ultraviolet illumination. Based on petrography and micro-fluorescence characteristics, HC-bearing inclusions in the Eocene rock salt can be classified into two different generations. The first generation was mainly trapped along the intragranular healed microfractures, and the liquid hydrocarbons within inclusions appear yellow or yellow-green fluorescence under UV light. The fluorescence colour indicates that the maturities of liquid hydrocarbons in inclusions are relatively low. While the second generation presents planar distribution within salt crystals, the liquid hydrocarbons appear light blue colour under UV light, indicating the maturities of them are relatively higher than those in the first generation. In addition, the abundance of the first generation HC-bearing inclusions is much higher than that of the second generation. The homogenisation temperatures (Th) of HC-bearing inclusions are different for each generation. The Th of the first generation range from 83 to 106 °C with an average of 95.4 °C, while the Th of the second generation vary from 105.2 to 128 °C with an average of 115.7 °C.

UV Raman has a high spectral resolution and can avoid or minimise the fluorescence effects of unsaturated hydrocarbons on Raman spectra, so this technique can be used to easily identify the types and structural organisation of hydrocarbons. In this research, the compositions of inclusion hydrocarbons in the Eocene rock salt were recognised by UV Raman with a 244 nm UV laser source, including saturated hydrocarbons, alkenes, aromatic hydrocarbons, bitumen and methane. Six types of HC-bearing inclusions representing two generations were identified by their hydrocarbon compositions and petrographic characteristics.

The presence of abundant HC-bearing inclusions is a direct evidence demonstrating that rock salt has been permeable to hydrocarbon fluids (oil and gas) during certain geological period. Based on petrography, micro-fluorescence, microthermometry and UV Raman analysis of HC-bearing inclusions, combining with the burial and thermal history, two stages of hydrocarbon fluid activities in rock salt in the Dongying Depression were determined. The first period occurred in the Late Oligocene (about 24 Ma) and another took place in the Late Pliocene (around 3 Ma). According to the difference in abundance of two generations of HC-bearing inclusions, the first period hydrocarbon fluid activity was considered to be strong, indicating certain regions of rock salt lost sealing capacity in the Late Oligocene. In contrast, the second was relatively weak, the overall sealing capacity of rock salt in the Late Pliocene was better than that in the Late Oligocene. The damage of sealing capacity of rock salt may be attributed to the opening of the faults cutting through rock salt layers and their associated fractures (pathways for hydrocarbon migration) caused by the regional tectonic movement, i.e., the Dongying movement. And the overpressure that existed under salt deposits when hydrocarbon migrated and / or accumulated in the Dongying Depression could provide a driving force for hydrocarbons to enter the rock salt along the faults and fractures.

## Acknowledgement

The research was co-funded by the National Natural Science Foundation of China (Grant No. 41172111, U1762108 and 41873070), the Fundamental Research Funds for the Central Universities (Grant No. 16CX06041A), and the Chinese Scholarship Council (No. 201606450054).

## References

Schoenherr J. et al. (2007) *A.A.P.G. Bull.* 91:1541-1557.

# Uranium bearing Lower Triassic sandstones of Peribaltic Syncline (N Poland) – preliminary mineralogical and microthermometric study

**Wołkowicz, K.<sup>1\*</sup> & Wołkowicz, S.<sup>1</sup>**

<sup>1</sup>Polish Geological Institute, National Research Institute, Poland; \*krystyna.wolkowicz@pgi.gov.pl

Triassic rocks in the Polish Lowlands commonly show the presence of uranium bearing horizons. The most widespread is the horizon found in the middle Bunter of the Paleozoic platform and Peribaltic Syncline (2 or 3 horizons). It is associated with clay-rich mudstones as well as with fine-grained sandstones or carbonate rocks. The uranium content of this level is sub-economic but ranges up to 300 ppm, in individual samples. The average weighted content occasionally reaches 100 ppm range over 0.5 m intervals.

To the east of Gdańsk in the middle part of Peribaltic Syncline in the rocks of Upper Bunter (Elbląg Formation) sandstone type uranium mineralisation occurs. The richest mineralisation, associated with fine-grained, gray and green-grey, slightly cemented sandstones, occurs on the Vistula Spit. In a single drill hole 4.43 m. interval, the weighted average uranium content is 0.26 wt%. In individual samples the uranium content reach 1.5 wt% (Miecznik et al., 2011). Uranium enrichment is accompanied by elevated V, Se, Mo, Pb, and As concentrations. Mineralogical studies show the presence of coffinite and nasturane as well as pyrite, galena and clausthalite. Two "tabular" type (Strzelecki, 1985) ore bodies were identified on the Vistula Spit at depths from 750 to 800 m.

Roentgenstructural studies of uranium-bearing sandstones identified nasturane, coffinite, clausthalite, galena, illite, dolomite, calcite and pyrite, which have high uranium content (Bareja, 1984). Scanning electron microscopy coupled with energy dispersive analyses indicated that uranium mineralisation occurs mainly in amorphous form in the porous clastic rocks, occurring as rims on grains, crack-fill in grains and cement. Microprobe analyses indicate the presence of uranium and variable amounts of silica, and vanadium. Uranium contents increase proportionally with titanium and silica probably due to uranium capture during leucoxene formation. Uranium from detrital organic matter forms clay-rich nasturane rims on quartz grains. Fragments of clay minerals were also enriched in uranium and vanadium.

Amorphous nasturane mineralisation is also present in association with pyrite, locally replacing it in numerous veinlets with (Pb, Fe, Ni, and Ag) selenides and calcite. Uranium (probably nasturane) mineralisation also occurs in the cavities between crystals of young calcite cement in sandstones. Elevated U and V concentrations were also observed in lead and iron oxides.

In highly altered porous sandstones with carbonate cement uranium mineralisation in the

form of rhombohedral crystals was observed, probably coffinite. U mineralisation also occurs as coatings on clasts of altered dolomite and feldspar, filling mineral embayment, and are often pressed into the micaceous. U-bearing mineralisation is also contemporaneous with alteration of the youngest K-feldspar.

A differentiation of the chemical composition of the carbonate cement was found using CL analysis. Calcite dominates, but dolomite and ankerite were also observed. In calcite, two types of fluid inclusions occur: two-phase (in large groups) and one-phase (in small groups). Rounded irregular-shaped two-phase inclusions reach maximum sizes of 0.08 mm. They are generally colourless and the vapour occupies less than 5 vol% of the fluid inclusion, while the remainder of the inclusions are filled with NaCl-KCl dominant brines.  $T_h$  values vary in the range from 194 to 220 °C. The second type of inclusions are gray-brown, large (0.2 mm), irregular in shape, but rounded. Preliminary studies indicate that they are filled with gas containing CO<sub>2</sub>, H<sub>2</sub>S and probably N<sub>2</sub>.

## References

- Bareja E. (1984) *Kwart. Geol.* 2:353-366.
- Miecznik J.B. et al. (2011) *Przeg. Geol.* 10:688-697.
- Strzelecki R. (1985) *Przeg. Geol.* 4:217-220.

# Fluid inclusion in beryl of Sherlovaya Gora deposit (Eastern Transbaikalia, Russian Federation)

Yurgenson, G.<sup>1</sup>, Prokofiev, V.<sup>2\*</sup>, Afanasieva, A.<sup>3</sup> & Kononov, O.<sup>3</sup>

<sup>1</sup>Institute of Natural Resources, Ecology and Cryology of the Siberian Branch, RAS, Russia; <sup>2</sup>Institute of Geology of Ore Deposits, Petrography, Mineralogy, and Geochemistry, RAS, Russia; <sup>3</sup>Lomonosov State University, Russia; \*vpr2004@rambler.ru

The deposit of bismuth, tin, tungsten and jewelry stones Sherlovaya Gora belongs to the South-Eastern Transbaikalia of Russia (Yurgenson et al., 2014). It is localised in the greisens of the Jurassic granite massif Sherlovaya Gora (154.6 - 147 million years). The deposit consists of miarols with beryl, topaz and quartz, which also contain ferberite, cassiterite, bismuthine, molybdenite and other minerals.

Fluid inclusions found in beryl can be divided into four types (Fig. 1): 1) gas inclusions - type 1, 2) vapour-liquid two-phase aqueous inclusions - type 2, 3) three-phase inclusions with NaCl daughter crystals - type 3, and 4) CO<sub>2</sub>-aqueous inclusions - type 4.

Microthermometrical studies of fluid inclusions were done with a THMSG-600 device (Linkam). Salt concentrations in fluid inclusions were assessed from ice or NaCl melting temperatures. Assessments of salt concentrations, densities of the aqueous fluid were done with FLINCOR software (Brown, 1989).

The analysis of the fluid bulk composition was carried out using monomineral 0.7 g beryl samples of -0.5/+0.25 mm size-fractions at the Central Research Institute for Geological Prospecting for Base and Precious Metals (analyst, Yu.V. Vasyuta) following the standard method (Kryazhev et al., 2006).

Type 1 are gas inclusions with  $T_{h_{liq}}$  from 419 to 642 °C. Salinity is between 8.7 and 23.6 wt% equiv. NaCl. Pressure 320-1590 bar.

Type 2 inclusions, with  $T_e$  from -61 to -21 °C, are water solutions containing Na and Ca, with salinities from 8.1 to 26.3 wt% eq. NaCl<sub>2</sub>.  $T_h$  is between 247 and 633 °C.

Type 3 L-V-S inclusions have  $T_h$  halite between 90-319 °C, and  $T_h$  of the vapour between 221 and 594 °C. Low  $T_e$  of -55 °C indicates Na and Ca chlorides, with salinities from 27.7 to 32.9 wt% eq. NaCl.

Type 4 CO<sub>2</sub>-aqueous inclusions have  $T_h$  319 °C and salinities 9.6 wt% eq. NaCl.

A study of the fluid composition by bulk analysis of the inclusions in beryl monofractions of productive veins showed that among the anions there were (‰) bicarbonate ions (3.8-768), Cl ions (0.4-96) while the cations are potassium (0.4-57), sodium (1.4-273), Ca (29) and magnesium (0.06-7.5): this is consistent with the data on the eutectic temperatures. The fluid also contains (‰) carbon dioxide (107-550), methane (0.9-8.1), B (1.7-16.7), As (0.95-6.3), Rb (0.01-1.2), Cs (0.01-1.7), Li (0.2-

3.0), and a number of trace components: Br, Sr, Sb, Mo, Ag, Cu, Zn, Cd, Pb, Bi, Th, U, Ga, Ge, Mn, Fe, Co, Ni, V, Cr, Y, Zr, Sn, Ba, W, Hg, Tl, and REEs. The main indices of the fluid composition are CO<sub>2</sub>/CH<sub>4</sub> = 20-44, Na/K = 3.3-5.0, and K/Rb = 32-58.

High temperatures and features of the chemical composition of fluids indicate a high proportion of magmatic components in the composition of the mineral-forming fluids of the Sherlovaya Gora deposit.

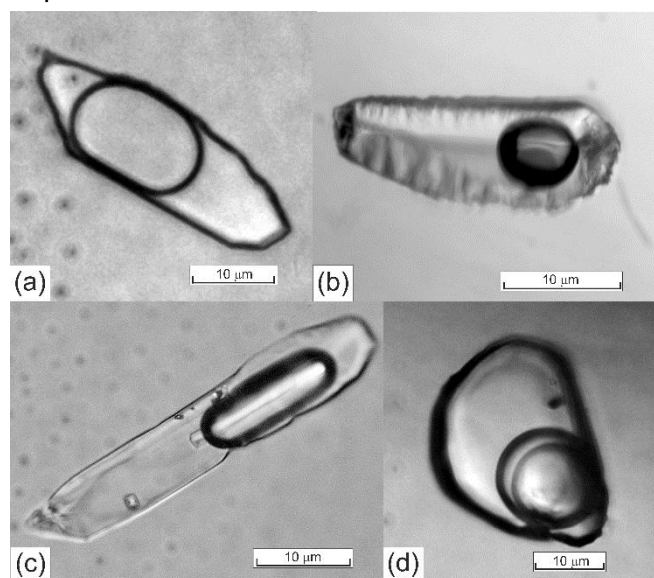


**Fig. 1.** Types of Fls: A) gas inclusions - type 1, B) vapour-liquid two-phase aqueous inclusions - type 2, C) L-V-S inclusions with NaCl daughter crystals - type 3; D) – carbon dioxide-water-salt fluid inclusions - type 4. Scale bar 10 µm.

## Acknowledgement

This work was financially supported by Russian Foundation for Basic Research (Grant no. 17-05-00387) and Project SB RAS IX 137.1.2.

## References

- Brown P. (1989) *Am. Mineral.* 74:1390-1393.
- Kryazhev S.G. et al. (2006) *Vestn. Mosk. U. Geol.* 4:30-36.
- Yurgenson G. et al. (2014) *Min. Almanac* 19:12-93.

# Evaluation of hydrocarbon migration pathways in Miocene (Badenian) sandstones by combining the GOI fluid inclusion technique and reservoir quality, Mezősas and Mezősas West fields, East Hungary

Zartasha, Z.<sup>1\*</sup>, Csoma, A.É.<sup>2</sup>, Bányai, Cs.<sup>2</sup>, Juhász, Gy.<sup>2</sup> & Orbán, R.<sup>2</sup>

<sup>1</sup>University of Miskolc, Hungary; <sup>2</sup>MOL Upstream, Hungary; \*[rzartasha@gmail.com](mailto:rzartasha@gmail.com)

The Mezősas and Mezősas West Fields of East Hungary have been producing from fractured Mesozoic basements and Miocene conglomerates, sandstones, and limestones for decades. Their complex structural evolution, resulted in horsts and grabens and complicated fracture patterns make it challenging to predict the presence and volume of hydrocarbon accumulations across the field.

The GOI technique (grains containing oil inclusion, Eadington et al., 1996) is a fast and cost-effective way to distinguish hydrocarbon migration pathways from hydrocarbon columns and water-saturated zone, and to reconstruct the charge history of a field by combining the results with well logs, well production data, petrographic and diagenetic analysis and organic geochemistry. This study introduces this technique for the first time in Hungarian sandstone reservoirs, in the Middle Miocene Badenian sandstones.

The GOI technique is a statistical approach that determines the ratio between grains containing oil inclusion(s) and the total number of grains. The ratio is expressed in GOI %. It has been established that GOI 5 % separates paleo oil columns from the residual zones and migration pathways, and the paleo OWC is marked by the sharp decline of GOI values (Lisk, 2012 and Eadington et al., 1996).

Cores from three wells (producers and dry) have been selected from the Badenian intervals. Sandstones and conglomerates with various textures and compositions underwent significant compaction, dissolution, and quartz and carbonate cementation. Hydrocarbon migration is one of the latest diagenetic events. The presence and quality of hydrocarbon inclusions (gas versus oil) correlates well with the well test data. GOI values (<5 %) document migration pathways in these sandstones rather HC column in alignment with the well test data. Preliminary data suggest that reservoir quality, in particular the presence of clay minerals between the quartz grains controls the entrapment of HC inclusions in the studied samples.

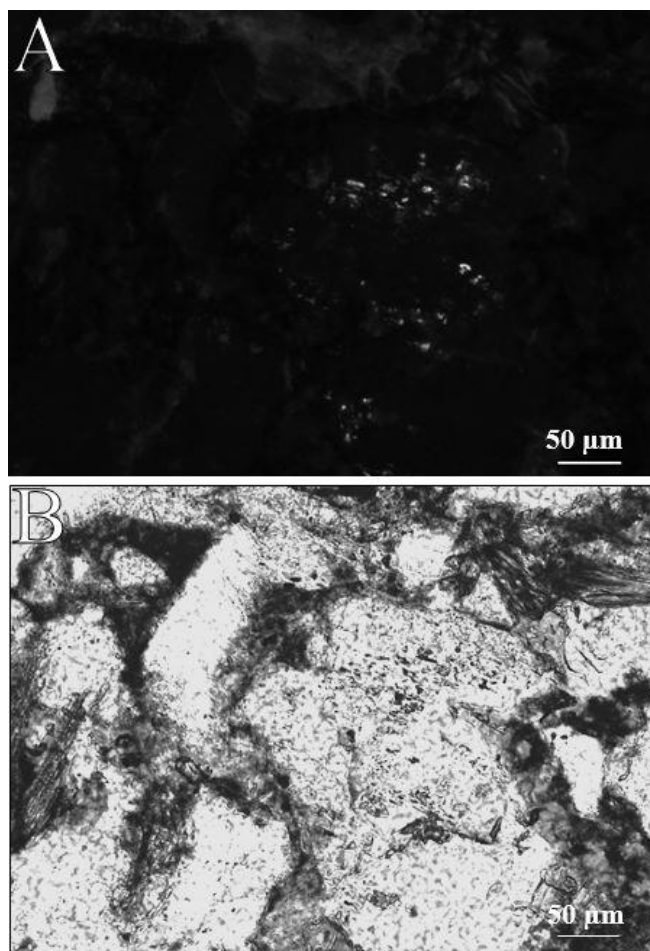


**Fig. 1.** Photomicrographs illustrating oil inclusions within a quartz grain. A) Oil inclusions under Ultraviolet light. B) Oil inclusions under transmitted light.

## References

- Eadington P.J. et al. (1996) United States Patent No.5543,616.  
Lisk M. (2012) PhD Thesis, Curtin University, Australia 734.

# The stages of petroleum accumulation in the middle of Junggar Basin, Northwest China: evidence from fluid inclusions studies

Zhang, H.<sup>1\*</sup>, Chen, Y.<sup>1</sup>, Lin, H.X.<sup>2</sup>, Wang, M.<sup>1</sup> & Ren, X.C.<sup>2</sup>

<sup>1</sup>School of Geosciences, China University of Petroleum, China; <sup>2</sup>Shengli Oilfield Company, SINOPEC, China; \*15694455138@163.com

The studied area is located in the Middle of Junggar Basin, Northwest China. It shows good prospect for petroleum exploration, but the petroleum accumulation history is still unclear.

Fluid inclusion analysis is an effective method to obtain information of oil and gas accumulation (Hu et al., 2017). The stages of petroleum accumulation were determined based on the petrography of fluid inclusions, microfluorescence and microthermometry. Petrographic observations indicate that there are two generations of hydrocarbon inclusions from the studied area. Hydrocarbon inclusions of the early generation were trapped in the microfractures within quartz grains and featured by yellow-green fluorescence colour (Fig. 1a, b). Hydrocarbon inclusions of the late generation were developed in the microfractures, cutting through the grains and represented by blue-white fluorescence (Fig. 1c, d). Based on the micro-spectrofluorimetry, we calculated the  $\lambda_{max}$  and Q650/500 values of the fluorescence of two generation fluid inclusions in this study. The  $\lambda_{max}$  of the early generation is from 504 to 515 nm (avg. = 509.81 nm) with the Q650/500 range from 0.43 to 0.72 (avg. = 0.60); while the hydrocarbon inclusions of the late stage show lower values of  $\lambda_{max}$  (462 – 469 nm, avg. = 465.83 nm) and Q650/500 (0.21 – 0.32, avg. = 0.27).

According to the microthermometry analysis, the homogenisation temperatures ( $T_h$ ) of the hydrocarbon inclusions of the early generation vary from 80 to 100 °C, and the  $T_h$  of their coeval aqueous inclusions are from 100 to 120 °C while the ice melting temperatures range from -6 to -4 °C (the salinity ranges from 6.45 to 9.21 NaCl wt%). The  $T_h$  of the hydrocarbon inclusions in the late stage show 60 – 80 °C, and 110 – 140 °C for their coeval aqueous inclusions with  $T_m$  value range from -2 to -4 °C (the salinity ranges from 3.39 to 6.45 NaCl wt%). Combined the history of tectonic evolution, burial and hydrocarbon generation, the stages of petroleum accumulation in the middle of Junggar Basin were determined, the early stage in the Early Cretaceous, and the late one in the Paleogene.

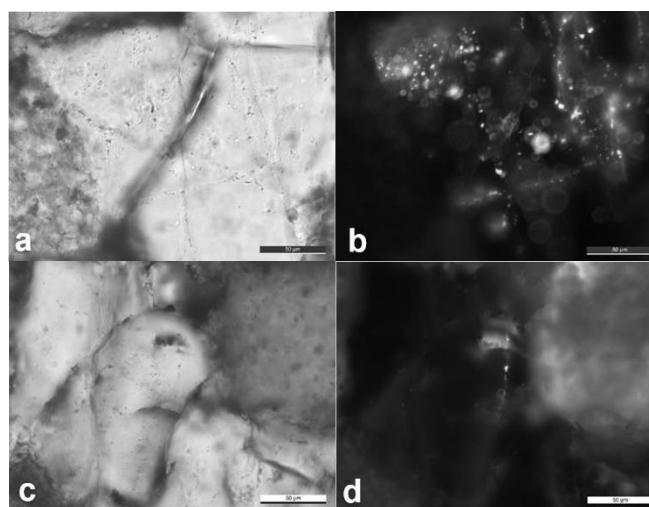


**Fig. 1.** Hydrocarbon inclusions in quartz A-B) early stage; C-D) later stage.

## Acknowledgement

This work was supported by the National Natural Science Foundation of China (No. U1762108 and 41873070) and the Key Research Projects of Shandong Province (No. 2017CXGC1608 and 2017CXGC1602).

## References

Hu H. et al. (2017) Geol. J. 7.

# Unexpected high-temperature behaviours of sulphate-water systems and their implications for rare earth mineralisation

**Zhong, R.C.<sup>1\*</sup>, Cui, H.<sup>1</sup>, Xie, Y.L.<sup>1</sup>, Brugger, J.<sup>2,3</sup>, Yuan, X.Y.<sup>4</sup>, Chen, H.<sup>1</sup>, Liu, W.H.<sup>5</sup> & Yu, C.<sup>1</sup>**

<sup>1</sup>Civil and Resource Engineering School, University of Science and Technology Beijing, China; <sup>2</sup>School of Earth, Atmosphere and the Environment, Monash University, Australia; <sup>3</sup>South Australian Museum, Australia; <sup>4</sup>MLR Key Laboratory of Metallogeny and Mineral Assessment, Institute of Mineral Resources, Chinese Academy of Geological Sciences, China; <sup>5</sup>CSIRO Minerals Recourses, Australia; \*zhongrichen@126.com

Sulphate salts are known for their two characteristics: (i) high melting temperatures that would not be significantly changed by the presence of water (884, 1069 and 1460 °C for crystalline Na<sub>2</sub>SO<sub>4</sub>, K<sub>2</sub>SO<sub>4</sub> and CaSO<sub>4</sub> at ambient pressure, respectively), and (ii) retrograde solubility, i.e., solubility decreasing with increasing temperatures. This implies that high-temperature geofluids should be expected to be poor in sulphate. However, sulphate-rich fluid inclusions containing sulphate daughter minerals are known to occur. A typical example is the syn-ore inclusions at the giant Maoniuping rare earth deposit in southwest China, which contain up to 70-75 vol% of hydrated K-Na-Ca-Sr-Ba sulphates as daughter minerals (Xie et al., 2014). Furthermore, microthermometric analysis of these inclusions shows that the sulphate daughter minerals melt at ~335 to 350 °C upon heating, a temperature range significantly lower than the expected melting points of sulphate salts with or without water.

In this study, we conducted hydrothermal diamond anvil cell (HDAC) experiments in the Na<sub>2</sub>SO<sub>4</sub>-SiO<sub>2</sub>-H<sub>2</sub>O and Na<sub>2</sub>SO<sub>4</sub>-Nd<sub>2</sub>(SO<sub>4</sub>)<sub>3</sub>-SiO<sub>2</sub>-H<sub>2</sub>O systems to simulate the high-temperature behaviour of sulphate in the presence of excess quartz. The SiO<sub>2</sub>-saturated systems are more close to the natural crustal geofluids compared to binary sulphate-water systems. Sulphate-oversaturated systems were prepared at room temperature by loading sulphate crystals, sulphate-saturated aqueous solution, and a piece of quartz as starting materials. The experiments were conducted from room temperature to ~550 °C. In the Na<sub>2</sub>SO<sub>4</sub>-SiO<sub>2</sub>-H<sub>2</sub>O system, the experimental system successfully reproduced the phase transitions observed in nature. The melting of the Na<sub>2</sub>SO<sub>4</sub> crystal initiated at ~270 °C (solidus temperature), and total homogenisation of the system took place at >~330 °C upon dissolution of sulphate melt into the aqueous solution. Similar phase transitions were observed in the Na<sub>2</sub>SO<sub>4</sub>-Nd<sub>2</sub>(SO<sub>4</sub>)<sub>3</sub>-SiO<sub>2</sub>-H<sub>2</sub>O system, and prograde dissolution of the Na-Nd-sulphate melting led to the formation an extremely Nd- and sulphate-rich fluid at ~420 °C.

For comparison, a quartz-free experiment was conducted in the Na<sub>2</sub>SO<sub>4</sub>-Nd<sub>2</sub>(SO<sub>4</sub>)<sub>3</sub>-H<sub>2</sub>O system. Both the Na<sub>2</sub>SO<sub>4</sub> and Nd<sub>2</sub>(SO<sub>4</sub>)<sub>3</sub> crystals remained in the solid state throughout the whole temperature range, and grew progressively upon heating due to

their retrograde solubility, leading to the formation of a REE-poor solution at high temperatures.

## References

Xie Y. et al. (2014) Ore Geol. Rev. 70:595-612

## Fluid inclusion characteristics of Ma Zhuang lead-zinc deposit in the Yishu fault zone

Zhong, S.<sup>1\*</sup>, Chen, Y.<sup>1</sup>, Liu, T.Y.<sup>1</sup>, Li, G.H.<sup>1</sup>, Zhang, S.K.<sup>2</sup> & Chen, J.J.<sup>2</sup>

<sup>1</sup>School of Geosciences, China University of Petroleum, China; <sup>2</sup>Shandong Institute of Geological Sciences, China; \*s18010052@s.upc.edu.cn

The Yishu fault zone is a large-scale fault zone in eastern China, which is a part of Tanlu fault zone in Shan Dong province. The Yishu fault zone is composed of four faults which strike north-east to north and called respectively Tang wu – Gegou fault, Yishui – Tangtou fault, Anqiu – Juxian fault, Changyi – Dadian fault from west to east. The Ma Zhuang lead-zinc deposit is located in Mazhan Sag which is between Tangwu – Gegou fault and Yishui – Tangtou fault. Ore-bearing fractures parallel the Yishu fault. The mineralization is constrained to the Early-Cretaceous Malangou Formation, comprised of yellow-green pebbly sandstone, tuff sandstone, and fuchsia sandstone. The ore minerals are galena, chalcopyrite, the gangue mineral is quartz, with abundant quartz veins in the host rock. The trend of quartz veins is consistent with the ore-bearing fractures.

With microscopic observation, field investigation and hand specimen analysis, three main stages of fluid activity were identified in study region: (1) the early fluid formed the quartz veins which cut through the wall rock, the quartz crystal are small and the fluid inclusions have irregular outlines with a single contained phase, small volume and distributed along microfractures, (2) the second stage is the metallogenic stage. Quartz cemented the early wall rock and formed breccia. The quartz crystals of this second stage are bigger and euhedral to subhedral. Galena precipitated in the quartz veins of second stage (Fig. 1), (3) the third and final stage is represented by quartz veins cross cutting both of the earlier veins. The fluid inclusions of third stage are secondary and aligned along tensional fractures. The vapor to liquid ratio of the fluid inclusions in metallogenic stage are from 5 % to 10 %, and range in size are from 8 to 30  $\mu\text{m}$  (Fig. 1). Homogenisation temperatures of the quartz-hosted inclusions of Ma Zhuang zinc-lead deposit are 147.8-204.05  $^{\circ}\text{C}$  with salinities ranging from 1.70 to 7.86 NaCl wt%, which indicate the low salinity fluid. Although there is minimal evidence to do so, we postulate, the fluids are the conjugate endmembers of boiling system. Thus, the trapping conditions obtained by PVT simulation show that the trapping temperatures are 179-210  $^{\circ}\text{C}$  and the trapping pressures are between 549 bar to 1571.39 bar (Bodnar et al. 1985; Bodnar and Vityk, 1994). Because the location of mineral deposit is quite shallow, the metallogenic fluid have been contaminated with meteoric water, resulting in the lower salinity and temperature. Laser Raman spectroscopy on liquid phase of inclusion, indicates that the liquid phases of inclusions are  $\text{H}_2\text{O}$ .

Generally, the ore deposit should be classified as an epithermal deposit, with the metallogenic input controlled by tectonic activity along the Yishu fault zone.

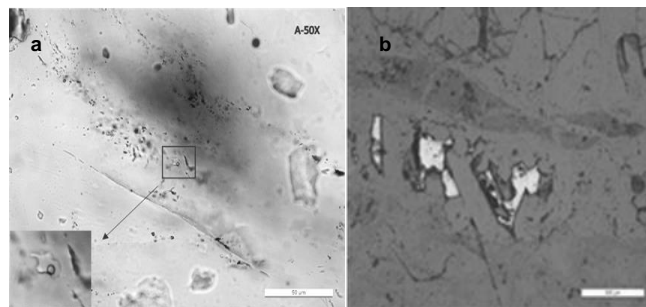


**Fig. 1.** A) fluid inclusions of the metallogenic stage, B) galena precipitated in quartz vein.

### Acknowledgement

This work was supported by the National Natural Science Foundation of China (No. U1762108) and the Key Research Projects of Shandong Province (No. 2017CXGC1602 and 2017CXGC1608).

### References

- Bodnar R.J. et al. (1985) *Geochim. Cosmochim. Ac.* 49:1861-1873.
- Bodnar R.J. and Vityk M.O. (1994) in: *Fluid Inclusions in Minerals. Methods and Applications* 117-130.

---

# **SPONSORS**

---

## SGA -The Society for Geology Applied to Mineral Deposits

<http://www.e-sga.org>

The Society for Geology Applied to Mineral Deposits (SGA) is an IUGS affiliated non-profit international scientific society that promotes the science of mineral deposits geology.



**The objectives of the SGA are:**

- To advance the application of scientific knowledge in the study and the development of mineral resources and their environment,
- To promote the profession of geology in science and industry,
- To cultivate personal contacts for mutually beneficial relationships,
- To protect and improve professional and ethical standards among its members.
- To foster and provide support to educational activities in mineral deposit geology to students and professionals from economically disadvantaged backgrounds.

The SGA was founded in 1965 in Heidelberg and incorporated in Switzerland in 1971. Its worldwide membership of over 1300 is composed of researchers, professionals and students from university, industry and government interested in economic geology, mineral resources, industrial minerals and environmental aspects related to mineral deposits. Continued increasing interest in student membership indicates that SGA is getting increasingly more attractive for younger geoscientists. The SGA Educational Fund helps to facilitate donations from corporations, institutions and members to provide sustained financial support for students and economically disadvantaged professionals to participate in SGA sponsored workshops and short courses, meetings and field trips. Its flagship publication, *Mineralium Deposita*, is recognized as a premier international scientific journal on mineral deposits geology. In addition to biennial scientific meetings, the SGA organizes international short courses and workshops and publishes Proceedings, a Newsletter and other Special Publications. The SGA-Newmont Gold Medal was established in 2006 to recognize "unusually original work in the mineral deposit sector, which shall be broadly interpreted to encompass major contributions to (1) the science through research, and (2) the development of mineral resources through mine geology, exploration and discovery". Since 2007, the SGA Young Scientist Award has been bestowed to young researchers with exceptional research achievements before the age of 40. The SGA gives a Best Paper Award to authors of an outstanding paper in *Mineralium Deposita*, on recommendation of the Board of Editors. Finally, but not least, the SGA recognizes excellent oral and poster presentations during its biennial meetings. Student participation in SGA Biennial Meetings is of paramount importance for the SGA and takes special care to recognize the best upcoming scientists in mineral deposit research.

### Upcoming SGA Biennial Meeting

15<sup>th</sup> SGA Biennial Meeting "Life with Ore Deposits on Earth" (Glasgow, Scotland, UK, August 2019)





**Molecular and Microanalysis**

- Raman Spectroscopy and AFM-Raman
- AFM
- Cathodoluminescence
- Fluorescence
- Surface Plasmon Resonance imaging

**Optical Spectroscopy**

- Diffraction Gratings
- Detectors
- OEM Spectrometers
- Monochromators

**Particle Characterization**

- Laser Diffraction
- Light Scattering
- Zeta Potential

**Elemental Analysis**

- ICP-OES
- C/S and O/N/H Analyzers
- XRF and  $\mu$ XRF Analyzers
- S Analyzers in Petroleum Products
- Sample Preparation

**Surface and Thin Film Characterization**

- Ellipsometry
- GD-OES
- PP-TOFMS™

**Forensics**

- Light Sources
- Image Treatment Software
- Databases

Follow us!



[www.horiba.com/scientific](http://www.horiba.com/scientific)

## O&G Development



1024 Budapest, Lövház u. 39.  
Tel.: +36 1 808 9001 • Fax: +36 1 808 9002  
E-mail: [info@shpbv.eu](mailto:info@shpbv.eu)  
[www.shpbv.eu](http://www.shpbv.eu)



ELTE Tudományos Tanács

## Index of authors

Abramov, S. ....	48	Carpentier, C. ....	34
Adlakha, E. ....	3, 70, 120	Castelli, D. ....	76
Afanasieva, A. ....	126	Caumon, M.C. ....	69, 96
Akinfiyev, N.N. ....	17, 101	Cendón, D.I. ....	75
Aleshin, A.P. ....	62	Cepedal, A. ....	40
Almeev, R.A. ....	100	Ceriani, A. ....	4
Alsuwaidi, M. ....	4	Chailan, O. ....	80
Andreeva, I.A. ....	5, 6	Chen, H. ....	129
Andreeva, O.A. ....	6	Chen, J.J. ....	130
Anisimova G.S. ....	56	Chen, L.S. ....	71
Antal, P. ....	60	Chen, Y. 25, 37, 71, 73, 121, 122, 123, 124, 128, 130	
Appel, P. ....	54	Chicherov, M. ....	101
Aradi, L.E. .... 7, 16, 17, 23, 43, 54, 63, 97, 98, 111		Chinchilla, D. ....	22
Aragón, D. ....	40	Chou, I-M. ....	26
Arias, D. ....	40	Chugaev, A.V. ....	117
Arribas, J. ....	45	Cipriani, M. ....	27
Avalos, N. ....	8	Costanzo, A. ....	27
Averin, A.A. ....	106	Csoma, A.É. ....	127
B. Kiss, G. ....	9, 74	Cui, H. ....	129
Badanina E.V. ....	56	Czifra, T. ....	63
Bain, W.M. ....	10, 11	Czuppon, Gy. .... 28, 74, 88	
Bakelli, A. ....	12, 84	Dal Corso, J. ....	23
Baker, D.R. ....	23	Damdinov, B.B. ....	29, 30
Bakker, R.J. ....	13, 14	Damdinova, L.B. ....	29, 30
Baksheev, I.A. ....	15	Davies, G.R. ....	21
Baldwin, G. ....	3	De Graaf, S. ....	31
Bali, E. .... 16, 18, 24, 91		Demény, A. ....	28
Banks, D.A. ....	20, 101	Demicco, R.V. ....	75
Bányai, Cs. ....	127	Dennis, P.F. ....	35
Bartoli, O. ....	23	Diamond, L.W. ....	32, 103
Baykara, O. ....	28	Dominici, R. ....	27
Bazarkina, E.F. ....	17	Dubessy, J. ....	17
Bendő, Zs. ....	9	Dublyansky, Y. .... 33, 39, 61	
Benkó, Zs. ....	74, 88	Dufresne, A. ....	10
Berkesi, M. 7, 18, 42, 43, 49, 63, 68, 72, 97, 98, 108, 111		Dumańska-Słowik, M. ....	55
Biró, T. ....	97	Eiler, J.M. ....	80
Bitte, M. ....	19	Elias-Bahnan, A. ....	34
Bocharov, V.N. ....	48	Elongo, V. ....	70
Bodnar, R.J. ....	58, 75, 98, 104, 110	Ersoy, Ö. ....	93
Borisova, A.Y. ....	117	Falck, H. ....	70, 120
Borovikov, A. ....	101, 118	Fall, A. ....	35
Bortnikov, N. ....	118	Fallick, A.E. ....	59
Botcharnikov, R.E. ....	67, 100	Fan, J.J. ....	36
Bouabalou, S. ....	84	Fayek, M. ....	51, 52
Boutaleb, A. ....	12	Feely, M. ....	27
Bozkaya, G. ....	20	Fehér, K. ....	97
Bozkaya, O. ....	20	Feng, Y.W. ....	37
Bracco Gartner, A.J.J. ....	21, 93	Ferrando, S. .... 38, 76, 102	
Brooks, H.L. ....	109	Filipčíková, P. ....	39
Brugger, J. ....	129	Frezzotti, M.L. ....	76, 102
Bryansky, N. ....	30	Friðleifsson, G.Ó. ....	16
Buhre, S. ....	67	Fuertes-Fuente, M. ....	40
Burke, J. ....	52	Futó, I. ....	43
Calisto, D. ....	22	Gajdošová, M. ....	41
Callegaro, S. ....	23	Gál, Á. ....	42
Capriolo, M. ....	23	Gale, J.F.W. ....	35
Caracciolo, A. ....	24	García-Veigas, J. ....	75
		Garrevoet, J. ....	67

Garrido, C.J.....	98	Krashennikov, S.P.....	67, 87, 100, 105, 113
Gasparini, G.....	89	Krüger, Y.....	61
Gaucher, E.C.....	34	Kryazhev S.....	118
Ge, Y.J.....	25	Krylova, T.L.....	62, 65
Gelencsér, O.....	43	Kubač, A.....	59
Ghahramani, S.....	44	Lamadrid, H.....	110
Giehl, C.....	54	Lange, T.P.....	63, 68
Gill, B.C.....	104	Laurent, O.....	59
Girard, J-P.....	80	Le, V.H.....	69
González-Acebrón, L.....	45	Lecumberri-Sanchez, P.....	58, 70, 120
Gráczner, Z.....	63	Leél-Óssy, Sz.....	28, 61
Graney, J.....	75	Legros, H.....	70
Greene, R.....	81	Li, G.H.....	71, 130
Griffin, W.L.....	72	Lin, H.X.....	128
Grishina, S.....	46, 47	Lin, K.....	28
Groschopf, N.....	67	Liptai, N.....	63, 68, 72, 98
Groznova, E.....	48, 118	Liu, S.B.....	36
Guðfinnsson, G.H.....	24, 91	Liu, T.Y.....	73, 121, 130
Gurenko, A.....	87	Liu, W.H.....	129
Guzmics, T.....	18, 49, 116	Lobanov, K.....	101
Halldórsson, S.A.....	24	Lovász, A.....	74
Haniçi, N.....	50, 53, 95	Lowenstein, T.K.....	75, 104
Hanley, J.J.....	3, 51, 52, 57, 83, 92, 120	Lu, X.S.....	36
Harangi, Sz.....	88, 91	Luciani, N.....	21
Hepvidinli, B.....	53	Lüders, V.....	101, 115
Herms, P.....	54	Lukács, R.....	88, 91
Hidas, K.....	98	Luo, Y.....	10
Holtz, F.....	100	Luptáková, J.....	60, 65
Hurai, V.....	41	MacHattie, T.....	92
Huraiová, M.....	41	Maffeis, A.....	76
Ionescu, C.....	42	Maia, M.....	77, 78, 79
Jannessary, M.R.....	44	Mangenot, X.....	80
Jarmołowicz-Szulc, K.....	55	Marsh, E.E.....	10, 11
Józsa, S.....	64, 108	Marshall, D.....	81
Juhász, Gy.....	127	Martin-Izard, A.....	40
Kahl, M.....	24	Marzoli, A.....	23
Kalko, I.A.....	15	Mas, J.R.....	45
Kardashevskaja, V.N.....	56	Maximovich, Y.....	46, 47
Karpukhina, V.S.....	117	Mazdab, F.K.....	10
Kasapçi, C.....	50	McDonald, I.....	82
Kennedy, N.....	3	McFall, K.A.....	82
Kerr, M.J.....	3, 57	McNeil, N.....	3
Kesjár, D.....	64, 68, 97	Meagher, D.....	83
Khabibullina, Y.N.....	15	Meddane, S.....	12, 84
Kis, B-M.....	88	Meng, F.C.....	121
Kiseleva, G.D.....	65	Meng, Q.Y.....	36, 85
Klimm, K.....	67	Mercadier, J.....	86
Kluge, T.....	61	Mercier-Langevin, P.....	83
Klyukin, Y.I.....	58	Migdisova, N.A.....	105
Koděra, P.....	59, 60	Milichko, V.....	101
Kolli, O.....	12, 84	Mills, B.J.W.....	23
Koltai, G.....	39, 61	Milovský, R.....	59
Komarov, V.I.B.....	62	Mirão, J.....	77, 78, 79
Komarova, M.M.....	15, 62	Mironov, N.L.....	67, 87, 100
Kononov, O.....	126	Molnár, Cs.....	63
Kontak, D.J.....	57	Molnár, K.....	74, 88
Koornneef, J.M.....	21	Molnár, M.....	28
Körmös, S.....	66	Moncada, D.....	8, 22
Kovács, I.....	42, 63, 64, 68, 97	Montenegro, T.....	115
Kovacs, M.....	64	Morad, D.....	89
Kovács, Z.....	64	Morad, S.....	89
Kővágó, Á.....	64	Moreira, N.....	77, 78, 79
Kovalenker, V.A.....	17, 65	Morozova, K.A.....	90

Mullis, J. ....	69, 80	Shishkina, T.A. ....	105
Nader, F.H. ....	89	Siklósy, Z. ....	28
Nagornaya, E.V. ....	15	Šimko, F. ....	60
Naumov, V.B. ....	114	Simonov, V.A. ....	117
Németh, B. ....	88, 91	Smirnov, S.Z. ....	47, 87
Newton, R.J. ....	23	Solovova, I.P. ....	106
Neyedley, K. ....	92, 120	Sonnenthal, E. ....	22
Nicol, C.A. ....	81	Sosa, G.M. ....	107, 115, 123
Nikogosian, I.K. ....	21, 93	Spiekermann, G. ....	110
Nogueira, P. ....	77, 78, 79	Spiess, R. ....	23
Nooitgedacht, C.W. ....	31	Spötl, C. ....	33, 39, 61
Noronha, F. ....	77, 78, 79	Spráñitz, T. ....	108
Novák, A. ....	63	Steele-MacInnis, M. ....	10, 11, 58, 109, 110, 121
O'Reilly, S.Y. ....	72	Steinbach, G. ....	66
Okunlola, O.A. ....	94	Sublett, D.M. ....	110
Ootes, L. ....	52	Süle, B. ....	63
Orbán, R. ....	127	Sushchevskaya, N.M. ....	105
Oriolo, S. ....	107	Szabó, Á. ....	16, 111
Óvári, M. ....	28	Szabó, Cs. ....	7, 16, 17, 18, 23, 42, 43, 49, 63, 64, 68, 72, 97, 98, 108, 111, 116
Oyedokun, M.O. ....	94	Szakács, A. ....	42
Özbaş, F. ....	95	Szanyi, Gy. ....	63
Öztürk, H. ....	50	Szűcs, E. ....	63
Padyar, F. ....	96	Takács, A. ....	60
Paicsu, L. ....	43, 88	Tarantola, A. ....	19, 44, 69, 80, 96, 112
Pálos, Zs. ....	63, 97	Tattitch, B. ....	82
Patkó, L. ....	63, 68, 72, 98	Timkó, M. ....	63
Pearson, D.G. ....	10	Tobelko, D.P. ....	87, 100, 113
Pérez-Garrido, C. ....	45	Toboła, T. ....	55
Petrov, V.A. ....	90	Tolstykh, M.L. ....	114
Pettke, T. ....	103	Tomilenko, A.A. ....	47
Pevzner, M.M. ....	114	Tóth, Á. ....	88
Pironon, J. ....	34, 99	Trottier, C. ....	52
Plessen, B. ....	115	Tsay, A. ....	51, 52, 83, 92
Plotinskaia, O. ....	48	Tutolo, B. ....	58
Polozov, A.G. ....	46	Tweedale, F. ....	51
Portnyagin, M.V. ....	67, 87, 100, 113	Uhlík, P. ....	59
Pourmoafi, M. ....	96	Ukar, E. ....	35
Pritchyn, M. ....	118	Váczi, T. ....	60
Prokofiev, V. ....	17, 90, 101, 117, 118, 119, 126	Valero, M. ....	19
Pujatti, S. ....	58	Van Bergen, M.J. ....	93
Puskarev, E. ....	13	Van den Kerkhof, A.M. ....	107, 115, 123
Raase, P. ....	54	Vanderhaeghe, O. ....	96
Racek, M. ....	60	Vetlényi, E. ....	116
Rahgoshay, M. ....	96	Vicente, S. ....	78
Ramlochund, P. ....	57	Vikent'eva, O. ....	118
Randi, A. ....	69, 112	Vikentyev, I.V. ....	117, 118
Reijmer, J.J.G. ....	31	Volkov, A.V. ....	119
Remigi, S. ....	102	Volynets, A.O. ....	114
Ren, X.C. ....	128	Vonhof, H.B. ....	31
Richter, L. ....	32, 103	Voudouris, P. ....	19
Rigaudier, T. ....	112	Wagner, A. ....	120
Robert, P. ....	69	Wang, M. ....	121, 128
Rohrbach, A. ....	54	Wang, X.T. ....	122, 123, 124
Rossi, C. ....	89	Wéber, Z. ....	63
Sami, L. ....	12, 84	Weldeghebiel, M.F. ....	75, 104
Scheffer, C. ....	19	Wesztergom, V. ....	63
Scherbakov, V.D. ....	67	Whitechurch, H. ....	44
Scholz, D. ....	33	Wignall, P.B. ....	23
Schubert, F. ....	66	Wilke, M. ....	67
Selektor, S. ....	101	Wołkowicz, K. ....	125
Sendula, E. ....	75, 98, 104, 110	Wołkowicz, S. ....	125
Sharpe, R. ....	51	Xie, Y.L. ....	129
Shen, C-C. ....	28		

Yarmolyuk, V.V. ....	6	Zhang, S.K. ....	130
Yazykova, Y.I. ....	65	Zhao, Z.Y. ....	37
Youbi, N. ....	23	Zhong, R.C. ....	129
Yu, Z.C. ....	85, 129	Zhong, S. ....	130
Yuan, X.Y. ....	129	Zhou, Y.Q. ....	25, 122, 123, 124
Yudovskaya, M.A. ....	106	Zhou, Z.Z. ....	25, 71
Yurgenson, G. ....	126	Zhuo, Q.G. ....	36
Zajacz, Z. ....	51, 52, 57, 83, 92, 116	Zierenberg, R. ....	16
Zartasha, Z. ....	127	Zinovieva, N.G. ....	106
Zhang, H. ....	128		

**ECROFI 2019 SCHEDULE**

<b>PRE-CONFERENCE PROGRAM SOUTHERN BUILDING</b>		<b>PLENARY SESSIONS NORTHERN BUILDING</b>				<b>FIELD TRIP</b>
Sunday 23 <sup>th</sup> June		Monday 24 <sup>th</sup> June	Tuesday 25 <sup>th</sup> June	Wednesday 26 <sup>th</sup> June	Thursday 27 <sup>th</sup> June	
07:45-08:00	Workshop 1 registration	07:45-08:30	Registration	08:00-08:30	Registration	
08:00-10:00	R.J. Bodnar Workshop 1	08:30-09:00	Opening ceremony	08:30-09:00	09:00-09:15	
10:00-10:30	<i>Coffee break</i>	09:00-09:30		09:15-09:30	09:15-09:30	Session 4
10:30-12:30	R.J. Bodnar Workshop 1	09:30-09:45		09:30-09:45	09:30-09:45	
12:30-13:30	<i>Lunch</i>	09:45-10:00	Session 3	09:45-10:00	09:45-10:00	Session 2
13:30-15:00	R.J. Bodnar Workshop 1	10:00-10:15		10:00-10:15	10:00-10:30	<i>Coffee break</i>
15:00-15:15	<i>Coffee break</i> Workshop 2 registration	10:15-10:30		10:15-10:30	10:30-10:45	
15:15-18:00	Lab Visits Workshop 2	10:30-11:00	<i>Coffee break</i>	10:30-11:00	10:45-11:00	
17:00-19:00	Conference registration	11:00-11:30		11:00-11:15	11:00-11:15	Session 2
18:00-21:00	Ice breaker party	11:30-11:45	Session 1	11:15-11:30	11:15-11:30	
		12:00-12:15		11:30-11:45	11:30-11:45	
		12:15-12:30		11:45-12:00	11:45-12:00	
		12:30-14:00	<i>Lunch</i>	12:00-13:40	12:00-13:30	<i>Lunch</i>
		14:00-14:15		13:40-14:00	13:30-13:45	
		14:15-14:30		14:00-14:15	13:45-14:00	Session 2
		14:30-14:45	Session 1	14:15-14:30	14:00-14:15	
		14:45-15:00		14:30-14:45	14:15-14:30	
		15:00-15:15		14:45-15:00	14:30-15:45	Plenary discussion & Closing ceremony
		15:15-15:30		15:00-15:30		
		15:30-16:00	<i>Coffee break</i>	15:30-15:45		
		16:00-16:15	Session 1	15:45-16:00		
		16:15-16:30		16:00-16:15		
		16:30-16:45		16:15-16:30		
		16:45-17:00	Session 5	16:30-16:45		
		17:00-17:15		16:45-17:00		
		17:15-17:30		17:00-18:15		
		17:30-19:00	Poster session	18:15-18:45		
				19:00-22:00		
						09:00-17:00 Buda Thermal Karst



# **ACTA MINERALOGICA-PETROGRAPHICA**

## **ABSTRACT SERIES**

VOLUME 10 2019

HU ISSN 0324-6523

HU ISSN 1589-4835

---